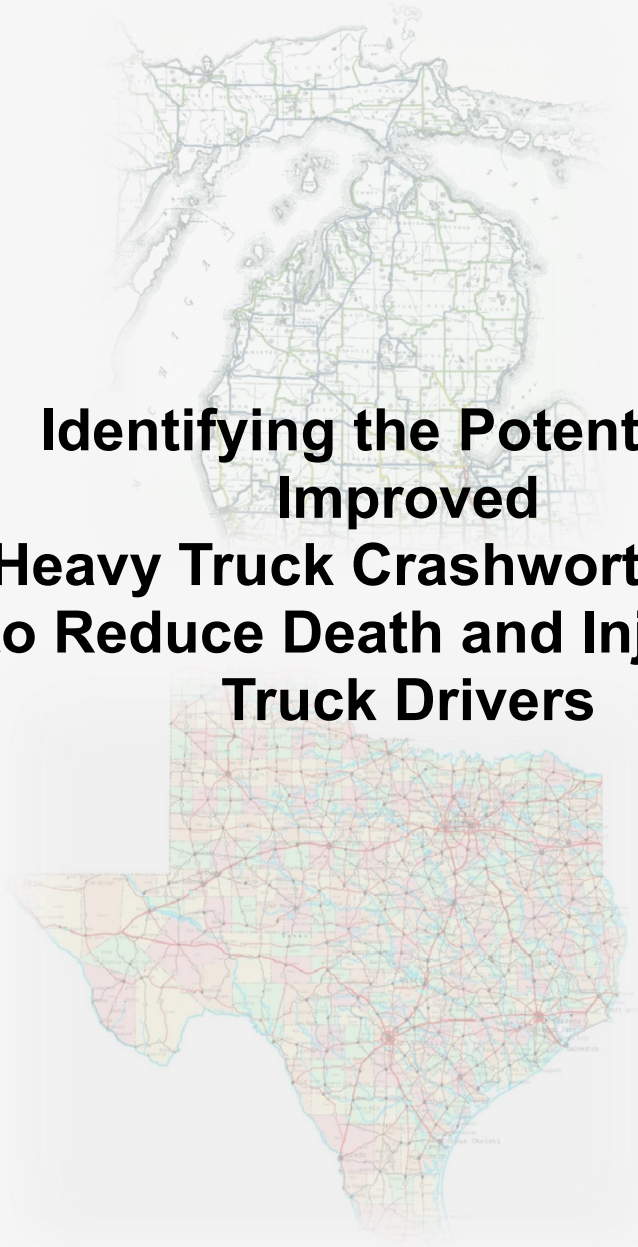




RESEARCH

A large, semi-transparent map of Texas is visible in the background, showing a dense network of roads and highways. The map is color-coded with various shades of green, yellow, and red, likely representing different road types or traffic volumes.

**Identifying the Potential of
Improved
Heavy Truck Crashworthiness
to Reduce Death and Injury for
Truck Drivers**

Identifying the Potential of Improved Heavy Truck Crashworthiness to Reduce Death and Injury for Truck Drivers

Report number: ATLAS-2015-4

**Chiara Silvestri Dobrovolny
Nathan D. Schulz
Texas A&M Transportation Institute, Texas A&M University**

**Daniel Blower
Marco Benedetti
University of Michigan Transportation Research Institute**



**University of Michigan
2901 Baxter Rd. Room 124
Ann Arbor, MI 48109-2150**

and

**Texas A&M Transportation Institute
Texas A&M University**

**3135 TAMU
College Station, TX 77843-3135**

July 2015

DISCLAIMER

The contents of this report reflect the views of the authors, who are responsible for the facts and the accuracy of the information presented herein. This document is disseminated under the sponsorship of the U.S. Department of Transportation's University Transportation Centers Program, in the interest of information exchange. The U.S. Government assumes no liability for the contents or use thereof.

ACKNOWLEDGEMENT

This research project was supported by the Center for Advancing Transportation Leadership and Safety (ATLAS Center). The ATLAS Center is supported by a grant from the U.S. Department of Transportation, Office of the Assistant Secretary for Research and Transportation, University Transportation Centers Program (DTRT13-G-UTC54). The ATLAS Center is a collaboration between the University of Michigan Transportation Research Institute (UMTRI) and the Texas A&M Transportation Institute (TTI).

Technical Report Documentation Page

1. Report No. ATLAS-2015-4		2. Government Accession No.		3. Recipient's Catalog No.	
4. Title and Subtitle Identifying the Potential of Improved Heavy-Truck Crashworthiness to Reduce Death and Injury for Truck Drivers				5. Report Date	
				6. Performing Organization Code	
7. Author(s) Chiara Silvestri Dobrovolny ¹ , Nathan D. Schulz ¹ , Daniel Blower ² , Marco Benedetti ²				8. Performing Organization Report No.	
9. Performing Organization Name and Address University of Michigan ² Texas A&M Transportation Institute ¹ 2901 Baxter Rd. Room 124 Texas A&M University Ann Arbor, MI 48109-2150 College Station, TX 77843-3135				10. Work Unit no. (TRAIS)	
				11. Contract or Grant No. DTRT13-G-UTC54	
12. Sponsoring Agency Name and Address Advancing Transportation Leadership and Safety (ATLAS) Center 2901 Baxter Rd., Room 124, Ann Arbor, MI 48109-2150 U.S.A				13. Type of Report and Period Covered	
				14. Sponsoring Agency Code	
15. Supplementary Notes Supported by a grant from the U.S. Department of Transportation, OST-R, University Transportation Centers Program					
16. Abstract Advanced crash avoidance technologies (ACATs) for trucks have been developed in recent years and are beginning to be deployed. Prior to the development of standards for heavy truck crashworthiness and occupant protection, additional characterization of the crash-injury problem, current medium/heavy truck crashworthiness, and the potential benefits of crashworthy structures in heavy straight trucks and in truck cabs and trailers is needed. The goal of the project is to determine the nature of truck crashes that would remain after full deployment of ACATs, and to assess them in terms of truck driver injury and prevention. Then, using finite element analysis and computer simulation, exemplar tractor-semitrailer crashes were simulated to identify opportunities to improve occupant protection. Rollover and frontal collisions account for most truck driver fatalities and serious injuries. It was estimated that full deployment of ACATs would reduce truck crashes by 10%, and up to 30% of riskiest crash types. However, rollover and frontal impacts would remain as the primary crash types to be addressed. A full truck cabin model was developed and employed in our FE computer simulations to analyze occupant behavior and injury risk during frontal and rollover crashes. An integral part of this truck cabin model was the development of the occupant compartment components as no publicly available heavy truck models exist that contains interior components in the cabin. Additionally, researchers provided a methodology that can be employed and /or adapted to conduct future research within heavy truck occupant safety with use of computational analysis. Analysis of restraint systems during frontal and rollover crashes revealed unacceptable results according to current injury criteria standards and future work needs to be conducted to develop more effective restraint systems to increase occupant safety.					
17. Key Words Heavy truck, truck cab crashworthiness, crash avoidance, finite element analysis, occupant protection, rollover, frontal impact, airbag, seatbelt				18. Distribution Statement Unlimited	
19. Security Classification (of this report) Unclassified		20. Security Classification (of this page) Unclassified		21. No. of Pages 317	22. Price

Table of Contents

1.	Introduction.....	1
2.	Technologies.....	4
2.1	Electronic stability control (ESC).....	4
2.2	Roll stability control (RSC).....	6
2.3	Forward collision warning and collision mitigation braking (FCW/CMB).....	6
2.4	Lane departure warning (LDW).....	7
3.	Background and relevant literature.....	8
3.1	Heavy truck crashworthiness - previous studies.....	8
3.1.1	Crash pulse.....	8
3.1.2	Occupant dynamic simulation input.....	10
3.1.3	Occupant/vehicle interaction data.....	12
3.1.4	Single degree of freedom model (SDOF).....	13
3.1.5	Three degrees of freedom model (TDOF).....	13
3.1.6	Rollover simulation and restraint systems.....	16
3.1.7	History and overview of the crash test dummy.....	19
3.1.8	Injury criteria.....	23
3.1.9	Restraint systems.....	26
3.1.10	Crash scenario.....	28
4.	Method to estimate residual crash population.....	30
4.1	Computation of adjusted weights to account for effectiveness.....	31
5.	Data.....	34
6.	How truck drivers are injured in crashes.....	35
7.	Baseline crash and driver injury distributions.....	38
8.	Effectiveness estimates on ACATs.....	40
8.1	Estimates for LDW, RSC, and FCW.....	40
8.2	Estimates for FCW and ACC.....	44
8.3	Estimates for FCW and collision mitigation braking (CMB).....	48
8.4	Estimates for ESC and RSC.....	53
8.5	Estimates for LDW.....	57
8.6	Estimated combined effect of ESC, FCW, and LDW.....	61

9.	Residual crashes, after full ACAT deployment	65
10.	Methodology for simulation	69
10.1	Interior design of heavy truck model	69
10.1.1	Introduction.....	69
10.1.2	Modified cab over engine cabin.....	70
10.1.3	Cloud point modeling	74
10.1.4	Surface modeling	76
10.1.5	Connection modeling	78
10.1.6	Crash test dummy finite element model	82
10.1.7	Statistics on frontal impacts drivers injury severity.....	83
10.2	Finite element seatbelt model development.....	90
10.3	Finite element airbag model development.....	93
10.3.1	Airbag overview.....	93
10.3.2	Implementation of the airbag model for use in frontal crash simulations	93
10.4	Frontal simulation methodology	96
10.4.1	Methodology introduction	96
10.4.2	Generation and application of crash pulse	96
10.4.3	Contact definition between dummy and truck cabin interior.....	101
10.5	Rollover simulation methodology.....	105
10.5.1	Introduction.....	105
10.5.2	TruckSim rollover event	105
10.5.3	Development of truck cabin model for rollover event.....	108
10.5.4	Application of rollover maneuver to truck cabin	108
10.5.5	Inclusion of Hybrid III 50 th percentile male dummy	109
10.5.6	Modifications to seatbelt.....	110
11.	FE Frontal computer simulation results – 35 mph.....	112
11.1	Frontal simulations without airbag – 35 mph	116
11.1.1	Frontal baseline simulation – 35 mph.....	116
11.1.2	Frontal no pretensioner simulation – 35 mph	126
11.1.3	Frontal 4 kN load limiter simulation – 35 mph.....	136
11.1.4	Frontal 8 kN load limiter simulation – 35 mph.....	146

11.1.5	Frontal lowered D-ring simulation – 35 mph	156
11.1.6	Comparison of Frontal Simulations without Airbag – 35 mph	166
11.2	Frontal simulations with airbag – 35 mph	170
11.2.1	Frontal baseline simulation – 35 mph.....	170
11.2.2	Frontal no pretensioner simulation – 35 mph	180
11.2.3	Frontal 4 kN load limiter simulation – 35 mph.....	190
11.2.4	Frontal 8 kN load limiter simulation – 35 mph.....	200
11.2.5	Frontal lowered D-ring simulation – 35 mph	210
11.2.6	Comparison of frontal simulations with airbag – 35 mph	220
12.	FE rollover computer simulation results.....	224
12.1	Comparison of fast dummy model to detailed dummy model.....	224
12.2	Unbelted rollover simulation	226
12.3	Lap belt rollover simulation.....	229
12.4	Shoulder and lap belt rollover simulation.....	233
12.5	Comparison of rollover simulations.....	237
13.	Summary and conclusions	240
13.1	Limitations	242
13.2	Implications for future research	243
14.	References.....	245
Appendix A.	FE frontal computer simulation results – 50 mph.....	247

List of Tables

Table 3-1 Interior model details (Source: Cheng et al., 1992).....	10
Table 3-2 Occupant and vehicle interaction data (Adapted from Cheng et al., 1992).	12
Table 3-3 Results for rollover simulation (Adapted from Cheng et al., 1992).	15
Table 3-4 Occupant motion details during rollover crash scenario according to different restraint conditions (Adapted from Cheng et. al. 1992).....	17
Table 3-5 Occupant motion details during frontal crash scenario according to different restraint conditions (Adapted from Cheng et. al. 1992).....	18
Table 3-6 Evolution of dummies.	21
Table 3-7 Injury criteria summary for the head.	24
Table 3-8 Injury criteria summary for the thorax.	25
Table 3-9 Injury criteria summary for the leg.....	25
Table 3-10 Different types of restraint systems.	28
Table 4-1 Penetration rates for roll and stability control by model year	33
Table 6-1 Crash Types by Serious Driver Injury Risk	36
Table 6-2 Driver injury by rollover	37
Table 6-3 Crash types by serious driver injury risk, belted drivers only	37
Table 6-4 Driver injury by rollover, belted drivers only	38
Table 6-5 Impact location on truck in collision crashes	38
Table 7-1 Baseline, pre-technology distribution of most harmful crash types	39
Table 7-2 Tractor-semitrailer driver injury severity	40
Table 8-1 Effectiveness estimates from Hickman for LDW, RSC, and FCW	42
Table 8-2 Crash types addressed by the Hickman analysis	42
Table 8-3 Reduction in crash involvements estimated from Hickman.....	43
Table 8-4 Reduction in driver injuries, based on Hickman	44
Table 8-5 Crash types addressed in Volvo FOT.....	45
Table 8-6 Effectiveness estimates for CWS and ACC, Volvo FOT.....	46
Table 8-7 Reduction in crash involvements by relevant crash type, Volvo FOT.....	46
Table 8-8 Reduction in crash involvements by most harmful event, Volvo FOT	47
Table 8-9 Reduction in driver injuries by ACAT device estimated from Volvo FOT	48
Table 8-10 FCW/CMB-relevant crash types, after Woodrooffe et al. (2012)	50
Table 8-11 Effectiveness estimates by technology.....	50
Table 8-12 Reduction in CMB-relevant crash types, estimated from Woodrooffe et al. (2012) .	51
Table 8-13 Reduction in crash involvements by most harmful event, estimated Woodrooffe et al. (2012).....	52
Table 8-14 Reduction in driver injuries, estimated from Woodrooffe et al. (2012).....	53
Table 8-15 Effectiveness estimates by technology, road condition, and crash type.....	54
Table 8-16 Crash types relevant to ESC and RSC, after Woodrooffe et al. (2009)	55

Table 8-17 Relevant crashes reduced by ESC & RSC, after Woodrooffe et al. (2009)	56
Table 8-18 Reduction in crash involvements by most harmful event, after Woodrooffe et al. (2009).....	56
Table 8-19 Reduction in driver injuries by ESC/RSC, after Woodrooffe et al. (2009).....	57
Table 8-20 LDW effectiveness estimates by crash type	59
Table 8-21 Distribution of LDW/RDW-relevant crashes, after Houser et al. (2009).....	59
Table 8-22 Reduction in LDW/RDW crashes	60
Table 8-23 Reductions in crash involvements by most harmful event, estimated from Houser et al. (2009).....	60
Table 8-24 Reduction in driver injuries estimated from Houser	61
Table 8-25 Combined ACAT effectiveness by MHE crash type	62
Table 8-26 Combined ACAT effectiveness on driver injury.....	63
Table 8-27 Effect of ACAT full deployment on rollover	64
Table 8-28 Effect of full deployment on collision crashes	65
Table 9-1 Current MHE crash population and after full deployment.....	66
Table 9-2 Distribution of fatal and serious injury crashes classified by precipitating event.....	68
Table 10-1 Parts Connection using constrained nodal rigid body.	78
Table 10-2 Parts connections using constrained spotweld.	79
Table 10-3 Parts connections using beam spotweld.	80
Table 10-4 Frontal collision injuries for CCTS drivers based on severity.	83
Table 10-5 Injury sources of frontal impacts for CCTS drivers based on belt use.....	84
Table 10-6 Percentages of injury sources based on belt use for CCTS drivers.....	86
Table 10-7 Injury source of body part for CCTS drivers in frontal impacts.	87
Table 10-8 Process for seatbelt modeling of retractor and pretensioner.	92
Table 11-1 Summary of simulation types, impact information and seatbelt.	112
Table 11-2 Injury criteria parameters for head and neck region.....	113
Table 11-3 Injury criteria parameters for chest region.	113
Table 11-4 Injury criteria parameters for leg region.....	114
Table 11-5 Summary of IARV's for injury criteria parameters.	115
Table 11-6 Frontal impact simulation frames side view (35 mph, baseline, no airbag).....	117
Table 11-7 Frontal impact simulation frames perspective view (35 mph, baseline, no airbag). 118	
Table 11-8 Frontal impact simulation frames side view (35 mph, no pretensioner, no airbag). 127	
Table 11-9 Frontal impact simulation frames perspective view (35 mph, no pretensioner, no airbag).	128
Table 11-10 Frontal impact simulation frames side view (35 mph, 4 kN load limiter, no airbag).	137
Table 11-11 Frontal impact simulation frames perspective view (35 mph, 4 kN load limiter, no airbag).	138
Table 11-12 Frontal impact simulation frames side view (35 mph, 8 kN load limiter, no airbag).	147

Table 11-13 Frontal impact simulation frames perspective view (35 mph, 8 kN load limiter, no airbag).	148
Table 11-14 Frontal impact simulation frames side view (35 mph, lowered d-ring, no airbag).	157
Table 11-15 Frontal impact simulation frames perspective view (35 mph, lowered d-ring, no airbag).	158
Table 11-16 Sequential frame comparison of frontal simulations at 35 mph without airbag (side view).	167
Table 11-17 Sequential frame comparison of frontal simulations at 35 mph without airbag (perspective view).	168
Table 11-18 Frontal impact simulation frames side view (35 mph, baseline, airbag).	171
Table 11-19 Frontal impact simulation frames perspective view (35 mph, baseline, airbag). ...	172
Table 11-20 Frontal impact simulation frames side view (35 mph, no pretensioner, airbag). ...	181
Table 11-21 Frontal impact simulation frames perspective view (35 mph, no pretensioner, airbag).	182
Table 11-22 Frontal impact simulation frames side view (35 mph, 4 kN load limiter, airbag).	191
Table 11-23 Frontal impact simulation frames perspective view (35 mph, 4 kN load limiter, airbag).	192
Table 11-24 Frontal impact simulation frames side view (35 mph, 8 kN load limiter, airbag).	201
Table 11-25 Frontal impact simulation frames perspective view (35 mph, 8 kN load limiter, airbag).	202
Table 11-26 Frontal impact simulation frames side view (35 mph, lowered d-ring, airbag).	211
Table 11-27 Frontal impact simulation frames perspective view (35 mph, lowered d-ring, airbag).	212
Table 11-28 Sequential frame comparison of frontal simulations at 35 mph with airbag (side view).	221
Table 11-29 Sequential frame comparison of frontal simulations at 35 mph with airbag (perspective view).	222
Table 12-1 Comparison of injury criteria for fast dummy and detailed dummy.	225
Table 12-2 Rollover unbelted simulation frames (front view).	226
Table 12-3 Rollover unbelted simulation frames (top view).	227
Table 12-4 Description of different contact points during rollover unbelted simulation.	228
Table 12-5 Rollover lap belt simulation frames (front view).	230
Table 12-6 Rollover lap belt simulation frames (top view).	231
Table 12-7 Description of different contact points during rollover lap belt simulation.	232
Table 12-8 Rollover shoulder and lap belt simulation frames (front view).	234
Table 12-9 Rollover shoulder and lap belt simulation frames (top view).	235
Table 12-10 Description of different contact points during rollover shoulder and lap belt simulation.	236
Table 12-11 Comparison of rollover sequential frames for different restraint systems (front view).	237

Table 12-12 Comparison of rollover sequential frames for different restraint systems (top view).	238
Table 12-13 Comparison of maximum lateral displacement for rollover simulations.	239
Table A-1 Summary of simulation types, impact information, and seatbelt.	247
Table A-2 Injury criteria parameters for head and neck region.	248
Table A-3 Injury criteria parameters for chest region	248
Table A-4 Injury criteria parameters for leg region.	249
Table A-5 Summary of IARVs for injury criteria parameters.	250
Table A-6 Frontal impact simulation frames side view (50 mph, baseline, no airbag).	252
Table A-7 Frontal impact simulation frames perspective view (50 mph, baseline, no airbag).	253
Table A-8 Frontal impact simulation frames side view (50 mph, no pretensioner, no airbag).	261
Table A-9 Frontal impact simulation frames perspective view (50 mph, no pretensioner, no airbag).	262
Table A-10 Frontal impact simulation frames side view (50 mph, 4 kN load limiter, no airbag).	270
Table A-11 Frontal impact simulation frames perspective view (50 mph, 4 kN load limiter, no airbag).	271
Table A-12 Frontal impact simulation frames side view (50 mph, 8 kN load limiter, no airbag).	279
Table A-13 Frontal impact simulation frames perspective view (50 mph, 8 kN load limiter, no airbag).	280
Table A-14 Frontal impact simulation frames side view (50 mph, lowered d-ring, no airbag).	288
Table A-15 Frontal impact simulation frames perspective view (50 mph, lowered d-ring, no airbag).	289
Table A-16 Sequential frame comparison of frontal simulations at 50 mph without airbag (side view).	297
Table A-17 Sequential frame comparison of frontal simulations at 50 mph without airbag (perspective view).	298

List of Figures

Figure 1-1 Percentage change from 2001 in truck and light vehicle driver fatalities.....	2
Figure 3-1 Crash pulse deceleration plot (Cheng et. al. 1992).	9
Figure 3-2 TDOF model for rollover phase (Cheng et. al. 1992).	13
Figure 3-3 SDOF and TDOF comparison chart (Cheng et. al. 1992).	14
Figure 3-4 Front and side view of transparent dummy with accelerometers.....	23
Figure 3-5 Crash pulse deceleration plot (Cheng et. al. 1992).	29
Figure 9-1 Fatal and A-injuries by MHE crash type, current and full ACAT deployment	67
Figure 9-2 Fatal and A-injuries in MHE collisions, current and full ACAT deployment	67
Figure 10-1 Original COE DoS cabin vs. morphed conventional cabin models.	72
Figure 10-2 UMTRI provided interior cloud points.	74
Figure 10-3 Cloud points with cabin.	75
Figure 10-4 Mesh grid step application process.	76
Figure 10-5 Perspectives of cloud points with surfaces in cabin.	77
Figure 10-6 Hybrid III 50 th percentile male dummy.....	82
Figure 10-7 Belt material force versus strain loading and unloading curves.	90
Figure 10-8 Seatbelt retractor curves representing force versus payout.	91
Figure 10-9 Different views of seatbelt and dummy showing seatbelt geometry.	92
Figure 10-10 Finite element computer model of the airbag.	94
Figure 10-11 Comparison of NCAC FE steering wheel (left) and truck cabin FE steering wheel (right).	94
Figure 10-12 Comparison of NCAC FE steering wheel (left) and truck cabin FE steering wheel (right) showing concealed airbag.....	94
Figure 10-13 Frontal simulation at time 0.03 seconds where airbag begins to inflate.	95
Figure 10-14 FE tractor-trailer model used to develop frontal crash pulse.	97
Figure 10-15 Cab mount locations in tractor vehicle for crash pulse application.	98
Figure 10-16 50 mph deltaV crash pulse at CG of truck cabin.	99
Figure 10-17 50 mph acceleration history at CG of truck cabin.....	99
Figure 10-18 35 mph deltaV crash pulse at CG of truck cabin.	100
Figure 10-19 35 mph acceleration history at CG of truck cabin.....	100
Figure 10-20 Dummy left foot resting behind clutch pedal.....	102
Figure 10-21 Dummy left foot resting on floor with no clutch pedal.....	102
Figure 10-22 Frontal simulation with lowered stiffness of dashboard causing large deformation.	103
Figure 10-23 Left edge of dashboard constrained to left door.....	103
Figure 10-24 Frontal simulation with constrained left edge of dashboard.	103
Figure 10-25 Large deformation of driver seat during frontal simulation.....	104
Figure 10-26 Simplified seat model with rigid bottom half and soft top half.	104
Figure 10-27 TruckSim tractor-trailer vehicle used to develop rollover simulation.	105
Figure 10-28 Rollover path that was input into TruckSim tractor-trailer rollover crash.....	106

Figure 10-29 Location of four cab mount for tractor vehicle.	107
Figure 10-30 Comparison of detailed dummy model (left) and fast dummy model (right).	109
Figure 10-31 Comparison of mesh size for detailed dummy model (left) and fast dummy model (right).	110
Figure 11-1 Modeled characteristics of the finite element simulation for the frontal impact (35 mph, baseline, no airbag).	116
Figure 11-2 Seatbelt retractor force time history (35 mph, baseline, no airbag).	119
Figure 11-3 HIC time history (35 mph, baseline, no airbag).	119
Figure 11-4 Neck injury time history (35 mph, baseline, no airbag).	120
Figure 11-5 Chest deflection time history (35 mph, baseline, no airbag).	121
Figure 11-6 KTH injury time history (35 mph, baseline, no airbag).	122
Figure 11-7 Tibia plateau fracture time history (35 mph, baseline, no airbag).	123
Figure 11-8 Tibia shaft fracture time history (35 mph, baseline, no airbag).	124
Figure 11-9 Injury probability as a function of IARV (35 mph, baseline, no airbag).	125
Figure 11-10 Modeled characteristics of the finite element simulation for the frontal impact (35 mph, no pretensioner, no airbag).	126
Figure 11-11 Seatbelt retractor force time history (35 mph, no pretensioner, no airbag).	129
Figure 11-12 HIC time history (35 mph, no pretensioner, no airbag).	129
Figure 11-13 Neck injury time history (35 mph, no pretensioner, no airbag).	130
Figure 11-14 Chest deflection time history (35 mph, no pretensioner, no airbag).	131
Figure 11-15 KTH injury time history (35 mph, no pretensioner, no airbag).	132
Figure 11-16 Tibia plateau fracture time history (35 mph, no pretensioner, no airbag).	133
Figure 11-17 Tibia shaft fracture time history (35 mph, no pretensioner, no airbag).	134
Figure 11-18 Injury probability as a function of IARV (35 mph, no pretensioner, no airbag). .	135
Figure 11-19 Modeled characteristics of the finite element simulation for the frontal impact (35 mph, 4 kN load limiter, no airbag).	136
Figure 11-20 Seatbelt retractor force time history (35 mph, 4 kN load limiter, no airbag).	139
Figure 11-21 HIC time history (35 mph, 4 kN load limiter, no airbag).	139
Figure 11-22 Neck injury time history (35 mph, 4 kN load limiter, no airbag).	140
Figure 11-23 Chest deflection time history (35 mph, 4 kN load limiter, no airbag).	141
Figure 11-24 KTH injury time history (35 mph, 4 kN load limiter, no airbag).	142
Figure 11-25 Tibia plateau fracture time history (35 mph, 4 kN load limiter, no airbag).	143
Figure 11-26 Tibia shaft fracture time history (35 mph, 4 kN load limiter, no airbag).	144
Figure 11-27 Injury probability as a function of IARV (35 mph, 4 kN load limiter, no airbag).	145
Figure 11-28 Modeled characteristics of the finite element simulation for the frontal impact (35 mph, 8 kN load limiter, no airbag).	146
Figure 11-29 Seatbelt retractor force time history (35 mph, 8 kN load limiter, no airbag).	149
Figure 11-30 HIC time history (35 mph, 8 kN load limiter, no airbag).	149
Figure 11-31 Neck injury time history (35 mph, 8 kN load limiter, no airbag).	150
Figure 11-32 Chest deflection time history (35 mph, 8 kN load limiter, no airbag).	151

Figure 11-33 KTH injury time history (35 mph, 8 kN load limiter, no airbag).....	152
Figure 11-34 Tibia plateau fracture time history (35 mph, 8 kN load limiter, no airbag).	153
Figure 11-35 Tibia shaft fracture time history (35 mph, 8 kN load limiter, no airbag).....	154
Figure 11-36 Injury probability as a function of IARV (35 mph, 8 kN load limiter, no airbag).155	
Figure 11-37 Modeled characteristics of the finite element simulation for the frontal impact (35 mph, lowered d-ring, no airbag).	156
Figure 11-38 Seatbelt retractor force time history (35 mph, lowered d-ring, no airbag).	159
Figure 11-39 HIC time history (35 mph, lowered d-ring, no airbag).	159
Figure 11-40 Neck injury time history (35 mph, lowered d-ring, no airbag).	160
Figure 11-41 Chest deflection time history (35 mph, lowered d-ring, no airbag).	161
Figure 11-42 KTH injury time history (35 mph, lowered d-ring, no airbag).	162
Figure 11-43 Tibia plateau fracture time history (35 mph, lowered d-ring, no airbag).....	163
Figure 11-44 Tibia shaft fracture time history (35 mph, lowered d-ring, no airbag).	164
Figure 11-45 Injury probability as a function of IARV (35 mph, lowered d-ring, no airbag). ..	165
Figure 11-46 Head injury probability comparison as a function of IARV (no airbag).	166
Figure 11-47 Neck injury probability comparison as a function of IARV (no airbag).	166
Figure 11-48 Chest injury probability comparison as a function of IARV (no airbag).....	169
Figure 11-49 KTH injury probability comparison as a function of IARV (no airbag).....	169
Figure 11-50 Modeled characteristics of the finite element simulation for the frontal impact (35 mph, baseline, airbag).	170
Figure 11-51 Seatbelt retractor force time history (35 mph, baseline, airbag).	173
Figure 11-52 HIC time history (35 mph, baseline, airbag).	173
Figure 11-53 Neck injury time history (35 mph, baseline, airbag).....	174
Figure 11-54 Chest deflection time history (35 mph, baseline, airbag).....	175
Figure 11-55 KTH injury time histories (frontal, 35 mph, belted, airbag).	176
Figure 11-56 Tibia plateau fracture time history (35 mph, baseline, airbag).	177
Figure 11-57 Tibia shaft fracture time history (35 mph, baseline, airbag).	178
Figure 11-58 Injury probability as a function of IARV (35 mph, baseline, airbag).	179
Figure 11-59 Modeled characteristics of the finite element simulation for the frontal impact (35 mph, no pretensioner, airbag).	180
Figure 11-60 Seatbelt retractor force time history (35 mph, no pretensioner, airbag).	183
Figure 11-61 HIC time history (35 mph, no pretensioner, airbag).	183
Figure 11-62 Neck injury time history (35 mph, no pretensioner, airbag).	184
Figure 11-63 Chest deflection time history (35 mph, no pretensioner, airbag).....	185
Figure 11-64 KTH injury time history (35 mph, no pretensioner, airbag).	186
Figure 11-65 Tibia plateau fracture time history (35 mph, no pretensioner, airbag).....	187
Figure 11-66 Tibia shaft fracture time history (35 mph, no pretensioner, airbag).	188
Figure 11-67 Injury probability as a function of IARV (35 mph, no pretensioner, airbag).	189
Figure 11-68 Modeled characteristics of the finite element simulation for the frontal impact (35 mph, 4 kN load limiter, airbag).....	190

Figure 11-69 Seatbelt retractor force time history (frontal, 35 mph, belted, airbag).....	193
Figure 11-70 HIC time history (35 mph, 4 kN load limiter, airbag).	193
Figure 11-71 Neck injury time history (35 mph, 4 kN load limiter, airbag).	194
Figure 11-72 Chest deflection time history (35 mph, 4 kN load limiter, airbag).	195
Figure 11-73 KTH injury time history (35 mph, 4 kN load limiter, airbag).....	196
Figure 11-74 Tibia plateau fracture time history (35 mph, 4 kN load limiter, airbag).	197
Figure 11-75 Tibia shaft fracture time history (35 mph, 4 kN load limiter, airbag).....	198
Figure 11-76 Injury probability as a function of IARV (35 mph, 4 kN load limiter, airbag).....	199
Figure 11-77 Modeled characteristics of the finite element simulation for the frontal impact (35 mph, 8 kN load limiter, airbag).....	200
Figure 11-78 Seatbelt retractor force time history (35 mph, 8 kN load limiter, airbag).....	203
Figure 11-79 HIC time history (35 mph, 8 kN load limiter, airbag).	203
Figure 11-80 Neck injury time history (35 mph, 8 kN load limiter, airbag).	204
Figure 11-81 Chest deflection time history (35 mph, 8 kN load limiter, airbag).	205
Figure 11-82 KTH injury time history (35 mph, 8 kN load limiter, airbag).....	206
Figure 11-83 Tibia plateau fracture time history (35 mph, 8 kN load limiter, airbag).	207
Figure 11-84 Tibia shaft fracture time history (35 mph, 8 kN load limiter, airbag).....	208
Figure 11-85 Injury probability as a function of IARV (35 mph, 8 kN load limiter, airbag).....	209
Figure 11-86 Modeled characteristics of the finite element simulation for the frontal impact (35 mph, lowered d-ring, airbag).	210
Figure 11-87 Seatbelt retractor force time history (35 mph, lowered d-ring, airbag).	213
Figure 11-88 HIC time history (35 mph, lowered d-ring, airbag).	213
Figure 11-89 Neck injury time history (35 mph, lowered d-ring, airbag).	214
Figure 11-90 Chest deflection time history (35 mph, lowered d-ring, airbag).	215
Figure 11-91 KTH injury time history (35 mph, lowered d-ring, airbag).	216
Figure 11-92 Tibia plateau fracture time history (35 mph, lowered d-ring, airbag).....	217
Figure 11-93 Tibia shaft fracture time history (35 mph, lowered d-ring, airbag).	218
Figure 11-94 Injury probability as a function of IARV (35 mph, lowered d-ring, airbag).	219
Figure 11-95 Head injury probability comparison as a function of IARV (airbag).	220
Figure 11-96 Neck injury probability comparison as a function of IARV (airbag).	220
Figure 11-97 Chest injury probability comparison as a function of IARV (airbag).....	223
Figure 11-98 KTH injury probability comparison as a function of IARV (airbag).....	223
Figure 12-1 Lateral displacement of dummy head during rollover unbelted simulation.	228
Figure 12-2 Lateral displacement of dummy head during rollover lap belt simulation.	232
Figure 12-3 Lateral displacement of dummy head during rollover shoulder and lap belt simulation.....	236
Figure A-1 Modeled characteristics of the finite element simulation for the frontal impact (50 mph, baseline, no airbag).	251
Figure A-2 Seatbelt retractor force time history (50 mph, baseline, no airbag).	254
Figure A-3 HIC time history (50 mph, baseline, no airbag).	254

Figure A-4 Neck injury time history (50 mph, baseline, no airbag).....	255
Figure A-5 KTH injury time history (50 mph, baseline, no airbag).....	256
Figure A-6 Tibia plateau fracture time history (50 mph, baseline, no airbag).....	257
Figure A-7 Tibia shaft fracture time history (50 mph, baseline, no airbag).....	258
Figure A-8 Injury probability as a function of IARV (50 mph, baseline, no airbag).....	259
Figure A-9 Modeled characteristics of the finite element simulation for the frontal impact (50 mph, no pretensioner, no airbag).....	260
Figure A-10 Seatbelt retractor force time history (50 mph, no pretensioner, no airbag).....	263
Figure A-11 HIC time history (50 mph, no pretensioner, no airbag).....	263
Figure A-12 Neck injury time history (50 mph, no pretensioner, no airbag).....	264
Figure A-13 KTH injury time history (50 mph, no pretensioner, no airbag).....	265
Figure A-14 Tibia plateau fracture time history (50 mph, no pretensioner, no airbag).....	266
Figure A-15 Tibia shaft fracture time history (50 mph, no pretensioner, no airbag).....	267
Figure A-16 Injury probability as a function of IARV (50 mph, no pretensioner, no airbag) ..	268
Figure A-17 Modeled characteristics of the finite element simulation for the frontal impact (50 mph, 4 kN load limiter, no airbag).....	269
Figure A-18 Seatbelt retractor force time history (50 mph, 4 kN load limiter, no airbag).....	272
Figure A-19 HIC time history (50 mph, 4 kN load limiter, no airbag).....	272
Figure A-20 Neck injury time history (50 mph, 4 kN load limiter, no airbag).....	273
Figure A-21 KTH injury time history (50 mph, 4 kN load limiter, no airbag).....	274
Figure A-22 Tibia plateau fracture time history (50 mph, 4 kN load limiter, no airbag).....	275
Figure A-23 Tibia shaft fracture time history (50 mph, 4 kN load limiter, no airbag).....	276
Figure A-24 Injury probability as a function of IARV (50 mph, 4 kN load limiter, no airbag).....	277
Figure A-25 Modeled characteristics of the finite element simulation for the frontal impact (50 mph, 8 kN load limiter, no airbag).....	278
Figure A-26 Seatbelt retractor force time history (50 mph, 8 kN load limiter, no airbag).....	281
Figure A-27 HIC time history (50 mph, 8 kN load limiter, no airbag).....	281
Figure A-28 Neck injury time history (50 mph, 8 kN load limiter, no airbag).....	282
Figure A-29 KTH injury time history (50 mph, 8 kN load limiter, no airbag).....	283
Figure A-30 Tibia plateau fracture time history (50 mph, 8 kN load limiter, no airbag).....	284
Figure A-31 Tibia shaft fracture time history (50 mph, 8 kN load limiter, no airbag).....	285
Figure A-32 Injury probability as a function of IARV (50 mph, 8 kN load limiter, no airbag).....	286
Figure A-33 Modeled characteristics of the finite element simulation for the frontal impact (50 mph, lowered d-ring, no airbag).....	287
Figure A-34 Seatbelt retractor force time history (50 mph, lowered d-ring, no airbag).....	290
Figure A-35 HIC time history (50 mph, lowered d-ring, no airbag).....	290
Figure A-36 Neck injury time history (50 mph, lowered d-ring, no airbag).....	291
Figure A-37 KTH injury time history (50 mph, lowered d-ring, no airbag).....	292
Figure A-38 Tibia plateau fracture time history (50 mph, lowered d-ring, no airbag).....	293
Figure A-39 Tibia shaft fracture time history (50 mph, lowered d-ring, no airbag).....	294

Figure A-40 Injury probability as a function of IARV (50 mph, lowered d-ring, no airbag).....	295
Figure A-41 Head injury probability comparison as a function of IARV (no airbag).	296
Figure A-42 Neck injury probability comparison as a function of IARV (no airbag).	296
Figure A-43 KTH injury probability comparison as a function of IARV (no airbag).....	299

Identifying the Potential of Improved Heavy Truck Crashworthiness to Reduce Death and Injury for Truck Drivers

1. Introduction

The University of Michigan Transportation Research Institute (UMTRI) and the Texas A&M Transportation Institute (TTI) conducted a joint project to identify and characterize opportunities to protect heavy-truck drivers and occupants through improved passive restraints and more protective cab interiors, in the context of current advanced crash avoidance technologies (ACATs). Crash types not addressed by current ACATs were identified and characterized to support finite element analysis (FEA) of heavy truck occupant kinematics in these crashes.

According to the Census of Fatal Occupational Injuries for 2013 from the Bureau of Labor Statistics, the transportation and warehousing sector, which includes truck driving, has the second highest rate of fatal occupational injuries annually, second only to agriculture and forestry. Truck driving also accounts for the second most fatal occupational injuries annually, only after construction. The fatality rate per worker is over four times the national average, and a large majority of fatalities to transportation workers occurs in traffic crashes (Bureau of Labor Statistics 2015). On average each year, about 526 truck drivers are killed in traffic crashes, 2,000 suffer incapacitating injuries, 6,200 non-incapacitating but evident injuries, and 7,400 minor injuries. In total, about 16,500 truck drivers are killed or injured in traffic crashes each year. It is clear that driving a truck is one of the most dangerous professions in the labor force.

Figure 1-1 shows the percentage change in the annual number of driver fatalities for truck drivers and for light vehicle drivers from 2001 to 2012, as reported in the National Highway Traffic Safety Administration (NHTSA) Fatality Analysis Reporting System (FARS) file¹. “Light vehicles” include passenger cars, SUVs, minivans, pickups and other light-duty vehicles. Over the period, the number of light vehicle drivers killed in traffic crashes fell by almost 28%, from 21,932 in 2001 to 15,842 in 2012. The number of light vehicle drivers killed in traffic crashes was either relatively stable in most years (e.g., 2001 through 2005) or declined (e.g., 2006 through 2012). The accelerated decline in 2008 was probably a response to the recession that began that year. The experience of truck drivers was quite different. The number of truck drivers killed in traffic crashes actually increased by almost 17% from 2001 to 2007, going from 603 in 2001 to 703 in 2007. The number then fell even more sharply in 2008 and 2009 before increasing again through 2012. In contrast with the fatality rate for light vehicles, which saw a roughly 28% decline over the whole period, truck driver fatalities in traffic crashes were down only 2.2% over the entire period. In 2001, 603 truck drivers were killed in traffic accidents. In 2012, the number of fatalities was 590.

¹ The FARS file is described in detail in section 55 below.

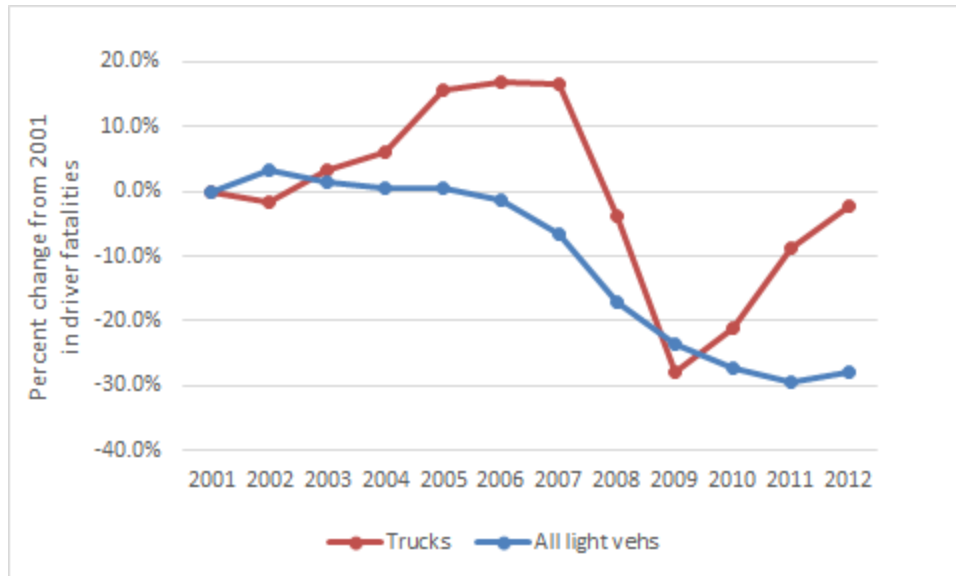


Figure 1-1 Percentage change from 2001 in truck and light vehicle driver fatalities

Among light vehicles, there have been numerous safety technologies implemented to make driving safer and decrease the carnage on the highways. In addition to safety belts and air bags (required for all passenger cars since the 1999 model year), the new car assessment program (NCAP) that was established in 1973, created market pressures for manufacturers to design safer cars. Crash testing and the NCAP star rating program have resulted in safer cars. The star-rating system, begun in 1994, was explicitly based on reducing the probability of serious injuries in traffic crashes, and has resulted in improvements in crashworthiness in frontal collisions, side impact, rollover, and occupant restraints (seat belts and air bags) (Hershman 2001).

In addition to these efforts to make cars more crashworthy (i.e., to protect occupants in the event of a crash), there has also been a substantial effort to assist drivers in avoiding crashes in the first place. Several advanced crash avoidance technologies (ACATs) have been developed. Electronic stability control (ESC), forward collision warning (FCW), lane departure warning and prevention (LDW/LDP), backing cameras, blind spot detection, and autonomous emergency braking have begun to be deployed in recent years (Blower 2014).

However, there has been significantly less development to protect truck drivers in crashes. Safety belt use is required by federal law under section 392.16 of the Federal Motor Carrier Safety Regulations. Usage rates of safety belts by commercial truck drivers have been increasing in recent years and currently are approaching those of light vehicle drivers. In 2007, about 65% of truck drivers were reported to be using safety belts in an observational study (FMCSA, 2007). By 2013, the rate had increased to 84% overall, with the highest rate reported for “box van” trucks, which includes tractor-semitrailers (FMCSA 2014). However, there has been no development of crashworthiness features for trucks that is comparable to that for light vehicles. That is, there is no NCAP for heavy trucks or requirement for air bags.

In terms of crash avoidance, however, while the situation for trucks may trail that of light vehicles, it is clearly moving in the same direction. Recent years have seen the development of LDW, FCW with autonomous emergency braking, blind spot detection, ESC, and roll stability control (RSC, a variant related to ESC) for heavy trucks. Some truck fleets have begun to adopt some of the ACATs, primarily ESC and RSC (Belzowski, Blower et al. 2009). Moreover, in June, 2015, a final rule was announced requiring ESC on heavy trucks beginning after the final publication date of the rule.

The goal of this project is to determine the nature of truck crashes that would remain after full deployment of ACATs, and to assess them in terms of truck driver injury and prevention. In other words, the project attempts to answer the following questions: What types of crashes would remain, even if the best of the current collision avoidance devices were fully deployed? What types of injuries would remain? What will be the nature of the remaining crashes, and what will be the challenge in terms of truck occupant protection? The goal was to determine the dimensions of the truck driver injury problem after all the current crash avoidance technologies had been, in effect, exhausted. The set of crashes and injuries remaining, then, would be a challenge for occupant restraints and other interventions to reduce driver injuries in the crashes that could not be avoided, given current technology.

Crash scenarios (and consequent occupant injury types) were selected using the results obtained by the crash data analysis conducted by UMTRI. The crash data analysis identified crash types and scenarios that presented the highest risk to truck drivers and account for the most fatalities and injuries. Then, the effect of the primary current crash avoidance technologies on the crash population was estimated, to determine the residual population of crashes that would remain after full deployment. This allowed researchers to focus on impact conditions that are overrepresented in the real world crash data, that would not be addressed by crash avoidance technologies, and for which there is room for improvement in terms of occupant safety. This analysis and simulation identified and characterized heavy truck crashes to define opportunities for improved truck crashworthiness to reduce truck driver fatalities and injuries.

The project employed numerical simulations to analyze heavy truck occupant kinematics in the most severe crash types for truck drivers. The work developed within this project consisted of finite element computer modeling and simulation to direct investigations on occupant safety. Finite element analysis (FEA) was used to analyze heavy truck occupant safety in terms of injury patterns and severity. While interior crash protection has received adequate attention for automobiles, very little is known about occupant safety in commercial vehicles such as heavy trucks. This report evaluated the effectiveness of passive safety restraints (such as seatbelts, airbags, etc.) by comparing occupant injury results obtained from simulations performed with and without these restraints. Understanding injury types and injury sources for heavy truck occupants in relation to different crash scenarios will help identify opportunities to reduce injury

severity through design of a more crashworthy occupant compartment and implementation of appropriate passive restraint systems.

TTI researchers used a currently available finite element (FE) dummy model for their computer simulations. The researchers analyzed the kinematics of the occupant during replicated crash scenarios. Employment of the dummy model in the simulation of different crash scenarios allowed collection of acceleration data from impact of different parts of the dummy with the interior components of the occupant compartment. The results were used to calculate injury levels for the occupant in different crash scenarios. The researchers evaluated the effectiveness of passive safety restraints (such as seatbelts, airbags, etc.) by comparing occupant injury results obtained from simulations performed with and without these restraints. The results of these simulations provide guidance on the effectiveness of the use of such occupant injury mitigation systems.

The results of this project present a first understanding of occupant kinematics and interaction with cab interior for heavy vehicles for different crash scenarios. It also provided guidance on the effectiveness of the use of occupant injury mitigation passive restraint systems. No previous research/testing was ever developed with this intent. Understanding injury types for heavy truck occupants in relation to different crash scenarios will help with development of mitigation strategies to reduce injury severity through design of the occupant compartment and appropriate passive restraint systems.

The truck type examined here was a tractor-semitrailer. This is a common truck configuration, colloquially called an “eighteen wheeler,” and is the workhorse truck of freight hauling in the U.S. Tractor-semitrailers were selected as the truck type to study because they are the primary truck configuration, because they account for most truck driver injuries and fatalities (Woodrooffe and Blower 2013), and because most of the studies on ACATs for trucks focus on the tractor-semitrailer combination.

2. Technologies

This section provides descriptions of each of the technologies evaluated. These specific technologies were selected because they are in relatively advanced development, there have been several useful studies of their effectiveness, and they are beginning to be deployed in the truck fleet.

2.1 Electronic stability control (ESC)

ESC is a system that monitors the stability of a vehicle and autonomously intervenes to help the driver maintain control (Houser, Pierowicz. et al., 2005b). ESC systems are designed to reduce rollover and loss-of-control crashes (LOC), in which a truck skids uncontrollably and crashes.

The system monitors two parameters, yaw and lateral acceleration. The degree of yaw is defined, effectively, as the difference between the direction a vehicle is going and the direction it is being steered toward. In understeer, the vehicle essentially “plows forward,” despite being steered one way or the other. Oversteer results in jackknife, when the tractor in a combination yaws more than the steering input.

ESC systems monitor the yaw rate and compare it to the steer angle to determine whether the vehicle is yawing excessively and to determine the direction of yaw. If an excessive yaw is observed, the system intervenes, essentially to align the vehicle with the direction the driver is trying to steer it.

To address excessive lateral acceleration, the system monitors the vehicle’s lateral acceleration and compares it with a limiting value, beyond which the vehicle would roll over. To determine this limiting value, the system estimates vehicle mass by monitoring engine torque and vehicle acceleration. Using the vehicle mass, it computes an allowable lateral acceleration, beyond which the vehicle would roll over. The amount of lateral acceleration that is observed by sensors is compared with the estimated amount that would be safe. If the observed value of lateral acceleration exceeds the limit, the system intervenes to reduce vehicle speed and regain control.

ESC systems intervene in a layered approach: By de-throttling the engine; by engaging the engine brake; and by applying the foundation brakes. De-throttling the engine, in other words, taking the foot off the accelerator, and engaging the engine brake both serve to slow the truck down. Applying the foundation brakes does so as well, but ESC also can selectively brake different axle ends in order to bring the truck under control. Thus, ESC can apply different brake force to the different corners of a vehicle to help straighten it out in the event of yaw or the beginning of rollover.

ESC is designed to be effective against two general types of crashes. The first crash type is untripped rollover, i.e., rollovers that are initiated by excessive lateral acceleration. Typical of untripped rollovers are crashes in which a truck attempts to steer through a curve at a speed that is too high. ESC will de-throttle the engine and engage the engine brake, and then apply the foundation brakes to slow the vehicle down. The second general set of crashes that ESC is designed to reduce are those initiated by on-road loss of control due to yaw. An example would be crashes on wet, low-friction roads that begin when the tractor yaws during a steering maneuver and the vehicle starts to skid. The ESC system will selectively apply the brakes on different axle ends to bring it back straight (Woodrooffe, Blower et al. 2009; Office of Regulatory Analysis and Evaluation 2012).

2.2 Roll stability control (RSC)

Roll stability control is similar to ESC though with less capability. ESC addresses instability related to both yaw and lateral acceleration, while RSC addresses only vehicle instability due to excessive lateral acceleration. Like ESC, RSC systems estimate vehicle mass by monitoring engine torque and acceleration. Vehicle mass is used to estimate a threshold value for lateral acceleration. Sensors monitor lateral acceleration and when it meets the threshold value, the system intervenes to reduce vehicle speed. Again, like ESC, RSC de-throttles the engine, applies the engine brake, and then applies the foundation brakes. RSC is designed to address only excessive lateral acceleration that results in untripped rollover. It does not have the capability to detect or intervene in LOC crashes (Houser, Murray et al. 2007; Murray, Shackelford et al. 2009b; Woodrooffe, Blower et al. 2009).

Both ESC and RSC are autonomous systems, that is, they intervene automatically and do not depend on driver response or initiative. They work by monitoring the stability of the vehicle. If one of the monitored parameters is exceeded, the systems automatically intervene to increase vehicle stability, which may help the driver bring the vehicle under control.

2.3 Forward collision warning and collision mitigation braking (FCW/CMB)

Forward collision warning and collision mitigation braking (sometimes also referred to as forward collision avoidance and mitigation (F-CAM) systems) are designed to address collisions with vehicles in the same lane and ahead of a vehicle; in other words, rear-end striking crashes. The systems have a forward-looking sensor, usually radar, which detects objects in front of the truck and determines the range, range-rate, and time-to-collision (TTC) of the object. Early systems were designed to detect automobiles and larger motor vehicles, but later generations can detect motorcycles, pedestrians, and other nonmotorists.

If a “conflict” such as a vehicle or other object is detected and the system determines that the TTC falls within a certain threshold, the system will issue an audible or haptic warning to the driver. The haptic warning pulses the brakes to warn the driver of a collision threat in front. In systems that are combined with autonomous braking, if the driver does not act or if the TTC falls below a threshold, the system will engage the engine-retarder or engine brake, and then apply the foundation brakes. Depending on the initial speed, the autonomous braking will either slow the vehicle enough to prevent the collision altogether or to at least reduce the impact speed.

Some systems also include adaptive cruise control (ACC). ACC uses the engine and transmission to control vehicle speed to maintain a set distance or time interval to the lead vehicle. In theory, a properly working ACC could maintain a safe following distance and thus prevent conflicts from developing in the first place.

More advanced FCW/CMB systems integrate camera systems to detect and evaluate objects that are effectively “fixed,” i.e., objects that were never detected moving. Such objects include motor vehicles that were already stopped prior to coming in range of the forward-looking sensor. But they would also include fixed roadside objects such as utility poles that might come in view of the sensor on a curve. Distinguishing between valid conflicts in the lane in front of the vehicles and nonthreatening roadside objects is one of the challenges of FCW/CMB design (McMillan, Carnell et al. 2007; Murray, Shackelford et al. 2009a; Woodrooffe, Blower et al. 2012).

2.4 Lane departure warning (LDW)

Lane departure warning systems monitor the vehicle’s position relative to lane markings and provide warnings to the driver when certain thresholds are reached. Current systems use camera-based systems to detect lane markings and to determine the speed and heading of the vehicle in relation to the roadway and lane boundaries. The cameras are typically mounted on the windshield to monitor the road ahead, and the images are interpreted to identify lane boundaries and roadway alignment ahead, e.g., whether the truck is traversing a curve. The system determines the truck’s position within lane, the distance to lane boundaries, the speed of the vehicle, including the lateral velocity toward the lane boundary, and the time-to-lane crossing.

Warning settings can be set to a variety of thresholds, to balance the frequency of false alarms to useful warning of unintentional drift out of lane. Warnings are typically issued by an audible tone and sometimes reinforced with a visual display. In addition, some systems can issue a haptic warning, such as by a vibration on one side of the driver’s seat, depending on the direction of lane excursion.

The systems are designed to warn in the event of unintentional lane excursions, so warnings are suppressed if the driver activates the turn signal. In addition, LDWs typically do not warn if the vehicle is travelling below a given travel speed, typically 30 to 35 mph. Only a warning is given; the systems do not prevent lane departure or steer a vehicle back into lane in the event of lane departure. Instead, the driver is responsible for maintaining the vehicle within lane boundaries.

Since the visual systems depend on detecting lane markings and interpreting them correctly, certain environmental conditions can reduce their effectiveness. Obviously, worn markings can be difficult to detect and the systems do not function if the marking is missing or covered with mud or snow. In addition, wet roadways, especially at night with reflections from street lights, can make it difficult to identify lane borders correctly. LDW systems typically notify the driver if they are not detecting lane boundaries (Houser, Pierowicz et al. 2005a; Orban, Hadden et al. 2006; Houser, Murray et al. 2009).

3. Background and relevant literature

3.1 Heavy truck crashworthiness - previous studies

Heavy truck crashworthiness studies that have been undertaken by many organizations over the past several years have shown that truck occupant safety is of higher concern due to lower deceleration levels and greater time durations in comparison with passenger car collisions, thus producing a more complex variation in the crash events (e.g. rollover crash scenario).

UMTRI performed a detailed analysis on heavy truck crashworthiness and reported its findings as a part of UMTRI occupant safety studies for both car and truck cases (Cheng et al., 1992).

The scope of this project was to investigate different means of evaluating truck occupant protection. The program was divided into several phases. In this report, Phase 1 will be highlighted which involves developing deceleration time histories also known as crash pulses and simulating occupant dynamics in heavy truck crashes using these crash pulses. Phase 1 is further divided into tasks, namely Task A, Task B and Task C.

Task A primarily involved selecting an accident scenario from examining the Fatal Accident Reporting System (FARS) database. The accident scenarios finalized within the study were:

- Frontal Collisions
- 90⁰ Rollover without subsequent collision
- 90⁰ Rollover with subsequent collision

Task B entailed development of crash pulses for the accident scenarios identified In Task A. It also concluded that the 180⁰ rollover of heavy truck was too complex to be dealt with in Phase 1 of the study.

Task C focused on analyzing the peak occupant excursion for the accident scenarios (mentioned above) and the crash pulses developed in Task B. The occupant response was studied for different types of restraint configurations (3-point belted, lap-belted, unrestrained) and cab style (cab-over engine and conventional) for each accident scenario. The information gathered in this phase was used to design test procedures and lead further investigations on truck occupant protection.

3.1.1 Crash pulse

One of the key aspects of this project was the development of the crash pulse. In this section, an overview of the development of the crash pulse is discussed. From previous studies (Rice, 1981 and Mark, et al., 1988), a typical shape resembling an automobile crash test deceleration is chosen which upon reviewing conforms to heavy truck crashes as well (Figure 3-1).

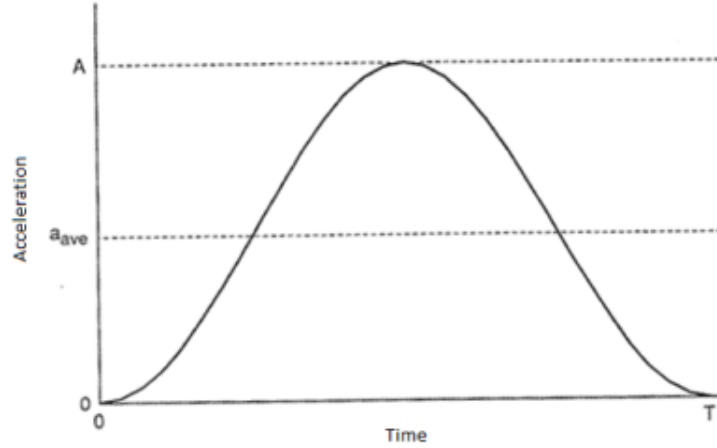


Figure 3-1 Crash pulse deceleration plot (Cheng et. al. 1992).

Deceleration profile is generated using Equation 2.1:

$$a(t) = \frac{1}{2} * A * \left(1 - \cos\left(\frac{2\pi t}{T}\right)\right) \quad (2.1)$$

Where, A is peak deceleration and T is pulse duration.

Change in velocity can be determined using Equation 2.2,

$$\Delta V = \frac{1}{2} * A * T \quad (2.2)$$

Average deceleration can be given by the Equation 2.3,

$$a_{ave} = \frac{1}{2} * A \quad (2.3)$$

The roll angular deceleration profile required to generate a roll over crash pulse is governed by the Equation 2.4:

$$\alpha(t) = \frac{1}{2} * \alpha_{max} * \left(1 - \cos\left(\frac{2\pi t}{T}\right)\right) \quad (2.4)$$

where, α_{max} is maximum angular deceleration and T is pulse period.

From above relation, average angular deceleration is given by Equation 2.5:

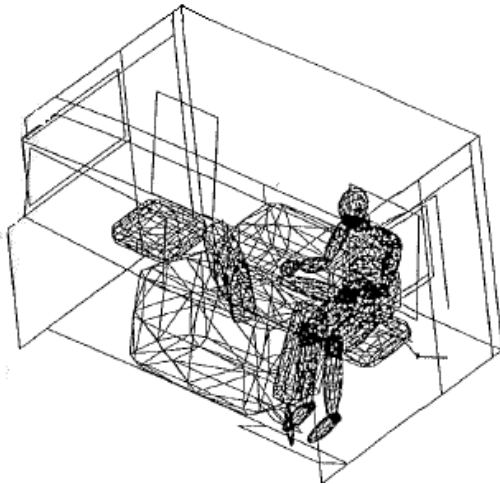
$$\alpha_{ave} = \frac{1}{2} * \alpha_{max} \quad (2.5)$$

3.1.2 Occupant dynamic simulation input

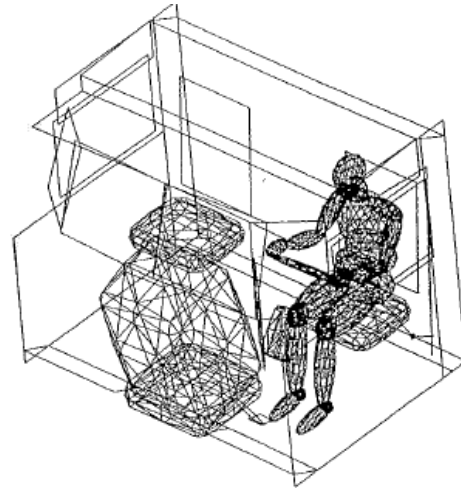
In the study conducted by Cheng et al. (1992), a typical cab interior geometry closest to cab-over-engine (COE) and conventional trucks was considered after studying 3 COE's and 6 conventional trucks. Standardized measurement details were provided to ensure consistency. The given values were compared with cab dimensions and the one with lowest root-sum-square (RSS) distance was selected. This set of dimensions was chosen considering various parameters, such as seat cushion location, lower dash (fore-aft location), floor height, side window, i.e. lateral distance, pillar locations, steering wheel location, restraint attachment and anchorage locations. Table 3-1 shows interior model details for both COE and conventional cabs.

Table 3-1 Interior model details (Source: Cheng et al., 1992).

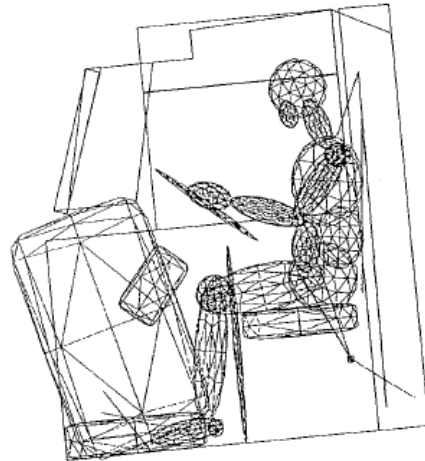
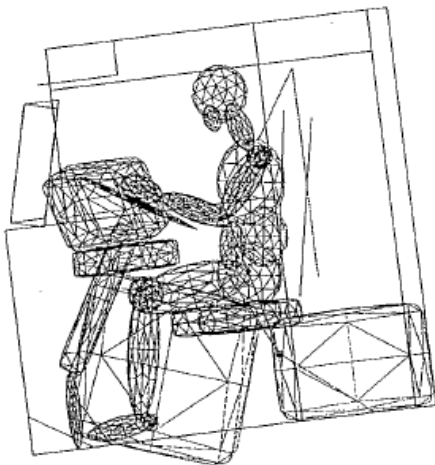
Cab-Over-Engine (COE)



Conventional Cab

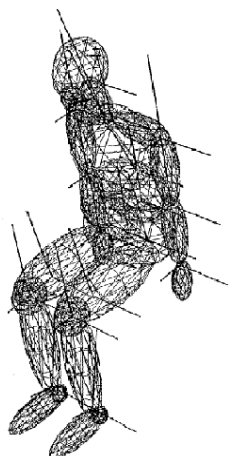


MADYMO Model – Isometric View



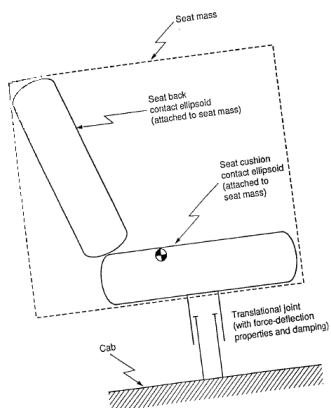
MADYMO Model – Side View

Table 3-1 Interior model details (Source: Cheng et al., 1992) (Continued).



(a) Dummy Model (Occupant Model)

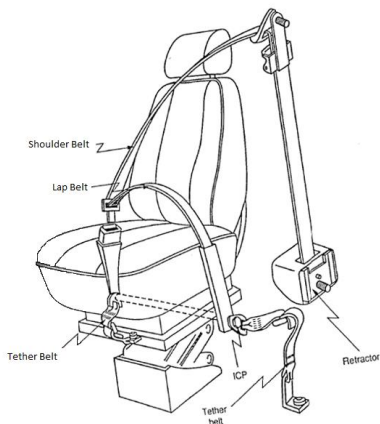
A model that is similar to the Hybrid III Anthropomorphic crash male dummy was chosen from the MADYMO database. The 22 body segments connected by mechanical joints possesses geometric and inertial and joint properties obtained from static, pendulum, and various other testing techniques.



For the seat model, a translational joint connects the cab to the suspended portion of the seat. The suspended portion of the seat accounts for inertial properties of seat cushion and back and the overall stiffness and damping properties of the air spring. The shock absorber is handled by the translational joint. These values were obtained from seat manufacturers and various literature sources. This MADYMO seat model was verified using vibration test transmissibility data and resulted in being in good agreement with test data.

(b) Seat Model

Components of the seat belt model are retractor to D-ring, D-ring to shoulder, shoulder to sternum, sternum to inboard ICP, inboard ICP to lower torso, lower torso to outboard ICP, inboard tether belt, outboard tether belt.



The 3 point resistant belt model includes all of the above mentioned components. The lap belted case excludes the retractor and shoulder belt segments, and in the unrestrained case, only the tether belts are included.

(c) Belt Model

3.1.3 Occupant/vehicle interaction data

A MADYMO model was used to prototype the primary dummy-vehicle interior interactions during a crash. This model employed a contact algorithm for ellipsoid-ellipsoid and plane-ellipsoid contacts which included contact parameters such as force-deflection curve, hysteresis and friction. Table 3-2 summarizes characteristics and results from the validated model for each of the accident scenarios.

Table 3-2 Occupant and vehicle interaction data (Adapted from Cheng et al., 1992).

Model Validation		
<p>Vehicle model: 1975 GMC Astro 95 COE tractor towing a loaded 1974 35 foot Trailco trailer</p> <p>Restraint Conditions: Unrestrained dummy – Driver position Lap belted dummy – Passenger position</p> <p>Dummy: Hybrid II; Triaxial head and chest accelerometers and femur load cells</p>		
Crash scenario	Deceleration	Damage
<p>Frontal: Tractor towing the trailer crashed into array of crushable steel drums at the rate of 29.2mph</p>	<p>2-2.5g at cab centerline over 750ms</p>	<p>Vehicle damage: limited to minor sheet metal distortion of frontal structure</p> <p>Unrestrained dummy: moved fwd. and contacted steering wheel with upper torso and head</p> <p>Lap belted dummy: Upper torso bent fwd. until it made contact with its upper legs</p>
<p>Rollover: 90⁰ rollover using GMC Astro 95 COE tractor towing flatbed trailer vehicle was directed to its left onto a 55⁰ side slope at 35mph</p>	<p>Main crash pulse lasted 150ms</p>	<p>Vehicle damage: Vehicle travelled down rolling to the left, producing longitudinal and lateral deceleration.</p> <p>Unrestrained dummy: Moved fwd. and left past the steering wheel and impacted head area with windshield and header cracking the windshield. Dummy body contacted driver side door and window.</p> <p>Lap restrained: Left leg and torso contacted engine tunnel. Head and chest did not contact any interior surfaces.</p>

3.1.4 Single degree of freedom model (SDOF)

It was noted that during the 90⁰ truck rollover accidents, the trailer shows less stability in comparison to the tractor, therefore the trailer initiates the rollover and pulls the tractor along with it. Due to this phenomenon, work-energy method is used to determine the trailer rollover rate at impact. The change in potential energy and work done by lateral overturning force from 0⁰ to 90⁰ was used in evaluating the increase in kinetic energy. The trailer rollover rate was used to calculate the impact velocity of the tractor. The significance of this method is its ability to determine the ground impact velocity of the tractor, which is a necessity in developing the crash pulse. This method does not provide rollover as a function of time.

A single degree of freedom (SDOF) rollover model of a trailer was developed to generate input data for the occupant dynamics simulations. This method assumes that the pivot (rotational axis) for the trailer is at tire-ground interface of outside tires. The lateral acceleration initiating the roll acts throughout the rollover motion. This method provides a qualitative agreement with observed tractor rollover motions, therefore it does not account for complex behavior of actual truck rollover. It is an easy tool and can be quickly adapted to any other heavy truck configurations and inertia conditions.

3.1.5 Three degrees of freedom model (TDOF)

The three degrees of freedom (TDOF) rollover model used a MADYMO model. It is a more complex computer model accounting for vertical, lateral, and rotational motion of heavy trucks. When comparing the results of the TDOF model with those of the SDOF model, very similar results were obtained up to a roll angle of 45⁰. After this point, however, the TDOF model allowed wheel lift off as there was no pivot constraint. Figure 3-2 demonstrates the rollover phase in the TDOF model (0.5 sec intervals from 0 to 2.5 sec ($\mu = 0.5$)).

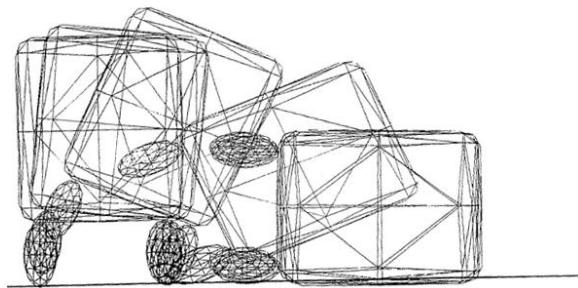


Figure 3-2 TDOF model for rollover phase (Cheng et. al. 1992).

Higher roll rates (25% higher) were predicted in SDOF system due to lateral acceleration persisting to act on the system as opposed to the TDOF model. A more reasonable prediction of truck rollover motions is provided by SDOF as compared with the TDOF model. Figure 3-3 shows the comparison of roll rate vs roll angle for SDOF and TDOF models (before impact).

Table 3-3 summarizes rollover simulation results with respect to roll direction, restraint configuration, cab style, occupant behavior, and recorded contact forces.

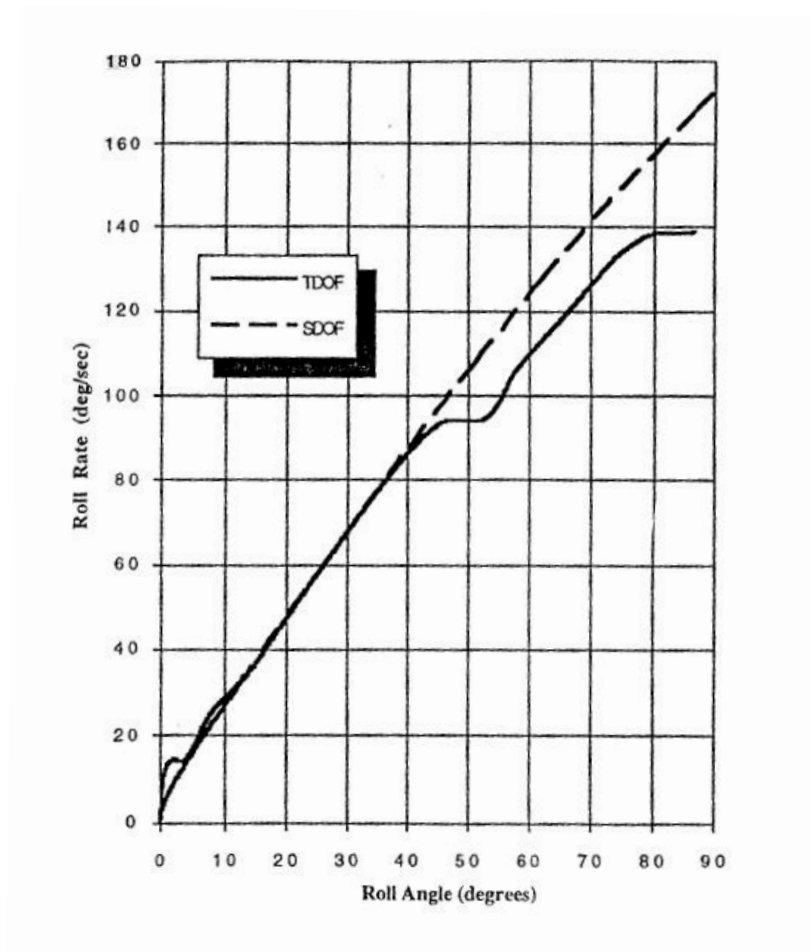


Figure 3-3 SDOF and TDOF comparison chart (Cheng et. al. 1992).

Table 3-3 Results for rollover simulation (Adapted from Cheng et al., 1992).

Rollover simulation Matrix						
Accident scenario	Roll direction Relative to driver	Restraint config	Cab style	Occupant behaviour	Forces	Conclusion
Rollover	Near	3-point	COE	Contacted side window with head at 340ms At ground impact occupant body moved laterally, impacting door and window at Lateral excursion of head = 13 inches Forward excursion of head = 5 inches Peak vertical movement = 6 inches up	Peak 3ms chest acc. = 44.8 g's Head impact on side roof rails = 2000 lbs HIC = 1172 lbs Peak shoulder belt force = 150lbs Max Lap belt force = 407 lbs	The inboard ICP Load higher than outboard ICP load Outboard tether belt load higher than inboard tether load
			Conventional	No significant difference from COE. Main impact occurred between head and side roof		Cab style had no significant influence on occupant dynamics. The peak responses slightly lower than COE Rollover.
Rollover	Near	Lap only	COE	Same as 3-point restraint for COE		Due to extensive occupant interaction with door, resulting in Peak responses slightly lower than COE rollover
Rollover	Far	Unrestrained	COE	Initially occupant driver leaned to his right At		Clearly unrestrained proved more catastrophic. The maximum
			Conventional	During initial rollover phase: occupant Rollover phase: Occupant remained on floor. Upon ground impact: occupant impacted		Different results from COE due to the absence of engine tunnel.
Rollover with subsequent collision	Near	3-point	COE	Occupant moved fwd and up. Effective in limiting occupant excursion, also prevented significant impacts	Max shoulder belt load = 1113 lbs Max tether belt load = 927 lbs Peak ICP load = 665lbs Head contact with side rail during Collision head impact with roof = 18lbs max fwd movement of head = 12 inches	The restraint was effective in limiting the occupant excursion preventing any significant impacts during collision.
			Conventional	Similar to COE 3 POINT case	Peak head to roof = 176lbs Peak shoulder belt load = 1056lbs	
Rollover with subsequent collision	Far	Lap only	COE	Occupant leaned to right, on ground impact, occupant moved vertical and lateral within the cab, head impacting roof. Subsequent collision, moved forward and struck head with roof header near vehicle centerline	HIC = 281lbs Head to roof peak contact force = 1929lbs Peak neck loading = 1300lbs Peak lap belt load = 904lbs (HIGHEST) Peak tether belt load = 803lbs	Lap belt was effective in reducing lateral excursion
			Conventional	Initial rollover, occupant leaned to right. Prior to ground impact, occupant leaned to left, head nearly in contact with driver side roof rail. Ground impact caused occupant project upward and lateral into the roof. Collision, occupant moved fwd and upward striking head to roof, head then slid beneath header, fwd movement into the center console.	Head to roof contact = 1427lbs Peak lap belt force = 1352lbs (50% Higher) Peak IPC = 664lbs Peak tether belt load = 1029lbs	Lap belt is effective in reducing lateral excursion It is not effective in preventing damage due to longitudinal excursion Low lap belt force due to additional lateral support to pelvis by engine tunnel Larger lateral excursion overcame the geometric adv of outboard in far side rollovers.
Rollover with subsequent collision	Near	Unrestrained	COE	Similar to restrained COE. Subsequent collision, occupant moves forward and upward within the cab striking head to roof header.	Peak Head to roof impact force = 1673lbs	
			Conventional	Similar to COE.	Peak head to roof impact force = 1188lbs	

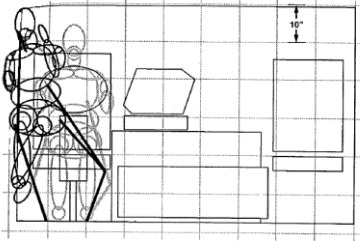
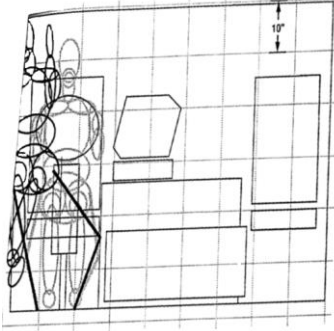
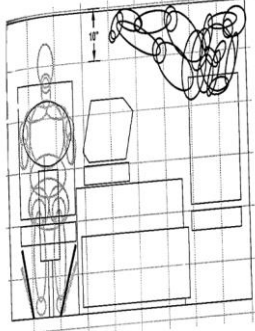
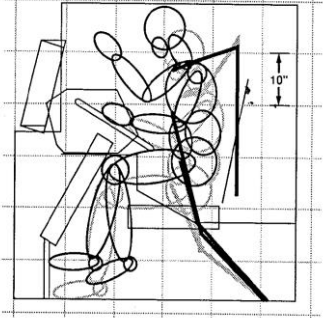
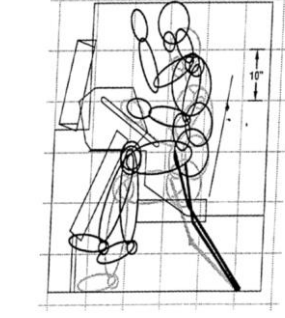
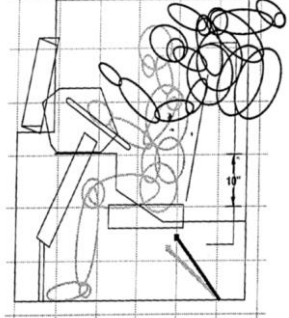
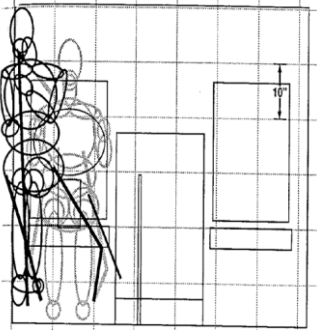
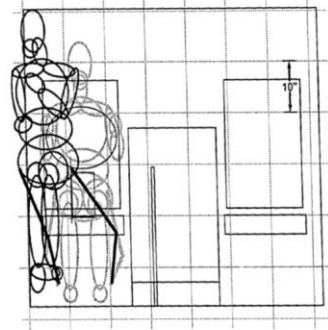
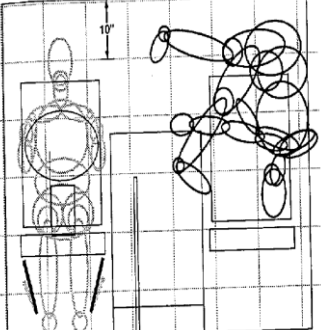
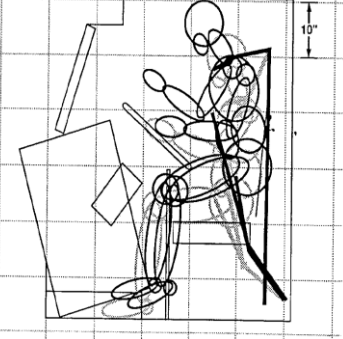
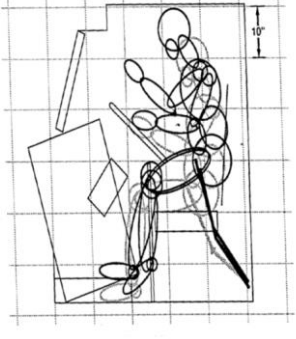
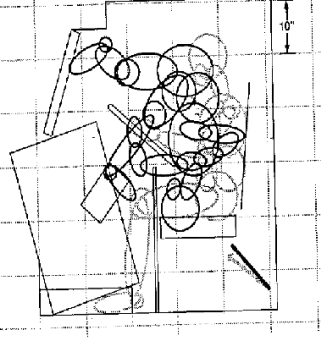
3.1.6 Rollover simulation and restraint systems

In far side rollovers, the use of restraints reduced the lateral excursion but was not very effective in controlling vertical excursions. In near side rollovers, the shoulder belt played a minimum role as it experienced very low loads. In subsequent collision rollover cases, the 3 point restraint system proved effective in reducing injuries due to forward excursions, but only the use of a lap belt was not effective in doing so. Higher loads on shoulders, lap, and tether belt were experienced in the case of subsequent collision after rollover.

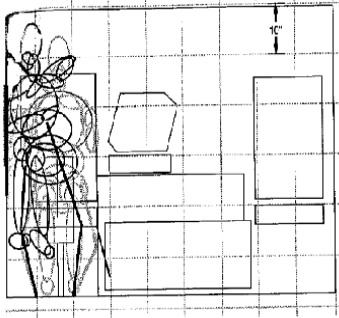
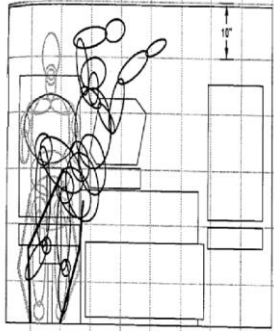

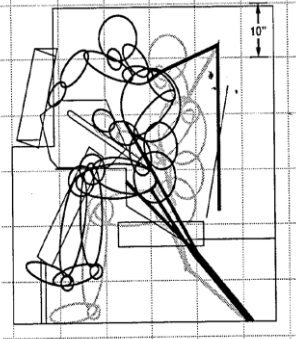
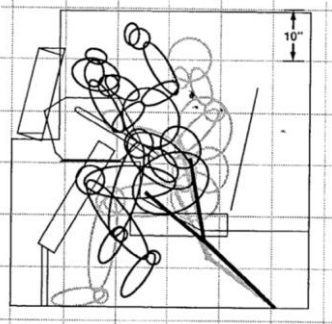

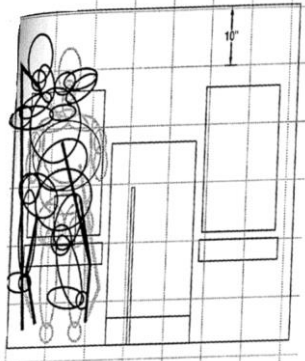
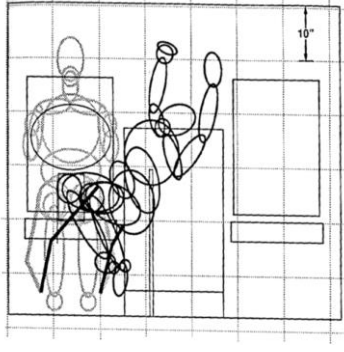
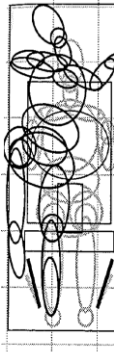
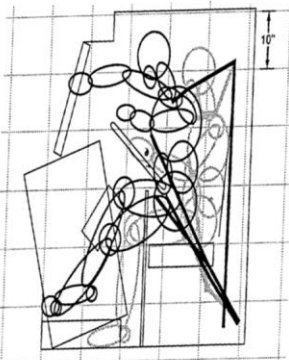
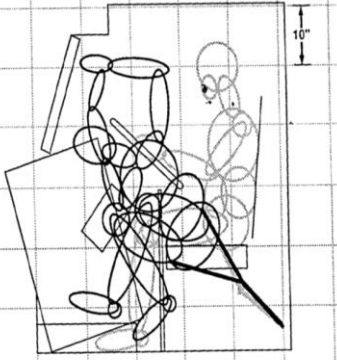

In near side rollovers, the COE and conventional cabs did not exhibit significantly different responses. In far side rollovers, especially in unrestrained case, the engine tunnel played an important role in distinguishing the responses. The absence of the engine tunnel resulted in 50% increase in maximum lap belt load.

In all simulations, the most common and significant injuries were head impacts with roof, roof header, and side roof rail. The most damaging of all appeared to be the cases of far side rollovers (unrestrained rollovers and lap belted rollovers with subsequent collisions). Use of shoulder belts proved to be beneficial in reducing head impact with roof header. In all the scenarios, high neck load of over 1,000 lbs was observed. Femur loads were generally low, except for in the case of a far side unrestrained simulation, where it exceeded 1,000 lbs, resulting from the knee impacting the roof. Table 3-4 and Table 3-5 summarize the motion experienced by the occupant during rollover and frontal impact scenarios, respectively. Three different occupant restraint conditions were considered (unrestrained, lap-belt, and 3-point belt).

**Table 3-4 Occupant motion details during rollover crash scenario according to different restraint conditions
(Adapted from Cheng et. al. 1992).**

Vehicle	Restraint	3-point	Lap belt	Unrestrained
COE	Rear view			
	Side view			
CONVENTION	Rear view			
	Side view			

**Table 3-5 Occupant motion details during frontal crash scenario according to different restraint conditions
(Adapted from Cheng et. al. 1992).**

Vehicle	Restraint	3-point	Lap belt	Unrestrained
COE	Rear view			
	Side view			
CONVENTION	Rear view			
	Side view			

3.1.7 History and overview of the crash test dummy

Crash test dummies in today's industrial society have had great significance in providing crucial information about the effects of vehicle impacts on the human body. Previous methods used to record data of simulated vehicle impacts have not been as effective. Mary Ward, who was the first recorded victim of an automobile crash in 1869, was only the first reminder of millions to come of how necessary it was to develop ergonomics research. When the number of fatalities for every 100 million vehicles had reached 15.6 in the 1930s, auto designers finally began to worry about how the rigidly manufactured vehicles at the time were transferring all of the impact force from accidents onto the drivers.

Researchers at Wayne State University were the first to study the effects of collisions on the body, with human cadavers being the first test subjects. The cadavers were often fitted with accelerometers and observed in high-impact collisions. Although human cadaver research saved thousands of lives annually, they were unreliable in terms of representing a wide demographic, because older white males were typically used, and certain parts of the body could be tested only once. Some researchers volunteered themselves to serve as crash test dummies and animal testing was used as a method to study survivability of accidents—a factor that could not be tested by cadavers. However, these methods were viewed as unethical and received much protest, and it was difficult to instrument the animals.

Data collected from cadaver and animal testing was used by Alderson Research Labs (ARL) and Sierra Engineering Company to create the first engineering dummy, "Sierra Sam" for aviation testing in 1949. This was a 95th percentile dummy, meaning that it modeled the 95th percentile of human males in height, width, and proportion. A subsequent 5th percentile female dummy was also produced. When General Motors and Ford requested a dummy, ARL and Sierra Engineering built two different competing models. GM, dissatisfied with both, combined the best characteristics of each to create a new dummy called Hybrid I in 1971. This was a 50th percentile male dummy, meaning that it represented the average male. A dummy with improvements in the shoulders, spine, and knees called Hybrid II was developed in 1972. The following year, Hybrid II 50th percentile dummy was introduced. The National Highway Traffic Safety Administration contracted with GM to improve a number of its features. A major setback to Hybrid I and II was that they could only be used to test the effectiveness of seat belt designs. GM researchers developed the current line of crash test dummies, Hybrid III, primarily to explore other areas of injury reduction.

The 50th percentile Hybrid III was introduced in 1976. He is 175 cm tall and has a mass of 77 kg. He is used to in frontal crash testing in the driver's seat. His family was soon expanded to include a 95th percentile male, a 5th percentile female, and three child dummies. Child dummies are an important recent addition as not much data is available on effects of vehicle accidents on children. The testing procedure for the Hybrid III dummies involve calibration, including calibrating the head, neck, and knees separately before a crash test. Calibration marks on the

dummy are used to aid researchers who review footage after a test. Between 30,000 and 35,000 data points can be collected through up to 58 data channels placed between the dummy's head and ankle. This data is downloaded and reviewed on the computer. One dummy can be tested multiple times and parts are replaceable. Since Hybrid III's main purpose is to assess effects of frontal impacts, other dummies, including the side impact dummy (measures rib, spine, and internal organ effects in side collisions), BioRID (observes rear impact effects), CRABI (measures effectiveness of child restraint devices), and THOR (advanced 50th percentile male dummy) were other dummies designed to study the effects of other types of impact.

In addition to real life dummies, the use of computer finite element models of humans and crash test dummies for high acceleration and impact biomechanics studies has proven valuable in studying the impacts of human injury. Specifically, combining computer modeled human elements and crash dummies increases the accuracy of predicting human response in high acceleration impacts. Substituting human elements on a finite element model of the Hybrid III dummy is validated by replicating tests of the human cadaver version of the element. Once validity is assured, the computer model can be used to predict a specific function of the element. Livermore Software Technology Corporation develops free or low cost finite element models and crash test dummies that come with sensors that measure forces, moments, displacements, and accelerations. They have many Hybrid III models. The Hybrid III 50th percentile male is a joint development with the National Crash Analysis Center at George Washington University.

Crash test dummies and computer models have greatly helped efforts to minimize injury. With the rise of automated vehicles in the use of transportation, there has been a greater push to develop protective systems. Crash test dummies, or anthropomorphic test devices, are now the most commonly used subjects to test protective systems. They have been proven to be close substitutes for humans, are more readily available than humans and animals, and therefore have the potential to make a greater impact in a faster and more reliable way.

Table 3-6 gives a detailed description of the evolution of dummy models.

Table 3-6 Evolution of dummies.






<p>Need for Change</p> 	<ul style="list-style-type: none"> • 1869: Mary Ward – first recorded victim of automobile crash • 1930s: Number of fatalities for every 100 million vehicles reached 15.6; Researchers at Wayne State University begin to study effects of collisions on the body
<p>Initial Methods</p> 	<ol style="list-style-type: none"> 1) Human cadaver testing Limitations: Represented narrow demographic by using mostly old white males; parts of the body could only be tested once; unethical 2) Animal testing Limitations: Unethical; difficulty in employing instrumentation 3) Volunteer Testing – Researchers volunteered themselves to serve as crash test dummies
<p>Introduction of Crash Test Dummies</p> 	<ul style="list-style-type: none"> • 1949: “Sierra Sam”—First engineering dummy created by Alderson Research Labs (ARL) and Sierra Engineering; Was a “95th percentile” male dummy; 5th percentile female dummy also created • 1971: Hybrid I created—GM combines two models from Sierra Engineering and ARL to create a 50th percentile male dummy • 1972: Hybrid II—improvements in shoulders, spine, and knees • 1973: Hybrid II 50th percentile dummy • Limitations of Hybrid I & II: Can only be used to test the effectiveness of seat belt designs

Table 3-6 Evolution of dummies (Continued).

<p>Current line of Hybrid III</p> 	<ul style="list-style-type: none"> • 1976: 50th percentile Hybrid III—175 cm tall, 77 kg; Used in frontal crash testing; family expanded to include 95th percentile male, 5th percentile female, and three child dummies • Livermore Software Technology Corporation’s Hybrid III 50th percentile—a joint development with the National Crash Analysis Center at George Washington University. • Dummies created to study effects of other impacts: side impact dummy, BioRID (rear impact), CRABI (child restraint device impact), and THOR (advanced 50th percentile male dummy)
<p>Computer Modeling</p> 	<ul style="list-style-type: none"> • Computer finite element models used for high acceleration and impact biomechanics studies • Can model elements of the human body to be tested independently or with crash test dummies • Process is validated by replicating tests of the human cadaver element

In this study, a Hybrid III 50th percentile dummy was used as the most representative dummy for occupants. To determine acceleration results of the dummy, several accelerometers were placed throughout the dummy in different body regions. The different accelerometers were placed in the head, chest, left and right femur and left and right tibia. Figure 3-4 illustrates the different locations of the dummy accelerometers.

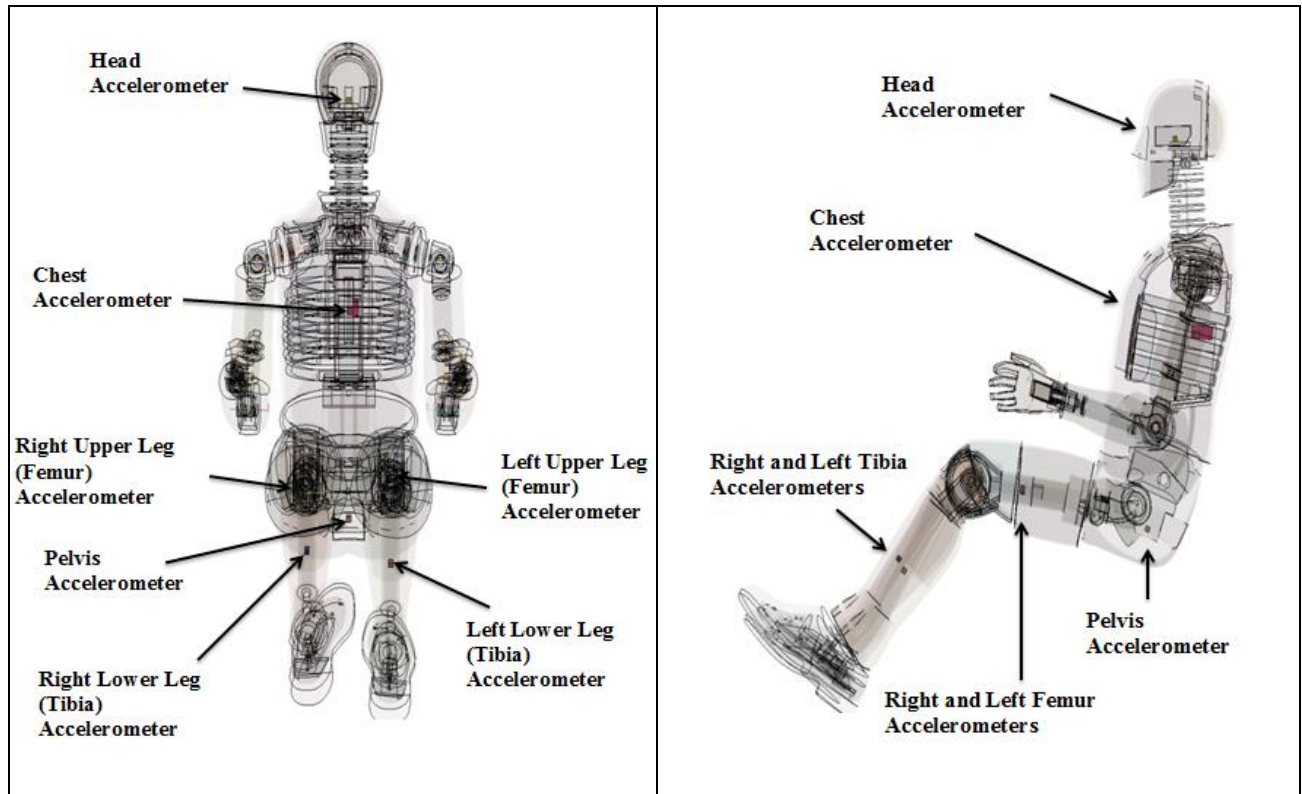


Figure 3-4 Front and side view of transparent dummy with accelerometers.

3.1.8 Injury criteria

Another critical aspect of this study is the validation of injury criteria. Injury criteria have been developed to address responses of dummies in terms of risk to life or injury to a living human. Several tests have previously been performed to analyze probabilities of injuries for the occupant in specific regions of the body. Many of these probabilities are determined based off of known accelerations of the dummy. The probability of injury is generally classified within the Abbreviated Injury Scale (AIS). This scale was created by the Association for the Advancement of Automotive Medicine (AAAM) and is used to classify and describe the severity of individual injuries. Below is a summary of injury criteria from previous tests for the different body regions of the dummy. A Hybrid III 50th percentile dummy was used in all the previous tests.

A study conducted by Eppinger et al. (1999) on developing improved injury criteria summarized equations for each injury criteria, all of which are further discussed in this section.

3.1.8.1 Head injury criteria

NHTSA performed injury analysis for frontal crashes to update frontal crash protection safety standards to improve protection of occupants. NHTSA regulations specify a head injury criterion (HIC), which is determined based on the acceleration of the head during the crash. These values were determined from tests where acceleration pulses were applied to the dummy.

Further head injury risk analysis was performed to determine the probability of skull fracture for injury severity greater than or equal to AIS 2. Along with head injury criteria NHTSA developed injury criteria for the neck. Injury criteria for the neck were developed based on tolerance limits for axial loads and bending moments. A standard 6-axis upper neck load cell records the values for axial loads and moments in all three directions. An injury risk curve was developed to determine the probability of injury based of the neck injury criteria. Table 3-7 further summarizes these injury criteria, equations, and parameters.

Table 3-7 Injury criteria summary for the head.

Injury Criteria	Equation	Parameters
Head Injury Criterion (HIC)	$HIC = \max \left[\left[\frac{\int_{t_2}^{t_1} a(t) dt}{t_2 - t_1} \right]^{2.5} (t_2 - t_1) \right]$	a(t) is resultant linear acceleration time of center of gravity of the head.
Probability of Skull Fracture (AIS \geq 2)	$p(fracture) = N \left(\frac{\ln(HIC) - \mu}{\sigma} \right)$	μ and σ are statistical parameters of an HIC injury risk curve.
Neck Injury Criteria	$N_{ij} = \frac{F_z}{F_{int}} + \frac{M_y}{M_{int}}$	<ul style="list-style-type: none"> - F_z is the axial load - F_{int} is the corresponding intercept value of load used for normalization - M_y is the flexion/extension bending moment - M_{int} is the corresponding intercept value used for normalization
Probability of Neck Injury	$p(AIS \geq 2) = \frac{1}{1 + e^{2.054 - 1.195N_{ij}}}$	N_{ij} is corresponding resultant neck injury criteria

3.1.8.2 Thoracic injury criteria

Seventy-one frontal impact sled tests were examined and analyzed to determine thoracic injury criteria for the dummy. Injury risk curves were developed to analyze the risk of injury based on the maximum chest deflection, spinal acceleration, and combined thoracic injury criteria. The probability of thoracic injury was determined for AIS injuries greater than or equal to 2. Table 3-8 summarizes the injury criteria and probability of injury for the thorax.

Table 3-8 Injury criteria summary for the thorax.

Injury Criteria	Equation	Parameters
Probability of thoracic injury	$p(AIS \geq 2) = \frac{1}{1 + e^{(1.8706 - 0.04439D_{max})}}$ $p(AIS \geq 2) = \frac{1}{1 + e^{(1.2324 - 0.0576Ac)}}$ $p(AIS \geq 2) = \frac{1}{1 + e^{(4.847 - 6.036CTI)}}$	- Dmax is maximum chest deflection - Ac is spinal acceleration - CTI is the resultant combined thoracic injury
Combined Thoracic Injury Criteria (CTI)	$CTI = \frac{A_{max}}{A_{int}} + \frac{D_{max}}{D_{int}}$	-A is value of spinal acceleration -D is value of dummy deflection.

3.1.8.3 Leg injury criteria

Analysis of the National Automotive Sampling System/ Crashworthiness Data System was conducted during the years 1993 to 1999 to determine the risk of injury to different regions of the body in frontal crashes. Specifically lower extremity injuries were analyzed due to being the most frequent AIS2+ injured body region for occupants in airbag equipped vehicles. Lower extremity injury criteria was determined for different regions of the lower body including, knee-thigh-hip complex fractures, knee ligament tears, tibial plateau/condyle fractures, tibia/ fibula shaft fractures, calcaneus, ankle and midfoot fractures, malleolar ligament, and ankle injuries. A summary for probability of injury to the different regions of the lower body can be seen in Table 3-9.

Table 3-9 Injury criteria summary for the leg.

Injury Criteria	Equation	Parameters
Probability of KTH injury	$p(AIS 2+) = \frac{1}{1 + e^{(5.7949 - 0.5196F)}}$ $p(AIS 3+) = \frac{1}{1 + e^{4.9795 - 0.326F}}$	F is femur axial force

Probability of Knee Ligament Injuries	$p(AIS 2+) = \frac{1}{1 + e^{(0.5204 - 0.8189F + 0.0686m)}}$	-F is upper tibia axial force - m is mass of subject
Injury Criteria for Tibia and Fibula Shaft Fractures	$TI = \frac{F}{F_c} + \frac{M}{M_c} < 1$	-F is measured compressive axial force - M is measured bending moment in the leg -M _c and F _c are critical values of bending moment and axial compressive force in tibia.
Probability of leg fracture versus Revised Tibia Index (RTI)	$p(AIS 2+) = 1 - \exp\left(-e^{\frac{\ln(RTI) - 0.2728}{0.2468}}\right)$ <p>where, $RTI = \frac{M}{240} + \frac{F}{12}$</p>	-F is measured compressive axial force - M is measured bending moment in the leg
Probability of Foot Injury	$p(AIS 2+) = \frac{1}{1 + e^{4.572 - 0.670F}}$	F is lower tibia axial force
Probability of ankle ligament and malleolar injury	$p(AIS 2+) = \frac{1}{1 + e^{6.535 - 0.1085M}}$	M is ankle joint moment due to dorsiflexion

3.1.9 Restraint systems

The development of restraint systems in recent history have been an important advocate in reducing the potential for serious injuries from automobile crash incidents. The following will include an overview of common seat-belt restraint systems including two- to six-point systems, belt-in-seats, and the process used to develop our restraint system.

Two-point belts that attach at two endpoints include lap belts and sashes. The lap belt was introduced in 1957 by Colonel John Paul Stapp. The primary purpose of the lap belt was to prevent occupants from crashing into the car interior since they moved with the car during a crash incident. Serious injury caused by crashing into the car's interior was an imminent problem for unrestrained occupants. The lap belt was a band that wrapped tightly around the occupant's pelvis and ran down to the floor where it was bolted down by screws. Lap belts were only successful in restraining occupants from crashing into the car's interior in large vehicles, as the

distance to the interior was larger than in smaller vehicles. Lap belts are now only primarily used in older cars. Sashes go over the shoulder and are buckled by the lap. Sashes are used in conjunction with lap belts. Otherwise, the occupant would slip out of the belt, resulting in a frontal collision.

To combat the issue unresolved by lap belts, Aldman proposed a combined lap and chest restraint, called the 3-point safety belt. Bohlin was credited with the first patent of this kind in 1958. Similar to the lap-and-sash belt, the 3-point belt spreads the impact of an accident over the chest, pelvis, and shoulders. Unlike the lap-and-sash belt, it operates as one function. The Belt-in-Seat is a special type of three-point belt where the shoulder belt is not attached to the vehicle but the seat itself. They are now mostly used in cars like convertibles where the occupants can choose to ride “open” allowing for no place to mount the upper part of the shoulder belt.

A 4-point belt involves two shoulder belts and the 5-point belt includes a belt between the legs. A 6-point belt has two lap belts between the legs. The 5-point belts are mostly used in child safety seats and racing cars. Due to the high number of restraint points, belts over 3-points can cause paralysis among other serious injuries in vehicle rollovers for vehicles not meant for that belt or in vehicles where rollover has a high chance of causing roof collapse.

To reduce the injuries that may occur as a result of the belt, some belts have force-limiting arrangements built into them, which limit the tensile force of the belt by the strength of a belt's seams. Other protective methods include the belt-pretensioner which tightens the belt earlier in the crash process. This reduces the slack that a normal belt allows and prevents the occupant from sliding forward considerably due to slack in the belt at the time of an event.

Our restraint system focuses on using a 3-point seat belt in the reduction of serious injuries in heavy truck crash incidents. Our focus is on using a finite element analysis model. Previous full-scale experiments completed using an FE model with integrated safety belts and Hybrid-III crash test dummies were studied. An FE-simulation based optimization of an adaptive restraint system was considered against multiple-crash load cases using LS-OPT. The parameters of crashworthiness being optimized include seat belt trigger time, seatbelt force level, and airbag response time, among others.

Specific to rollover crashes, simulations were performed by optimizing a modeled seatbelt to improve prevention from head excursion. Seven factors were analyzed to observe their effects on occupants' vertical head excursion in rollovers. These include lap belt angle, D-ring position, pretension force, type of latch plate, initial slack length, coefficient of friction between occupant and seat, and clearance between seatback and occupant. The physical properties and dummy response of the seat structure and belt were studied with FE frontal crash simulations. Responses measured include lap and torso belt force, chest deflection, neck and head, and ride-down efficiency. The option of a seat-integrated safety built was also considered, and MADYMO (a

mathematical model) was used to evaluate the effectiveness of design changes of this system during a frontal impact.

Table 3-10 Different types of restraint systems.

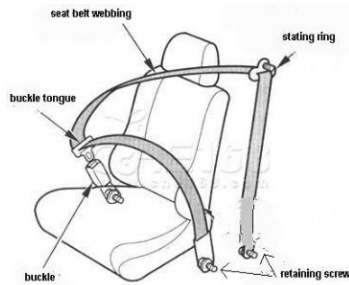
Lap Belt



Lap and Shoulder Belt



3-Point Belt



Belt-in-Seat



4-Point Belt



5-Point Belt



3.1.10 Crash scenario

Previous tests have been performed for tractor-trailer crashes to analyze injury criteria. Two different scenarios have been determined as appropriate crash scenarios for heavy vehicles which include a frontal crash and a rollover crash. An SAE paper on tractor-trailer rollover crash test by James Chinni et al. (2007) provides recommendations for test procedures to conduct simulated dynamic rollover restraint system tests for heavy vehicle applications. For the test dummy a Hybrid-III 50th percentile male is recommended for testing. Accelerometers should be used to measure acceleration, forces, and moments at different body regions of the dummy. To simulate vehicle rollover, acceleration pulses are used and applied to the heavy vehicle over time. Angular acceleration can be analytically expressed as seen in Equation 2.6. Furthermore, Figure 3-5 represents a typical plot of angular acceleration versus time.

$$\alpha(t) = \frac{1}{2}\alpha_p \left(1 - \cos\left(\frac{2\pi}{T}t\right)\right) \quad (2.6)$$

where: $\alpha_p = 6875 \text{ degrees/s}^2$
 $T = 0.05 \text{ s}$

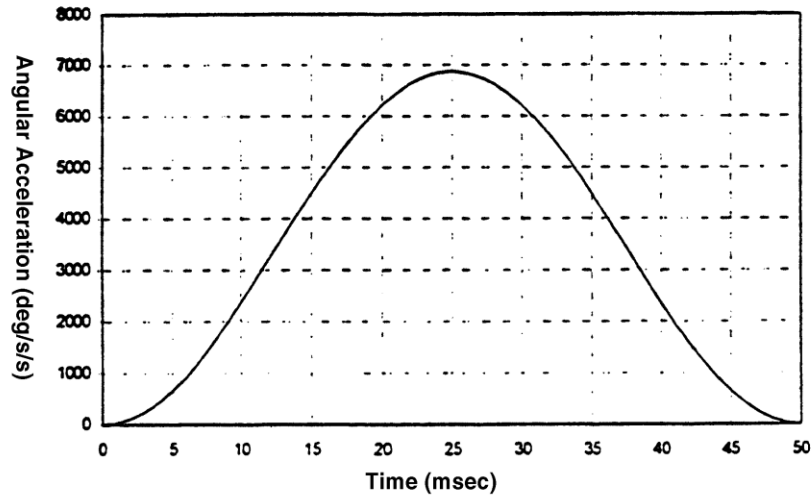


Figure 3-5 Crash pulse deceleration plot (Cheng et. al. 1992).

Since the previous studies have a limitation of being unable to include pre-deceleration roll history data (i.e., it does not account for forward velocity of the model), in this study, a simulation software, TruckSim, is used to simulate the possible maneuver of the trailer-tractor model.

Previous testing of a tractor-trailer rollover test was performed by IMMI. The tractor-trailer was driven by a remote control and overturned onto its driver's side during an overcorrecting maneuver at 40 mph. This test was conducted to observe the vehicle dynamics of a rollover and assess occupant protection during the rollover crash. The overcorrecting maneuver, which involves a truck departing the roadway and overturning while maneuvering back onto the roadway, was determined to be the most representative case of heavy vehicle rollover crashes based on real world crash data. By selecting this most representative case, it was determined that the tractor-trailer vehicle would make an evasive maneuver to the left followed by an overcorrecting maneuver to the right. The occupant safety system included a suspension seat system, and a seat-mounted rollover airbag. TruckSim modeling software was used to simulate the rollover crash of a tractor-trailer model. The resulting behavior of the tractor-trailer from the

simulation was compared to the behavior of the tractor-trailer in the real crash test. Results from the test show that the occupant was successfully protected throughout the test. The recorded injury criteria were well below reference values showing favorable results for occupants in this type of rollover event.

4. Method to estimate residual crash population

This section describes the process used to develop estimates of the crash populations that would be affected by the ACATs, potential reduction in those crashes, and the residual set of crashes after full deployment. In broad view, the process consisted of the following steps:

1. Identify the most sound evaluations of the effectiveness of ACATs in the literature.
2. Determine the crash types and conditions under which each technology will be effective.
3. Extract effectiveness estimates from the literature for each technology. This includes the specific crash types, environmental conditions, and driver conditions that could influence the effectiveness of the ACATs.
4. Using national crash databases, identify the set of crashes and circumstances to which each ACAT is applicable.
5. Apply the effectiveness estimates to the crash population, adjusting for the current penetration of the technologies into the truck fleet.
6. Assess the remaining crashes in terms of driver injury and the types of crashes.

A variety of resources were used to identify evaluations of ACATs for heavy trucks. These included Google Scholar, SCOPUS, TRID, as well as the UMTRI Library. Google Scholar is a search service provided by Google to search for scholarly literature across a broad range of resources, including scientific journals, court documents, and many other sources². Scopus provides a citation database of literature from scientific journals, conference proceedings, and research reports³. TRID is an integrated database that provides access to the Transportation Research Board (TRB) Transportation Research Information Services (TRIS) database of research reports and journal articles on all aspects of transportation⁴. The UMTRI library, through the University of Michigan Mirlyn service, provides access to an extensive collection of literature on traffic safety⁵. Of course, there is significant overlap across these resources, but this diverse set of databases ensured a comprehensive survey.

Searches were conducted for literature on active safety for trucks. The specific technologies were ESC, RSC, FCW, LDW, and CMB. General searches for evaluations of active safety were conducted, including different aspects of active safety as well as particular systems. For example, search terms included “driver assistance,” “collision avoidance,” “autonomous braking,” “AEB,”

² <http://scholar.google.com/>

³ <http://www.scopus.com/>.

⁴ <http://trid.trb.org/>

⁵ <http://libguides.umtri.umich.edu/drc>

“autonomous emergency braking,” “collision imminent braking,” “intelligent speed adaption.” Other key search terms included “driver reaction time,” “forward collision warnings,” “kinematics models,” “potential benefits,” “rear-end collision avoidances,” “rear-end collisions,” and “system effectiveness.” In all cases, we were searching for evaluations of the effectiveness of ACATs for heavy trucks.

The search process identified approximately 45 relevant reports. Each was evaluated for usability for the current project. To be useful, the report needed certain qualities:

- The crash types addressed must be identified with sufficient specificity that they could be identified in the available crash databases. This means that the technologies had to be evaluated against specific crash types.
- The crash types had to be able to be identified in the available crash databases. They needed to be specified in a way that could be mapped to the fields in FARS and GES, specifically.
- Any limitations on the effectiveness of the technology had to be described in a way that could be applied in the national crash data files.

Beyond those requirements, there was also a hierarchy of preference used in selecting reports for use. The evaluations employed diverse methodologies; preference was given to those most realistically tied to actual operations. Reports based on engineering evaluation, track testing, simulation, and field operational tests (FOTs), were given preference. Evaluating the technologies in general deployment is not currently possible. First, because the penetration of the ACATs into the general truck population is at an early stage (see section 4.1 for information on current penetration rates). Secondly, even if there was widespread use of the ACATs, none of the available crash databases has any information on whether trucks in crashes have the technologies. There were some useful reports that included analysis of the experience of specific fleets that had deployed one or more technologies and these were used where possible.

Accordingly, for each technology, the most useful reports were identified. Then, for each report and each technology, the target crash population was specified, along with any factors that would reduce the effectiveness, and algorithms developed to identify the crash types in the crash population. Effectiveness estimates were extracted from the reports, and applied to the crash population to produce an estimate of the remaining population. This process is discussed below in more detail with respect to each report and technology. The method of applying effectiveness estimates extracted from the reports is described in the next section.

4.1 Computation of adjusted weights to account for effectiveness.

Estimates of the effectiveness of the technologies were applied to the crash population by adjusting case weights, to produce new estimates of the affected crash populations. The method

accounts for the estimated effectiveness of the technologies as well as the penetration of the technologies into the fleet represented by the crash data. This section outlines how the weight adjustments were computed.

In the crash data, each case has a case weight. The case weight is contained in a variable called WEIGHT. FARS is a census file, so the weight of each FARS case is effectively 1. GES is the product of a stratified sample of police reported crashes, so each case has a weight equal to the inverse of its probability of selection. If the probability of selection is 0.2 (meaning a 20% chance of selection), the WEIGHT variable is set to 5, and so on. These weight variables are adjusted for crashes falling into specific crash categories, to reflect the estimated effect on all crashes of that type.

The process can be illustrated by an example. Let us say that technology X is estimated to be 30% effective against crash type Y. In the crash data, an algorithm is developed to identify the current population of crash type Y. The algorithm selects all records that meet the criteria for crash type Y. The effect of technology X is to reduce that population by 30%. To apply the technology effectiveness estimates for crashes meeting specific crash criteria, case weights for crash type Y are multiplied by (1-effectiveness estimate), on in this case 0.7. For FARS cases, the effectiveness case weight would be 0.7 (0.7*1). For GES cases, the effectiveness case weight would be 0.7 * WEIGHT.

$$\text{Effectiveness weight} = (1-E_{tech}) * \text{case weight} \quad \text{Eq. 1.}$$

Where E_{tech} is the estimated effectiveness of a technology for a specific crash type
Case weight is the FARS or GES case weight

A second adjustment was made to account for the penetration of several technologies into the fleet represented by the crash population. It is necessary to account for existing deployment of the technologies, so that crashes are not “prevented” twice. Some of the trucks represented in the crash population were equipped with one or more of the ACATs. Since the technologies were already on some trucks, it is assumed that, for the trucks with the technology, the crashes were representative of the population that would occur despite the technology. However, the crash data do not include information on what ACATs each vehicle was equipped with. Accordingly, it is necessary to adjust case weights to reflect existing deployment of the technology across the fleet. It is assumed that the technologies actually in deployment have the effectiveness that was estimated in the literature.

The presence of the technologies for each vehicle is not recorded in any crash data available to date. However, sales of the technologies were obtained by model year. Some of the information was obtained from official filings by the Truck & Engine Manufacturers Association, and other information was provided by a major truck manufacturer (Truck & Engine Manufacturers

Association 2012). See also Office of Regulatory Analysis and Evaluation (2012) and Belzowski, Blower et al. (2009). This information is summarized in Table 4-1.

Table 4-1 Penetration rates for roll and stability control by model year

Stability control system	Model year										
	2002	2003	2004	2005	2006	2007	2008	2009	2010	2011	2012
Roll control (RSC) *	0.1%	0.6%	3.6%	6.4%	6.9%	7.6%	12.3%	16.3%	16.7%	15.2%	17.3%
Full stability control (ESC) *	0.0%	0.0%	0.0%	0.4%	5.3%	15.5%	23.0%	21.5%	26.7%	34.4%	33.6%
Forward collision warning (FCW) †	0.0%	0.0%	0.0%	0.0%	0.0%	0.0%	0.0%	0.0%	1.0%	15.0%	24.0%
Lane departure warning (LDW) †	0.0%	0.0%	0.0%	0.0%	0.0%	0.0%	0.0%	0.0%	2.0%	0.5%	1.0%

Source: * (Truck & Engine Manufacturers Association 2012)

† Personal communication from a representative of a major truck manufacturer.

For trucks in the crash population that were already equipped, the technology-relevant crashes have already been prevented. It would not be valid to, in effect, prevent them twice. Accordingly, for model years in which the technology is deployed, a population adjustment is made so that the effectiveness of the technology is reduced in direct proportion to the penetration of the technology. If the technology was deployed 100% through the fleet, the adjustment to the crash population to reflect further deployment of the technology would be zero, because the fleet was already saturated. On the other hand, if no trucks had the technology, the adjustment would be one, allowing the full effectiveness of the technology

The adjustment for technology penetration is made to the effectiveness estimates, by model year because the penetration of the various technologies is known by model year. The case weighting factor is as follows:

$$\text{Case weight adjustment factor} = 1 - (E_{\text{crash_type}} * (1 - P_{\text{mod_year}})) \quad \text{Eq. 2.}$$

Where E_{tech} is the estimated effectiveness for a specific crash type.

$P_{\text{mod_year}}$ is the penetration proportion for a model year.

If the technology is not relevant to a crash type, effectiveness is zero and the crash weight adjustment factor goes to 1.

If penetration of the technology was complete ($P_{\text{mod_year}} = 1$), then the term $(1 - P_{\text{mod_year}})$ would equal zero and the CWAFF would be 1, meaning no effect of the technology.

The adjustment factor is then multiplied by the case weight to obtain the distribution of crashes that would remain if the technology was deployed across the entire fleet, accounting for existing deployment.

$$\text{Final case weight} = \text{CWAF} * \text{case weight} \quad \text{Eq. 3.}$$

5. Data

Crash data from the National Highway Traffic Safety Administration (NHTSA) Fatality Analysis Reporting System (FARS) and the National Automotive Sampling System General Estimates System (GES) were used to characterize the population of tractor-semitrailer traffic crashes.

FARS is a census file of all fatal motor vehicle crashes in the U.S. The data are compiled by analysts in each state and compiled by NHTSA. The state analysts code the data from police crash reports, coroner's records, driver history files, and other investigative materials. The data provide a comprehensive, though general purpose, record of all motor vehicles and persons involved in fatal crashes (NHTSA 2014). Data are collected at the crash, vehicle, and person level. The data provide, among other things, a relatively detailed identification of the vehicles involved, the environment at the scene of the crash, details about how the crashes occurred, and the injuries sustained by each person involved. Over 100 variables are coded. The fact that FARS is a census file means that it includes records on every fatal motor vehicle crash in the country. FARS provides the best and most detailed information available on fatal crashes.

The GES crash file is part of NHTSA's National Automotive Sampling System (NASS). GES is a nationally-representative sample of the estimated 6.4 million police-reported crashes that occur annually. GES is the product of a sample survey with clustering and stratification. To compile annual GES files, police reports are sampled and data are coded entirely from those sampled police reports. Case weights allow national estimates to be computed from the samples (NHTSA 2011b). Unlike FARS, GES includes all crash severities, from fatal crashes to property damage only crashes. As such, GES provides the best available data on traffic crashes of all severities in the U.S.

Three years of data were combined for this study, using data from 2010 through 2012. Multiple years of data were used to provide robust estimates of deaths and injuries. In the tables, where frequencies are provided, the numbers represent annual counts averaged over the three years 2010 to 2012.

Since 2010, the variables collected in FARS and GES have been harmonized, meaning the files use the virtually the same variables and code levels. Harmonization allows results to be easily combined. In this analysis, data from FARS and GES were combined. Because FARS is a census

file, it has the most accurate and comprehensive information on fatal crashes. GES provides the most accurate and comprehensive national data on nonfatal crashes. To combine the files to make a crash file covering both fatal and nonfatal crashes, fatal crashes were deleted from the GES data and data from FARS were substituted. Because variables from the two data systems have been harmonized, combining results was relatively straightforward.

6. How truck drivers are injured in crashes

The initial step in determining how ACATs may change how truck drivers are injured in traffic crashes is to determine how they are injured currently. A crash typology was developed to identify crash types that present the greatest risk of severe injury to truck drivers. The classification was developed from a field that captures the most harmful events (MHE) at the vehicle level, meaning for each vehicle in a crash. The MHE was the event judged to result in the most severe injury to occupants of the vehicles or the greatest damage to the vehicles when no occupant was injured (NHTSA 2011a). There is one exception, however. If the most severe injury was to a nonmotorist such as a pedestrian or bicyclist, that event was recorded as the MHE, rather than any injury to a truck occupant or damage to the truck. Other than that situation, the MHE variables captured injury to vehicle occupants.

MHE includes collision events with other vehicles, and it was considered important to determine the type of other vehicle, since an impact with another truck on its face should present less of an injury risk to a truck driver than an impact to a light vehicle. Accordingly, the general type of the other vehicle was determined. The other motor vehicles in the collisions were classified as either other trucks and buses, light vehicles (GVWR less than 10,000 lbs.), or vehicles of unknown type. In addition, fixed objects were categorized by the probability of a severe injury. Objects such as buildings, embankments, and bridge structures, which posed a higher than average probability of injury, were classified as “hard.” Fixed objects with a lower than average probability of severe injury, such as sign posts, shrubbery, and fences, were classified as “soft.”

It is important to keep in mind that other severe events may have occurred in a crash, in addition to the MHE. For example, the MHE rollover category does not capture all vehicle rollovers, just those judged to account for the most severe injury in the vehicles. If a rollover was followed by a fire and the fire was judged to be the cause of the most severe injuries, the MHE would be coded as “fire.” Rollover can be determined from a separate rollover variable.

The most dangerous crashes to tractor-semitrailer drivers were rollovers, collisions with other trucks or hard fixed objects, and fires. Table 6-1 shows the MHE crash typology developed, along with the percentage of serious injuries (fatal or A-injury) to drivers, the percentage of all involvements, and the ratio of those two percentages. Serious injury involvement ratios over 1 indicate the degree to which a crash type presented a greater injury risk than average, and ratios less than 1 indicate crashes that pose a less than average injury risk.

Table 6-1 Crash Types by Serious Driver Injury Risk

Most harmful event		Percent of serious/fatal driver injuries	Percent of all involvements	Serious injury involvement ratio
Rollover		52.4%	4.0%	13.0
Fire		5.9%	0.4%	15.9
Other non-collision		1.0%	2.1%	0.5
Collision with	Truck/bus	11.8%	8.5%	1.4
	Light vehicle	9.4%	62.6%	0.2
	Unknown motor vehicle	5.6%	5.8%	1.0
	Train	0.3%	0.2%	1.5
	Pedestrian/bicyclist/animal	0.1%	2.0%	0.1
	Other non-fixed object	0.3%	4.0%	0.1
	Hard fixed object	11.3%	3.9%	2.9
	Soft/other fixed object	1.4%	6.1%	0.2
Unknown		0.5%	0.4%	1.2
Total		100.0%	100.0%	1.0

Rollover was coded as the MHE in only 4.0% of tractor-semitrailer involvements but accounted for 52.4% of fatal and A-injuries in crashes, for a serious injury involvement ratio of 13.0, meaning that the probability of a fatal or A-injury was 13.0 times higher in rollover than overall. Collisions with trucks or buses, or with hard fixed objects also had involvement ratios over 1.0 and accounted for 11.8% and 11.3% of fatal and serious injuries, respectively. Along with MHE fire, these four crash types accounted for 81.4% of all tractor-semitrailer driver fatal and A-injuries in crashes, for an overall involvement ratio of 4.8. Collisions with light vehicles were the most common MHE (62.6%), but accounted for only 9.4% of fatal and A-injuries, for a ratio of 0.2.

As suggested above, not all rollovers were classified as the MHE for a tractor-semitrailer in a crash. MHE rollover accounted for about 88% of all rollovers, with most of the rest classified as following a collision with a hard fixed object, another truck or bus, or a light vehicle. However, when rollover as such was isolated from all other crash types, the result was the same: Rollover accounted for a clear majority of tractor-semitrailer driver fatal and A-injuries in motor vehicle crashes. (See Table 6-2.) Rollover was the primary serious injury mechanism in crashes.

Table 6-2 Driver injury by rollover

Driver injury	Rollover	No rollover	Total
Fatal/serious	59.9%	40.1%	100.0%
Other injury	34.5%	65.5%	100.0%
No injury	2.7%	97.3%	100.0%
Total	4.6%	95.4%	100.0%

The use of safety belts by the drivers did not make a significant difference in terms of the types of crashes that posed the highest risk to truck drivers. The same crash types were identified as presenting the high serious injury risk to tractor-semitrailer drivers regardless of safety belt use. Table 6-3 and Table 6-4 are restricted to tractor-semitrailer drivers that were coded as belted. Among belted tractor-semitrailer drivers, MHE rollover accounted for 50.0% of fatal/serious driver injuries, collisions with a truck or bus 15.4%, and collisions with hard fixed objects 10.0%. Table 6-4 shows that rollover accounted for 55.9% of fatal/serious injuries among belted drivers, which was almost as high as among all drivers, belted and unbelted (59.9% in Table 6-2.)

Table 6-3 Crash types by serious driver injury risk, belted drivers only

Most harmful event		Percent of fatal/serious driver injuries	Percent of all involvements	Serious injury involvement ratio
Rollover		50.0%	3.9%	12.7
Fire		2.9%	0.4%	7.5
Other non-collision		0.9%	2.1%	0.4
Collision with	Truck/bus	15.4%	8.2	1.9
	Light vehicle	12.4%	63.6	0.2
	Unknown motor vehicle	6.3%	5.6	1.1
	Train	0.1%	0.2	0.5
	Pedestrian/bicyclist/animal	0.1%	2.1	0.1
	Other non-fixed object	0.4%	3.6	0.1
	Hard fixed object	10.0%	4.0	2.5
	Soft/other fixed object	0.9%	5.9	0.2
Unknown		0.7%	0.5%	1.5
Total		100.0%	100.0%	1.0

Table 6-4 Driver injury by rollover, belted drivers only

Driver injury	Rollover	No rollover	Total
Fatal/serious	55.9%	44.1%	100.0%
Other injury	33.6%	66.4%	100.0%
No injury	2.7%	97.3%	100.0%
Total	4.5%	95.5%	100.0%

A collision with another vehicle or fixed object was the other primary crash type with an elevated injury risk for truck drivers. Impacts with other trucks and buses or with hard fixed objects were overrepresented among fatal and serious injuries to truck drivers. And among collisions, impact to the front of the truck posed the highest risk. Table 6-5 shows that frontal collisions accounted for almost 60% of fatal and serious injuries in collision events. Frontal impacts were 2.5 times as likely to produce serious injury as collisions as a whole. Right or left side impacts accounted for roughly similar percentages of serious injuries and were less likely to cause serious injuries than frontal impacts. Right and left-side impacts include both impacts to the cab, which can be severe, as well as to the area behind the cab and the trailer, which pose a much lower risk. Collisions with the rear of the tractor-semitrailer accounted for only 1.3% of fatal/serious injuries and were the least likely, obviously, to be serious.

Table 6-5 Impact location on truck in collision crashes

Impact location	Percentage of fatal/serious driver injuries	Percentage of all involvements	Serious injury involvement ratio
Front of truck	59.5%	23.5%	2.5
Right side	20.3%	28.5%	0.7
Back	1.3%	12.0%	0.1
Left side	16.7%	26.7%	0.6
Other/unknown	2.3%	9.2%	0.2
Total	100.0%	100.0%	1.0

7. Baseline crash and driver injury distributions

This section shows the baseline annual crash distribution for tractor-semitrailers, before the application of the estimated effects of crash avoidance technologies. These baseline distributions are used to illustrate the net effect of the ACATs, in terms of reductions from the current (2010-2012) situation. The crash population here was derived from the combined FARS and GES files. Clearly, there has been some penetration of some of the technologies into the fleet, so some of

the vehicles involved in crashes already were equipped with some of the technologies. Penetration of crash avoidance technologies are accounted for in estimating the net effect of complete deployment, as explained in section 4.1.

Table 7-1 shows the distribution of annual tractor-semitrailer involvements by crash type. The crash type used here is based on the MHE that occurred to the tractor-semitrailers in the crashes, and calls out the crash types that are the highest risk to truck drivers, as described in section 6. The frequencies in the table are counts of tractor-semitrailers in crashes of all severities. The types are based on the MHE in the crash; many crashes involve more than one harmful event, so, for example, the rollover category does not necessarily include all rollovers. Table 6-1 above showed that rollover and collisions with trucks or buses or hard fixed objects presented the greatest risk of serious (fatal or incapacitating) injury to tractor-semitrailer drivers. The MHE was rollover for only 4.0% of tractor-semitrailers, but those involvements accounted for almost 60% of fatal and serious injuries. In other words, MHE rollover occurred in only 4% of tractor-semitrailer traffic crashes, but in almost 60% of crashes in which the driver was killed or seriously injured. In contrast, colliding with a light vehicle (passenger car, pickup, sport utility vehicle, and so on) was the MHE in 62.6% of all involvements, but those crashes produced only 9.4% of serious injuries.

Table 7-1 Baseline, pre-technology distribution of most harmful crash types

Most harmful event		N	%
Rollover		5,023	4.0
Fire		461	0.4
Other non-collision event		2,615	2.1
Collision with	Truck/bus	10,612	8.5
	Light vehicle	78,178	62.6
	Unknown motor vehicle	7,215	5.8
	Train	247	0.2
	Pedestrian/bike/animal	2,467	2.0
	Other non-fixed object	5,047	4.0
	Hard fixed object	4,827	3.9
	Soft/other fixed object	7,642	6.1
Unknown		501	0.4
Total		124,834	100.0

Table 7-2 shows the average number of truck drivers injured in crashes, 2010-2012. This set of driver injuries is the baseline set of injuries against which the technologies are measured. The technologies are run against the crashes to estimate the effect on the crashes, including their

estimated effect on driver fatalities and injuries. Only the drivers of tractor-semitrailers are included in the table, since the focus of the study is on crash avoidance technologies deployed on tractor-semitrailers. It is clear that most crashes did not present significant injury risk to the truck occupants. Most (88.7%) tractor-semitrailer crashes did not result in any injury to the driver. On average, about 328 tractor-semitrailer drivers were fatally injured and 785 received A-injuries (incapacitating), but those two severities combined accounted for less than 1% of the drivers.

Table 7-2 Tractor-semitrailer driver injury severity

Driver injury	N	%
Fatal	328	0.3
A-injury	785	0.6
B-injury	3,147	2.5
C-injury	2,594	2.1
Injured, unknown severity	211	0.2
No injury	110,479	88.7
Other/unknown	7,012	5.6
Total	124,557	100.0

8. Effectiveness estimates on ACATs

8.1 Estimates for LDW, RSC, and FCW

Hickman, Guo, et al. (2013) estimated the effectiveness of three ACATs, based on carrier crash data. The three ACATs were LDW, RSC, and FCW. A total of 14 carriers provided crash and travel data for the evaluation. The researchers reviewed data on each crash to identify crash configurations and events potentially relevant to the different technologies. Data from the 14 carriers were combined into a single file for analysis. Among the strengths of this report is that the effectiveness estimates were based on the actual operating performance of the technologies in revenue service (Hickman, Guo et al. 2013).

LDW was defined as relevant to the following crash types:

- Run off road, in which a truck departed the road and collided with a roadside object or overturned.
- Head-on, in which a truck collided head-on with another vehicle after departing its lane.
- Same direction sideswipe, in which a truck departed its lane and sideswiped a same-direction vehicle.

- Opposite direction sideswipe, in which a truck departed its lane and sideswiped a vehicle going in the opposite direction.

FCW was defined as relevant to two crash types:

- Head-on collisions, in which a truck collided head-on with another vehicle after departing its lane (same as an LDW crash type).
- Rear-end crashes, in which a truck collided with another vehicle in front of it.

RSC was defined as relevant to first-event rollovers. These are rollovers in which the roll occurred prior to striking any other vehicle and not as the consequence of a collision.

In addition to identifying crashes to which each technology was relevant, the researchers also identified and excluded conditions where the technologies likely would not be effective.

For LDW, the technology would not be effective if the lane departure followed an avoidance maneuver; if the driver used a turn signal (which typically disables a warning); if lane markings were covered or missing; if the driver was incapacitated.

RSC would not be effective for tractor-only combinations (since RSC is trailer-based), if the driver was incapacitated, on unpaved roads, if the rollover followed a prior collision, at low speeds (<15 mph), or if the rollover was tripped.

FCW was determined to not be relevant for collisions following an avoidance maneuver, if the truck is travelling slower than 30 mph (systems not active at low speeds), if the target was stopped when it came into the sensor range, or if the driver was incapacitated.

The analysis was done at the vehicle level. For each truck in the fleets, the researchers had data on the technologies installed, the vehicle miles traveled (VMT), and crash involvement. Using these data, the researchers divided the trucks into equipped and not equipped, and computed crash rates (involvements in relevant crash types per VMT). Poisson regression was used to model crash counts. The statistical model was intended to control for potential confounding factors such as more than one ACAT on a truck. The specific statistical method employed accounted for possible “over-dispersion,” meaning a possible high degree of variability in the data. Overdispersion does not affect the point estimates of the parameters (such as effectiveness estimates for specific technologies), but can underestimate the width of the confidence intervals for the point estimates. The modeling technique used accounted for overdispersion to produce more realistic confidence intervals.

Table 8-1 shows the effectiveness estimates determined by the researchers for each technology against the crashes relevant to the technology. LDW was estimated to reduce relevant crashes relevant by 47.8%, and RSC by 35.7%. Crashes relevant to LDW include runoff road, same and

opposite direction sideswipes, and some head-on crashes. Untripped, first-event rollover was assumed to be relevant RSC. No effect was found for FCW. The estimated effect was actually -0.3%, which was not statistically different from zero, and in practice not different from zero. Only one of the carriers operated trucks with FCW; the researchers concluded that there was insufficient data to make a valid analysis of FCW.

Table 8-1 Effectiveness estimates from Hickman for LDW, RSC, and FCW

Technology	Effectiveness estimate
LDW	47.8%
RSC	35.7%
FCW	-0.3%*
* Not statistically significant (Hickman, Guo et al. 2013)	

To apply the effectiveness estimates from Hickman, Guo, et al. (2013) to the current crash population in FARS and GES, algorithms were developed to identify the crashes relevant to each technology. The descriptions in Hickman were sufficiently detailed and specific to identify the appropriate crashes in the available data, including conditions where the each technology would not be effective, such as with impaired drivers or in low speed conditions. Table 8-2 shows the crash types, annual frequency of involvement, and percentage distribution developed in the current project of the crash types addressed in Hickman as affected by the set of ACATs they analyzed. These are the crashes that can potentially be addressed by full deployment of the technologies represented in Hickman. These crash types were estimated to account for 16.5% of all tractor-semitrailer involvements.

Table 8-2 Crash types addressed by the Hickman analysis

Crash types	N	%
Run off road	2,855	2.3
Head-on	1,707	1.4
Same direction sideswipe	7,578	6.1
Rear-end striking	7,185	5.8
Rollover	1,281	1.0
All other crash types	104,229	83.5
Total	124,834	100.0

The effectiveness estimates developed in Hickman were applied to the crash population, taking into account estimated penetration of LDW, FCW, and RSC into the crash population, as described in section 4.1. Table 8-3 shows the estimated effect of the technologies on the crash population, that is, the number of crashes that could be avoided annually if the various technologies were fully deployed, along with the percentage avoided for each crash type. The crash population is categorized in terms of the MHE, to identify crash types that pose the highest risk to tractor-semitrailer drivers. The greatest effect of the ACATs addressed in the Hickman report was on rollover (15.4% reduction), collisions with hard fixed objects (11.3% reduction), and collisions with trucks or buses (5.6% reduction). Each of these crash types were identified as high risk to tractor-semitrailer drivers. Overall, however, only 5.0% of tractor-semitrailer crash involvements were estimated to be saved.

Table 8-3 Reduction in crash involvements estimated from Hickman

Most harmful event		Number reduced	Percent reduced
Rollover		775	15.4
Fire		19	4.1
Other non-collision event		10	0.4
Collision with	Truck/bus	593	5.6
	Light vehicle	3,744	4.8
	Unknown motor vehicle	144	2.0
	Train	0	0.0
	Pedestrian/bike/animal	3	0.1
	Other non-fixed object	0	0.0
	Hard fixed object	544	11.3
	Soft/other fixed object	348	4.6
Unknown		56	11.1
Total		6,237	5.0

Table 8-4 shows the estimated effect of full deployment of the technologies on tractor-semitrailer driver injury. Interestingly, the most severe driver injuries are estimated to show the greatest percentage reduction. It is estimated that deployment would result in saving 64 driver fatalities annually and 110 A-injuries, reducing the incidence for tractor-semitrailer drivers by 19.4% and 14.1% respectively.

Table 8-4 Reduction in driver injuries, based on Hickman

Driver injury	Number reduced	Percent reduced
Fatal	64	19.4
A-injury	110	14.1
B-injury	368	11.7
C-injury	95	3.7
Injured, unknown severity	9	4.2
All injuries	647	9.2

Most of the reduction in fatalities was attributed to the reduction in rollovers and collisions with hard fixed objects. The reduction in these events in turn were attributed to the reduction in run off road crashes, which resulted in either a subsequent rollover or a collision with a hard fixed object. Thus, a secondary effect of the technology aimed at lane departure was to reduce high risk events that occurred after the lane departure: off-road rollover and impacts on unyielding fixed objects like bridge abutments.

8.2 Estimates for FCW and ACC

McMillan, et al. (2007) tested three technologies in an FOT. The technologies were collision warning system (CWS), ACC, and advanced braking system (AdBS). CWS used sensors to detect conflicts in front of the truck and issued visual and audible warnings to the driver. The system basically was designed against rear-end crashes in which the truck was the striking vehicle, so crashes in which the other vehicle was in lane in front of the truck. (CWS was the term used in the report; it is fundamentally similar to FCW in this report.) The ACC maintained a driver-selected fixed distance between the truck and vehicles in lane in front of the truck. If there was no vehicle in front of the trucks, the ACC system would maintain a driver-selected speed. AdBS used disc brakes and an electronically-actuated braking system to enhance the trucks braking and shorten stopping distances. Disc brakes can supply more stopping power than conventional drum brakes, and electronically-controlled brakes are not subject to the latency of air brakes, which can take up to a second to develop full braking power.

The systems were evaluated by means of a field operational test (FOT). The FOT consisted of 50 trucks equipped with the safety systems and 50 trucks that served as a control group. Within the control group, half operated with none of the safety systems for the first 18 months and only CWS for the remaining period. The other set of control trucks had CWS in operation for the entire test. The test lasted for approximately two years.

The effectiveness of the systems was estimated in terms of conflicts avoided or reduced. Because crashes are rare and the FOT was limited in terms of number of trucks and duration, there could not be enough crashes to measure changes using actual crashes. Instead, a set of safety critical forward conflict situations was defined in terms of time to collision (TTC) and deceleration rates to avoid a collision. Short TTC (0.5s) and high deceleration (0.4g) were defined as aggressive; longer TTC (1.5s) and lower deceleration rates (0.2g) to avoid were considered as conservative.

The systems tested were all designed to reduce the number and severity of forward collisions, specifically rear-end truck striking crashes. Three crash situations were evaluated: lead vehicle (LV) at a constant speed, LV slowing, and LV change lanes in front of the truck. Specific crash definitions were supplied in Appendix B of the report, which was adapted to estimate the population of relevant crashes in the FARS and GES datasets used for this report. Table 8-5 shows estimates of the annual number of crashes relevant to the technologies tested in McMillan, et al., by specific crash type. Taken together, about 8.8% of tractor-semitrailer crash involvements were considered relevant to the technologies. LV slower/stopped (i.e., constant speed) was the most numerous, with about 6,500 involvements annually, and 3.2% of all fatal and A-injuries to tractor-semitrailer drivers. LV slowing accounted for only about 4,100 (3.3%), and LV change lanes only about 400 (0.3%). Taken together, these crash types pose a lower risk of fatal or serious injury to truck drivers, except when the lead vehicle is another truck or if the collision results in a rollover.

Table 8-5 Crash types addressed in Volvo FOT

Crash type	Number of involvements	% of involvements	% of serious (K+A) driver injuries
LV slower/stopped	6,481	5.2	3.2
LV slowing	4,091	3.3	3.4
LV change lanes	405	0.3	0.1
All else	113,857	91.2	93.4
Total	124,834	100.0	100.0

Table 8-6 shows the effectiveness estimates used in recomputing the crash population, based on full deployment of the technologies (McMillan et al. 2007). McMillan, et al., provided estimates based on aggressive, conservative, and moderate assumptions. For the purposes of re-estimating the crash population, we chose effectiveness ratios based on moderate assumptions. The table shows effectiveness estimates for three forward crash types and three combinations of forward collision avoidance technologies: CWS only, ACC only, and CWS+ACC. (AdBS was paired with ACC in the test.) For each forward crash type, the combination of CWS+ACC was most

effective. The effectiveness of CWS+ACC is less than the sum of CWS and ACC alone because there is some overlap of crashes avoided.

Table 8-6 Effectiveness estimates for CWS and ACC, Volvo FOT

Crash type	Effectiveness estimates by technology		
	CWS	ACC	CWS+ACC
LV slower/ stopped	49%	22%	60%
LV slowing	1%	6%	7%
LV change lanes	30%	37%	56%

Source: (McMillan, Carnell et al. 2007)

Table 8-7 displays the result of applying the effectiveness estimates to the crash population. Almost all the crash reduction comes from the LV slower/stopped group, accounting for 3,817 out of the total of 4,328 crashes estimated to be eliminated. The LV slowing set of crashes was about two-thirds the size of the LV slower/stopped group, but the estimated effectiveness for the LV slower group was only about 7%. Overall, CWS accounted for most of the crash reduction, with about 3,300. ACC alone, which includes AdBS, was estimated to eliminate almost 1,800 tractor-semitrailer crash involvements. The column showing percentage reduced was slightly lower than the effectiveness estimates themselves because penetration of the technology into the fleet was also taken into account. Overall, it was estimated that the combination of CWS plus ACC would only eliminate about 3.5% of tractor-semitrailer crash involvements in total.

Table 8-7 Reduction in crash involvements by relevant crash type, Volvo FOT

Crash type	Number reduced by technology			Percent reduced by both
	CWS	ACC	CWS+ACC	
LV slower/stopped	3,117	1,400	3,817	58.9
LV slowing	41	244	285	7.0
LV change lanes	121	149	226	55.8
Total	3,279	1,793	4,328	3.5

The estimated effect of the Volvo safety systems on truck driver injury was significantly less than for systems that directly address rollover. Table 8-8 shows the effect of the safety systems on the distribution of MHE for tractor-semitrailer drivers in crashes. The most serious crashes in terms of truck driver injury were rollover, collisions with trucks or buses, and collisions with hard fixed objects. The effect of collision avoidance devices on forward collisions only indirectly addressed some of these crash types. MHE rollover was only reduced by 0.8%, and collisions with hard fixed objects were only reduced by 0.1%. Both rollover and an impact with a hard

fixed object would have to occur as a subsequent event to a rear-end striking collision for it to be affected by CWS or ACC, and apparently that did not occur often in the crash data used here. Collisions with trucks and buses were identified above as posing a significant risk of serious injury to tractor-semitrailer drivers, and it was estimated that the combination of CWS plus ACC would reduce their incidence by about 4.9%. The reduction in collisions with light vehicles, significantly less risk for truck drivers, was of similar magnitude.

Table 8-8 Reduction in crash involvements by most harmful event, Volvo FOT

Most harmful event		Number reduced by technology			Percent reduced by both
		CWS	ACC	CWS+ACC	
Rollover		28	17	38	0.8
Fire		15	13	23	5.1
Other non-collision event		4	3	6	0.2
Collision with	Truck/bus	388	217	517	4.9
	Light vehicle	2,772	1,497	3,641	4.7
	Unknown motor vehicle	59	39	85	1.2
	Train	0	0	0	0.0
	Pedestrian/bike/animal	0	0	1	0.0
	Other non-fixed object	0	0	0	0.0
	Hard fixed object	3	2	4	0.1
	Soft/other fixed object	9	4	11	0.1
Unknown		1	1	2	0.4
Total		3,279	1,793	4,328	3.5

After examining Table 8-8, one would expect only a modest impact on truck driver injury, and that proved to be the case. Fatal injuries to tractor-semitrailer drivers were estimated to be reduced by only 5.5% (Table 8-9). Overall, it was estimated that the combination of safety systems tested in the Volvo FOT would reduce the total number of tractor-semitrailer drivers injured in crashes by only 3.1%. Most of the reduction in fatalities was related to the impact of the safety systems on the number of collisions with trucks or buses, unknown motor vehicle types, and fires. The unknown motor vehicle types were probably large vehicles, such as farm tractors or construction equipment, given the effect on driver injury. The fires probably occurred subsequent to a forward impact, and eliminating the forward impact eliminated the fire. The number of B-injuries reduced was somewhat anomalous and seems to be the result of the fact that GES is the product of a sample and one of the GES records for a driver with a B-injury had a large sample weight. Overall, it is estimated that the combination of safety systems in the Volvo FOT would reduce the total number of injured drivers by 3.1%.

Table 8-9 Reduction in driver injuries by ACAT device estimated from Volvo FOT

Driver injury severity	Number reduced by technology			Percent reduced for both
	CWS	ACC	Both	
Fatal	14	7	18	5.5
A-injury	3	3	6	0.7
B-injury	105	65	144	4.6
C-injury	38	20	49	1.9
Injured, unknown severity	1	0	1	0.5
All injuries	161	95	217	3.1

8.3 Estimates for FCW and collision mitigation braking (CMB)

A report by Woodrooffe et al., analyzed the effectiveness of an FCW with collision mitigation braking for NHTSA. This project (Woodrooffe, et al. 2012) employed track testing to establish the capabilities and performance characteristics, crash data analysis to identify and characterize the relevant crashes, and computer simulation to estimate the effect of the technologies on the relevant crash population.

The technology tested consisted of a forward collision warning system and an autonomous braking system. The FCW system issued audible and haptic warnings to the driver in the event of a forward conflict. Forward conflicts were defined as vehicles in lane ahead of the truck that presented a collision risk, as assessed by a time-to-collision of less than about 1.3 seconds. If the driver did not respond in time or with sufficient braking, once a collision was imminent, the autonomous braking system would de-throttle the engine and apply the foundation brakes. Three different versions of the integrated system (warning and braking) were tested, called CMB1, CMB2, and CMB3. In the CMB1 system, the forward collision warning system did not trigger for objects that the forward sensors (radar) had never detected moving. This means that a forward vehicle that was stopped when the CMB1-equipped vehicle came in range would not trigger a warning to the driver. The CMB2 and CMB3 systems added a camera to enhance the ability to detect and evaluate forward stopped vehicles, so both CMB2 and CMB3 triggered (issued warnings and braked) for any vehicle in lane ahead of the truck. In addition, CMB2 applied braking force up to 0.3 g for all stopped vehicles and up to 0.6 g for moving vehicles; and CMB3 braked up to 0.6 g for both moving and stopped forward vehicles.

Track testing was used to establish and verify the functioning of the systems in different crash scenarios. The systems were tested against both moving and stopped targets, and the performance of the systems was parameterized for use in simulation. National crash data were analyzed to establish the scope and characteristics of the crashes relevant to the systems. Then

simulation was used to establish estimates of the effectiveness of the different versions of FCW with CMB.

The computer simulation was based on naturalistic driving data. Naturalistic driving data was used to generate a virtual population of crashes relevant to the technologies under consideration. Within the naturalistic driving data, a set of episodes were identified in which a tractor-semitrailer was following a slowing or slower lead vehicle within a certain distance, i.e., with a potential forward collision for the tractor-semitrailer. In the naturalistic data, there were no such actual collisions, but a set of virtual crashes was generated by imposing delays on the response of the tractor-semitrailer driver to produce a simulated crash. These delays in response were “tuned” in order to generate a set of rear-end crashes that had the same characteristics and distributions as the real population of rear-end crashes from the crash data analysis. Then the simulated crashes were re-run, in effect, with the actions of the FCW/CMB systems overlaid, to determine the effect of the technologies on preventing or reducing the impact of the collisions.

Four crash types were identified as relevant to the FCW/CMB systems: lead vehicle (LV) stopped, LV slower (than the following vehicle), LV decelerating, and LV cut-in. In the LV cut-in type, a vehicle cuts in front of the truck and slows down, presenting a collision risk. These crash types are all essential rear-end crashes, in which a vehicle strikes another vehicle in lane ahead in the rear.

The Woodrooffe et al. (2012) report included the algorithms and filters used to establish the crash population relevant to the FCW/CMB technologies. These algorithms were used in the current report to identify the set of relevant crashes. In addition, the report identified several circumstances in which the technology would not be effective. These included low friction roads (i.e., not dry), vehicle loss of control due to a vehicle failure (tire blowout; brake, steering, or suspension failure), and aggressive driving or coded road rage. In each case, the technology was not considered to be effective, either because of limitations on the effectiveness of braking (slick roads or blown tires) or because the driver had pushed the vehicle beyond its limits (aggressive driving or road rage).

As defined in the Woodrooffe, et al. (2012), report, about 8.6% of tractor-semitrailer crash involvements could be addressed by the FCW/CMB technologies. (Please see Table 8-10.) The LV stopped crash type accounted for the largest share of the relevant crashes with about 3.9%, or 4,814 estimated annually. The next largest share was crashes in which the LV decelerated in front of the trucks, with 2.8% or 3,481. LV cut-in crashes were relatively rare, with on 0.4% of all crashes, and only 5% (541 of 10,744) of the relevant rear-end striking crashes.

Table 8-10 FCW/CMB-relevant crash types, after Woodrooffe et al. (2012)

Crash types	N	%
LV stopped	4,814	3.9
LV slower	1,908	1.5
LV decelerating	3,481	2.8
LV cut-in	541	0.4
All others	114,090	91.4
Total	124,834	100.0

According to the report, the LV stopped crash type actually consisted of two types: crashes in which the LV came to a stop while within sensor range of the striking vehicle and crashes in which the LV was stopped prior to coming in range. This is an important distinction because the CMB1 version of the technology would activate for the former but not the latter. The Woodrooffe et al. (2012) report reviewed a sample of rear-end striking crashes where the LV was coded as stopped to determine the proportion of those crashes in which the LV came to a stop within a range in which the FCW/CMB sensors could have detected movement and therefore activated.

The foregoing explains why the Woodrooffe (2012) report had positive effectiveness estimates for the CMB1 for the LV stopped crash type. Table 8-11 presents the effectiveness estimates for the relevant crashes types for each of the technology combinations. The estimates range from 9.7% in the case of CMB1 for the LV stopped crash type, to 58.5% for the CMB3 (triggers for all stopped vehicles and brakes very aggressively) for the same crash type. The table shows generally higher rates of effectiveness for the more advanced versions of FCW/CMB, either because the sensors activate for more crashes or because the system triggers more aggressive braking.

Table 8-11 Effectiveness estimates by technology

Crash type	FCW + CMB1	FCW + CMB2	FCW + CMB3
LV stopped	9.7%	9.7%	58.5%
LV slower	15.8%	36.6%	36.6%
LV decelerating	20.3%	25.1%	25.1%
LV cut-in	27.6%	40.0%	40.0%

Source:(Woodrooffe et al. 2012)

Table 8-12 shows the number of crashes of each type reduced by each of the FCW/CMB systems, along with the percentage of relevant crashes reduced by the most effective system,

FCW + CMB3. Overall, the systems would reduce all tractor-semitrailer crash involvements by 3.1%. And each advancement in the systems resulted in significant increases in the proportion of relevant crashes prevented. The combination of FCW + CMB1, which did not activate against stopped vehicles that had never been seen and braked the least aggressively, was estimated to prevent only 16.1% of relevant crashes. CMB2 added detection of never-seen stopped vehicles, and braked more aggressively for other crash types, increasing the percentage to 27.6% of prevent relevant crashes. CMB3 braked the most aggressively for all crash types, and clocked in with a prevention ratio of 36.6%. The table also shows FCW + CMB3 system effectiveness against each relevant crash type.

Table 8-12 Reduction in CMB-relevant crash types, estimated from Woodrooffe et al. (2012)

Crash type	Number reduced by technology			% reduced by FCW+CMB3
	FCW + CMB1	FCW + CMB2	FCW + CMB3	
LV stopped	628	1,201	2,169	45.1
LV slower	296	686	686	36.0
LV decelerating	698	863	863	24.8
LV cut-in	147	213	213	39.3
Total	1,769	2,962	3,931	3.1
% relevant crashes reduced	16.5%	27.6%	36.6%	

The effect was significantly less in terms of the crash types that present the highest risk to tractor-semitrailer drivers. Table 8-13 shows the number of crashes, classified by MHE, prevented by each technology. The primary categories prevented were collisions with other trucks and buses and collisions with light vehicles. It was estimated that 4.3% of impacts with other trucks and buses and 4.2% of collisions with light vehicles. The prevented collisions were all rear-end, truck striking crashes, so in cases where the LV was a truck, preventing those crashes could reduce serious tractor-semitrailer driver fatalities and serious injuries. In contrast, collisions with light vehicles pose relatively little risk to the truck driver. It was estimated that 3.6% of MHE fires could be prevented, and MHE fire poses a very high risk to truck drivers, but they are relatively rare, so the net effect was not large. Overall, deploying the most effective version of FCW/CMB technologies was estimated to prevent only 3.1% of crashes, or about 3,931 annually.

Table 8-13 Reduction in crash involvements by most harmful event, estimated Woodrooffe et al. (2012)

Most harmful event		Number reduced by technology			% reduced by FCW+CMB3
		FCW + CMB1	FCW + CMB2	FCW + CMB3	
Rollover		11	24	25	0.5
Fire		7	15	17	3.6
Other non-collision event		0	1	1	0.0
Collision with	Truck/bus	225	387	461	4.3
	Light vehicle	1,461	2,441	3,309	4.2
	Unknown motor vehicle	60	85	107	1.5
	Train	0	0	0	0.0
	Pedestrian/bike/animal	0	0	0	0.0
	Other non-fixed object	0	0	0	0.0
	Hard fixed object	1	2	3	0.1
	Soft/other fixed object	3	7	7	0.1
Unknown		0	1	1	0.2
Total		1,769	2,962	3,931	3.1

Table 8-14 shows the estimated reduction in tractor-semitrailer driver injury for each of the three FCW/CMB combinations, plus the percentage reduced for each driver injury severity. Compared with some of the other technologies, the effect on the most serious driver injuries was modest. Overall, it was estimated that the most effective version of FCW/CMB would reduce all tractor-semitrailer driver injuries by 2.4%, including 4.7% of driver fatalities, 1.4% of A-injuries, and 3.1% of B-injuries. FCW + CMB3 was about three times as effective in preventing fatalities as the least effective system, which makes sense given its more aggressive braking and broader range of rear-end crashes addressed.

Table 8-14 Reduction in driver injuries, estimated from Woodrooffe et al. (2012)

Driver injury severity	Number reduced by technology			% reduced by FCW+CMB3
	FCW + CMB1	FCW + CMB2	FCW + CMB3	
Fatal	5	9	15	4.7
A-injury	8	10	11	1.4
B-injury	44	87	97	3.1
C-injury	18	30	42	1.6
Injured, unknown severity	0	1	1	0.4
Total injuries	75	137	166	2.4

Analysis showed that most of the fatalities prevented were due to the effect on MHE fire and collisions with other trucks and buses. Most rear-end collisions for tractor-semitrailers did not result in serious or fatal injuries to the drivers, unless the LV was a truck or a fire occurred. Accordingly, the primary effect of FCW/CMB systems was in the reduction of fatal and serious injuries in the struck and other vehicles, rather than the driver of the striking vehicle. Nevertheless, it was clear that reducing these crash types would result in some decrease in truck driver injury.

8.4 Estimates for ESC and RSC

Estimates for the effectiveness of ESC and RSC were used from a report to NHTSA by Woodrooffe et al., from UMTRI. The project used a set of integrated methodologies to estimate the effectiveness of ESC and RSC in different crash scenarios, including simulation, clinical review of in-depth crash investigations, and analysis of national crash data files. FARS and GES crash data were used to identify the set of crashes relevant to ESC and RSC. Hardware-in-the-loop (HiL) simulation was used to define and characterize how the ESC and RSC would act to help maintain the stability of the truck. Effectiveness estimates were established from an engineering review of a representative set of 164 crash investigations from the Large Truck Crash Causation Survey (LTCCS) (Woodrooffe, Blower et al. 2009).

The analysis of the national crash files identified a set of crash types that were relevant to RSC and ESC. The crash types were untripped rollover, and crashes precipitated by on-road loss of control (LOC). RSC helps maintain the stability of trucks in excessive lateral acceleration, such as a truck entering a curve at too high a speed. It senses that the rollover threshold is being approached and slows the truck down by de-throttling the engine and applying the foundation brakes, if necessary. ESC includes the same capability, but also monitors vehicle yaw, which occurs when the direction of motion is different from the direction the driver is attempting to

steer. ESC also can also apply the brakes to different wheels in order to straighten the vehicle out—bring the direction of motion back in line with the direction the driver is attempting to steer. Given these applications, the crash types identified as relevant to the technologies were untripped rollover and loss of control. The study also estimated effectiveness for different scenarios relevant to how the technologies worked. Separate estimates were developed by the cross-classification of roadway alignment (straight or curved) and roadway condition (dry or wet).

HiL simulation was used to establish the performance characteristics of ESC and RSC in different representative scenarios. The HiL incorporated the physical operation of the ESC and RSC technologies into the simulation of exemplar crashes. In the simulation, maneuvers that led to crashes such as entering a curve at speed. An algorithm simulated the activity of the vehicle sensors and sent the appropriate signals to a physical mockup of tractor-semitrailer brake layout. Brakes were fired according to the commands of the ESC and the resulting brake forces fed back into the simulation to drive the path of the truck and resulting vehicle control. These results were used to characterize the effectiveness of the technologies in different scenarios and conditions.

The final component informing the effectiveness estimates was an engineering review of in-depth crash investigations from the Large Truck Crash Causation Study (LTCCS). Detailed data, crash diagrams, scene photos, and the researchers narrative were reviewed to estimate the effectiveness of the technologies in preventing or mitigating sample rollover and loss of control crashes. The engineering judgment was based on the analysis of the crashes informed by the results of the HiL simulation. The LTCCS crashes selected for review corresponded to the crash scenarios identified in the national crash data, and the results were used to compute effectiveness estimates for those scenarios.

Table 8-15 shows the effectiveness estimates from Woodrooffe, et al., (2009) for ESC and RSC for each of the crash scenarios defined. Depending on the circumstances, the effectiveness ranged from 0.0% against rollover on straight, not dry (wet, snow-covered, icy) roads to 75.1% for ESC on curved not dry roads. Overall, ESC had higher effectiveness estimates than RSC, and was more effective on curved roads than straight, dry roads than wet, and against rollover than loss of control.

Table 8-15 Effectiveness estimates by technology, road condition, and crash type

Road alignment	Road surface	ESC		RSC	
		Rollover	LOC	Rollover	LOC
Straight	Dry	21.1%	17.8%	16.4%	0.6%
	Not dry	0.0%	20.6%	0.0%	1.8%
Curve	Dry	75.1%	31.6%	71.2%	14.0%
	Not dry	55.6%	39.6%	45.6%	11.5%

Source: (Woodrooffe, Blower et al. 2009)

The rollover crashes relevant to ESC or RSC are basically first-event, untripped rollovers. These are rollovers that occurred when lateral acceleration overcame roadway friction and the vehicles rolled over. Typical untripped rollover crashes occurred on-road when a vehicle attempted to traverse a curve at a too-high a speed and the lateral acceleration caused the vehicle to rollover. Rollovers that occurred after a collision with another vehicle or after roadway departure, unless the ESC would have enabled the driver to keep his vehicle on the road by slowing it prior to roadway departure, were not included. Relevant LOC crashes were initiated by on-road yaw, primarily due to low friction (e.g., wet road surfaces). LOC due to vehicle failure (e.g., tire blowout or other vehicle failure), were excluded.

Woodrooffe, et al., (2009) included the crash data filters used to identify the relevant crash types. Since the report used the same crash data files as were used in the current report, they were directly applicable here, though some minor modification was needed to accommodate some changed variables in years of FARS and GES used here. ESC- and RSC-relevant crashes encompassed about 7.2% of all tractor-semitrailer crashes (Table 8-16). In the report, three fundamental crash types were evaluated: rollover only, rollover following loss of control, and loss of control only. About 2,300 relevant rollover-only crashes were identified in the data, 1,645 rollover and LOC, and 4,970 LOC-only crash involvements. These are estimated counts of annual tractor-semitrailer crash involvements.

Table 8-16 Crash types relevant to ESC and RSC, after Woodrooffe et al. (2009)

Crash type	N	%
Roll only	2,311	1.9
Roll & LOC	1,645	1.3
LOC only	4,970	4.0
All others	115,908	92.8
Total	124,834	100.0

Effectiveness estimates contained in Table 8-15 were applied to the crash data to determine the number of crash involvements that would have been prevented by the technologies. ESC proved to be more effective than RSC in reducing the crashes relevant. ESC would have prevented almost 40% of roll-only crashes, about half of roll and LOC crashes, and about 21.1% of LOC-only crashes (Table 8-17). Overall, it was estimated that full deployment of ESC would prevent about 2.2% of all tractor-semitrailer crashes.

Table 8-17 Relevant crashes reduced by ESC & RSC, after Woodrooffe et al. (2009)

Crash types	Reduced by technology		% reduced by ESC
	ESC	RSC	
Roll only	916	859	39.7
Roll & LOC	824	736	50.1
LOC only	1,047	186	21.1
Total	2,788	1,782	2.2

Table 8-18 shows the effect of ESC and RSC on the distribution of crashes, by MHE. Not surprisingly, the greatest effect is on MHE rollover, with ESC estimated to reduce by 36.3%, or about 1,823 MHE rollovers annually. The relative large number of “other non-collision events” reduced was from a reduction in the number of jackknives. Since ESC addresses tractor yaw, it can reduce the number of jackknife events initiated by tractor yaw. The other area of greatest impact was a reduction in collisions with hard fixed objects (as well as soft fixed objects) following roadway departure due to loss of control. Overall, ESC was estimated to reduce disproportionately crash types most risky to truck drivers.

Table 8-18 Reduction in crash involvements by most harmful event, after Woodrooffe et al. (2009)

Most harmful event		Reduced by tech.		% reduced by ESC
		ESC	RSC	
Rollover		1,823	1,601	36.3
Fire		5	2	1.1
Other non-collision event		269	47	10.3
Collision with	Truck/bus	16	3	0.2
	Light vehicle	77	17	0.1
	Unknown motor vehicle	34	4	0.5
	Train	0	0	0.0
	Pedestrian/bike/animal	0	0	0.0
	Other non-fixed object	1	0	0.0
	Hard fixed object	382	80	7.9
	Soft/other fixed object	164	22	2.2
Unknown		15	6	3.0
Total		2,788	1,782	2.2

Not surprisingly in light of the effect on the most risky crash types, ESC, and to a lesser extent RSC, would reduce the incidence of truck driver serious injuries substantially. (Table 8-19.) Overall, it was estimated that ESC would prevent 984 injuries annually, or about 13.9% of all tractor-semitrailer driver traffic injuries. About 35 truck driver fatalities would be prevented by ESC, along with 187 A-injuries. Almost all of the fatalities and A-injuries would be prevented by the reduction in MHE rollover. Reducing the number of MHE rollovers accounted for 28 of the 35 driver fatalities and 173 of the 187 driver A-injuries prevented. The effect on deaths and injuries related to LOC was significantly less. Only 7 of the prevented fatalities were attributed to a reduction in LOC crashes, and only 16 of the A-injuries prevented were because of fewer LOC crashes. Generally speaking, ESC was less effective in preventing LOC crashes than in preventing untripped rollovers, for each of the crash scenarios, as shown in Table 8-20. Moreover, since RSC does not address yaw events, its effectiveness against LOC crashes was limited.

Table 8-19 Reduction in driver injuries by ESC/RSC, after Woodrooffe et al. (2009)

Driver injury	Reduced by tech.		% reduced by ESC
	ESC	RSC	
Fatal	35	28	10.6
A-injury	187	170	23.8
B-injury	490	392	15.6
C-injury	231	148	8.9
Injured, unknown severity	41	36	19.4
Total	984	773	13.9

8.5 Estimates for LDW

Houser, Murray, et al., provided estimates of the effectiveness of an LDW system in a form that was usable for this project. The purpose of the Houser report was to estimate costs, benefits, and return on investment for motor carriers of an LDW system. They used data from a field operational test and from a survey of motor carriers to estimate effectiveness for specific crash types. The carrier data included crash data and comprehensive crash cost data for a number of accident types, including those relevant to LDW. Crash costs were estimated separately for rollovers, sideswipes, run-off-road, rear-end, and jackknife crashes. In addition, the carriers estimated, based on their experience, the effectiveness of LDW systems against the relevant crash types, chiefly sideswipes and run-off-road crashes (Houser, Murray et al. 2009).

The FOT evaluated an LDW in operation in a test involving a single motor carrier. The LDW was installed on 22 tractor-semitrailers with tank cargo bodies, and operated over a 12 month

period. The test was divided into baseline and operational periods. During the baseline period, the device was inactive, but collecting data on driving patterns. Lane departure was noted but no warnings were issued to the drivers. In the operational period, the LDW warning system was activated and the drivers received feedback from the system. System effectiveness was measured by changes in the number of relevant conflicts, such as unsignaled lane crossings (Orban, Hadden et al. 2006).

The crash types addressed by the LDW system, as specified in the studies, included:

- Single-vehicle road departure, collision;
- Single-vehicle road departure, rollover;
- Same-direction lane departure, sideswipe;
- Opposite-direction lane departure, sideswipe; and,
- Opposite-direction lane departure, head-on collision.

In addition, the LDW system was not considered to be effective against the crash types specified in the case of loss of control prior to roadway exit, either due roadway conditions or avoidance maneuvers; vehicle failure such as tire blowout or some other mechanical problem; or driver incapacitation due to sleep, a medical condition, or other condition.

Both studies estimated crash reductions based on an evaluation of the GES file, and supplied lists of the variables and code levels used to identify the relevant crashes within GES. This information was used in the current study to identify the same population of crashes. The data years used in the two studies were older than those used in the current study. There have been some modest changes made by GES in the structure of the specific variables used, so the algorithms were modified to adapt them to the format of the years of the GES file used in the current study.

Table 8-20 shows the effectiveness estimates derived from Houser that were used here. Houser presents two effectiveness estimates: one based on the FOT results and one based on the responses of motor carriers. The responses from motor carriers were essentially their estimates of the proportion of relevant crashes that would be prevented by an LDW system. As far as can be determined from the report, the motor carrier estimates were not based on actual experience with the systems. The estimates from the FOT were determined by the observed reduction in LDW-relevant conflicts from actual operations. For the present purposes, the effectiveness estimates based on the FOT results were used here. Overall, it was estimated that the LDW system would reduce relevant crashes by about 23%.

Table 8-20 LDW effectiveness estimates by crash type

Crash type	Effectiveness estimates
Single-vehicle roadway departure (SVRD)	23.5%
Same-direction lane departure (SDLD)	23.0%
Opposite-direction lane departure (ODLD)	23.0%

The LDW-relevant crash types accounted for about 5.1% of all tractor-semitrailer crashes, as defined by the crash types identified in the reports and excluding crashes where the LDW system would not be expected to work, such as on-road loss of control and driver incapacitation (Table 8-21). Road departure crashes were the predominant type affected, with about 3,100 annually, 2.5% of all crashes. Lane departure crashes, both opposite direction and same direction, were of similar magnitude, with about 1,500 to 1,700 annually.

Table 8-21 Distribution of LDW/RDW-relevant crashes, after Houser et al. (2009)

Crash type	N	%
Road departure	3,103	2.5
Lane departure, opposite	1,513	1.2
Lane departure, same	1,796	1.4
All else	118,421	94.9
Total	124,834	100.0

Table 8-22 shows results of applying the effectiveness estimates to the LDW-relevant crash population. The reductions were modest in terms of overall impact. In sum, it was estimated that full deployment of the LDW system would prevent about 1.2% of tractor-semitrailer crashes annually. The effect on LDW-relevant crashes was obviously greater, but the size of the LDW-relevant crash population, as defined in the reports, was small enough that the overall reduction was not large.

Table 8-22 Reduction in LDW/RDW crashes

Crash type	Involvements reduced	% reduced
Road departure	730	23.5
Lane departure, opposite direction	349	23.1
Land departure, same direction	415	23.1
Total	1,494	1.2

Despite the modest size of the effect overall, the impact on crash types most risky to the truck drivers was somewhat larger. It was estimated that MHE rollovers would be reduced by 211 or 4.2% annually, and collisions with hard fixed objects would decline by 280, or 5.8% (Table 8-23). Collisions with another truck or bus would go down by 2.8% and MHE fire would also decline by 2.5%. These are all crash types that present a disproportionate risk to truck drivers, so even though the effect on crashes overall is modest, the effect on truck driver injury would be significant. As a result, it is estimated that fatal driver injuries would decline by 33, 10.2% of all tractor-semitrailer driver fatalities; and 29 A-injuries (3.7% of all) would be prevented.

Table 8-23 Reductions in crash involvements by most harmful event, estimated from Houser et al. (2009)

Most harmful event		Crash involvements reduced	% reduced
Rollover		211	4.2
Fire		12	2.5
Other non-collision event		5	0.2
Collision with	Truck/bus	293	2.8
	Light vehicle	442	0.6
	Unknown motor vehicle	48	0.7
	Train	0	0.0
	Pedestrian/bike/animal	1	0.1
	Other non-fixed object	32	0.6
	Hard fixed object	280	5.8
	Soft/other fixed object	149	1.9
Unknown		21	4.3
Total		1,494	1.2

Table 8-24 Reduction in driver injuries estimated from Houser

Driver injury	Number reduced	% reduced
Fatal	33	10.2
A-injury	29	3.7
B-injury	119	3.8
C-injury	20	0.8
Injured, unknown severity	1	0.4
Total injuries reduced	202	2.9

The positive effect of LDW on tractor-semitrailer driver injury stemmed largely from preventing run-off-road crashes and, to a lesser extent, head-on collisions. Same-direction sideswipes typically have low relative velocity, so that same-direction collisions themselves posed relatively low risk of injury to truck drivers. However, run-off road events can result in rollover or collisions with hard objects such as embankments or bridge structures, which are the most threatening for the drivers. Almost all of the reduction in driver fatalities was from preventing roadway departure, including 20 fatalities reduced from off-road rollover, and 11 fatalities prevented from collisions with hard fixed objects. In terms of truck driver injury, the primary benefit of LDW would be from keeping the truck on the road.

8.6 Estimated combined effect of ESC, FCW, and LDW

This section examines the joint effect of the ACATs on tractor-semitrailer crashes under the assumption of full deployment within the truck fleet. Under this assumption, all tractor-semitrailers would be equipped with the most effective implementation of each crash avoidance technology. Effectiveness estimates for each technology are applied to the relevant crash types across the whole set of truck crashes simultaneously and the resulting effect computed.

The method of estimating the net effect of full deployment for all the technologies proceeded as follows. For each crash, it was determined which technology, if any, was applicable. If only one technology was applicable, then the appropriate effectiveness estimate for that crash was selected. Where more than one technology could address a specific crash, the most effective technology was selected. In other words, if more than one device could reduce the likelihood of a crash, the applicable prevention probability was the most effective relevant device. For these crashes, the case sample weight would be recomputed accordingly, as described in section 4.1. Where no technology was relevant, the original case sample weight was used.

In the crash population, there was relatively little overlap between the technologies in terms of crashes addressed. Most of the technologies addressed very specific crash types and

circumstances, and the way the crash types were defined in the evaluations were typically narrowly focused on specific, well-defined events. Therefore it is not surprising that there was not much redundancy. Overlap of the ACATs only amounted to about 0.8% of tractor-semitrailer crashes, and occurred between ESC and LDW. Some untripped rollovers were initiated by lane departure; for example, if a truck drifted out of lane and then the driver over-corrected to steer back into lane. These crashes could be addressed either by an LDW that prevented the initial wandering or an ESC that helped the driver maintain control following the over-correction. In estimating the joint effect of the technologies in such a case, the one with the highest probability of success was assumed.

Table 8-25 shows the combined ACAT effectiveness on the MHE crashes for tractor-semitrailer drivers. Overall, about 10.9% of crash involvements would be prevented, which is about 14,000 tractor-semitrailer crashes annually. However, it is interesting to note that the effect was greater on the crash types that posed the highest risk for truck drivers. MHE rollover was identified above as the primary cause of driver fatal and serious injury in traffic crashes, and it is estimated that the combination of all the ACATs would reduce MHE rollover by almost 43%, preventing 2,145 tractor-semitrailer rollovers annually. Collisions with hard fixed objects would go down by 17.8%, and with other trucks or buses by 11.8%.

Table 8-25 Combined ACAT effectiveness by MHE crash type

Most harmful event		Crash involvements reduced	Percent reduced
Rollover		2,145	42.7
Fire		48	10.4
Other non-collision event		286	10.9
Collision with	Truck/bus	1,248	11.8
	Light vehicle	8,168	10.4
	Unknown motor vehicle	302	4.2
	Train	0	0.0
	Pedestrian/bike/animal	4	0.2
	Other non-fixed object	1	0.0
	Hard fixed object	859	17.8
	Soft/other fixed object	514	6.7
Unknown		71	14.2
Total		13,646	10.9

MHE fire, though rare, would also decline by 10.4%. None of the technologies specifically addressed fire. MHE fire typically occurred after rollover or serious collisions with other vehicles or fixed objects. Fire often developed slowly and if the driver was unable to extricate himself, the fire could become the most harmful event. The ACATs helped to reduce MHE fire by preventing the collisions or rollovers that resulted in fires.

With respect to truck driver injury, the combined effect of all the ACATs evaluated was estimated to reduce tractor-semitrailer driver injuries in crashes by 1,581 annually, or about 22.4% (Table 8-26). It is notable that the most severe driver injuries were reduced substantially more than less serious injuries. Overall, the ACATs would reduce tractor-semitrailer crashes by 10.9%, but fatal injuries were estimated to be reduced by 32.7%, A-injuries by 30.0%, and B-injuries by 26.9%. The ACATs tended to target the crash types that pose the greatest threat to truck drivers, rollover and frontal collisions. Accordingly, truck driver injury would be reduced far more than crash involvements as a whole.

Table 8-26 Combined ACAT effectiveness on driver injury

Driver injury severity	Driver injuries avoided	% reduced
Fatal	107	32.7
A-injury	236	30.0
B-injury	847	26.9
C-injury	345	13.3
Injured, unknown severity	46	21.6
Total	1,581	22.4

Most of the change in truck driver fatalities was produced by preventing MHE roll (46 fatalities prevented) and collisions with hard fixed objects (21 prevented), which in turn was related to reducing road departure. Interestingly, the next greatest number of fatalities prevented was MHE fire, with an estimated 18 fewer fatalities. Reducing MHE fire accounted for about 17% of the decline in driver crash-related deaths. These fires were very likely secondary events in the crashes, following collisions or rollovers. Analysis showed that about 20% of MHE fires followed run off road crashes and about 80% occurred in collisions with other vehicles. It should be noted, however, that about half of the collisions with other vehicles were crashes with more than two vehicles where the truck was not involved in the initial collision. Those crashes are unlikely to be addressable by truck-based crash avoidance technology.

Preventing rollover, both tripped and untripped, accounted for most of the reduction in truck driver serious injuries. ESC and RSC address untripped rollover directly, by reducing the speed

of the trucks when rollover threatens, and, in the case of ESC by helping the driver maintain control in skids. But it appears that the joint effect of the ACATs will also reduce tripped rollover by reducing collisions (F-CAM and LDW) and by helping to keep the trucks on the road and avoiding impacts with fixed objects. Table 8-27 shows the predicted effect of the ACATs on all rollovers, whether MHE or not. Untripped rollovers were predicted go down by 53.4% overall, but tripped rollovers by 28.3%. Most of these occurred in run-off road crashes. In these crashes, the trucks ran off the road and rolled over, or struck an object, usually fixed, and rolled over. By keeping trucks on the road, subsequent harmful events would also be eliminated, producing significant benefits.

Table 8-27 Effect of ACAT full deployment on rollover

Rollover status	Current crash involvements	Crash involvements reduced		K & A-injury crashes reduced	
		N	%	N	%
No rollover	119,125	11,381	9.6	74	16.6
Tripped rollover	2,630	744	28.3	123	33.4
Untripped rollover	1,991	1,063	53.4	137	60.0
Roll, unknown type	1,087	459	42.2	9	13.4
All rollovers	5,709	2,265	39.7	269	40.4
Total	124,834	13,646	10.9	343	30.8

Again, it appears that the positive effect of reducing rollover was greater for more severe crashes for truck drivers. In terms of the crashes in which truck drivers received fatal or A-injuries, it was estimated that the ACATs would reduce 60.0% of untripped rollovers and 33.4% of tripped (Table 8-27). This result is consistent with previous results that estimated the ACATs preferentially address the highest risk truck crashes.

In terms of MHE collisions, full deployment of the ACATs was estimated to reduce a significant number of such collisions and to reduce frontal collisions, which pose the greatest risk to truck drivers, more than other types. Overall, the ACATs were estimated to reduce all MHE collisions by 9.5%. (Please see Table 8-28, which is restricted to crashes involving a collision with another vehicle or object.) All MHE frontals were estimated to decline by 21.1%, while right and left impacts were estimated to go down by 7.1% and 8.2% respectively. The reduction in frontals was primarily attributable to the F-CAM technology. LDW contributed through reducing run-off-road crashes that resulted in frontal impacts with fixed objects. Because frontal MHE collisions were strongly associated with serious truck driver injury, reducing frontals tended to reduce serious-injury crashes more than crashes of lesser severities. It was estimated that full deployment of the ACATs discussed here would reduce tractor-semitrailer driver fatal and A-

injuries in collisions by about 14.8% overall, and reduce fatal and A-injuries in frontal collisions by 18.3%.

Table 8-28 Effect of full deployment on collision crashes

Side of truck struck	Current collision crash involvements	Crashes all severities reduced		K & A-injuries reduced	
		N	% of crashes	N	% of K/A
Front	27,151	5,730	21.1	42	18.3
Right	32,952	2,355	7.1	6	8.2
Back	13,977	36	0.3	0	0.0
Left	30,933	2,533	8.2	7	11.0
Other/unknown	10,661	363	3.4	2	20.1
Total	115,674	11,017	9.5	58	14.8

About three-quarters of the reduction of MHE collision involvements was estimated to come in crashes with light vehicles. Reducing those crashes would not make a significant impact on truck-driver injury, though of course it would have substantial benefits to the occupants of those vehicles. The forward sensors do not discriminate between trucks or light vehicles, but obviously the benefit to truck drivers would be much greater from avoiding a crash with another truck. About 30% of the reduction in driver fatal or A-injuries was estimated to come from reducing collisions with other trucks and buses, and almost half from collisions with fixed objects. Preventing run-off-road crashes was estimated to have a very substantial effect on truck driver injury through avoiding collisions with fixed objects, in addition to the effect from avoiding rollovers that occur off-road.

9. Residual crashes, after full ACAT deployment

The above analysis shows that full deployment of ACATs would prevent almost a third of driver fatalities and about 30% of A-injuries among truck drivers. However, the overall number of truck crashes would only be reduced by 10%, leaving a significant number of crashes. Table 9-1 shows the current distribution of tractor-semitrailer crash involvements classified by the MHE to truck drivers, along with the estimated distribution after full deployment and estimated crash involvements avoided. Although significant numbers of the crash types most likely to put drivers at risk were predicted to be avoided, substantial numbers of crashes will remain: almost 3,000 annual rollovers; over 9,000 collisions with trucks or buses; and almost 4,000 impacts with hard fixed objects, to identify only the riskiest crash types.

Table 9-1 Current MHE crash population and after full deployment

Most harmful event		Current crash population	Assuming full deployment	Involvements avoided
Rollover		5,023	2,877	2,145
Fire		461	414	48
Other non-collision event		2,615	2,329	286
Collision with	Truck/bus	10,612	9,364	1,248
	Light vehicle	78,178	70,010	8,168
	Unknown motor vehicle	7,215	6,913	302
	Train	247	247	0
	Pedestrian/bike/animal	2,467	2,463	4
	Other non-fixed object	5,047	5,046	1
	Hard fixed object	4,827	3,967	859
	Soft/other fixed object	7,642	7,128	514
Unknown		501	430	71
Total		124,834	111,188	13,646

In terms of reducing the harm to truck drivers in crashes, of course, the main focus is on the most severe injuries. Figure 9-1 shows the frequency of fatal and A-injuries by MHE crash type currently and assuming full ACAT deployment. Although the ACATs were estimated to reduce certain crash types substantially, it is clear that many serious injury crash involvements will remain, including many of the target crash types. Rollover would be reduced the most by ACAT deployment, but would still account for by far the greatest number of serious driver injuries, 335 out of the total of 770 projected. In fact, even after full deployment, the same crash types would remain as the primary sources of truck driver injury in traffic crashes: rollover, collisions with a truck or bus, and collisions with hard fixed objects.

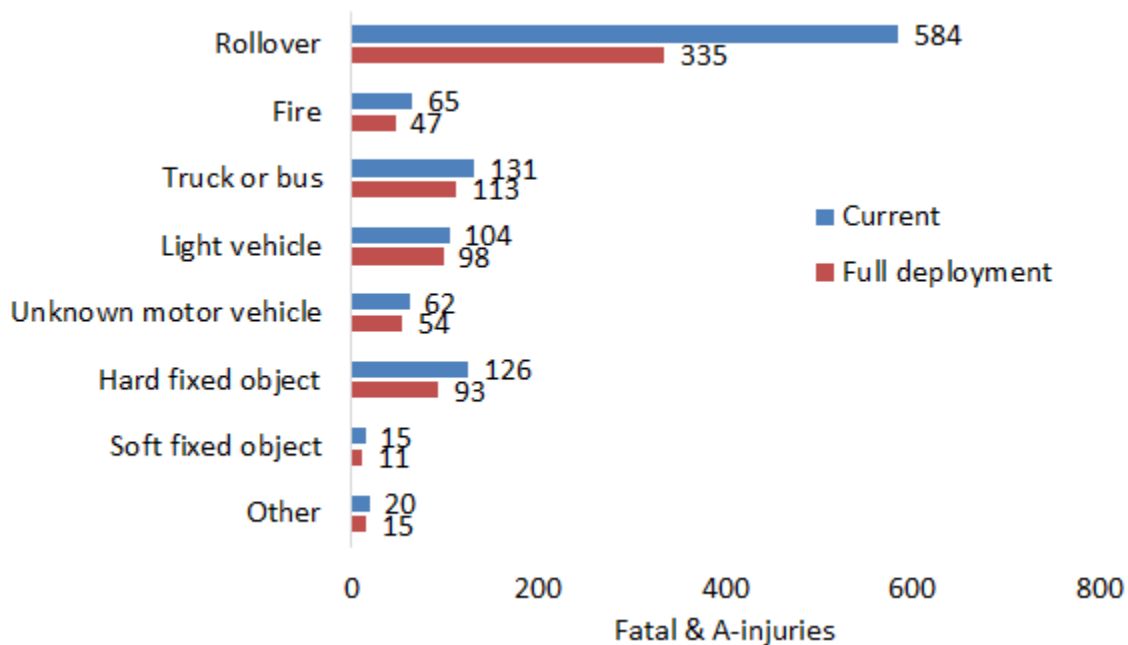


Figure 9-1 Fatal and A-injuries by MHE crash type, current and full ACAT deployment

Similarly, though full ACAT deployment was estimated to result in about a 15% reduction in driver fatalities and A-injuries in MHE collision crashes, a significant number would remain and most would still be frontal impacts. Figure 9-2 shows the current distribution of fatal and A-injuries by the side of impact in collision crashes, plus the distribution of crashes that would remain after full deployment. The greatest effect would be on frontal impacts, but frontal collisions would still dominate among fatal and serious collision-related injuries.

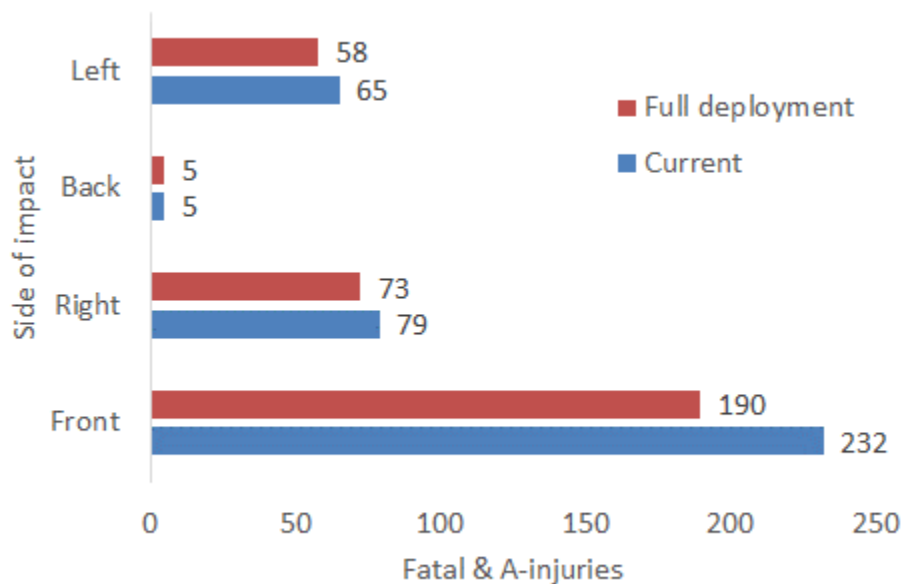


Figure 9-2 Fatal and A-injuries in MHE collisions, current and full ACAT deployment

The ACATs address relatively simple crash types: forward, in-lane collisions for F-CAM; untripped on-road rollovers for RSC, and the same plus loss of control for ESC; and lane/road departure for LDW. The analysis above showed that many of these simple crash types will remain even after full deployment. In the future, some of these may be addressed as ACAT systems are made more effective. However, more complex crashes will remain. For example, untripped rollover was addressed relatively effectively by RSC and ESC. But those technologies are not effective against tripped rollover. Thus, a greater share of rollovers following deployment would be more complex, involving a series of events that culminated in rollover, rather than simple rollovers.

Table 9-2 shows a distribution of classified using the ACC_TYPE field in the GES and FARS files. ACC_TYPE records the relative position and movement of vehicles at the point of initial collision. In effect, it records the precipitating event in crashes. In the table, the crashes are categorized as single vehicle, a set of crashes types with other vehicles, on-road untripped rollovers, and other crashes, including multivehicle crashes in which the truck was not involved in the initial crash. Percentage distribution of current crashes and after full deployment is shown.

Table 9-2 Distribution of fatal and serious injury crashes classified by precipitating event

Precipitating event		Current crashes	Full deployment
Single vehicle	Ran off road	9.3%	8.2%
	Hit object in road	6.1%	6.8%
Collision with another vehicle	Rear-end striking	9.1%	5.5%
	Rear-end struck	7.0%	7.8%
	Same direction sideswipe, truck over lane line	9.4%	7.3%
	Same direction sideswipe, other over lane line	9.1%	10.2%
	Head-on or sideswipe, truck over centerline	1.5%	0.9%
	Head-on or sideswipe, other over centerline	2.0%	2.2%
	Truck turn across path	8.3%	9.3%
	Other turn across	4.3%	4.8%
	Straight, crossing paths	3.0%	3.4%
	On-road untripped rollover	1.1%	0.6%
Other, including multivehicle		29.7%	32.9%
Total		100.0%	100.0%

Among current crashes, about 9.3% were initiated by running off the road, either as a result of loss of control, an avoidance maneuver, or simple drifting off the road. After full deployment, it was estimated that those crashes would account for 8.2%, a significant reduction. There would also be a reduction in the proportion of rear-end striking (9.1% to 5.5%) and same direction sideswipes where the truck crossed over the lane line (9.4% to 7.3%).

However, more complex crash types would remain and indeed increase in share of total crashes. Crashes in which the truck turned across the path of another vehicle would increase from 8.3% of crashes to 9.3%. Crashes where the other vehicle turned across the truck's path would also increase, as would crashes in which both vehicles were going straight, but crossing paths, as at an intersection. These are more difficult crashes to address by avoidance technologies. Where one or the other vehicle was turning, the other vehicle would only be directly in front of the truck immediately prior to the crash. The situation is not like a rear-end striking crash, where in the great majority of crashes, the other vehicle was in front of the truck for most of the pre-crash interval.

Similarly, in crossing paths crashes—for example, where one or the other vehicle ran through a stop sign or red light—the geometric relationship is much more difficult than the rear-end situation. In these crashes, in the initial stages the other vehicle moves across the front of the truck prior to the crash. Sensors would require a wider field of view to detect crossing vehicles, estimate travel speeds, and compute time-to-collision. Roadside fixtures such as signs and buildings, parked vehicles, and other in-transport vehicles will make sorting out the specific threat much more difficult.

10. Methodology for simulation

10.1 Interior design of heavy truck model

10.1.1 Introduction

To date, not much research has been performed to support development of safety systems and especially to evaluate occupant protection in heavy trucks, when compared to the effort made for occupants for passenger cars and pickup trucks. An analysis of previously projects developed at UMTRI involving accident reconstruction (Cheng et al., 1992) and occupant dynamic simulation (Cheng et al., 1994) for both car and truck cases was used to develop our current safety restraint system for heavy truck occupants. One of the main focuses of this project is to improve seatbelt design for use on heavy trucks. Specifically, one significant component of this proposed study is the use of finite element computer simulations to model the frontal portion of the heavy truck and analyze the effects of suggested restraint systems. This was not available during the time of UMTRI's studies. In fact, the previously developed UMTRI's studies employed MADYMO models, instead. Recent advances in computer hardware and finite element methodologies have given researchers in the roadside safety and physical security communities the ability to

investigate complex dynamic problems involving vehicular impacts into barrier systems. FEA has been used extensively to evaluate both vehicle components and crashworthiness of safety barriers and hardware. The FEA discussed herein were performed using the LS-DYNA finite element code. LS DYNA is a general purpose, explicit finite element code (Hallquist, 2015). LS-DYNA is widely used to solve nonlinear, dynamic response of three-dimensional problems and is capable of capturing complex occupant interactions and dynamic load-time history responses that occur during vehicle impacts.

Next, a brief overview of the process undertaken to create the front interior of the heavy truck is presented, as well as explanation on the choice for the dummy employed in simulations, and the methodology to study proposed restraint systems effectiveness within developing simulations. LS-PrePost software was used to make many of the modifications and restore parts used in the heavy truck model.

10.1.2 Modified cab over engine cabin

Recently, the Roadside Safety and Physical Security Division at the Texas A&M Transportation Institute (TTI) was involved in a project supported by the Department of State (DoS) to scan the outline of a Cab Over Engine (COE) heavy truck. The scanning of the truck supported the development of finite element computer models of the truck components. Although this proposed study is considering employment of a heavy truck conventional cab, the provided COE DoS cabin model was morphed to fit the conventional cab style by flattening it out and making adequate adjustments in order to fit the proper geometry. The main adjustments made are listed below:

- Dimension from Front of Cabin to Back of Cabin:
Old DoS Cabin = 81.1'' (2060.12 mm)
Morphed Cabin = 81.1'' (2059.22 mm)
- Dimension from Left Cabin to Right Cabin:
Old DoS Cabin = 94.4'' (2396.27 mm)
Morphed Cabin = 94.4'' (2396.27 mm)
- Dimensions from Top of Cabin to Bottom of Cabin:
Old DoS Cabin = 74.3'' (1887.49 mm)
Morphed Cabin = 92.1'' (2339.02 mm)

As shown above, the biggest adjustment made was with respect to the vertical dimension from the cabin top to the cabin bottom. This was needed mainly to adjust cabin's floor dimensions and characteristics. In fact, since in the COE model the truck engine is located right underneath the driver, the floor is higher than it would be in a conventional cab. The widths in the lateral dimensions did not change significantly.

The original COE DoS model included many additional parts that were not essential to be included in this project's cab model, since they did not interfere with the occupants' safety during a simulated crash scenario. In order to maintain a simplified truck model, some of these truck cab parts were removed. Below is a list of parts removed from the original COE DoS cabin model:

- Spring board assembly
- Rubber mount assembly
- Cab back
- Cab roof inside brace back
- Cab roof inside brace front
- FL Support 1
- FL Support 2
- Wall support
- Cab FR bracket 1
- Cab FR bracket 2
- Cab back inside
- Cab front inside mesh
- Cab front inside surface
- Wall support 2
- Cab right inside
- Cab connection
- Undercab center beam
- Undercab main beam mesh
- Undercab roller connection bottom
- Undercab roller connection front bracket
- Undercab roller connection left flange
- Cab floor inside surface
- Cab floor inside main floor
- Cab left inside
- Top body assembly
- Bottom plate connection
- Right plate connection
- Left plate connection
- Top latch assembly
- Top beam shells
- Inner door
- Inner door piece 2
- Outer channel
- Undercab roller connection casing
- Arm Support
- Door latch base

Figure 10-1 shows different perspectives of the original COE DoS cabin model and the morphed conventional model.

Original COE DoS Cabin

Morphed Conventional DoS Cabin



Figure 10-1 Original COE DoS cabin vs. morphed conventional cabin models.

Original COE DoS Cabin

Morphed Conventional DoS Cabin

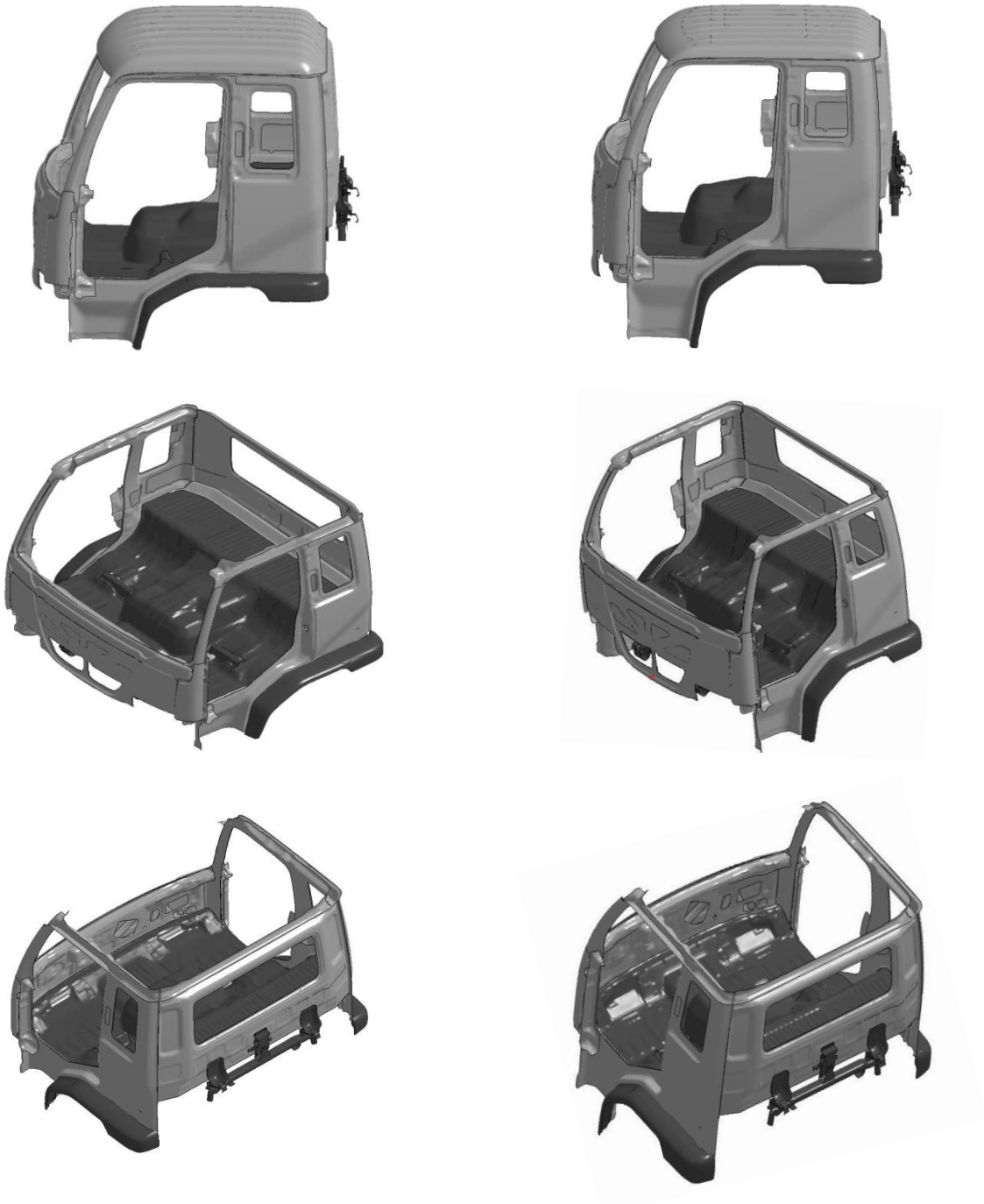


Figure 10-1 Interior views of original cabin vs. morphed cabin models (Continued).

10.1.3 Cloud point modeling

Cloud points were used as a basis for the 3-D development of the frontal interior of the truck. UMTRI used scanners and probes over the interior pieces of an actual truck to create an outlined image of cloud points on the computer. These dotted images were then used to create the finite element model employed in the computer simulations. Figure 10-2 gives views of the original cabin interior cloud point's scans provided by UMTRI. Figure 10-3 shows the surfaces of the conventional cabin model when superimposed to the cloud points.

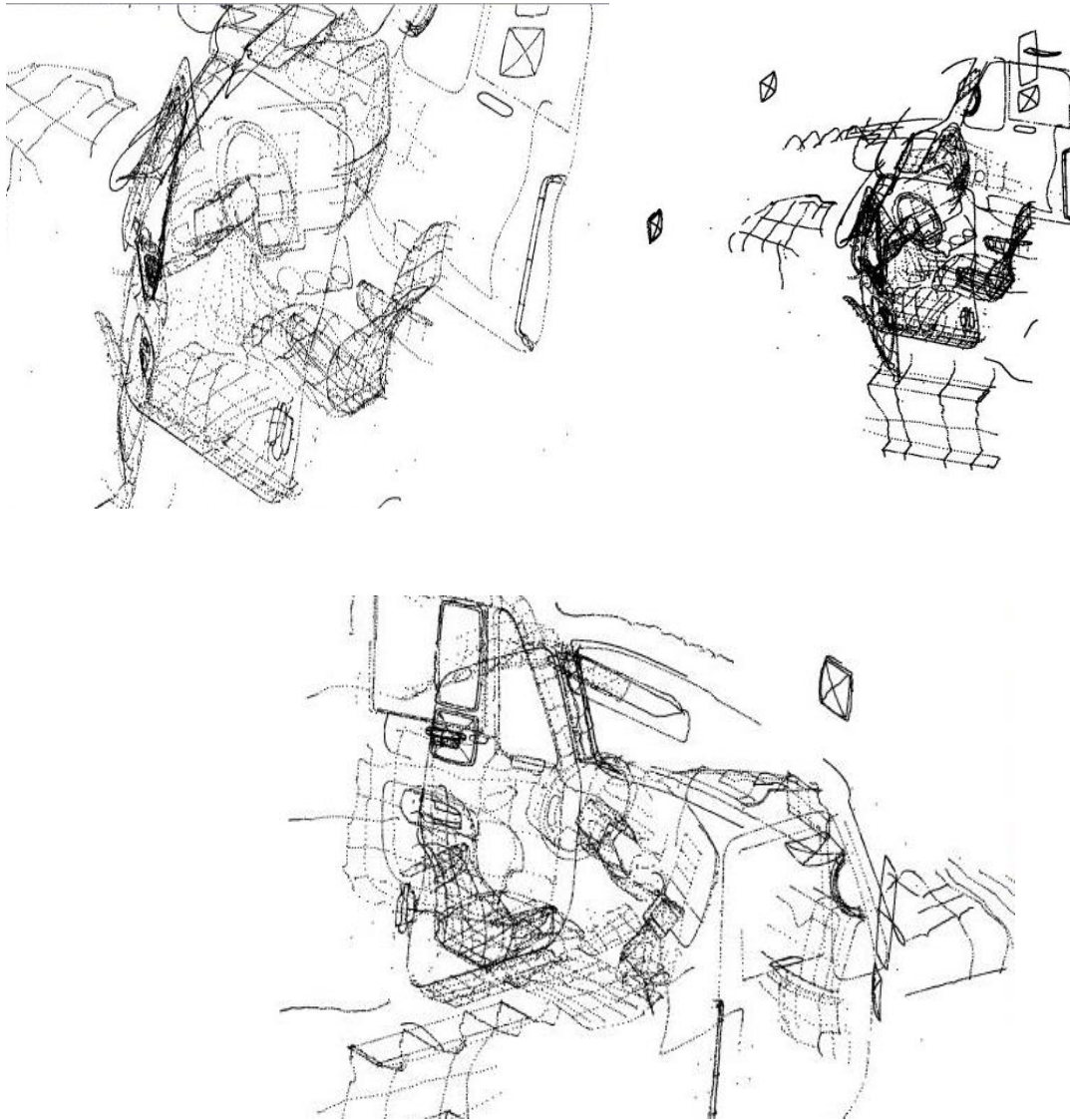
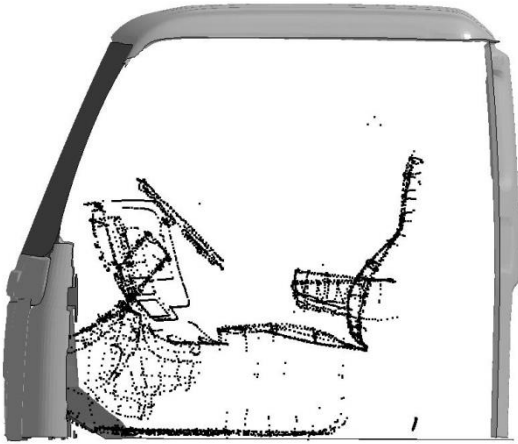
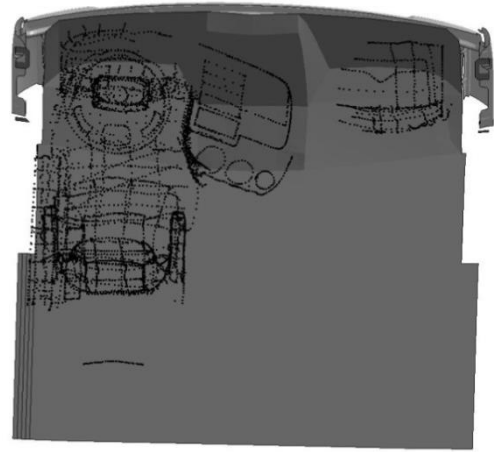


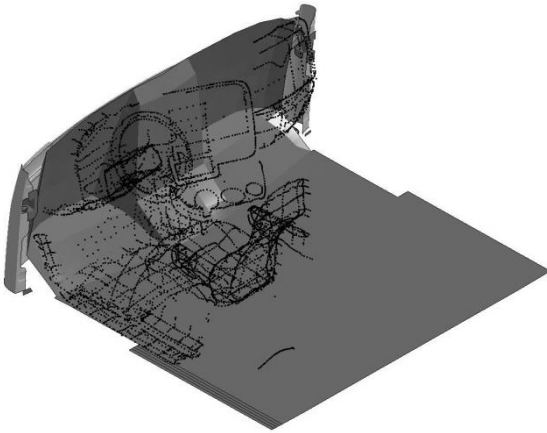
Figure 10-2 UMTRI provided interior cloud points.



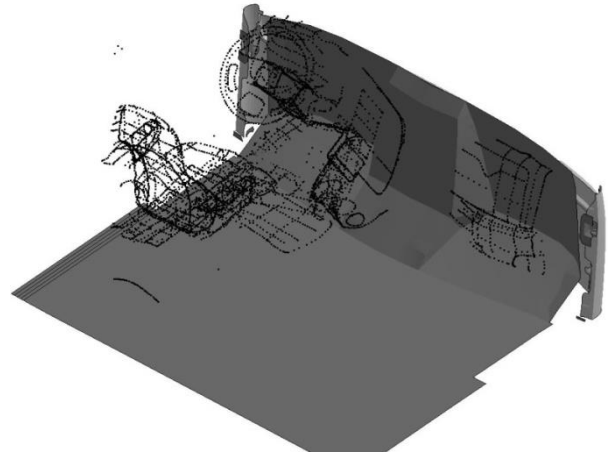
(a) Side View



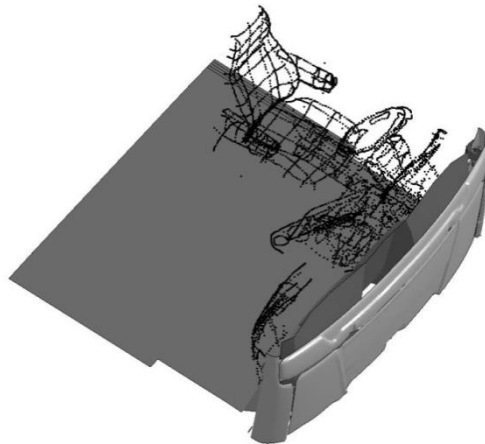
(b) Top View



(c) Left View



(d) Right View



(e) Frontal View

Figure 10-3 Cloud points with cabin.

10.1.4 Surface modeling

A mesh grid was applied over the image using LS-PrePost software to create a 3-D computer model. Figure 10-4 shows steps of this process to specifically create the seat surfaces. This same methodology was employed to complete the surfaces for all other modeled cabin parts (Figure 10-5). The cloud points were used as a reference to apply surfaces to these other parts of the interior.

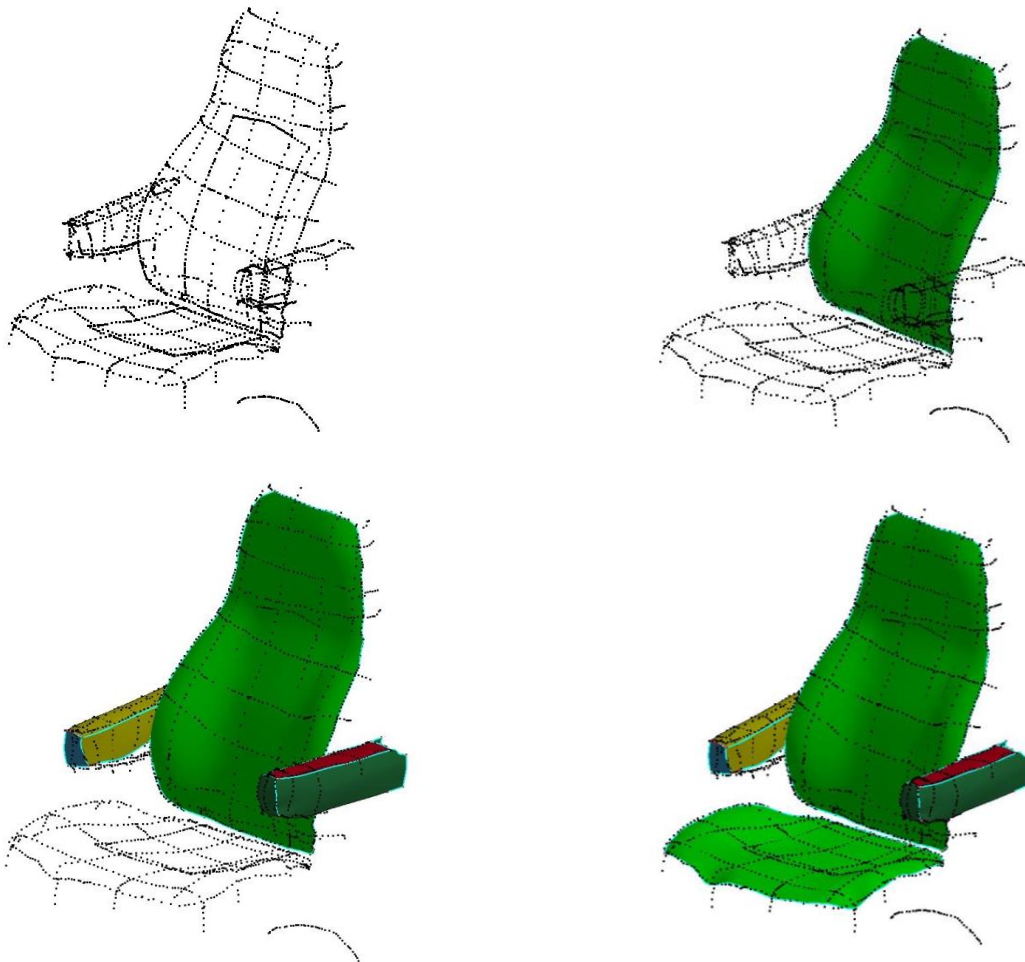
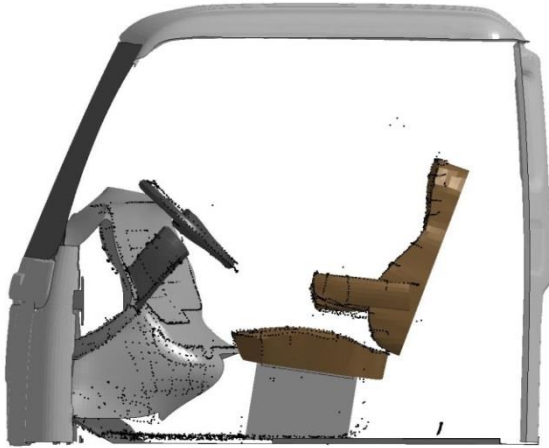
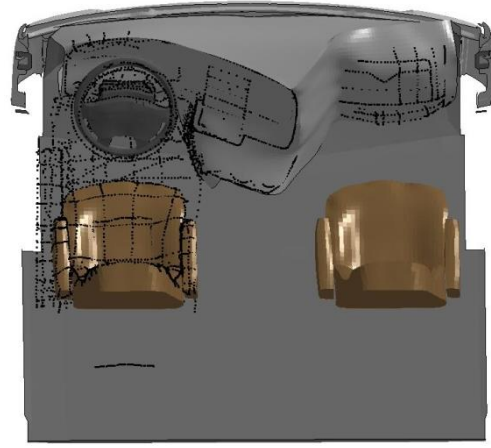


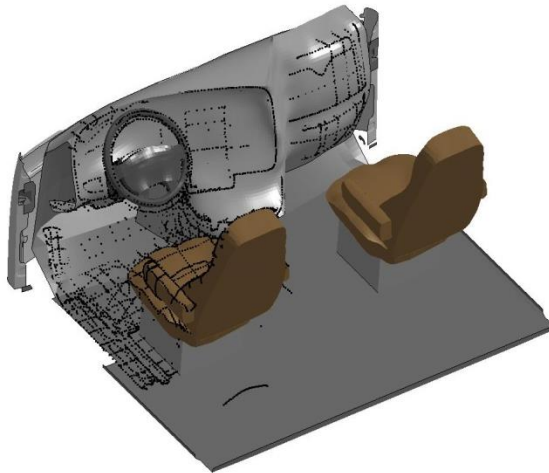
Figure 10-4 Mesh grid step application process.



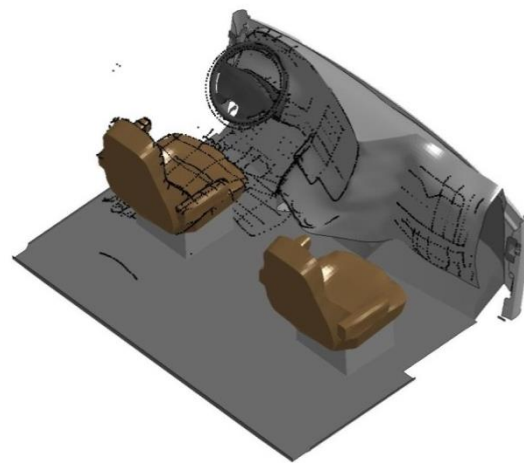
(a) Side View



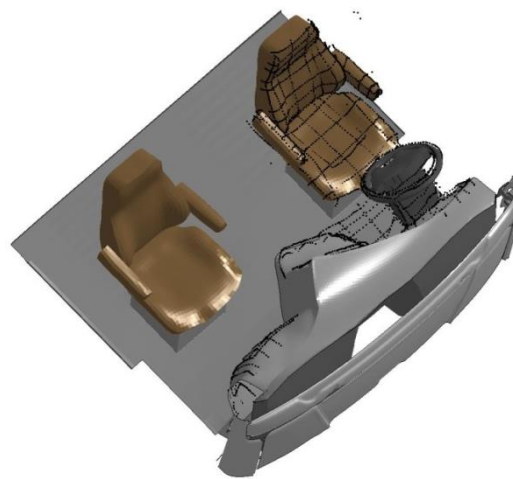
(b) Top View



(c) Left View



(d) Right View



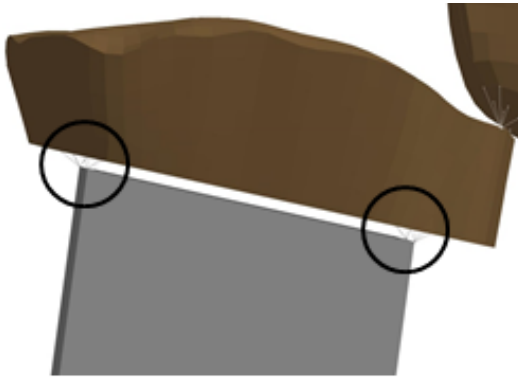
(e) Frontal View

Figure 10-5 Perspectives of cloud points with surfaces in cabin.

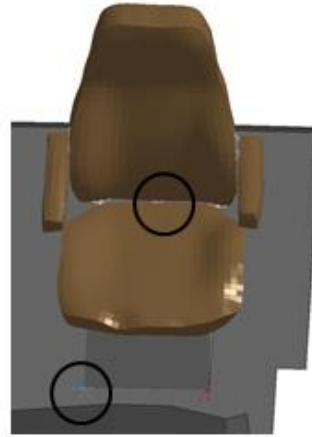
10.1.5 Connection modeling

There were three distinct methods used to create smooth connections between the meshed surfaces of the interior pieces and the surface of the cabin in LS-Post: constrained nodal rigid bodies (Table 10-1), spot-welds (Table 10-2), and beam spot-welds (Table 10-3).

Table 10-1 Parts Connection using constrained nodal rigid body.



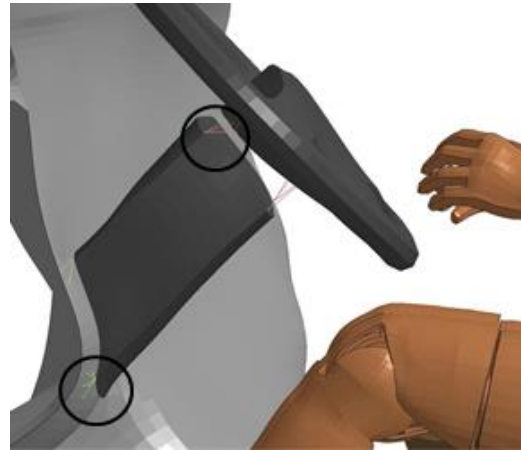
(a) Box Seat and seat bottom



(b) Seat parts



(c) Seat and floor



(d) Steering wheel and Column

Table 10-2 Parts connections using constrained spotweld.

Driver Windshield

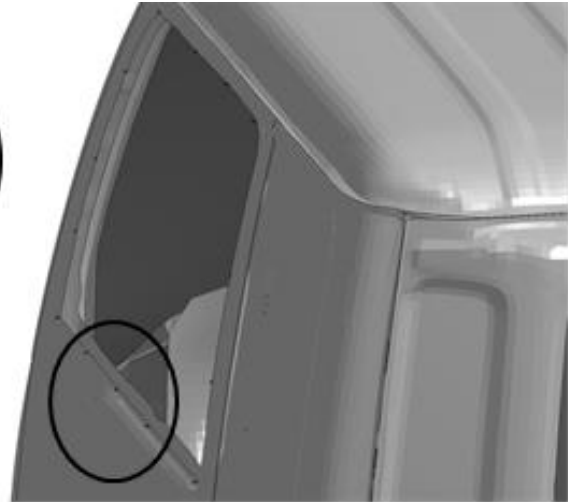
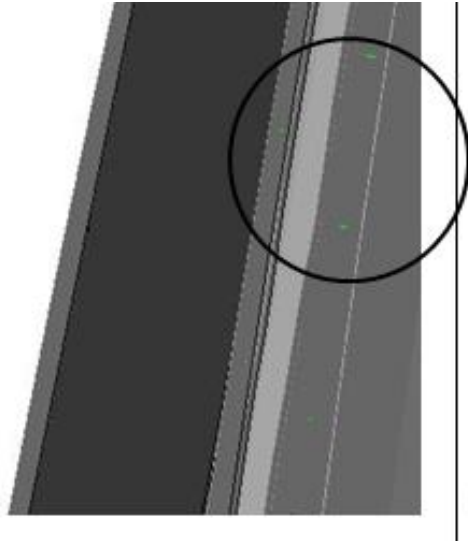
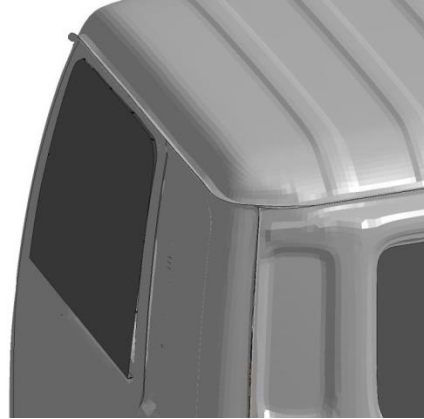
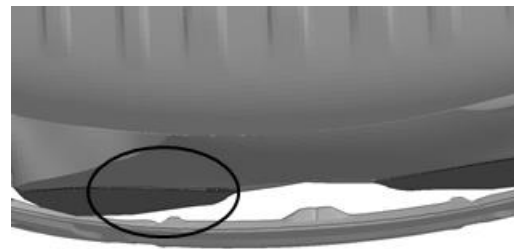
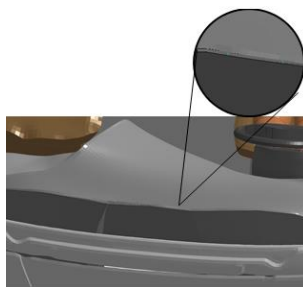
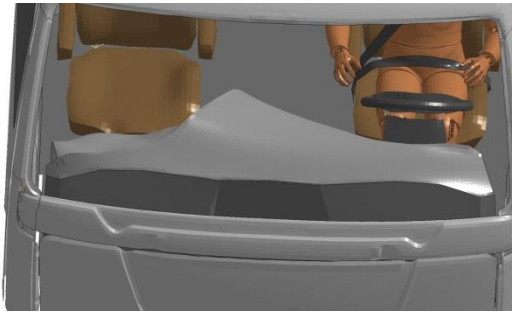


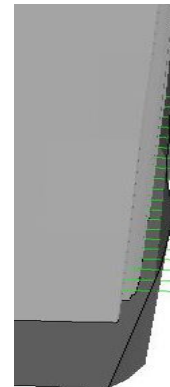
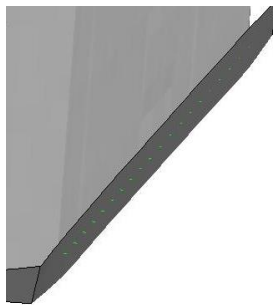
Table 10-3 Parts connections using beam spotweld.

Dashboard



(a) Front cabin and dashboard

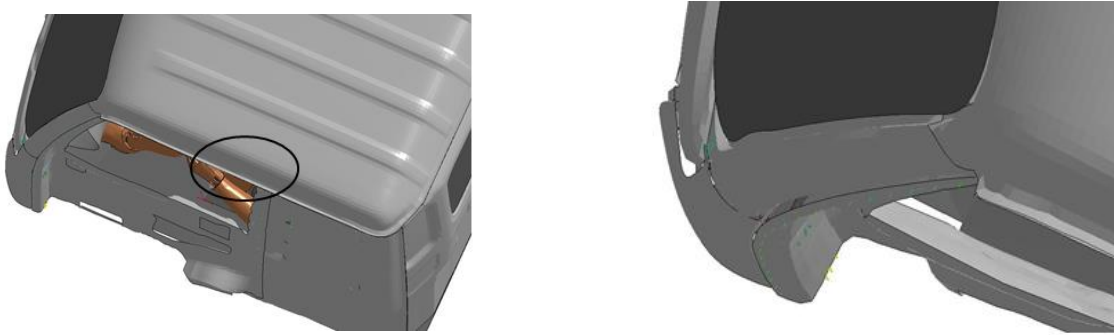
Floor



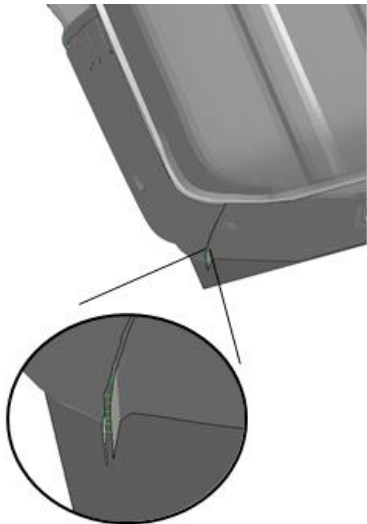
(b) Floor to back of cabin

Table 10-3 Parts connections using beam spotweld (Continued).

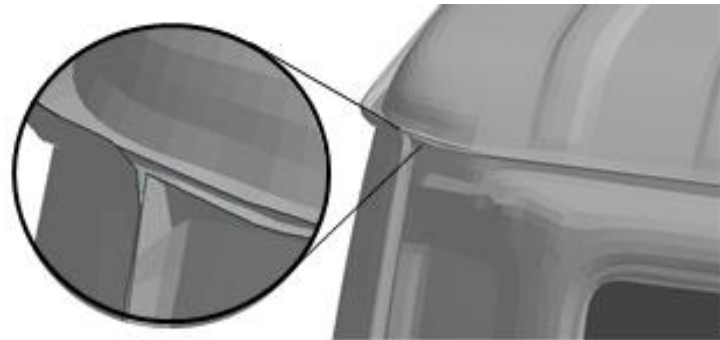
Driver Door



Cabin



(c) Front and back of cabin



(d) Top and back of cabin

10.1.6 Crash test dummy finite element model

A finite element model of the Hybrid III (H3) 50th percentile male anthropomorphic test device (ATD) (also called dummy) was selected for employment in the study's computer modeling and simulations. The dummy model used in this project's simulations was provided by the Livermore Software Technology Corporation (LSTC). This finite element H3 model includes models of accelerometers located at critical body locations (head, chest, pelvis, left and right femur, and left and right tibia). The H3 dummy provides an adequate model to evaluate injury criteria for frontal collisions. Figure 10-6 shows different views of the H3 finite element dummy model along with accelerometer locations.

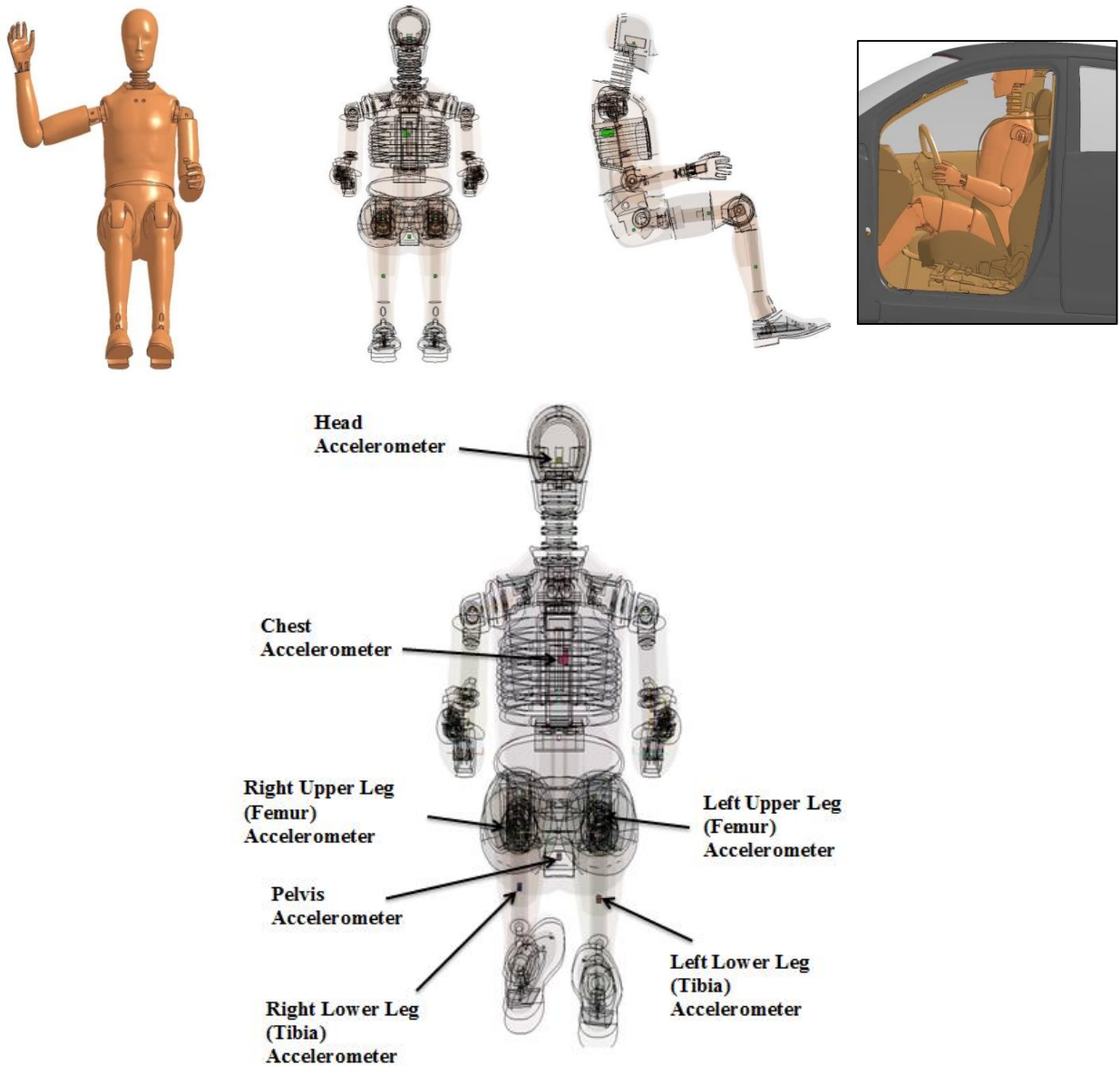


Figure 10-6 Hybrid III 50th percentile male dummy.

10.1.7 Statistics on frontal impacts drivers injury severity

A statistics report on different types of frontal impacts and the severity of collisions for drivers in conventional cab, tractor-semitrailers (CCTS) was provided as part of this research study. Table 10-4 shows the weighted distribution of drivers in conventional cab, tractor-semitrailers involved in frontal collisions. The table is classified by most severe injury to the driver. This focus of this research study is to prevent injuries with a degree of severity within “severe to maximum severity” range. Table 10-4 shows that the frequency of injuries and degree of severity are inversely related. About 53.9% of all drivers of frontal impact collisions walked away with no injuries. However, the highly severe injuries are more likely to lead to death, and therefore call for a greater need of the development of better safety equipment.

Table 10-4 Frontal collision injuries for CCTS drivers based on severity.

Degree of Severity	Frequency (#)	Percent (%)
0- No Injury	21,968	53.9
1- Minor	12,647	31.0
2- Moderate	3,475	8.5
3- Serious	1,135	2.8
4- Severe	1,003	2.5
5- Critical	308	0.8
6- Maximum	199	0.5
Injury Unknown Severity	50	0.1
Total	40,784	100.0

Table 10-5 lists the weighted frequencies based on injury source by belt use upon frontal impact for CCTS drivers. The table includes all injury severities. The injury sources were sorted according to three levels of restraints of drivers: belted, not belted and not ejected, and ejected. UMTRI classifies belted as drivers with the shoulder and lap belt. The not belted, not ejected, and ejected categories classify drivers with improper belt usage or without a seatbelt.

The largest number of injuries for belted drivers came from the collision with the steering wheel rim (8,517 injuries). None of the other injury sources came nearly as close to creating that many injuries for belted drivers. The second highest number of injuries for belted drivers came from the belt restraint webbing/buckle (3,746). Other injury sources that closely follow include the left instrument panel, the steering wheel, and the seat back support. The main causes of injuries are objects that directly entrap the driver or immediately surround the vicinity of the driver. It is

interesting to note that the airbag did not cause any injuries. The data from this table helps prove that a better seatbelt design is needed and that the airbag is a safety design mechanism that does not cause additional harm.

The not belted, not ejected drivers did not have nearly as many injuries from the steering wheel rim as the belted drivers, so the total number of injuries for them was also fewer. Their top injury sources were the left instrument panel, the windshield, the window, and the left side interior surface (around 2,000 injuries each). Although the total number of injuries was fewer than those of the belted drivers, the severity of the injuries for non-belted drivers was probably much higher. For example, all of the injuries for the ejected drivers were listed as a result of making impact with the ground. Direct impact with the ground has a higher probability of death than injuries caused by collision with the cab's interior objects.

Table 10-5 Injury sources of frontal impacts for CCTS drivers based on belt use.

Injury Source	Belted	Not Belted Not Ejected	Ejected	Total
Windshield	600	2,887	0	3,487
Steering wheel rim	8,517	713	0	9,230
Steering wheel (combination of codes 004 and 005)	1,928	1,357	0	3,285
Cellular telephone or CB radio	0	224	0	224
Left instrument panel and below	2,914	2,496	0	5,410
Center instrument panel and below	688	473	0	1,162
Glove compartment door	688	0	0	688
Win. incl. 1/+:fr header,A(A1/A2)-pillar,instr. panel,mirror,or steering assembly(driver)	0	2,205	0	2,205
Left side interior surface, excluding hardware or armrests	524	2,133	0	2,657
Left side hardware or armrest	65	688	0	753
Left B-pillar	412	0	0	412
Left side window glass	0	375	0	375
Left side window frame	250	0	0	250
Lt side win. glass incl. 1/+:frame,win. sill,A(A1/A2)-pillar,B-pillar,or roof side rail	0	375	0	375
Seat, back support	1,364	319	0	1,683
Belt restraint webbing/buckle	3,746	0	0	3,746

Table 10-5 Injury sources of frontal impacts for CCTS drivers based on belt use (Continued).

Injury Source	Belted	Not Belted Not Ejected	Ejected	Total
Head restraint system	204	0	0	204
Interior loose objects (specify)	262	0	0	262
Fold down armrest first row	751	0	0	751
Roof left side rail	33	135	0	168
Roof or convertible top	0	125	0	125
Roof maplight/console	0	24	0	24
Floor (including toe pan)	209	416	0	625
Floor or console mounted transmission lever, including console	0	424	0	424
Foot controls including parking brake	290	0	0	290
Other rear object(specify)	262	0	0	262
Airbag	0	24	0	24
Outside hardware(e.g., outside mirror, antenna)	0	125	0	125
Ground	0	0	5,292	5,292
Other vehicle or object (specify)	487	0	0	487
Fire in vehicle	131	0	0	131
Flying glass	166	0	0	166
Other noncontact injury source (specify)	388	0	0	388
Injured, unknown source	0	0	0	0
Unknown injury source	2,094	3,636	0	5,730
Total	26,977	19,157	5,292	51,426

Table 10-6 gives an overall summary of the percentages of injuries for each injury source. Injuries caused by the steering wheel accounts for almost a quarter of all injuries. Designing a seatbelt that will prevent the upper part of the driver to fall too far forward, but without creating too much stress on the driver would be the most effective design.

Table 10-7 shows the weighted counts of injuries for each injury source based on body part for all CCTS drivers. The totals for all CCTS drivers, for just belted drivers, and for not belted, not ejected drivers are listed at the bottom of the table. Table 10-7 shows that the face (13,882) and upper extremities (11,231) encountered the highest number of injuries out of all the body parts for all drivers. The belted and not belted, not ejected drivers also showed similar results, with

the face (4,428 for non-belted and 8,788 for belted) having the highest number of injuries. Most of the injuries to the face came from impact with the steering wheel rim, which was listed as the highest injury causing source from the previous table. The upper extremities (4,629) showed the second highest number of injuries for not belted, not ejected drivers. The second highest number of injuries for belted drivers was on the lower, not upper extremities. Most of these injuries for the upper and lower extremities were caused by the left instrument panel. The belt restraint caused injury to the upper extremities as well.

Overall, the face and upper and lower extremities are the areas that lead to the highest number of injuries during frontal impacts.

Table 10-6 Percentages of injury sources based on belt use for CCTS drivers.

Aggregated injury source	Belted	Not belted, not ejected	Ejected	Total
Windshield, front header, sun visor	2.2	15.3	0.0	6.8
Flying glass	0.6	0.0	0.0	0.3
Steering wheel	38.7	10.9	0.0	24.4
Instrument panel	15.9	15.7	0.0	14.2
Windshield, A pillar etc.	0.0	11.6	0.0	4.3
Left roof rail	0.1	0.7	0.0	0.3
Left side, any	4.6	18.9	0.0	9.4
Other roof	0.0	0.8	0.0	0.3
Seat back, head restraint mount	5.8	1.7	0.0	3.7
Any belt	13.9	0.0	0.0	7.3
Other interior	4.7	2.4	0.0	3.4
Exterior object	1.8	0.7	100.0	11.5
Noncontact, including fire	1.9	0.0	0.0	1.0
Floor, foot controls	1.9	2.2	0.0	1.8
Unknown	7.8	19.2	0.0	11.2
Total	100.0	100.0	100.0	100.0

Table 10-7 Injury source of body part for CCTS drivers in frontal impacts.

Injury Source	Head	Face	Neck	Thorax	Abdomen	Spine	Upper Extremities	Lower Extremities	Unspec.
Windshield	884	713	138	0	0	0	1,622	131	0
Steering wheel rim	260	7,353	0	263	46	138	1,188	46	0
Steering wheel (combination of codes 004 and 005)	0	815	0	1,804	60	600	6	0	0
Cellular telephone or CB radio	154	70	0	0	0	0	0	0	0
Left instrument panel and below	0	0	0	0	0	0	3,042	2,400	0
Center instrument panel and below	148	148	0	0	148	0	28	688	0
Glove compartment door	0	0	0	0	0	0	688	0	0
Win. incl. 1/+:fr header,A(A1/A2)-pillar,instr. panel,mirror,or steering assembly(driver)	1,103	965	0	0	0	138	0	0	0
Left side interior surface, excluding hardware or armrests	0	0	0	2,133	0	50	474	0	0
Left side hardware or armrest	0	0	0	0	688	65	0	0	0
Left B-pillar	391	0	0	0	0	0	21	0	0
Left side window glass	125	250	0	0	0	0	0	0	0
Left side window frame	125	125	0	0	0	0	0	0	0
Lt side win. glass incl. 1/+:frame,win. sill,A(A1/A2)-pillar,B-pillar,or roof side rail	0	0	0	0	0	0	375	0	0
Seat, back support	0	0	0	69	69	1,030	161	474	0

Table 10-7 Injury source of body part for CCTS drivers in frontal impacts (Continued).

Injury Source	Head	Face	Neck	Thorax	Abdomen	Spine	Upper Extremities	Lower Extremities	Unspec.
Belt restraint webbing/buckle	0	0	0	894	907	84	1,078	783	0
Head restraint system	204	0	0	0	0	0	0	0	0
Interior loose objects (specify)	131	0	131	0	0	0	0	0	0
Fold down armrest first row	0	0	0	0	0	688	63	0	0
Roof left side rail	101	68	0	0	0	0	0	0	0
Roof or convertible top	125	0	0	0	0	0	0	0	0
Roof maplight/console	0	24	0	0	0	0	0	0	0
Floor (including toe pan)	69	347	0	0	0	0	0	209	0
Floor or console mounted transmission lever, including console	0	0	0	297	128	0	0	0	0
Foot controls including parking brake	0	0	0	0	0	0	0	290	0
Other rear object(specify)	131	131	0	0	0	0	0	0	0
Airbag	0	0	0	0	0	0	24	0	0
Outside hardware(e.g., outside mirror, antenna)	125	0	0	0	0	0	0	0	0
Ground	1,512	0	0	0	0	1,512	1,512	756	0
Other vehicle or object (specify)	0	0	0	0	0	0	281	206	0
Fire in vehicle	96	0	0	32	0	0	131	0	32
Flying glass	0	50	0	0	0	0	117	0	0

Table 10-7 Injury source of body part for CCTS drivers in frontal impacts (Continued).

Injury Source	Head	Face	Neck	Thorax	Abdomen	Spine	Upper Extremities	Lower Extremities	Unspec.
Other noncontact injury source (specify)	0	0	0	0	0	317	0	131	0
Injured, unknown source	161	485	0	208	70	0	70	208	0
Unknown injury source	1,919	2,339	0	773	1,268	262	351	663	939
Total	7,767	13,882	269	6,473	3,385	4,885	11,231	6,986	971
Total for Belted	2,047	8,788	131	2,167	907	2,077	4,809	5,361	688
Total for Not belted, not ejected	3,823	4,428	138	3,463	1,108	1,114	4,629	204	250

In conclusion, the steering wheel, instrument panel, and the left side are causes of a high number of injuries regardless of belt use. The face and upper and lower extremities are the areas most affected by these injury sources. By reviewing the above reported data, a better idea was provided in terms of which components were needed for inclusion in the finite element model of the heavy truck occupant compartment.

10.2 Finite element seatbelt model development

An LS-DYNA finite element model of a three-point belt system was developed and modeled as a load-limiting seatbelt. The belt system consists of general 1D seatbelt elements and 2D shell elements. Also, several specialized elements were used to model specific parts of the seatbelt such as the pretensioner, retractor, and D-ring.

The general seatbelt element is represented with a material that contains loading and unloading curves based on force vs. engineering strain. Figure 10-7 represents the material curves used in this study. The beam-like elements exert force only in tension and generate zero force whenever the strain is negative.

UMTRI researchers provided a working FE model of a seatbelt and the material, retractor, and pretensioner curves were implemented in the seatbelt model used in this study.

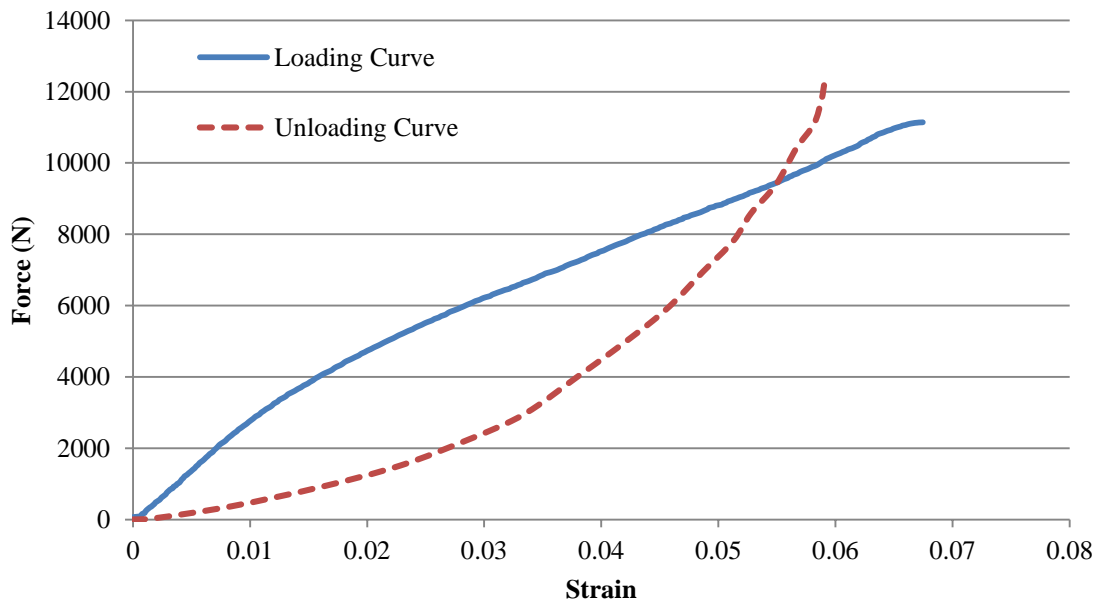


Figure 10-7 Belt material force versus strain loading and unloading curves.

A load-limiting belt system is modeled through the use of a retractor system. Retractors operate in two different ways and allow belt material to be paid out or reeled in. The first way in which a retractor operates is in the unlocked role, which is when belt material is paid out, or reeled in under constant tension. The second way a retractor operates is the locked role, where a user-defined force-pullout curve applies. A seatbelt sensor element fires and acts on a retractor causing it to enter into a locked state and allowing the force-pullout relationship to take over. Typically, seatbelt sensors fire after a specified time after the simulation has begun. This

approach for seatbelt sensors was similarly used for this study. Figure 10-8 shows the force-pullout curve applied to the seatbelt. The retractor will follow the loading curve in tension and will follow the unloading curve when no tension is in the belt. When the belt is in tension the retractor will give out belt material by lengthening the last element attached to the retractor. The last element will lengthen based on the force-pullout relationship of the retractor.

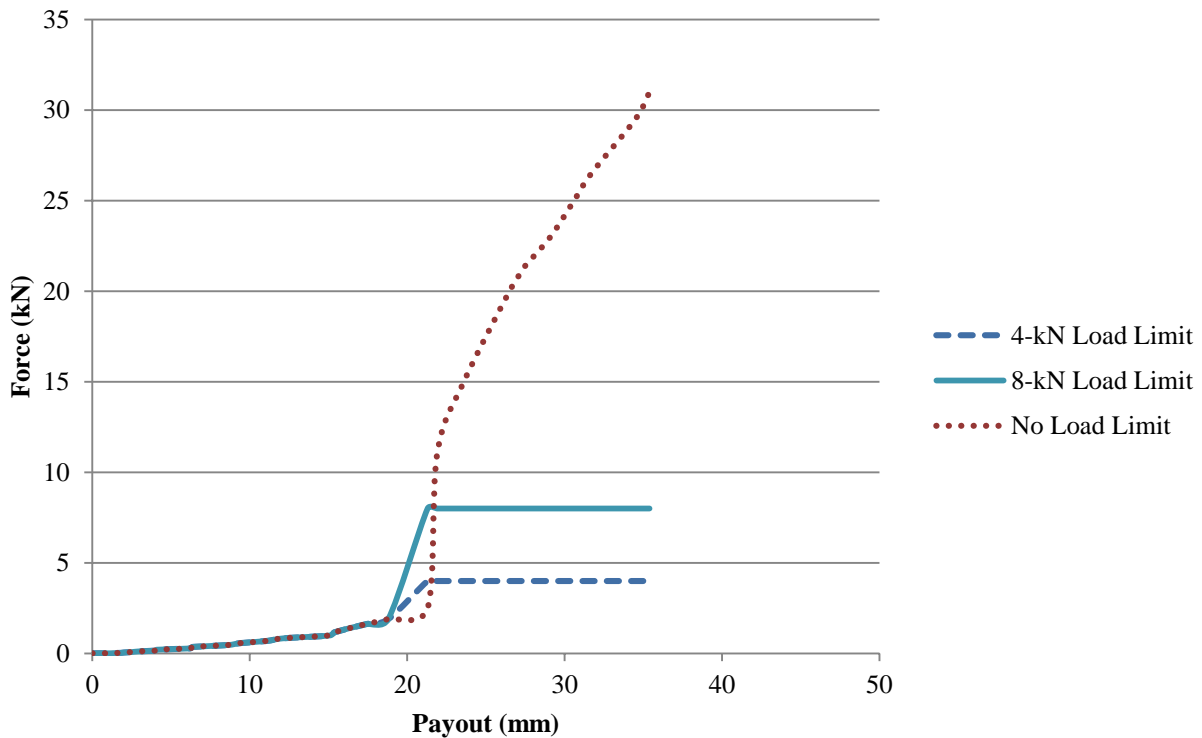


Figure 10-8 Seatbelt retractor curves representing force versus payout.

The retractor curves were determined based on highest belt force expected during the simulation which was around 11 kN with no load limit. The no load limit curve is used to represent this case. The 4-kN load-limit curve is a relatively low limit and will allow for much higher payout of belt material during the simulation. The 8-kN load-limit curve represents approximately 70% of the expected maximum tension and is a medium level for the force limit. These force-payout curves were provided by UMTRI.

A pretensioner was used in conjunction with the retractor and controls seatbelt elements to remove initial slack. Similar to the retractor, the pretensioner fires based on of a timed seatbelt sensor. Shortly after the retractor engages and locks the pretensioner fires and engages and pulls in belt material to create 1.8 kN of tension in the belt. Once the tension in the belt reaches 1.8 kN the pretensioner disengages and the retractor takes over again. Table 10-8 shows a step-by-step process of the retractor and pretensioner working together.

Table 10-8 Process for seatbelt modeling of retractor and pretensioner.

Event	Action
1 ms	Retractor sensor fires – enters locked mode
10 ms	Pretensioner sensor fires – enters locked mode
1.8 kN tension reached	Pretensioner disengages – retractor active
4 kN tension reached	Load limiter 1 engages (load limit case 1 only)
8 kN tension reached	Load limiter 2 engages (load limit case 2 only)

There are two D-ring elements used in the three-point belt system. One is used for the lap belt and the other is used for the shoulder belt. D-rings allow the seatbelt to be redirected with the option of adding some friction to the moving seatbelt.

The location of the D-ring and anchor positions is very important when modeling a seatbelt. Exact positions were provided by UMTRI as part of the cloud point scans for the D-ring and anchors. After the D-ring and anchor points were set for the FE seatbelt model an LS-PrePost seatbelt fitting tool was used to fit the seatbelt around the dummy chest and pelvis. Figure 10-9 shows the final geometry of the seatbelt and how it fits to the dummy.

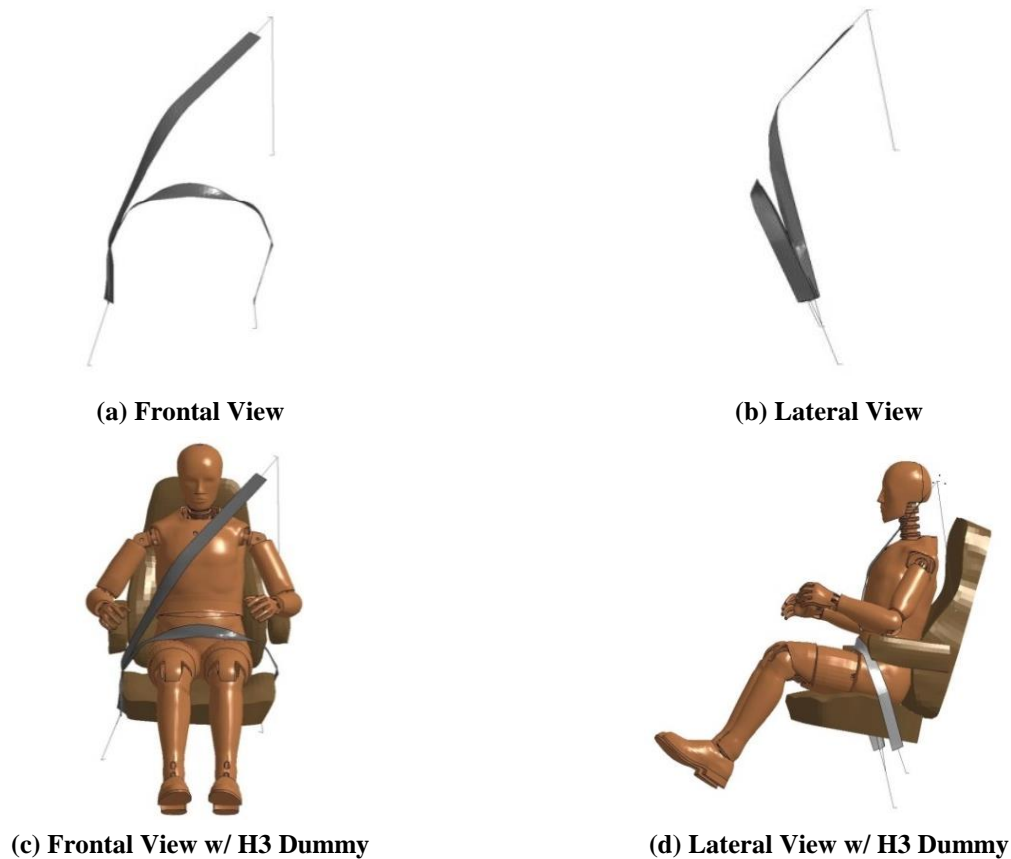


Figure 10-9 Different views of seatbelt and dummy showing seatbelt geometry.

10.3 Finite element airbag model development

10.3.1 Airbag overview

The primary purpose of airbags is to protect passengers in head-on collisions. One airbag is located in the steering wheel column on the driver's side and the other is located in the dashboard on the passenger side. It is a folded nylon bag which becomes inflated with nitrogen gas after impact. According to the Insurance Institute for Highway Safety, the use of airbags with the seatbelt reduced the number of deaths from automobile crashes by 24%. NHTSA now requires that cars made after 1998 contain both driver and passenger side airbags.

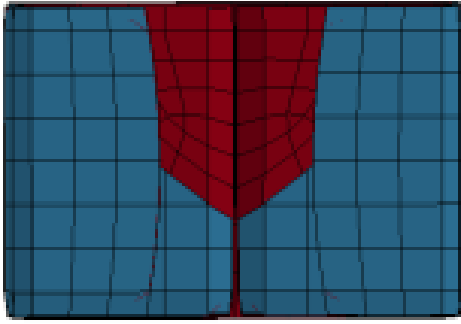
An airbag responds within milliseconds of a crash. It is made up of two systems. The first system is the impact sensor. The airbag deploys when it senses an accident that is greater than or equal to a 10-15 mph crash into a rigid wall. The sensors detect automobile deceleration through two or more deceleration sensors at the front of the car. If the deceleration of the car happens rapidly, the sensors are tripped, sending an electric current to the airbag unit, causing it to deploy.

The airbag control unit comprises the second system. It consists of an inflator assembly, a nylon bag, and a breakaway cover. A mechanical switch is flipped when there is a mass shift that closes an electrical contact. The sensors receive information about it from an accelerometer built into a microchip. The airbag system ignites a solid propellant which burns rapidly to create a large volume of gas to inflate the bag. The addition of the solid propellant ensures that the nitrogen gas reaction is going off at the correct time. The inflation system reacts sodium azide with potassium nitrate to produce nitrogen gas to inflate the bag. Inflation takes an average of 30 milliseconds. When the occupant impacts with the airbag, the gas is forced back through the vents, which takes another 45 milliseconds. Overall, the process is very fast.

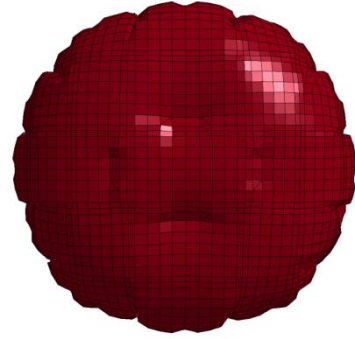
10.3.2 Implementation of the airbag model for use in frontal crash simulations

The National Crash Analysis Center (NCAC) developed a working FE model of a steering wheel and airbag that is publicly available for download on their website. This airbag model was used in our frontal simulation to analyze the effects of an airbag restraint system on occupant injury criteria. Figure 10-10 shows (a) the folded FE airbag before inflation and (b) the fully inflated airbag.

The steering wheel used in the heavy truck cabin has a different geometrical shape relative to the FE steering wheel containing the airbag. Therefore the airbag was placed within our truck cabin steering wheel and connected to the steering wheel in a similar manner. Figure 10-11 and Figure 10-12 compare the NCAC steering wheel to the truck cabin steering wheel.



(a) Folded airbag before inflation process



(b) Inflated airbag

Figure 10-10 Finite element computer model of the airbag.

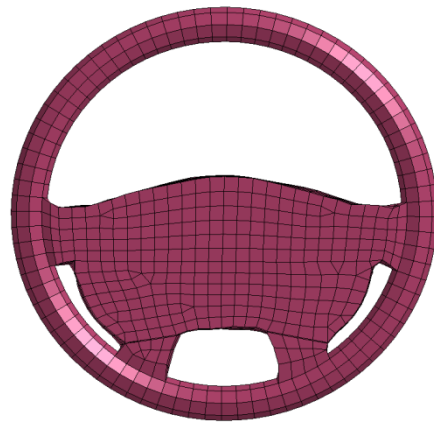
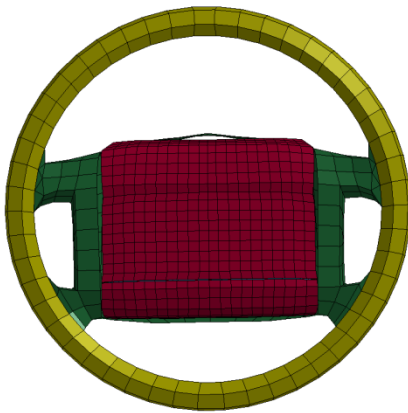


Figure 10-11 Comparison of NCAC FE steering wheel (left) and truck cabin FE steering wheel (right).

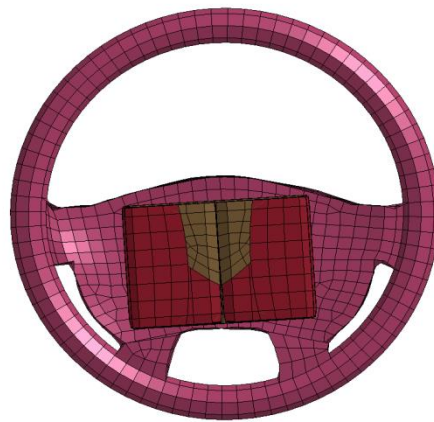
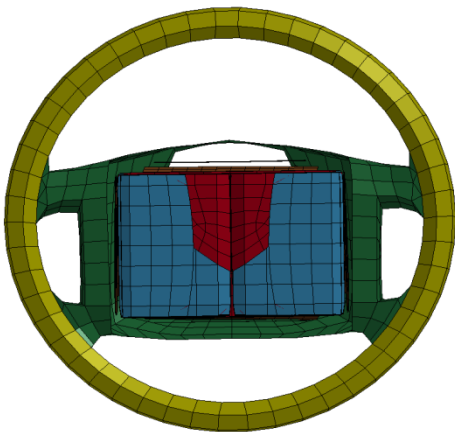


Figure 10-12 Comparison of NCAC FE steering wheel (left) and truck cabin FE steering wheel (right) showing concealed airbag.

According to previous research conducted on airbags, the input curve used to inflate the airbag was developed. Thirty milliseconds after impact the airbag begins to inflate, and it takes approximately 25 milliseconds to achieve full inflation. The airbag inflation input curve from the NCAC model was modified according to those two parameters. Figure 10-13 shows snapshots from one of the frontal simulations where the airbag model was implemented. The airbag was only implemented and analyzed for the frontal crash scenario.



(a) 0.03 sec, airbag starts to inflate



(b) 0.08 sec, airbag fully inflated

Figure 10-13 Frontal simulation at time 0.03 seconds where airbag begins to inflate.

10.4 Frontal simulation methodology

10.4.1 Methodology introduction

The purpose for conducting the frontal crash simulation is to analyze restraint systems and their effect on occupant injury criteria. As previously discussed, a truck cabin model with interior components was developed for use in the frontal simulation. Also, a publicly available FE tractor-trailer model was used to generate the crash pulse used in the frontal simulation. The step-by-step methodology performed to develop a successful FE frontal crash simulation is described next.

A significant input for the frontal crash simulation was the impact speed. Currently there are no standards for heavy truck frontal impact crash testing and as a result there is no standard impact speed. Originally, researchers selected the impact speed to be 50 mph, which was based on average impact speed in crash data analysis of heavy truck crashes. The methodology provided was then conducted at the selected 50 mph impact speed. However, after further discussion and deliberation, researchers decided to change the impact speed to 35 mph. There were several reasons for selecting the 35 mph as the impact speed. The main reason is that Federal Motor Vehicle Safety Standard (FMVSS) 208 and the New Car Assessment Program (NCAP) testing standards set the impact velocity to be between 30 and 35 mph for passenger vehicles. No current standard exists for heavy trucks, so researchers wanted to replicate a similar impact speed to the FMVSS 208 standard. Furthermore, the 50 mph average impact speed determined by crash data analysis did not consider relative velocity of other vehicles. Therefore the deltaV crash history may have been less than the 50 mph impact speed. Researchers included the results from the 50 mph simulations in 0.

10.4.2 Generation and application of crash pulse

Crash pulse application is a major part of finite element crash studies and was used for the purposes of this study. Crash pulses are acceleration or velocity histories from full crash simulations or tests that can be applied to a simplified model to replicate the same full frontal crash scenario. A full scale crash test was simulated with a tractor-trailer model impacting a rigid barrier and the crash pulse generated is later applied to the truck cabin model.

In order to generate the crash pulse for the frontal crash scenario a computer simulation was created that consisted of a FE tractor-trailer model impacting a rigid barrier head on at the specified impact speed.

The tractor-trailer model used to generate the crash pulse was downloaded from the NTRCI website. The FEM models are some of the most advanced publicly available models in terms of material property, and geometric detail. The tractor cabin was a conventional day cabin with a 194 inch wheelbase. The trailer that connects to the tractor has a length of 45 feet. The FEM combined tractor-trailer model consists of 391390 nodes, 345537 elements and 563 parts. Figure 10-14 shows the tractor cabin and combined tractor-trailer FE model.

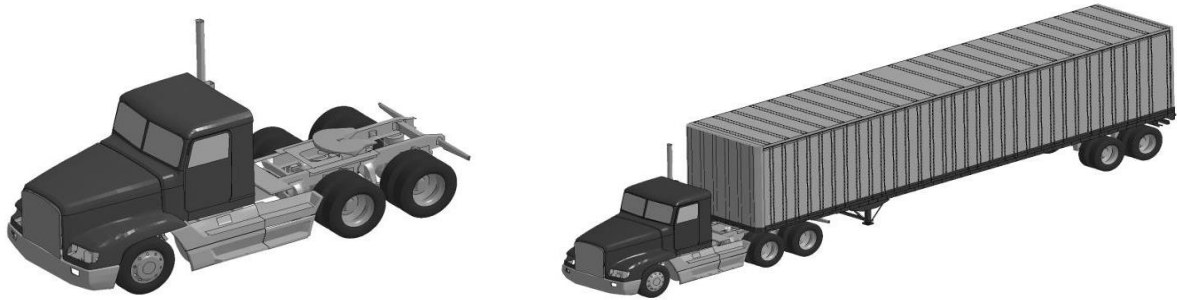


Figure 10-14 FE tractor-trailer model used to develop frontal crash pulse.

From the frontal crash simulation x, y, and z velocities were output at four different locations which represent cab mount connections (Figure 10-15). A node was picked at these four locations to easily output velocity versus time from the simulation. The velocity curves were applied as a crash pulse in our truck cabin model at the same nodes.

Several issues arose with application of the crash pulse to our truck cabin model. The cabin did not correctly follow the x, y, and z velocity curves input by BOUNDARY_PRESCRIBED_MOTION cards. A simplified approach was tried by applying the velocity curve only in the x-direction at each of the four nodes. The velocity in the y and z direction for these nodes was very small and insignificant, so it was an appropriate approach.

There were still some small issues occurring when applying the crash pulse only in the x-direction. The truck cabin was still experiencing major rotation in the y and z direction, which was not accurate. To fix this issue, first the cabin floor was rigidized with MAT_RIGID input card. Second, within the MAT_RIGID card the floor cabin was constrained to not allow rotation and to only allow translational movement. Due to rigidizing the cabin only one overall velocity was applied to the cabin. Figure 10-16 through Figure 10-19 represents the deltaV curves at the center of gravity and acceleration history for the 50 mph and 35mph frontal crash.

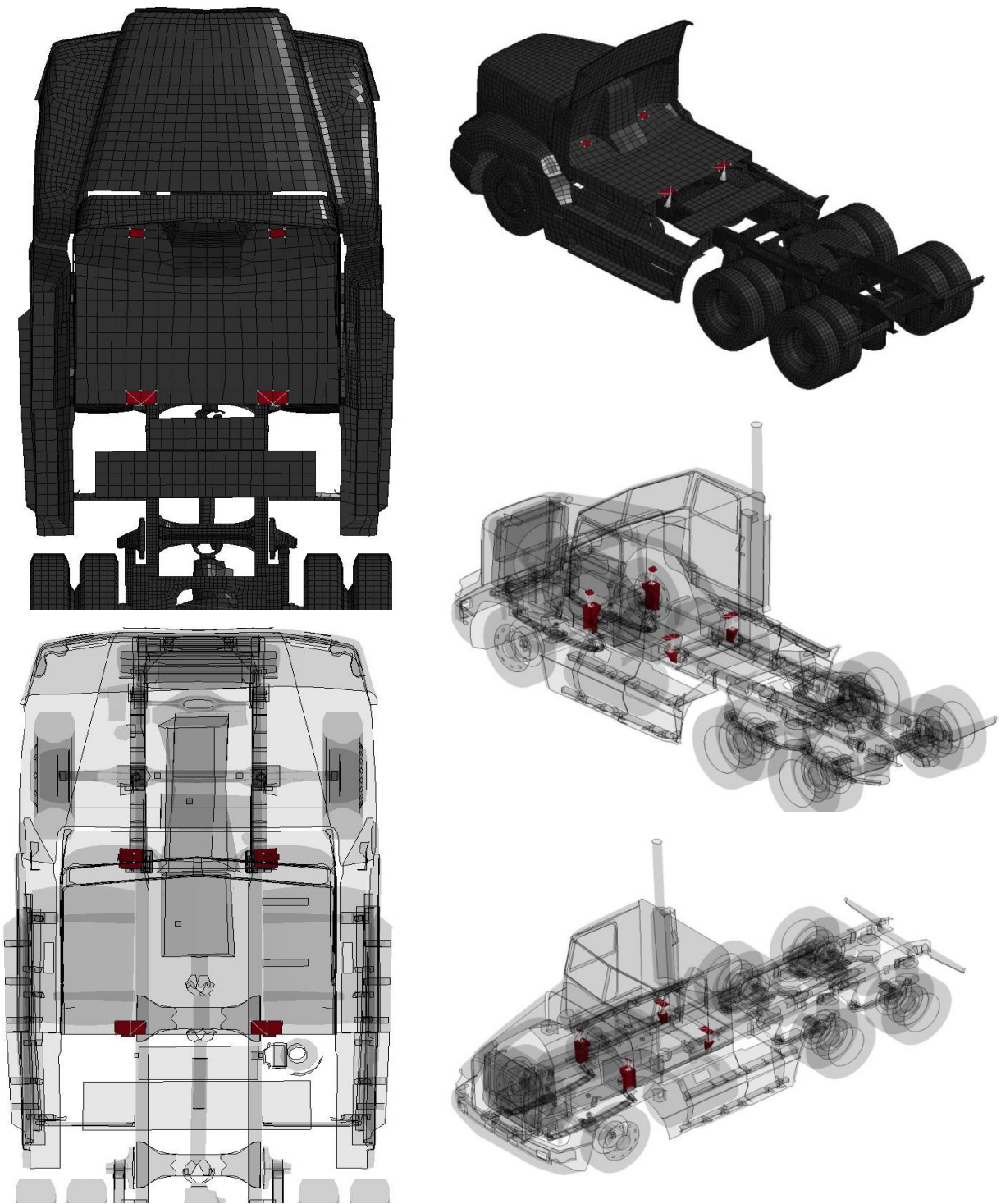


Figure 10-15 Cab mount locations in tractor vehicle for crash pulse application.

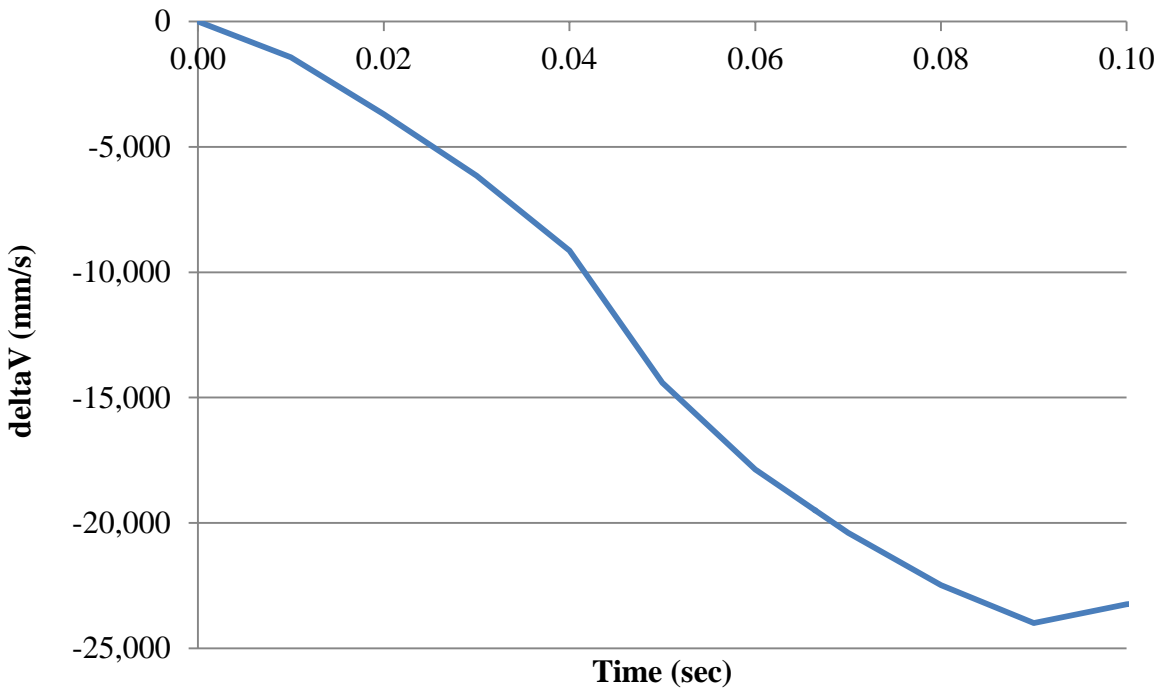


Figure 10-16 50 mph deltaV crash pulse at CG of truck cabin.

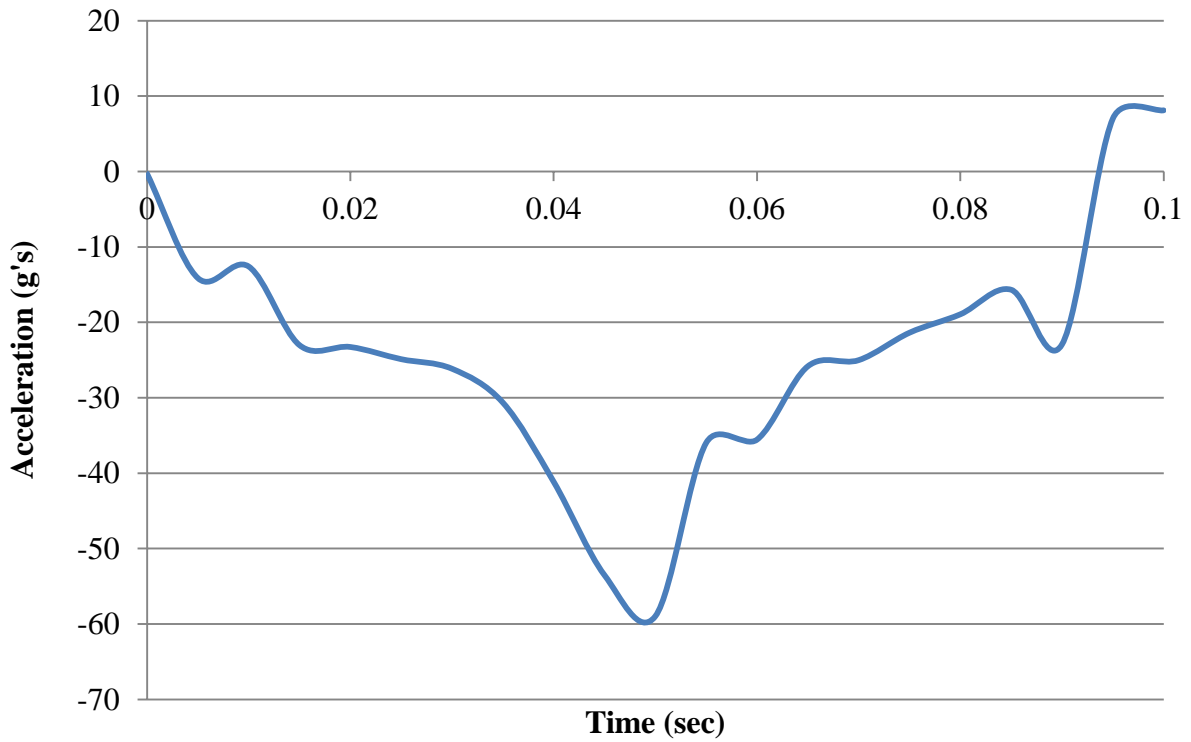


Figure 10-17 50 mph acceleration history at CG of truck cabin.

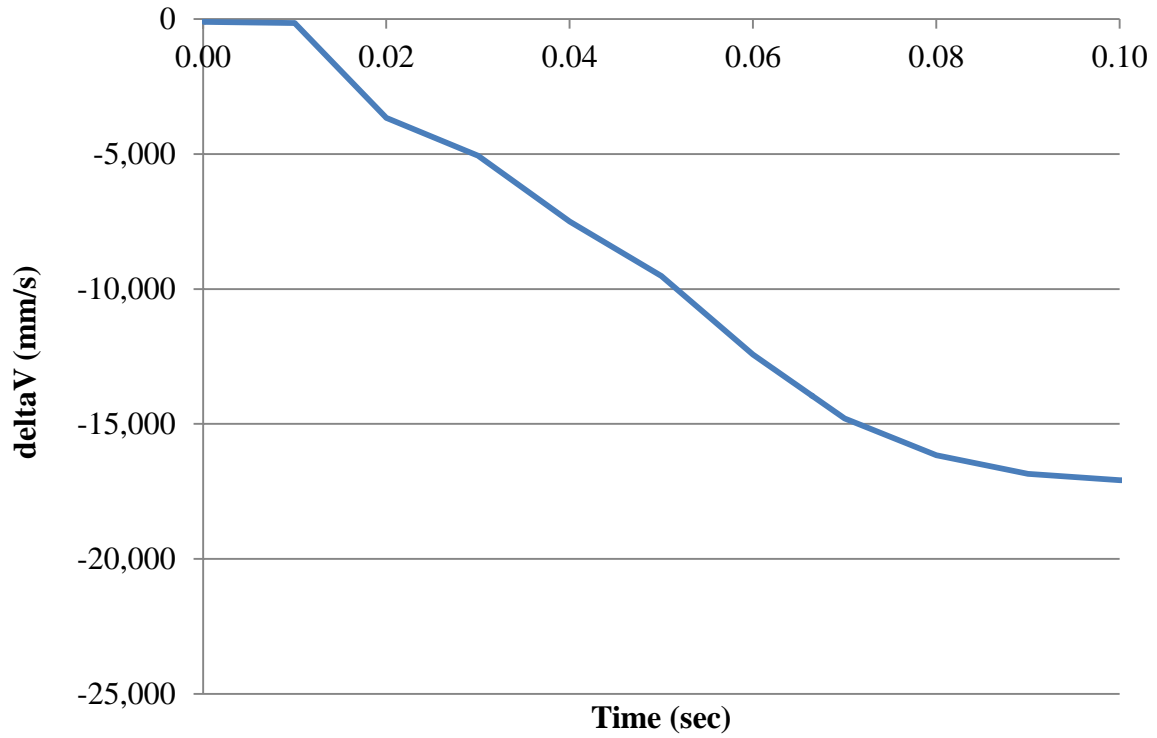


Figure 10-18 35 mph deltaV crash pulse at CG of truck cabin.

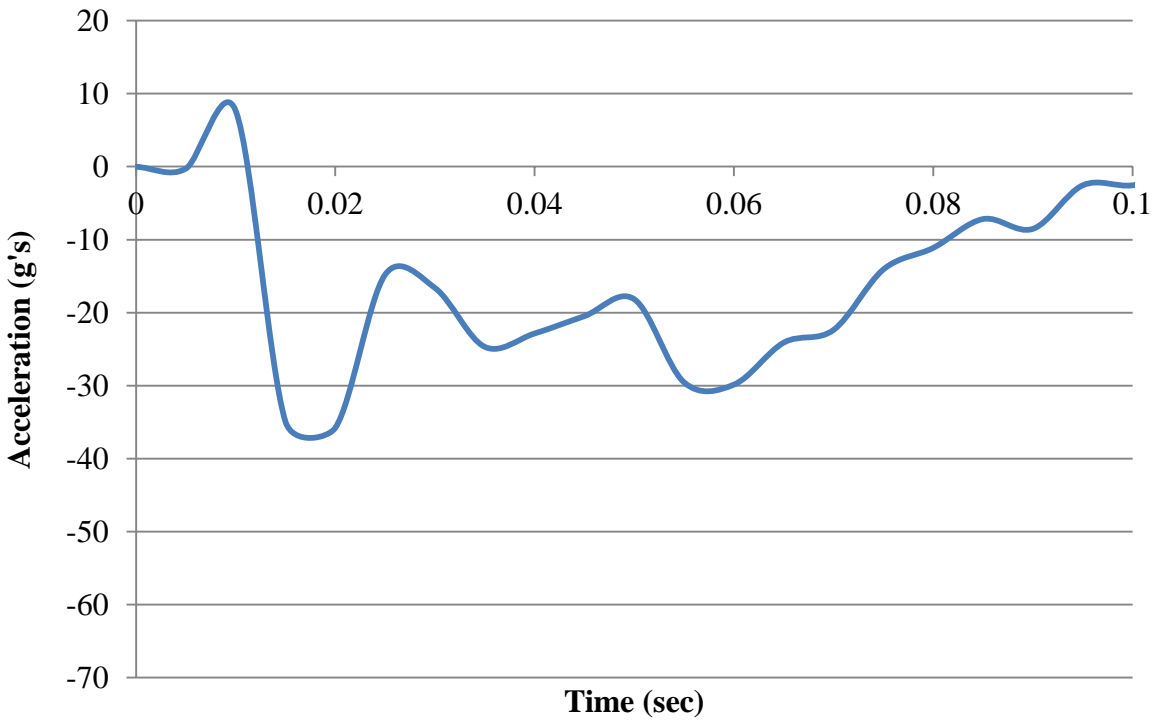


Figure 10-19 35 mph acceleration history at CG of truck cabin.

10.4.3 Contact definition between dummy and truck cabin interior

After developing a successful model that correctly applied the crash pulse to the cabin, the Hybrid III 50th percentile male dummy model was included within the model and positioned on the driver seat. To shorten simulation time the dummy was pre-positioned in the driver seat by conducting a pre-simulation of a dummy sinking into the foam seat. The pre-simulation was conducted according to a step-by-step methodology provided by LSTC. As a result simulations were run that did not have an initial wait time to allow the dummy to sink in to the seat.

In the LS-DYNA program contacts must be defined between all the different parts that are interacting together. The simplest LS-DYNA contacts are AUTOMATIC_SINGLE_SURFACE and AUTOMATIC_SURFACE_TO_SURFACE, which were both used for a majority of the different contact interactions. Contact interactions are influenced by a number of input parameters and material properties of the individual parts.

Several complications were faced when defining contact between the dummy and the truck cabin. This was due to the fact that the material properties that were assigned to a majority of the cabin interior components were not validated. The material properties that were assigned to the cabin interior were taken from a FE Toyota Yaris model with interior components that were not validated.

The first issue was contact between the dummy feet and the floor pedals. Originally we tried to model the dummy with the right foot resting on the brake pedal and the left foot resting behind the clutch pedal (Figure 10-20). This approach was unsuccessful because there was a high impact between the left foot and the clutch pedal, which produced negative volume error terminating the simulation early. Negative volume error occurs simply when a solid element experiences large deformation and the volume of the element becomes less than zero. We then decided to move the left foot to the left of the clutch pedal, so that it was resting near the door. This approach did not work because the dummy was not flexible enough to rotate its leg to the left. Finally we decided to remove the clutch pedal and move the left foot to the original position (Figure 10-21). The contact between the pedals and the feet was successful with this approach; however it does result in some high lower tibia forces for the left foot. This is later explained in the results section but is not a serious issue that needs to be fixed.

Another issue was the contact between the knees of the dummy and the dashboard area. Again this issue was due to the drastic difference in stiffness between the dummy knees and dashboard. The solution to the problem came by a trial and error process. Several different reasonable approaches were tried each resulting in some type of error in the simulation until a final approach was produced that resulted in successful interaction between the dummy knees and the dashboard. A brief summary of some of the major approaches tried is provided.

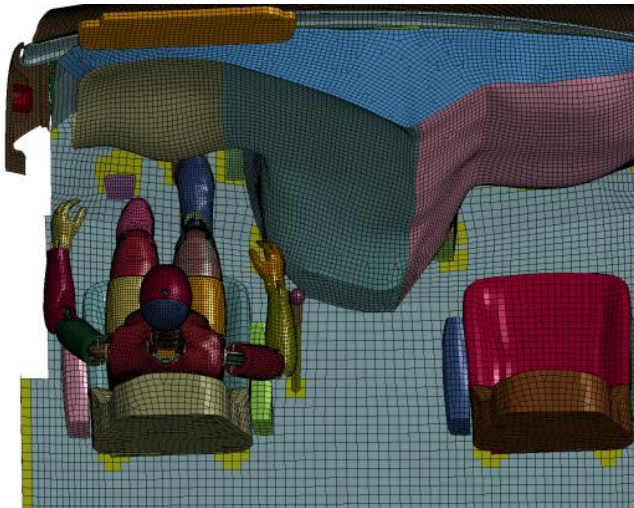


Figure 10-20 Dummy left foot resting behind clutch pedal.

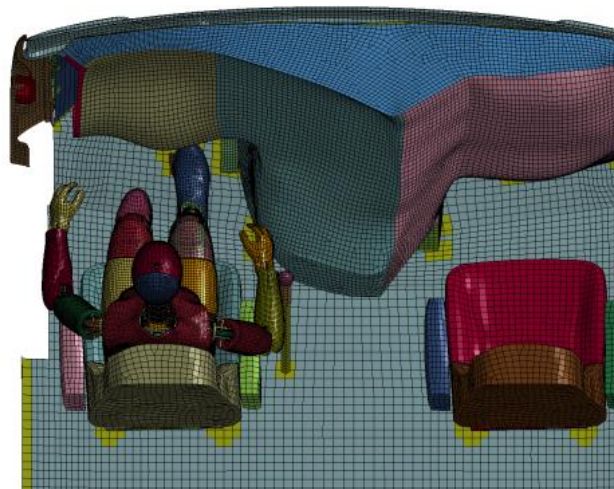


Figure 10-21 Dummy left foot resting on floor with no clutch pedal.

Because the issue was coming from the difference in material stiffness, the modulus of elasticity was lowered for the dashboard part to allow for less difference between the knees and the dashboard. This approach produced a more realistic result as far as contact interaction but did create another problem with large unrealistic deformation of the dashboard (Figure 10-22). It was determined that the dashboard was not connected adequately to prevent such large deformations upon impact of the dummy knees. In order to combat this issue, the left side of the dashboard was rigidly constrained to the neighboring left door (Figure 10-23). This significantly helped produce a more realistic contact interaction between the dummy knees and the deformation was much less as seen in Figure 10-24.

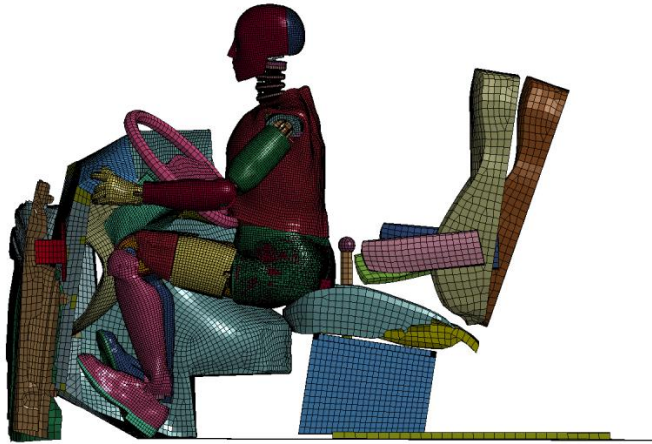


Figure 10-22 Frontal simulation with lowered stiffness of dashboard causing large deformation.

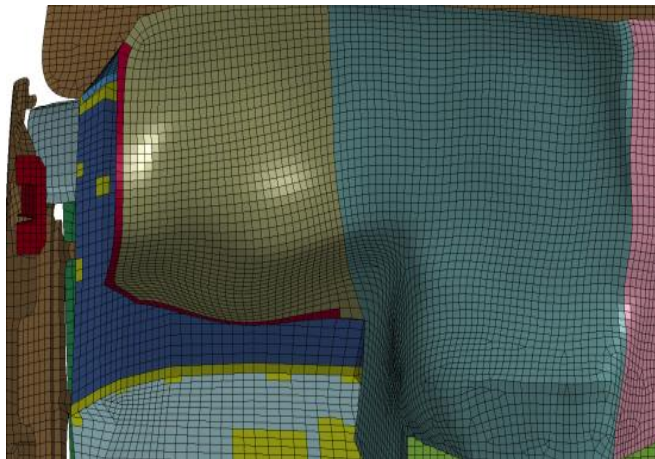


Figure 10-23 Left edge of dashboard constrained to left door.

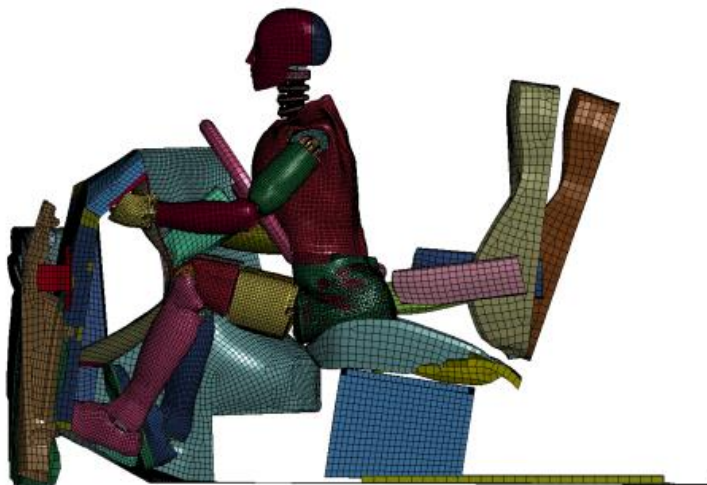


Figure 10-24 Frontal simulation with constrained left edge of dashboard.

A third issue that arose was deformation in the seat. Over the duration of the simulation the seat experienced large deformation (Figure 10-25). This was caused by the seat being modeled as a foam material and having a very low stiffness. A simple seat model was redefined by creating a rigid bottom half of the seat and the same soft upper half of the seat (Figure 10-26). This approach worked well and prevented deformations of the seat.

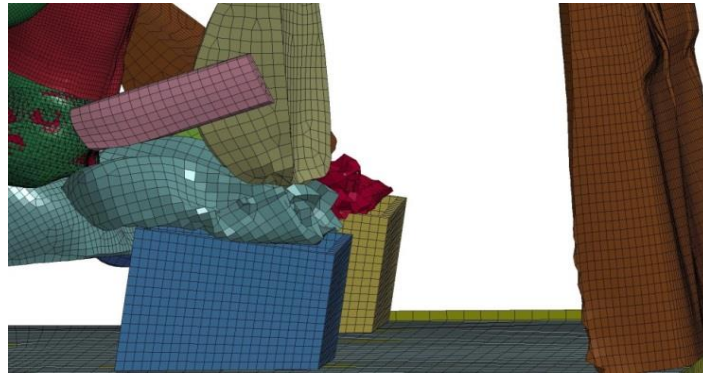


Figure 10-25 Large deformation of driver seat during frontal simulation.

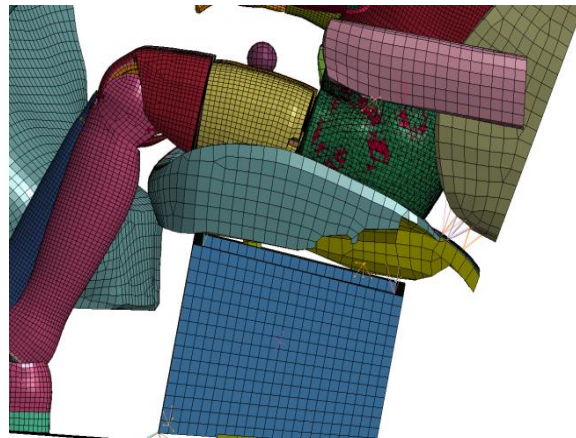


Figure 10-26 Simplified seat model with rigid bottom half and soft top half.

After fixing all these issues a successful baseline simulation with the seatbelt was run. In order to analyze the effects of the seatbelt upon the dummy injury criteria, four different parametric simulations were run and compared to the baseline simulation. Those four parameters include no pretensioner, a 4 kN load limiter, an 8 kN load limiter, and a lowered d-ring height. Lastly we concluded the frontal crash simulation with analysis of the effects of an airbag on the occupant. Further explanation of the additional simulations is provided in the results section.

After developing a successful frontal simulation with a 50 mph impact, all the simulations were run with a 35 mph impact. The same methodology was used for the 35 mph impact as the 50 mph impact.

10.5 Rollover simulation methodology

10.5.1 Introduction

Rollover crashes for heavy trucks can cause significant injury to occupants and have become an increasing area of concern for roadside safety researchers. The purpose of this rollover study is to analyze vehicle kinematics during a rollover crash and to analyze occupant kinematics and safety. The following is a step-by-step methodology to develop a finite element computer simulation that accurately captures vehicle and occupant kinematics during a rollover crash.

10.5.2 TruckSim rollover event

One of the first steps conducted for this rollover study was selecting the type of rollover event. There are several different ways in which heavy trucks can rollover in a crash, so it is necessary to determine what type of event is most critical. Based off of a previous real-world crash data study conducted by Indiana Mills and Manufacturing Inc. (IMMI), it was determined that one of the most critical rollover events is where the vehicle performs an evasive maneuver to the left followed by an overcorrecting maneuver to the right (Chinni et al., 2007).

In order to develop a FE computer model of a truck cabin that can perform a rollover crash, it is necessary to know the kinematics of the cabin throughout the rollover. TruckSim is a dynamic vehicle modeling software for heavy trucks that was used to replicate the rollover event and analyze the kinematics of the truck. The truck model used was a tractor-trailer vehicle with a 3-axle tractor and a 2-axle trailer (Figure 10-27).

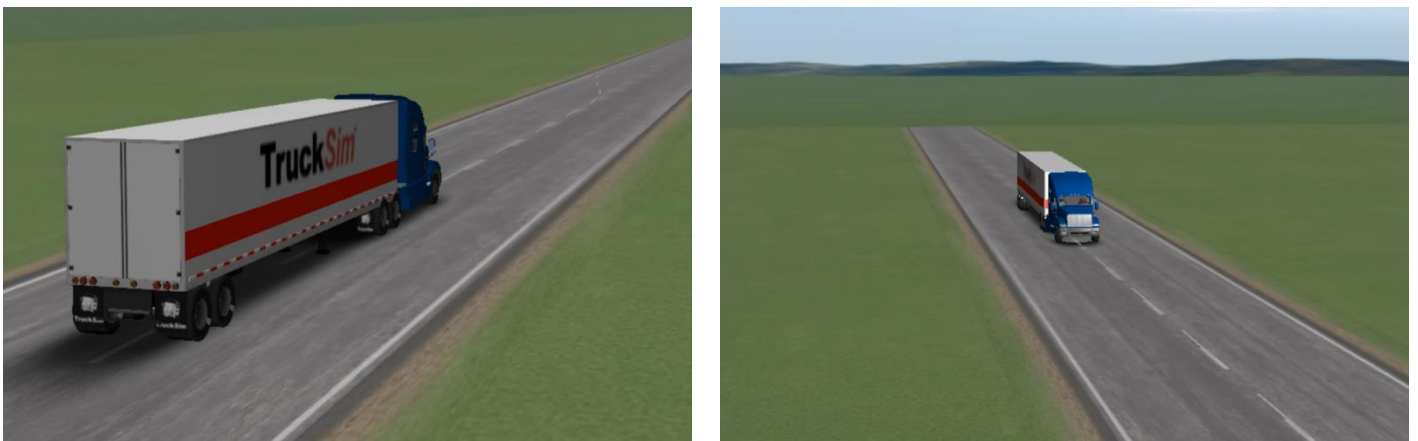


Figure 10-27 TruckSim tractor-trailer vehicle used to develop rollover simulation.

The rollover crash in TruckSim was conducted by inputting a path for the tractor-trailer to follow. The rollover path was determined from an IMMI study (Figure 10-28) (Chinni et al., 2007).

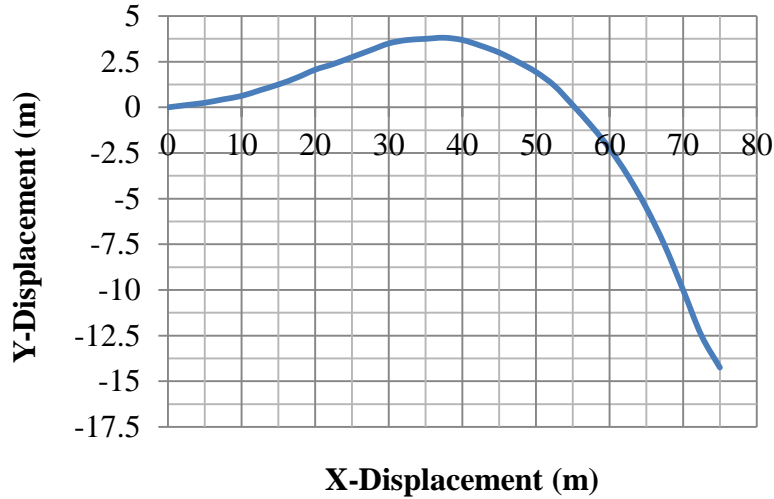


Figure 10-28 Rollover path that was input into TruckSim tractor-trailer rollover crash.

Outputs of interest from the TruckSim rollover simulation were displacements at four cab mount locations. Measurements were taken in a FE model of a tractor-trailer for the exact locations of the cab mounts to determine where to output displacements from TruckSim. At these four locations x, y and z displacements were output over time. Figure 10-29 shows where the cab mounts are located in the FE tractor-trailer model. These displacement curves were then applied in our truck cabin model by BOUNDARY_PRESCRIBED_MOTION cards at the four locations.

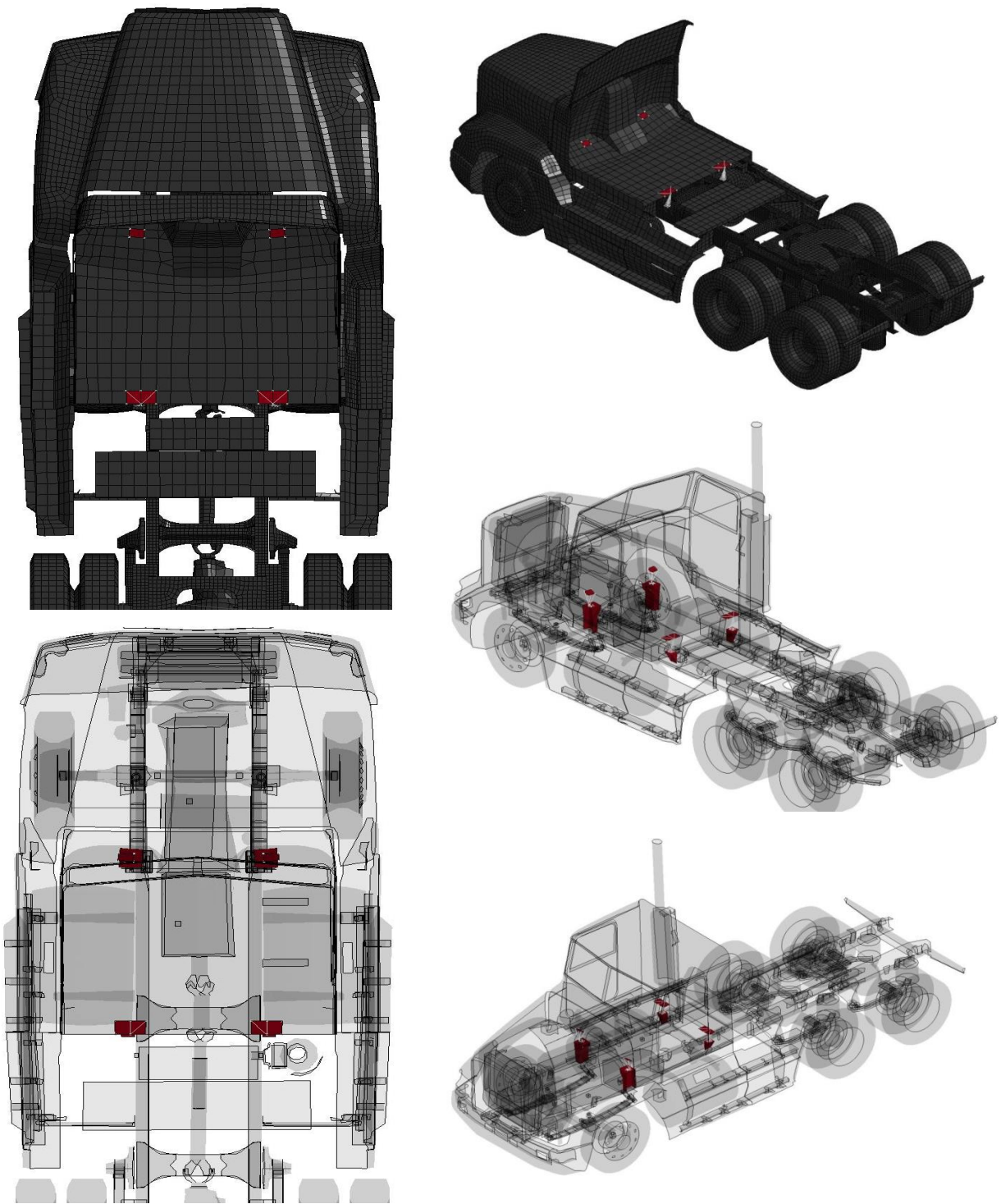


Figure 10-29 Location of four cab mount for tractor vehicle.

10.5.3 Development of truck cabin model for rollover event

There is a significant difference between the time it takes for a frontal crash event to occur and a rollover event to occur. A typical complete frontal crash impact can occur in about 0.5 seconds, whereas a complete rollover crash event can occur in about 4 seconds. The TruckSim full rollover crash was completed in 3.4 seconds. For finite element simulations a simulation time of that length can take several days of run time to obtain results. This is a result of the large number of computations that have to be performed. For the purposes of this study it was not feasible to allow such lengthy and costly simulations. Therefore, several changes were made to the truck cabin to simplify the model which would significantly reduce simulation run time.

First, the entire cabin was completely rigidized by changing all the material cards to MAT_RIGID. Only the dummy was not rigidized in our complete model. A majority of finite element computation time is spent on material stiffness; therefore, changing the parts to “infinite” stiffness drastically cut down simulation time.

Second, all truck cabin parts were constrained to follow the floor by the CONSTRAINED_RIGID_BODIES card. Originally the parts were connected together by beam spotwelds or constrained nodal rigid bodies. These types of connections only work for parts that have non-rigid material properties. This approach no longer worked for the rigidized cabin resulting in the constrained rigid bodies approach. Essentially, this approach combines all the rigid truck cabin parts together and treats it as one big rigid part.

Finally, the contact definitions were reduced to one CONTACT_AUTOMATIC_SURFACE_TO_SURFACE contact between the dummy and the rest of the truck cabin. Contact algorithms are another aspect of finite element computer simulations that can cause long computation time. Therefore, removing extra contacts and developing one simple contact definition significantly reduced run time.

10.5.4 Application of rollover maneuver to truck cabin

Taking the displacements at the four cab mount locations from TruckSim and applying them to our truck cabin model proved to be a difficult process. Several different approaches were tried to apply the displacements but many of them did not successfully capture accurate rollover kinematics. A brief summary is provided explaining the general approaches and the resulting final approach.

Initially the approach was to apply x, y and z displacements at four nodes at the location of the cab mounts via BOUNDARY_PRESCRIBED_MOTION cards. Several variations of this approach were tried but none of them proved successful. Investigation of the LS-DYNA manual BOUNDARY_PRESCRIBED_MOTION card showed that no more than one node should be prescribed or unexpected results may be obtained. Accordingly, it was determined that applying displacement and rotation at the center of the floor would prove to be a better approach.

TruckSim was used again to output x, y, and z displacement along with x, y and z rotation at the center of the floor. These displacement and rotation curves were applied at the center node of the floor but the truck cabin was not able to successfully complete the rollover maneuver.

Another approach was tried by applying x, y, and z velocity instead of the displacement curves. The resulting simulation successfully captured a rollover maneuver. Therefore, this method was used to re-create the rollover crash for the truck cabin model.

10.5.5 Inclusion of Hybrid III 50th percentile male dummy

After developing a successful truck cabin model that could perform a rollover maneuver, a detailed Hybrid III 50th percentile male dummy was positioned in the driver seat. An initial simulation was run with the positioned dummy and no seatbelt. The total simulation time was 3.4 seconds, which is the length required to complete the rollover maneuver. At about 0.8 seconds the simulation terminated due to numerical stability in the dummy. It was determined that a lower time step would be needed to allow the simulation to run the full length but this would result in very long and costly simulations. Due to time and budget constraints researchers proceeded to include a simplified version of the Hybrid III model referred to as the fast model. Figure 10-30 and Figure 10-31 compare the fast model to the detailed model. The fast Hybrid III model allowed a successful rollover simulation run and was used for all rollover simulations conducted. There were concerns with the accuracy of the fast dummy model and these are addressed in the results section.

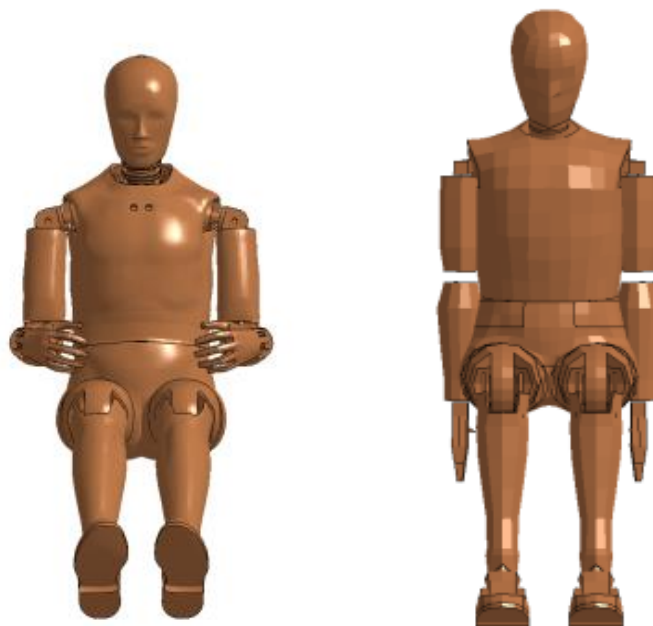


Figure 10-30 Comparison of detailed dummy model (left) and fast dummy model (right).

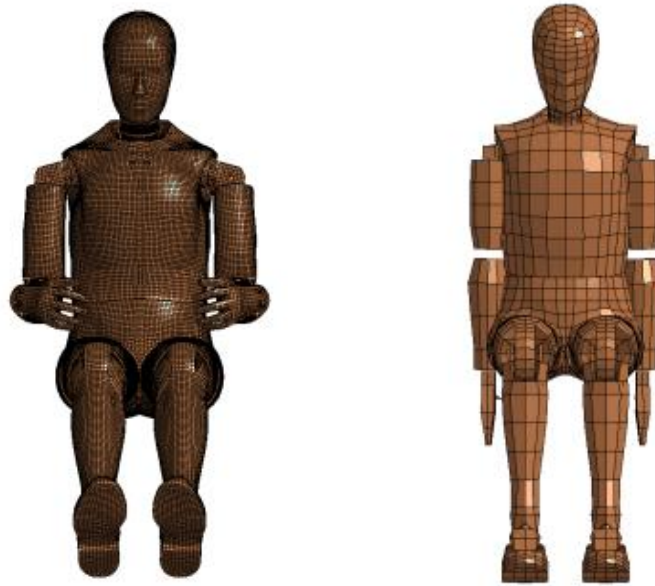


Figure 10-31 Comparison of mesh size for detailed dummy model (left) and fast dummy model (right).

10.5.6 Modifications to seatbelt

To analyze the effects of a restraint system on the occupant during a rollover crash, a 3-point seatbelt was included in our FE computer model. An initial simulation was performed with the seatbelt fitted to the dummy but the simulation terminated due to numerical instability occurring in the seatbelt. Several changes were made to the seatbelt to improve the performance of the restraint system.

A significant input that affects the performance of the seatbelt is the material properties. The belt model currently used was provided by UMTRI researchers and `MAT_PIECEWISE_LINEAR_PLASTICITY` was used to represent the seatbelt material. Another approach to material modeling was tried by using `MAT_FABRIC` to represent the seatbelt material. A 3-point seatbelt model available on the LSTC website was downloaded that implemented `MAT_FABRIC` for their seatbelt. The same material input cards were replicated in our seatbelt model. After implementing the new material for the seatbelt model, a simulation was produced that resulted in much better performance of the seatbelt. However, it was noticed that the contact between the dummy and the seatbelt was not working properly.

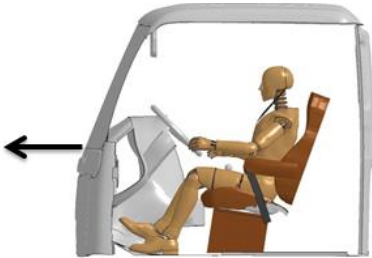








Defining a proper contact between the dummy and the seatbelt is a challenge because of the difference in material stiffness between the two parts. Contact inputs contain several different parameters that affect the contact interaction. Upon further investigation of the contact inputs for

the dummy and seatbelt, it was noticed that the coefficient of friction was scaled quite high to a value of 3.0. This was not a reasonable value and it was lowered to a value of 0.8. Additionally the soft constraint contact input was changed from a value of 2 to 1. According to LS-DYNA manual, a soft value of 1 invokes an interface stiffness based on the nodal mass and the global time step size. This method of computing the interface stiffness will typically give much higher stiffness value than would be obtained by using the bulk modulus. After these two significant changes were made the contact interaction was more realistic than previously. The contact interaction was not perfect and there were still minor issues occurring during the simulation; therefore, researchers suggest future work be conducted to optimize the contact interaction between the dummy and the seatbelt.

11. FE Frontal computer simulation results – 35 mph

TTI researchers performed an array of crash tests to determine the crashworthiness of the heavy truck. The variations in crash tests were based on initial impact speed and seatbelt condition. With regard to initial impact speed, the simulations were carried out at 35 mph. The other category for differentiation among crash tests was the seat belt condition. The baseline simulation incorporated the basic seatbelt model with a pretensioner and no load limiter. The second type did not include the pretensioner. The following two types included a 4 and 8 kN load limiters, respectively. Last, in the final simulation, the location of the D-Ring was lowered compared to the baseline simulation. Table 11-1 summarizes the different simulation types.

Table 11-1 Summary of simulation types, impact information and seatbelt.

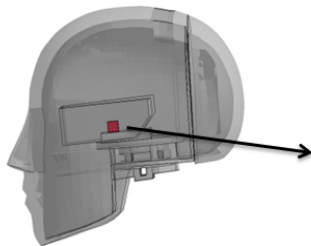
<p>Impact Type : Frontal Initial Impact Speed : 35 mph Seatbelt Conditions:</p> <ul style="list-style-type: none"> • Baseline • No Pretensioner • 4 kN Load Limiter • 8 kN Load Limiter • Lowered D-Ring <p>Airbag : No</p>			
<p>Impact Type : Frontal Initial Impact Speed : 35 mph Seatbelt Conditions:</p> <ul style="list-style-type: none"> • Baseline • No Pretensioner • 4 kN Load Limiter • 8 kN Load Limiter • Lowered D-Ring <p>Airbag : Yes</p>			
<p>Impact Type : Frontal Initial Impact Speed : 50 mph Seatbelt Conditions:</p> <ul style="list-style-type: none"> • Baseline • No Pretensioner • 4 kN Load Limiter • 8 kN Load Limiter • Lowered D-Ring <p>Airbag : No</p>			

To assess the potential threat to occupants, the injury criteria of the H3 50th percentile male dummy was analyzed and a parametric evaluation was performed. The injury criterion used for the evaluation included head and neck injury criteria, chest injury criteria, and leg injury criteria. Table 11-2 through Table 11-4 summarize the injury criteria parameters for the different body regions.

Table 11-2 Injury criteria parameters for head and neck region.

a) Head Injury Criteria (HIC₁₅)

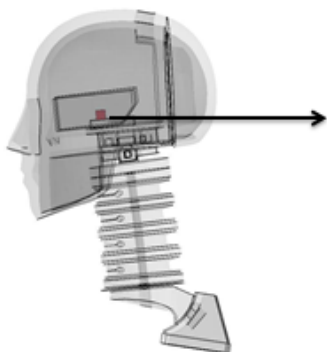
Head acceleration recorded during the impact event is employed to calculate the HIC₁₅ value, which represents the probability of skull fracture



$$HIC = \max \left[\frac{\int_{t_1}^{t_2} a(t) dt}{t_2 - t_1} \right]^{2.5} (t_2 - t_1)$$

b) Neck Injury Criteria

Dummy injury criteria for the neck are evaluated based on the Normalized Neck Injury Criteria- Nij which is defined as the sum of normalized values of loads and moments.



$$N_{ij} = \frac{F_z}{F_{int}} + \frac{M_y}{M_{int}}$$

Table 11-3 Injury criteria parameters for chest region.

Chest deflection recorded during the impact event is employed to calculate the chest injury criteria value and probability of injury.

$$p(AIS3+) = \frac{1}{1 + e^{10.5456 - 1.568 * D^{0.4612}}}$$

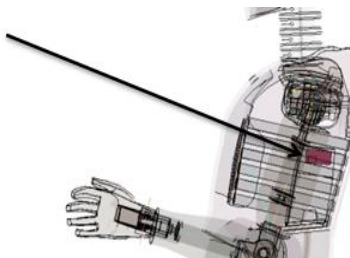
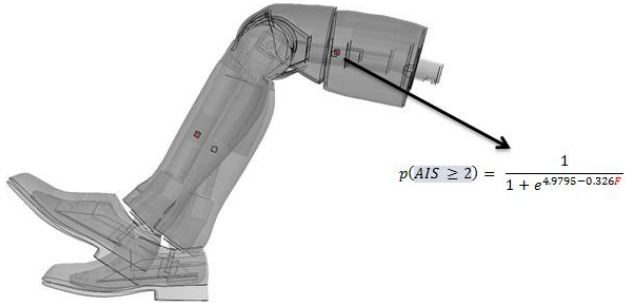


Table 11-4 Injury criteria parameters for leg region.

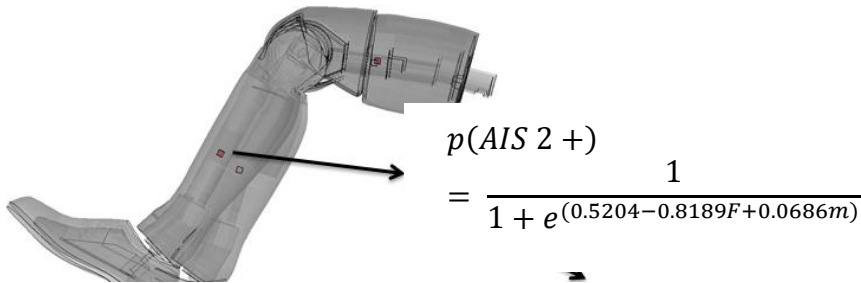
a) KTH Injury Criteria

Dummy injury criteria for the KTH are evaluated based on the formulation for probability of injury as a function of femur axial force.



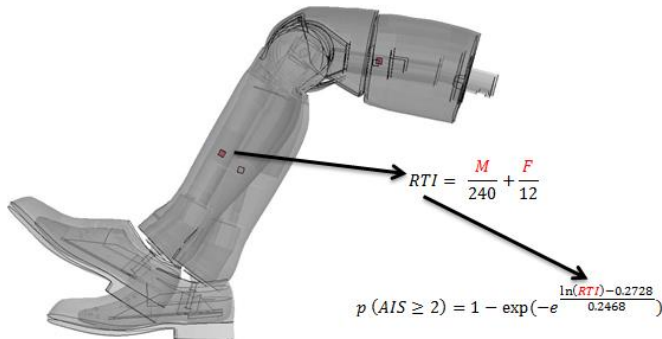
a) Tibia Plateau Fractures

Dummy injury criteria for tibia plateau fractures are evaluated based on upper tibia axial forces and dummy mass.



b) Leg Shaft Fracture

Dummy injury criteria for tibia plateau fractures are evaluated based on a normalized formulation that combines bending moments and axial compressive loads.



In 1978, Mertz developed the Injury assessment reference values (IARVs) to assess the efficacy of General Motors (GM) restraint system designs under a series of simulated frontal crash events using the Hybrid III midsize adult male dummy as the occupant. It was a comparative analysis which evaluated whether or not the values from the simulation exceeded the IARVs. The injury event was termed “unlikely” if the associated injury value did not exceed the IARVs. They were published as a part of the GM petition of NHTSA to authorize the use of the Hybrid III midsize adult male dummy in FMVSS No. 208 testing standard. Table 11-5 contains IARVs for the different injury criteria parameters analyzed in the simulations. Typically, injury criteria values are represented as a percentage of IARV, and this approach was used for each simulation.

Table 11-5 Summary of IARV’s for injury criteria parameters.

Head and Neck	Parameter	IARV
	HIC-15	700
	Nij	1
	Neck axial tension(kN)	4.17
	Neck axial compression(kN)	4
Chest		
	Deflection (mm)	63
Leg and Foot		
	Left Femur axial force(kN)	-10
	Right Femur axial force(kN)	-10
	Left Tibia Index	1
	Right Tibia Index	1
	Left Tibia axial force(kN)	-8
	Right Tibia axial force (kN)	-8

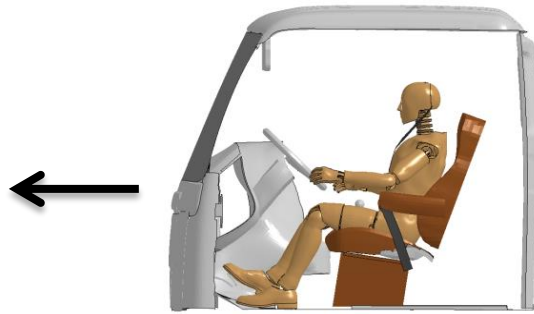
11.1 Frontal simulations without airbag – 35 mph

11.1.1 Frontal baseline simulation – 35 mph

1.1.1.1 Simulation frames and summary

The following documents the post processed results of the finite element simulation of a frontal impact event with initial speed of 35 mph, inclusion of a belted HIII 50th percentile male dummy in the driver position, and no application of airbag. Table 11-6 and Table 11-7 summarize the resulting simulation with frames at different times throughout the simulation. The details of the simulation are summarized below and in Figure 11-1:

- Impact Type : Frontal
- Initial Impact Speed : 35 mph
- Seatbelt Condition: Belted (Baseline)
- Airbag : No



(a) Lateral View of the FE Computer Model with Indication of Impact Orientation



(b) Seatbelt Model



(c) No Use of Airbag Model

Figure 11-1 Modeled characteristics of the finite element simulation for the frontal impact (35 mph, baseline, no airbag).

Table 11-6 Frontal impact simulation frames side view (35 mph, baseline, no airbag).





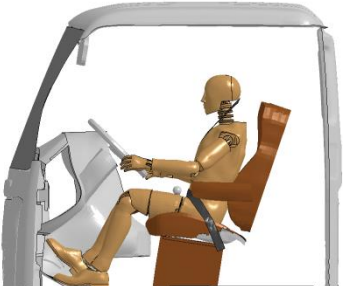

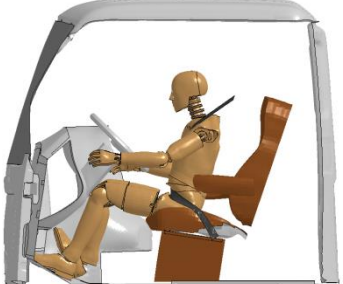

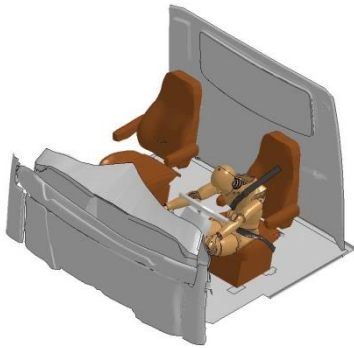

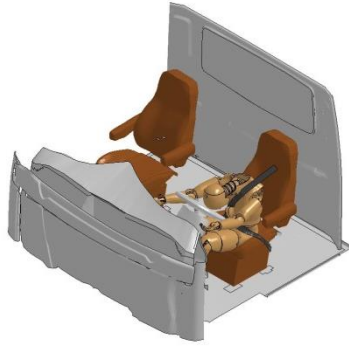
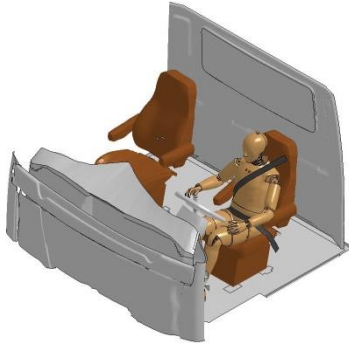
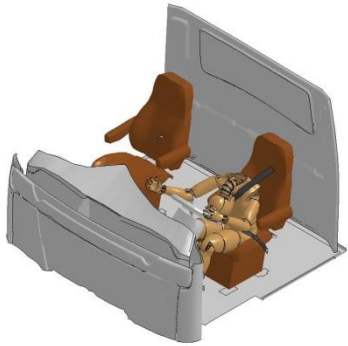

Time (Sec)	Sequential Frames	Time (Sec)	Sequential Frames
0.000		0.074	
0.015		0.089	
0.030		0.105	
0.055			

Table 11-7 Frontal impact simulation frames perspective view (35 mph, baseline, no airbag).

Time (Sec)	Sequential Frames	Time (Sec)	Sequential Frames
0.000		0.074	
0.015		0.089	
0.030		0.105	
0.055			

The seatbelt retractor force for the resulting simulation is plotted in Figure 11-2. The retractor contained no load limiter for this simulation and reached a peak of about 9.5 kN.

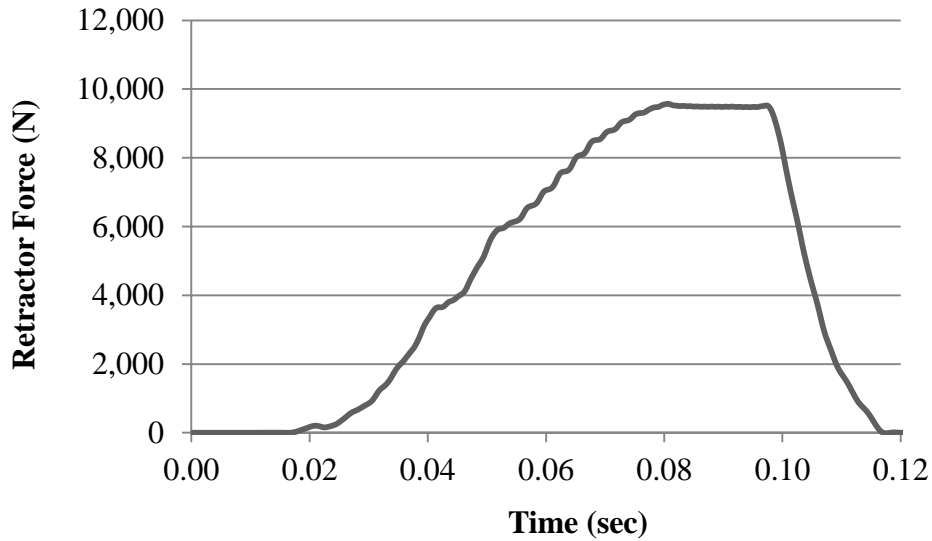


Figure 11-2 Seatbelt retractor force time history (35 mph, baseline, no airbag).

1.1.1.2 Head Injury Criteria

Dummy injury criteria for the head are evaluated with respect to the HIC₁₅ criteria. Head acceleration recorded during the impact event is employed to calculate the HIC₁₅ value. Figure 11-3 illustrates details for the head injury criteria and the recorded curves from this specific impact condition and passive restraint systems employment.

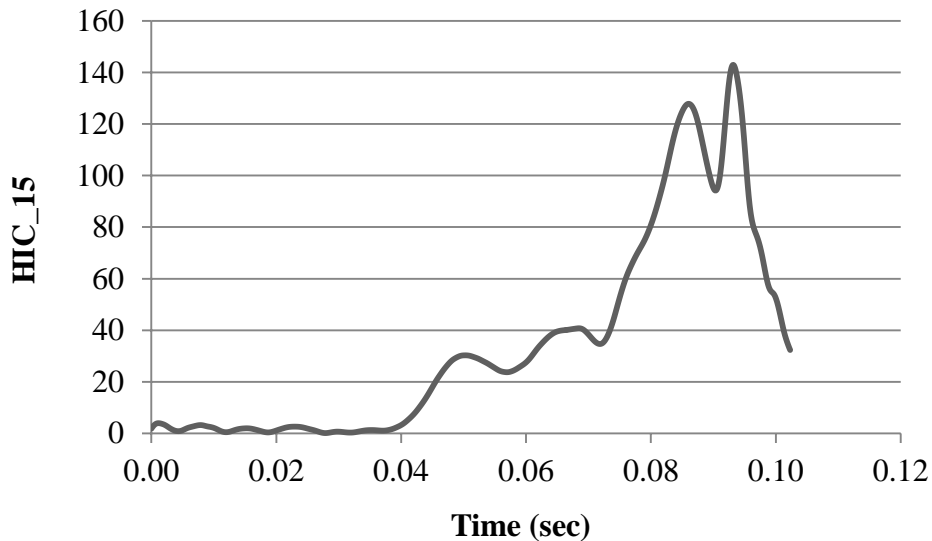
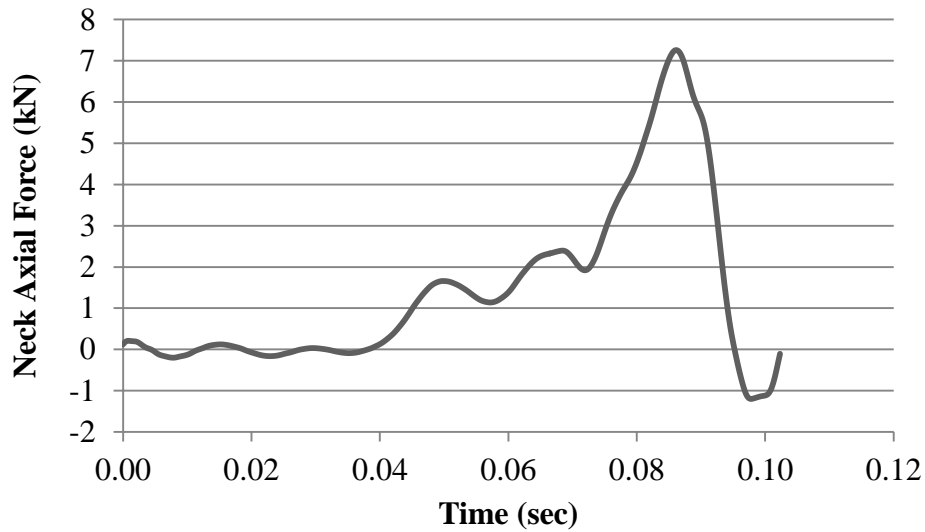


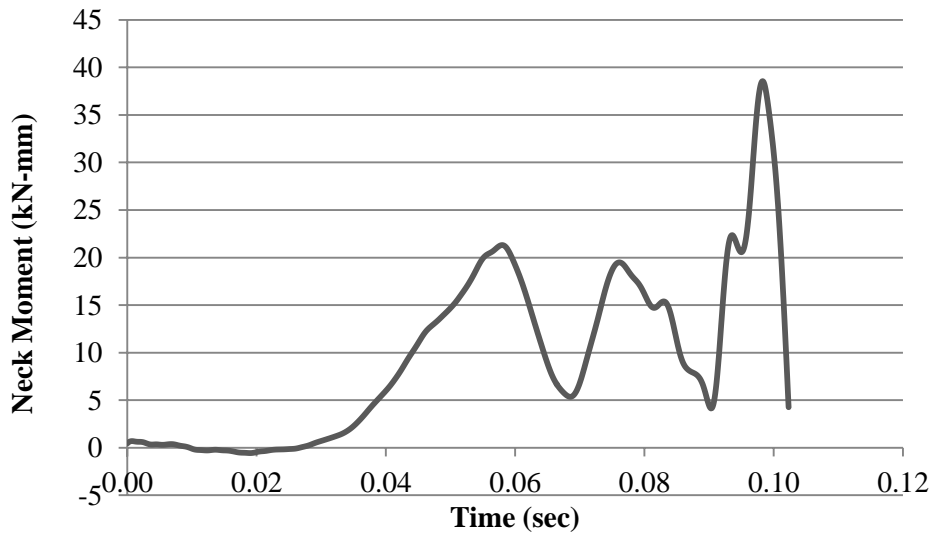
Figure 11-3 HIC time history (35 mph, baseline, no airbag).

1.1.1.3 Neck Injury Criteria

Dummy injury criteria for the neck are evaluated based on the normalized neck injury criteria, N_{ij} , which is defined as the sum of normalized values of loads and moments. Figure 11-4 illustrates details for the neck injury criteria and the recorded curves from this specific impact condition and passive restraint systems employment.



(a) Neck Axial Force Time History



(b) Neck Bending Moment Time History

Figure 11-4 Neck injury time history (35 mph, baseline, no airbag).

1.1.1.4 Chest Injury Criteria

Dummy injury criteria for the chest are evaluated based on the chest deflection values. Figure 11-5 illustrates details for the chest injury criteria and the recorded curves from this specific impact condition and passive restraint systems employment.

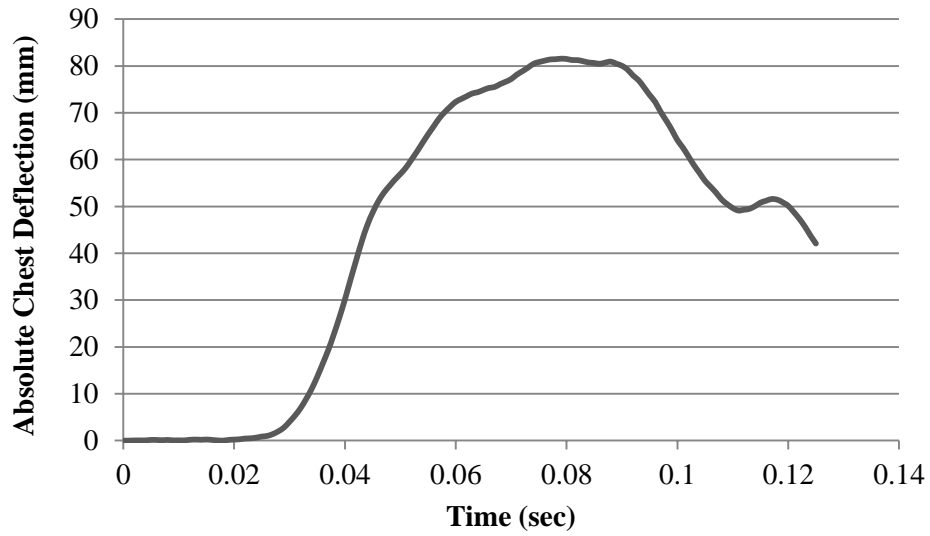
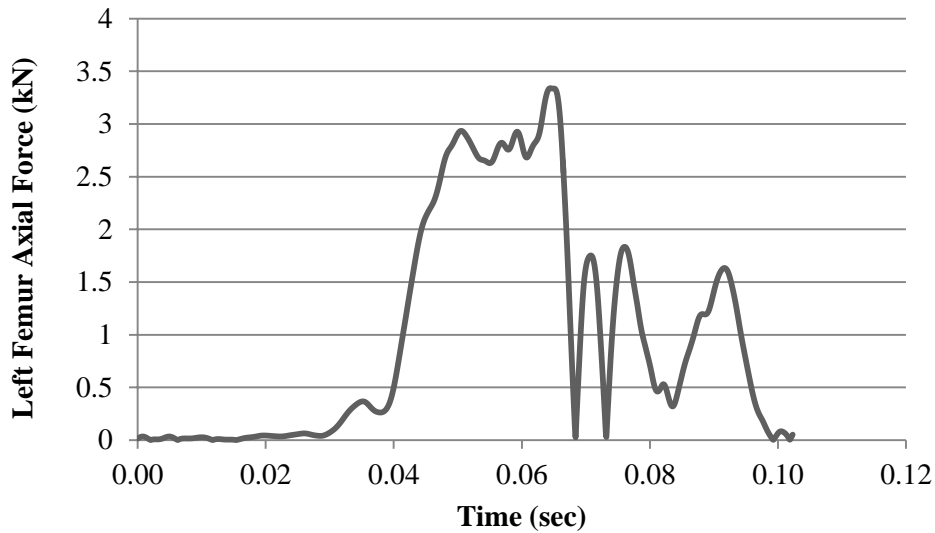


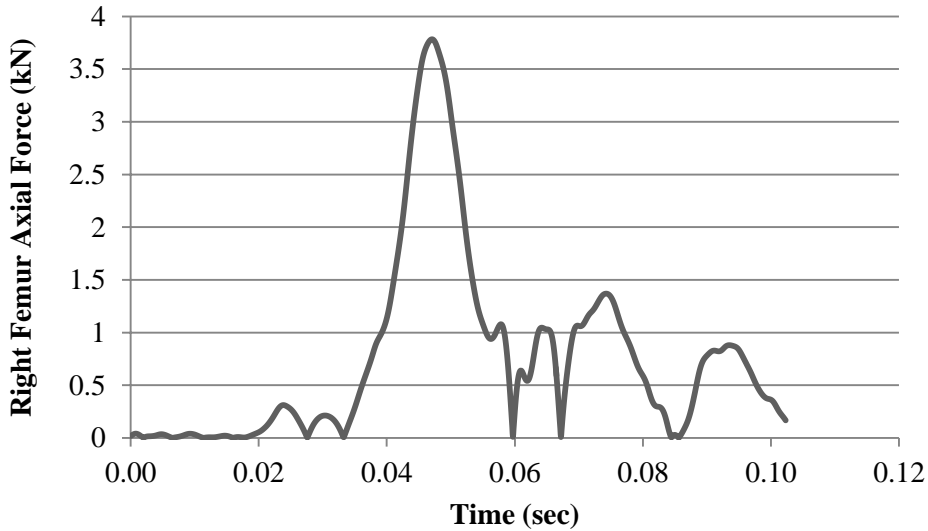
Figure 11-5 Chest deflection time history (35 mph, baseline, no airbag).

1.1.1.5 KTH Injury Criteria

Dummy injury criteria for the KTH are evaluated based on the formulation for probability of injury as a function of femur axial force. Figure 11-6 illustrates details for the KTH injury criteria and the recorded curves from this specific impact condition and passive restraint systems employment.



(a) Left Femur Axial Force Time History

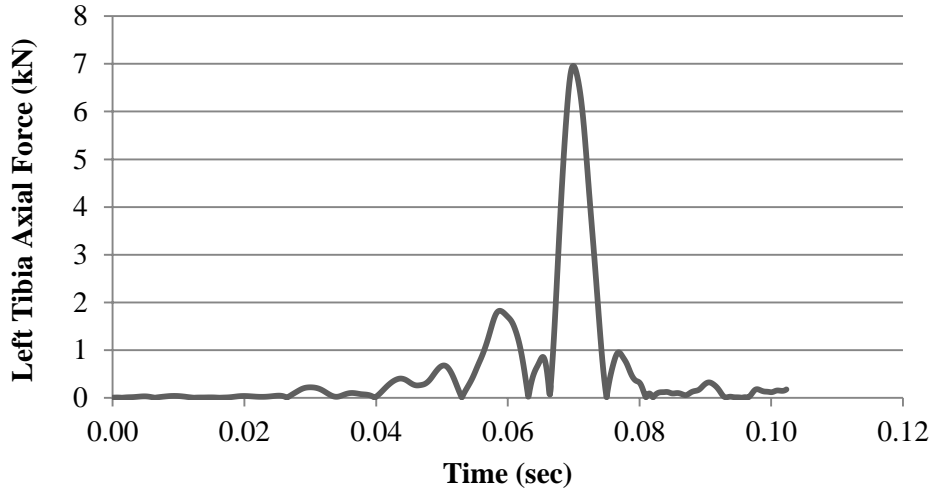


(b) Right Femur Axial Force Time History

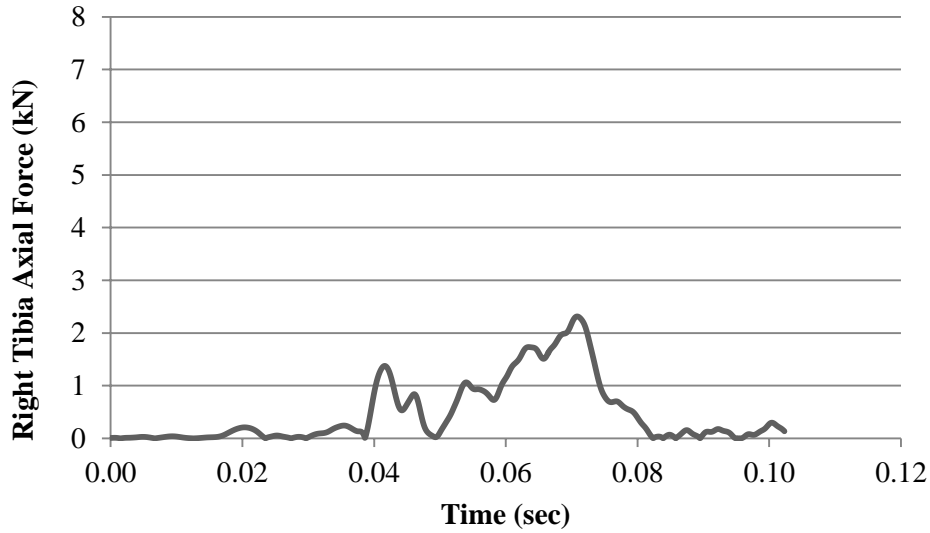
Figure 11-6 KTH injury time history (35 mph, baseline, no airbag).

1.1.1.6 Tibia Plateau Fracture Injury Criteria

Dummy injury criteria for tibia plateau fractures are evaluated based on axial compressive loads. Figure 11-7 illustrates details for the tibia plateau injury criteria and the recorded curves from this specific impact condition and passive restraint systems employment.



(a) Left Tibia Axial Force Time History

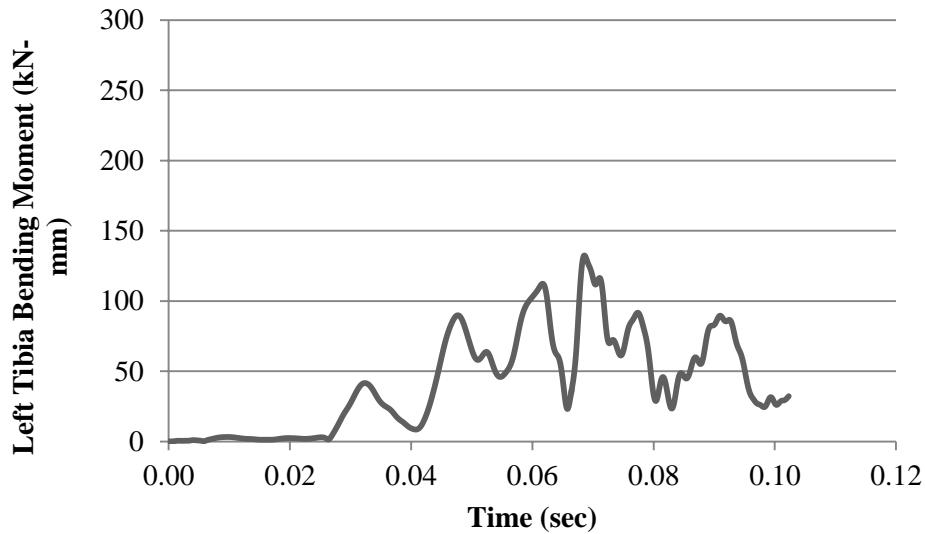


(b) Right Tibia Axial Force Time History

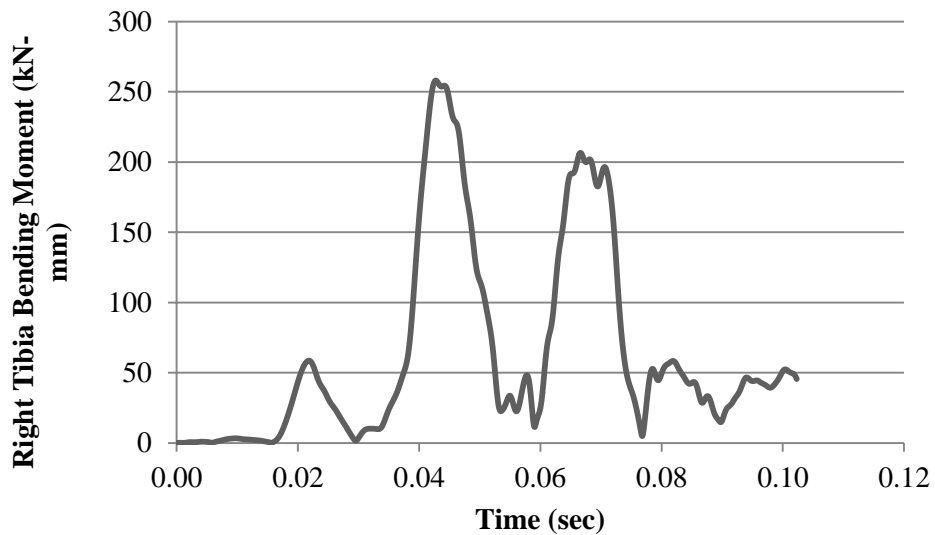
Figure 11-7 Tibia plateau fracture time history (35 mph, baseline, no airbag).

1.1.1.7 Tibia Shaft Fracture Injury Criteria

Dummy injury criteria for tibia shaft fractures are evaluated based on a normalized formulation that combines bending moments and axial compressive loads. Figure 11-8 illustrates details for the tibia shaft injury criteria and the recorded curves from this specific impact condition and passive restraint systems employment.



(a) Left Tibia Resultant Bending Moment Time History



(b) Right Tibia Resultant Bending Moment Time History

Figure 11-8 Tibia shaft fracture time history (35 mph, baseline, no airbag).

1.1.1.8 Conclusions

The injury criteria values for various parts of the body were compared to the IARV requirements. The simulation injury criteria results as a percentage of the IARV values are shown in Figure 11-9.

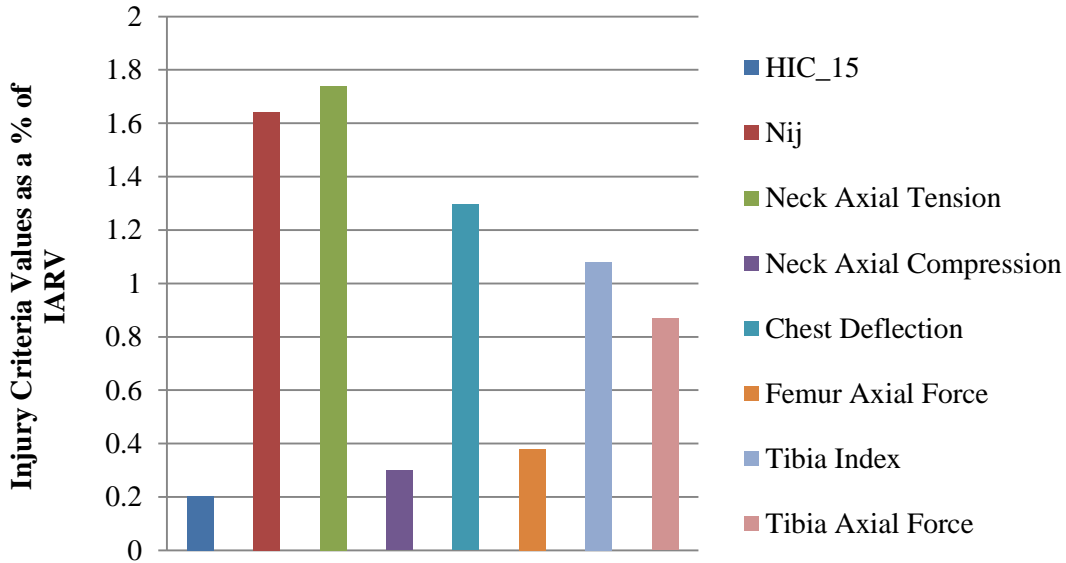


Figure 11-9 Injury probability as a function of IARV (35 mph, baseline, no airbag).

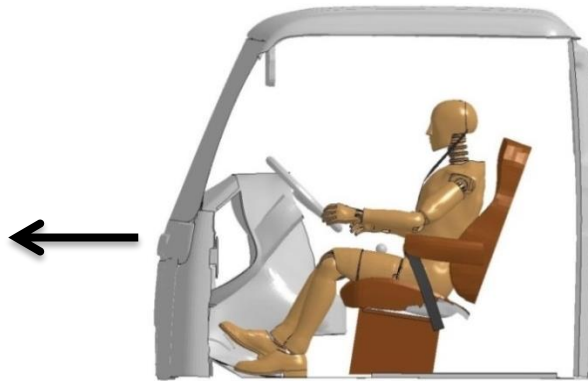
For the frontal baseline simulation without airbag, the probability of injury for the head and KTH regions is unlikely because the injury criteria values stay below the threshold IARV. The injury criteria values for the neck and chest regions exceeded the threshold IARV which is unacceptable according to current standards.

11.1.2 Frontal no pretensioner simulation – 35 mph

1.1.1.9 Simulation frames and summary

The following documents the post processed results of the finite element simulation of a frontal impact event with initial speed of 35 mph, inclusion of a belted H3 50th percentile male dummy in the driver position, and no application of airbag. Table 11-8 and Table 11-9 summarize the resulting simulation with frames at different times throughout the simulation. The details of the simulation are summarized below and in Figure 11-10:

- Impact Type : Frontal
- Initial Impact Speed : 35 mph
- Seatbelt Condition: Belted (No Pretensioner)
- Airbag : No



(a) Lateral View of the FE Computer Model with Indication of Impact Orientation



(b) Seatbelt Model



(c) No Use of Airbag Model

Figure 11-10 Modeled characteristics of the finite element simulation for the frontal impact (35 mph, no pretensioner, no airbag).

Table 11-8 Frontal impact simulation frames side view (35 mph, no pretensioner, no airbag).










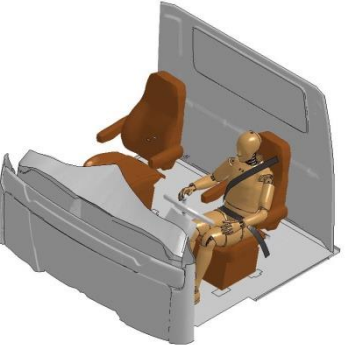
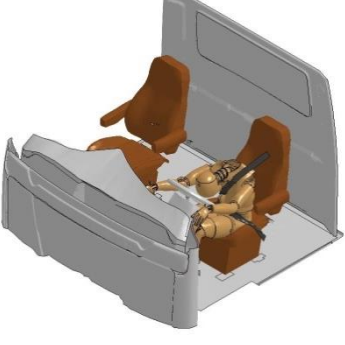
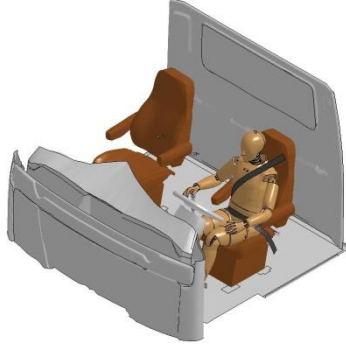
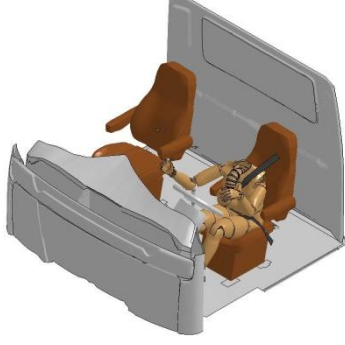
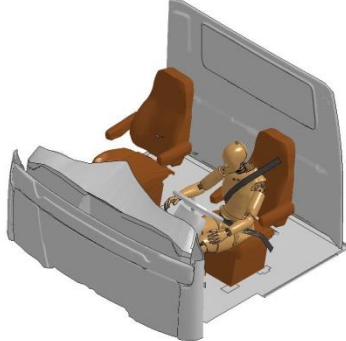
Time (Sec)	Sequential Frames	Time (Sec)	Sequential Frames
0.000		0.074	
0.015		0.089	
0.030		0.105	
0.055			

Table 11-9 Frontal impact simulation frames perspective view (35 mph, no pretensioner, no airbag).

Time (Sec)	Sequential Frames	Time (Sec)	Sequential Frames
0.000		0.074	
0.015		0.089	
0.030		0.105	
0.055			

The seatbelt retractor force for the resulting simulation is plotted in Figure 11-11. The retractor contained no load limiter for this simulation and reached a peak of about 9.5 kN.

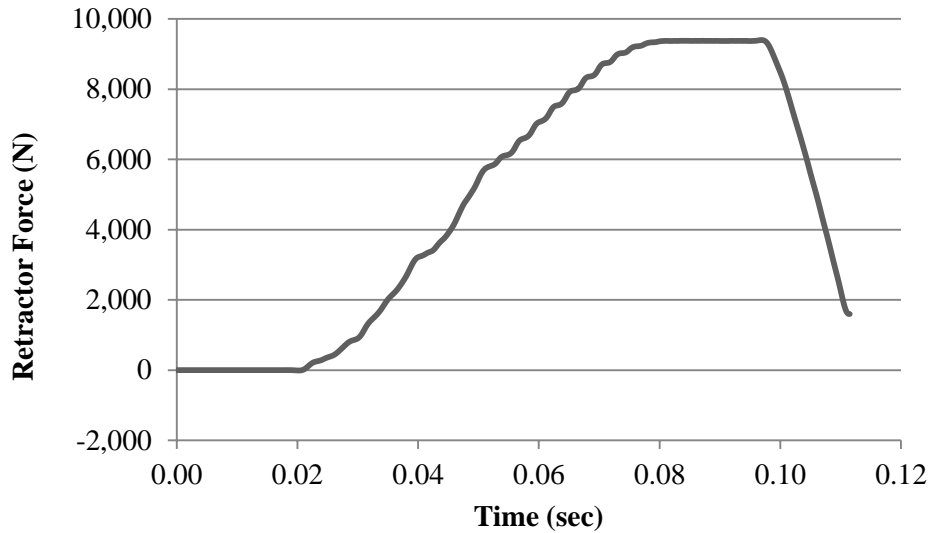


Figure 11-11 Seatbelt retractor force time history (35 mph, no pretensioner, no airbag).

11.1.2.1 Head injury criteria

Dummy injury criteria for the head are evaluated with respect to the HIC₁₅ criteria. Head acceleration recorded during the impact event is employed to calculate the HIC₁₅ value. Figure 11-12 illustrates details for the head injury criteria and the recorded curves from this specific impact condition and passive restraint systems employment.

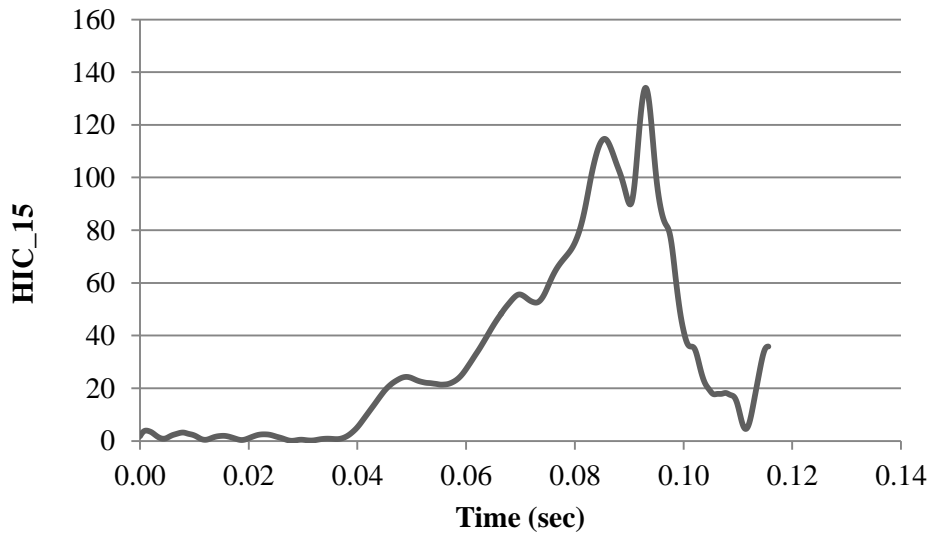
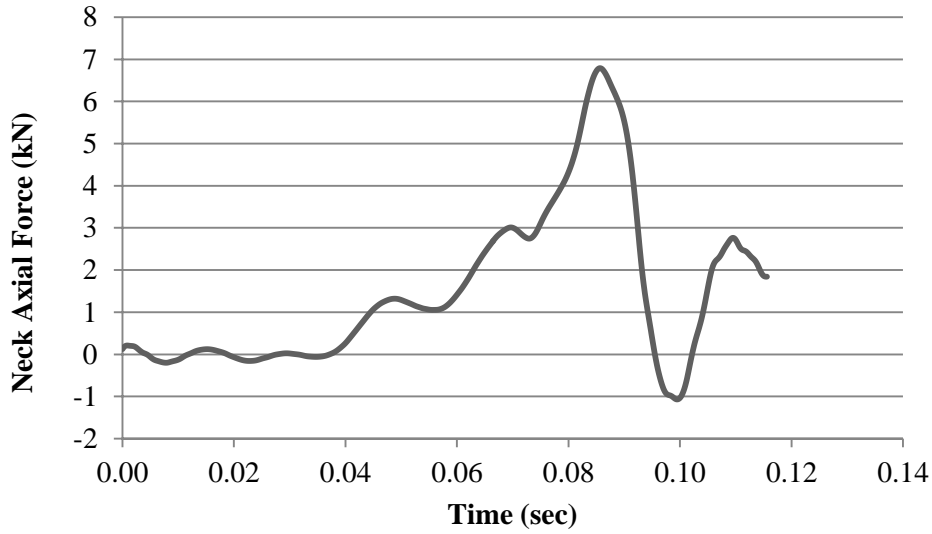


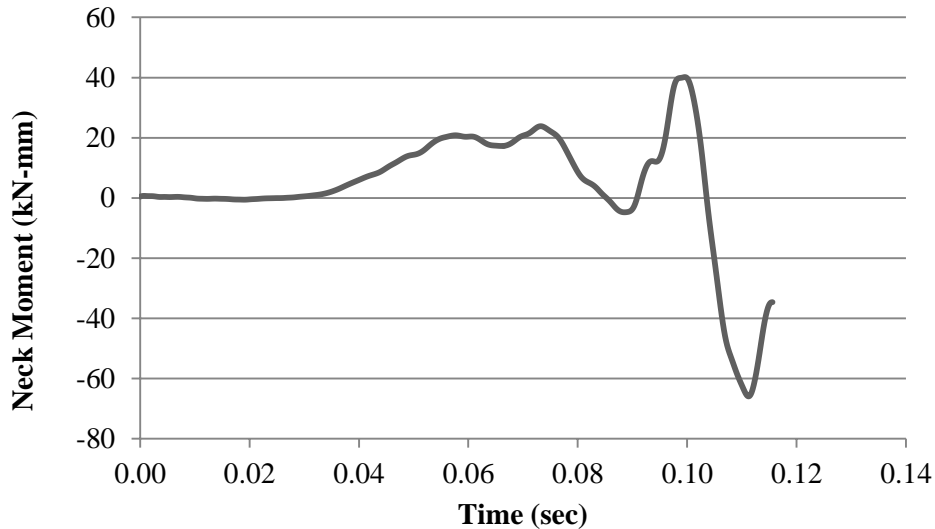
Figure 11-12 HIC time history (35 mph, no pretensioner, no airbag).

1.1.1.10 Neck Injury Criteria

Dummy injury criteria for the neck are evaluated based on the normalized neck injury criteria, N_{ij} , which is defined as the sum of normalized values of loads and moments. Figure 11-13 illustrates details for the neck injury criteria and the recorded curves from this specific impact condition and passive restraint systems employment.



(a) Neck Axial Force Time History



(b) Neck Bending Moment Time History

Figure 11-13 Neck injury time history (35 mph, no pretensioner, no airbag).

1.1.1.11 Chest Injury Criteria

Dummy injury criteria for the chest are evaluated based on the chest deflection values. Figure 11-14 illustrates details for the chest injury criteria and the recorded curves from this specific impact condition and passive restraint systems employment.

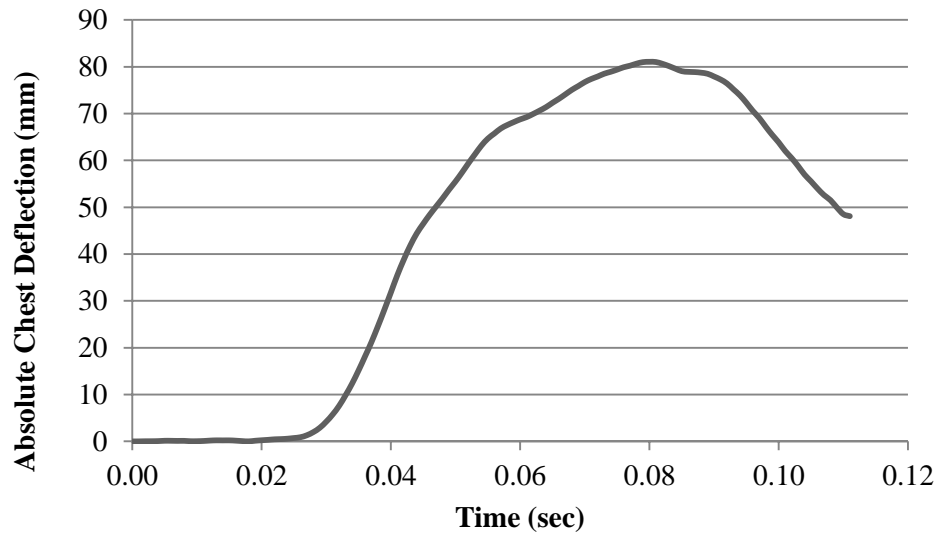
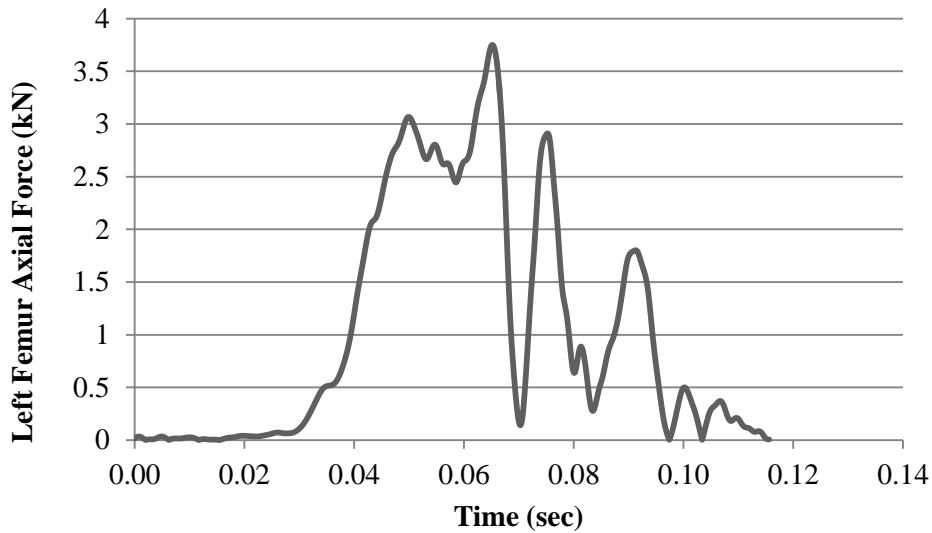


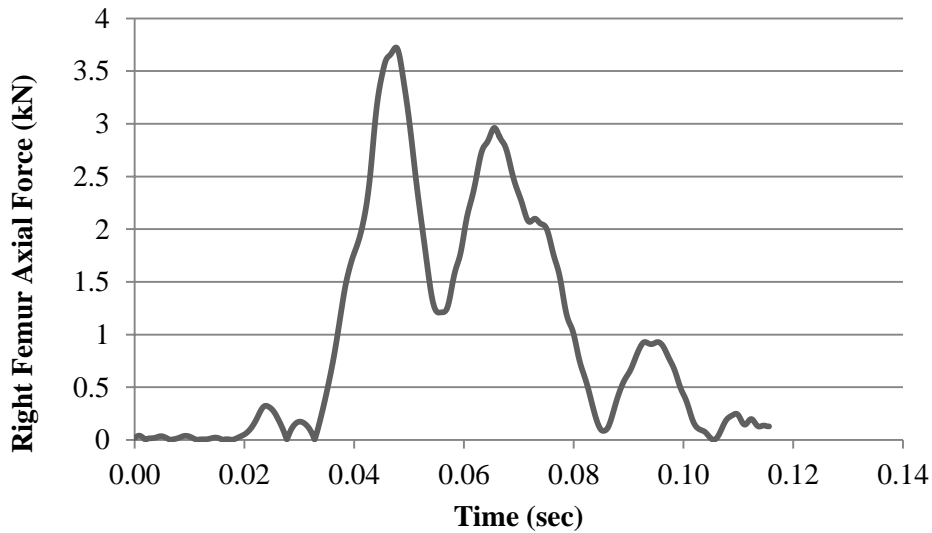
Figure 11-14 Chest deflection time history (35 mph, no pretensioner, no airbag).

1.1.1.12 KTH Injury Criteria

Dummy injury criteria for the KTH are evaluated based on the formulation for probability of injury as a function of femur axial force. Figure 11-15 illustrates details for the KTH injury criteria and the recorded curves from this specific impact condition and passive restraint systems employment.



(a) Left Femur Axial Force Time History

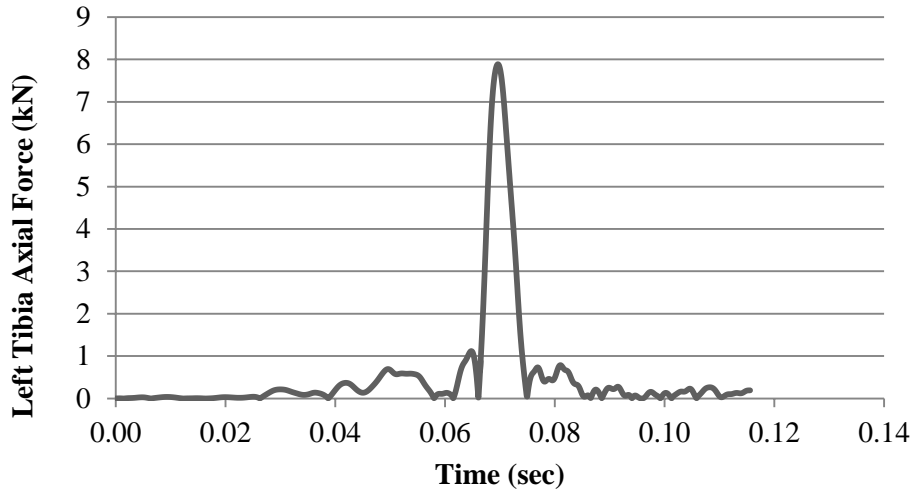


(b) Right Femur Axial Force Time History

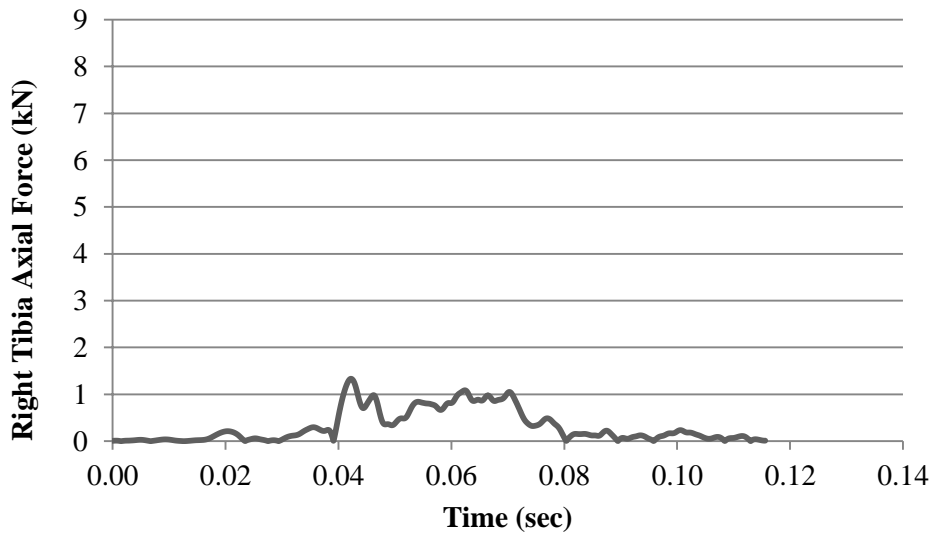
Figure 11-15 KTH injury time history (35 mph, no pretensioner, no airbag).

1.1.1.13 Tibia Plateau Fracture Injury Criteria

Dummy injury criteria for tibia plateau fractures are evaluated based on axial compressive loads. Figure 11-16 illustrates details for the tibia plateau injury criteria and the recorded curves from this specific impact condition and passive restraint systems employment.



(a) Left Tibia Axial Force Time History

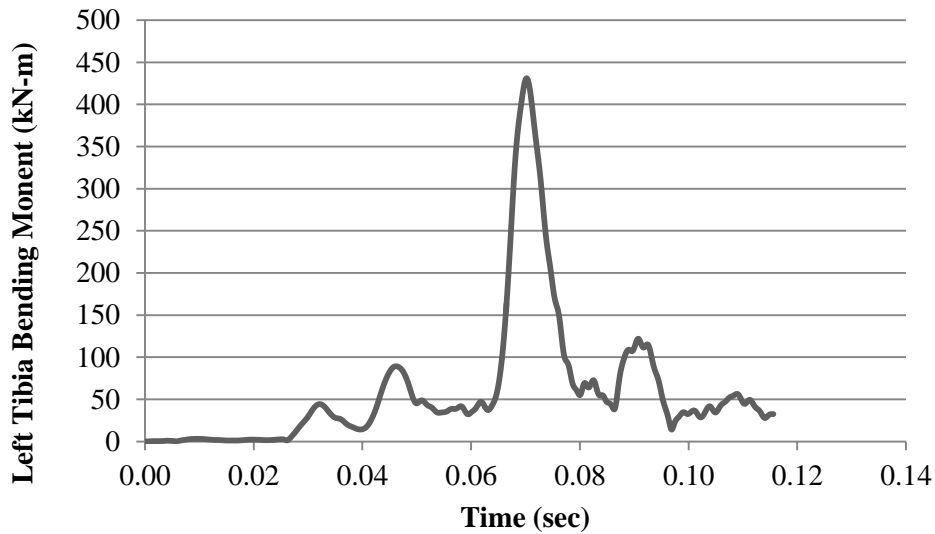


(b) Right Tibia Axial Force Time History

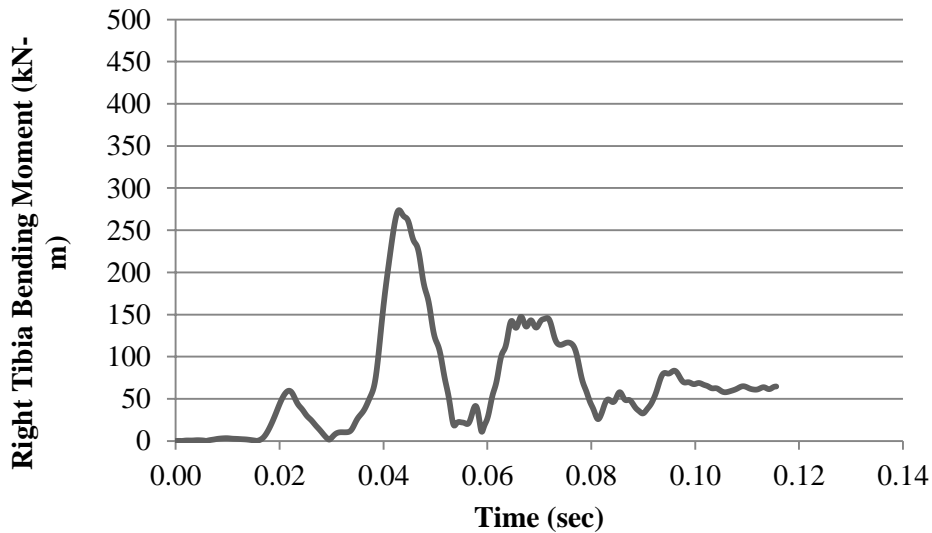
Figure 11-16 Tibia plateau fracture time history (35 mph, no pretensioner, no airbag).

1.1.1.14 Tibia Shaft Fracture Injury Criteria

Dummy injury criteria for tibia shaft fractures are evaluated based on a normalized formulation that combines bending moments and axial compressive loads. Figure 11-17 illustrates details for the tibia shaft injury criteria and the recorded curves from this specific impact condition and passive restraint systems employment.



(a) Left Tibia Resultant Bending Moment Time History



(b) Right Tibia Resultant Bending Moment Time History

Figure 11-17 Tibia shaft fracture time history (35 mph, no pretensioner, no airbag).

1.1.1.15 Conclusions

The injury criteria values for various parts of the body were compared to the IARV requirements. The simulation injury criteria results as a percentage of the IARV values are shown in Figure 11-18.

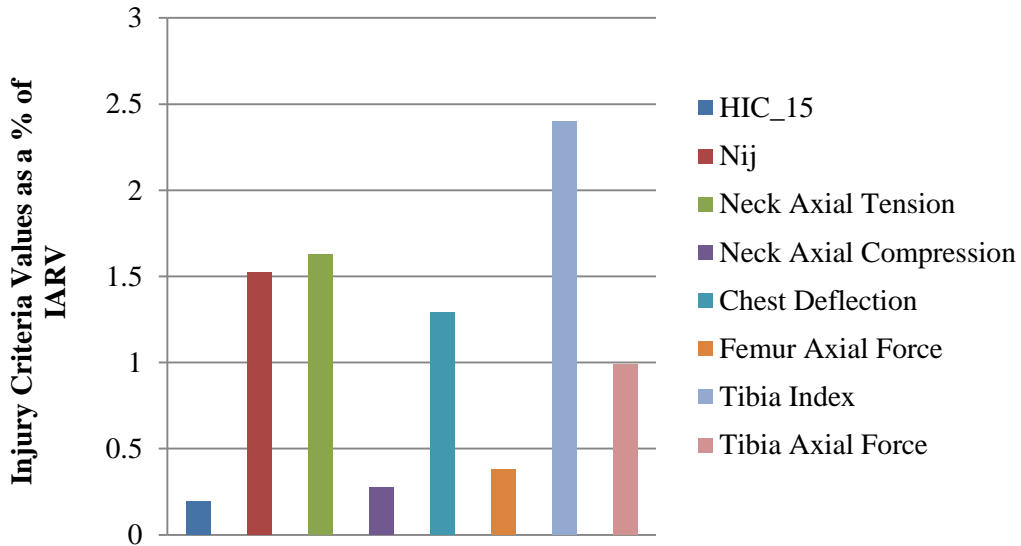


Figure 11-18 Injury probability as a function of IARV (35 mph, no pretensioner, no airbag).

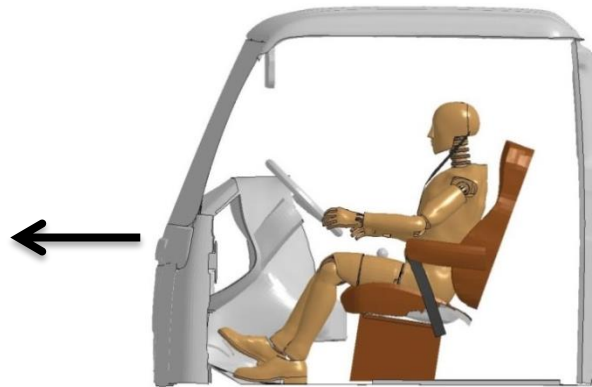
For the frontal no pretensioner simulation without airbag, the probability of injury for the head and KTH regions is unlikely because the injury criteria values stay below the threshold IARV. The injury criteria values for the neck and chest regions exceeded the threshold IARV which is unacceptable according to current standards.

11.1.3 Frontal 4 kN load limiter simulation – 35 mph

11.1.3.1 Simulation frames and summary

The following documents the post processed results of the finite element simulation of a frontal impact event with initial speed of 35 mph, inclusion of a belted H3 50th percentile male dummy in the driver position, and no application of airbag. Table 11-10 and Table 11-11 summarize the resulting simulation with frames at different times throughout the simulation. The details of the simulation are summarized below and in Figure 11-19:

- Impact Type : Frontal
- Initial Impact Speed : 35 mph
- Seatbelt Condition: Belted (4 kN load limiter)
- Airbag : No



(a) Lateral View of the FE Computer Model with Indication of Impact Orientation



(b) Seatbelt Model



(c) No Use of Airbag Model

Figure 11-19 Modeled characteristics of the finite element simulation for the frontal impact (35 mph, 4 kN load limiter, no airbag).

Table 11-10 Frontal impact simulation frames side view (35 mph, 4 kN load limiter, no airbag).









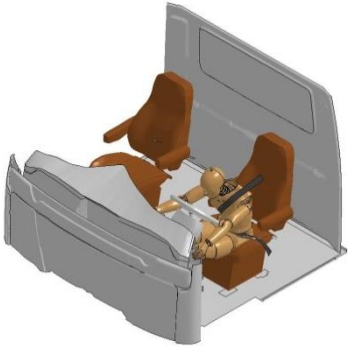

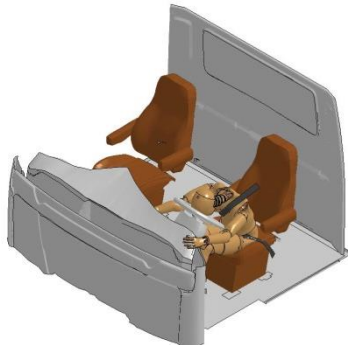
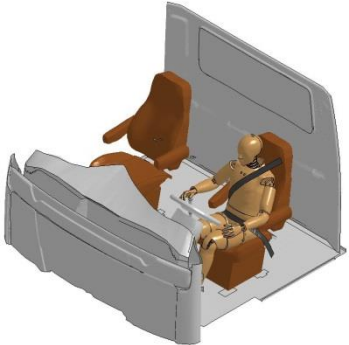

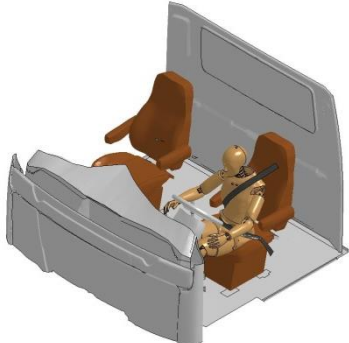
Time (Sec)	Sequential Frames	Time (Sec)	Sequential Frames
0.000		0.074	
0.015		0.089	
0.030		0.118	
0.055			

Table 11-11 Frontal impact simulation frames perspective view (35 mph, 4 kN load limiter, no airbag).

Time (Sec)	Sequential Frames	Time (Sec)	Sequential Frames
0.000		0.074	
0.015		0.089	
0.030		0.118	
0.055			

The seatbelt retractor force for the resulting simulation is plotted in Figure 11-20. The retractor contained a 4 kN load limiter.

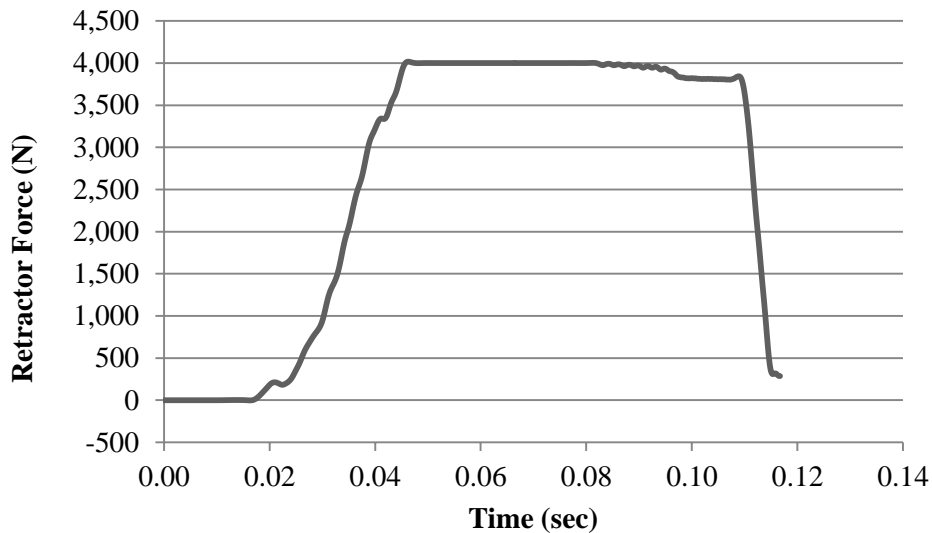


Figure 11-20 Seatbelt retractor force time history (35 mph, 4 kN load limiter, no airbag).

1.1.1.16 Head Injury Criteria

Dummy injury criteria for the head are evaluated with respect to the HIC₁₅ criteria. Head acceleration recorded during the impact event is employed to calculate the HIC₁₅ value. Figure 11-21 illustrates details for the head injury criteria and the recorded curves from this specific impact condition and passive restraint systems employment.

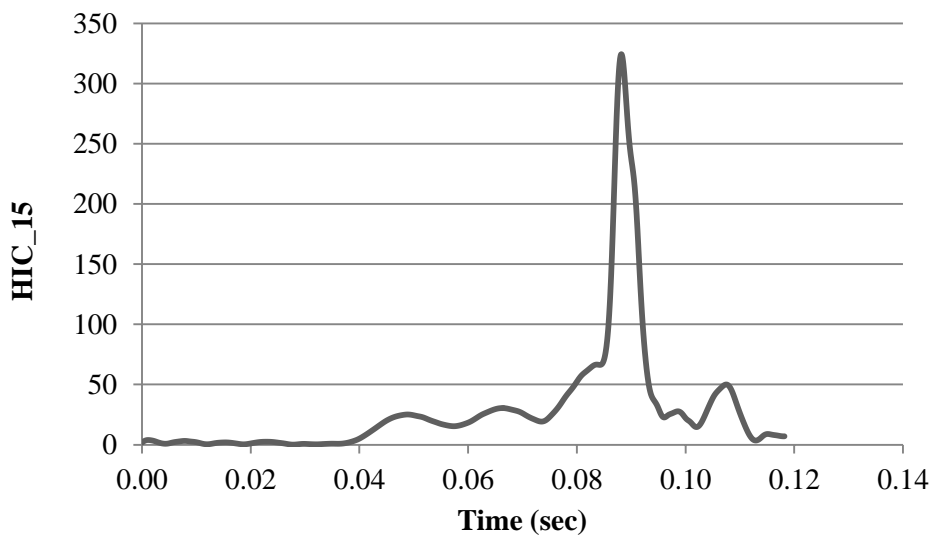
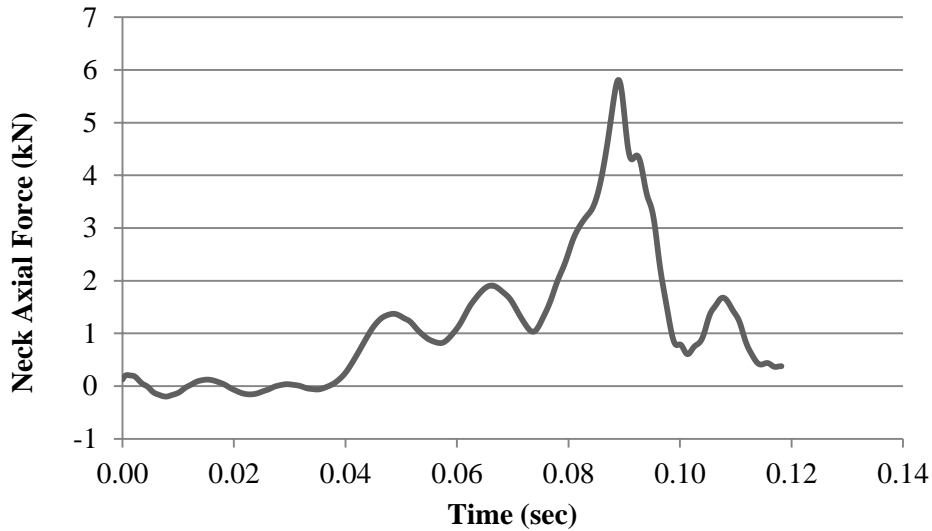


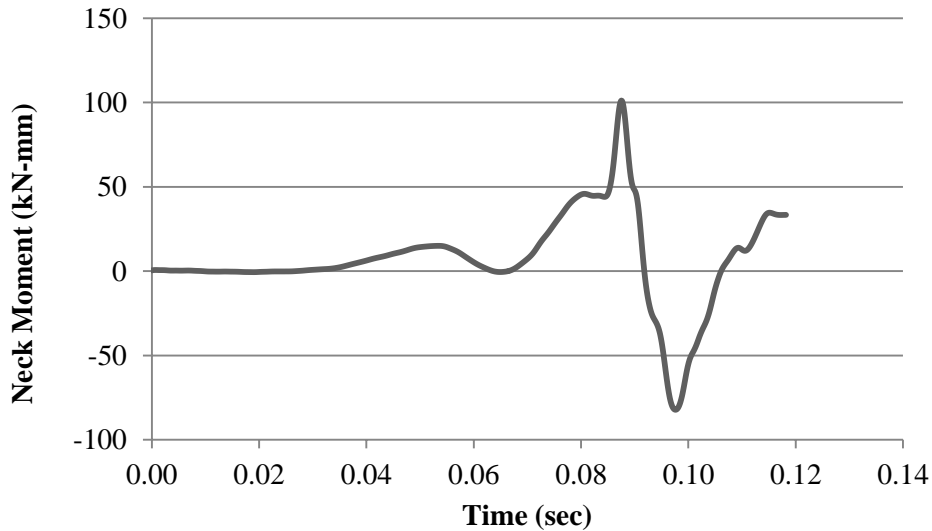
Figure 11-21 HIC time history (35 mph, 4 kN load limiter, no airbag).

1.1.1.17 Neck Injury Criteria

Dummy injury criteria for the neck are evaluated based on the normalized neck injury criteria, N_{ij} , which is defined as the sum of normalized values of loads and moments. Figure 11-22 illustrates details for the neck injury criteria and the recorded curves from this specific impact condition and passive restraint systems employment.



(a) Neck Axial Force Time History



(b) Neck Bending Moment Time History

Figure 11-22 Neck injury time history (35 mph, 4 kN load limiter, no airbag).

1.1.1.18 Chest Injury Criteria

Dummy injury criteria for the chest are evaluated based on the chest deflection values. Figure 11-23 illustrates details for the chest injury criteria and the recorded curves from this specific impact condition and passive restraint systems employment.

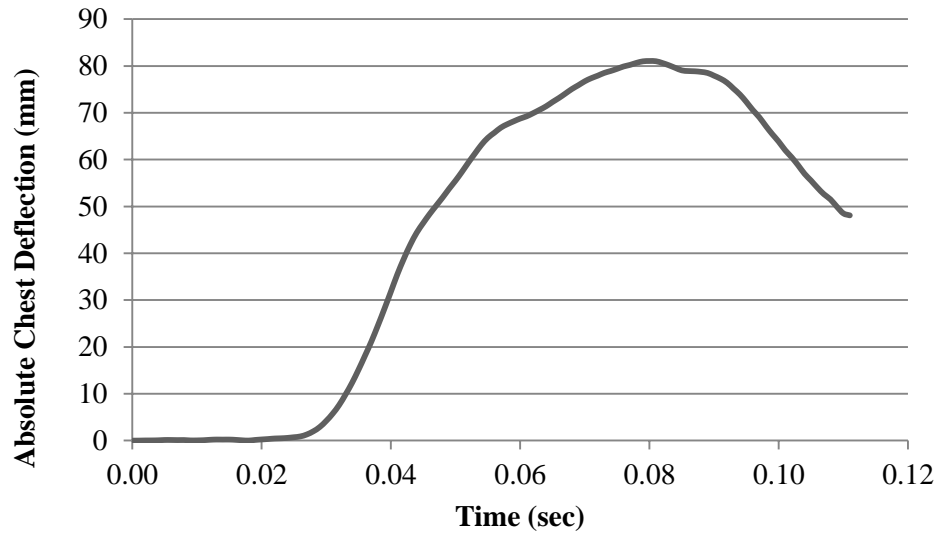
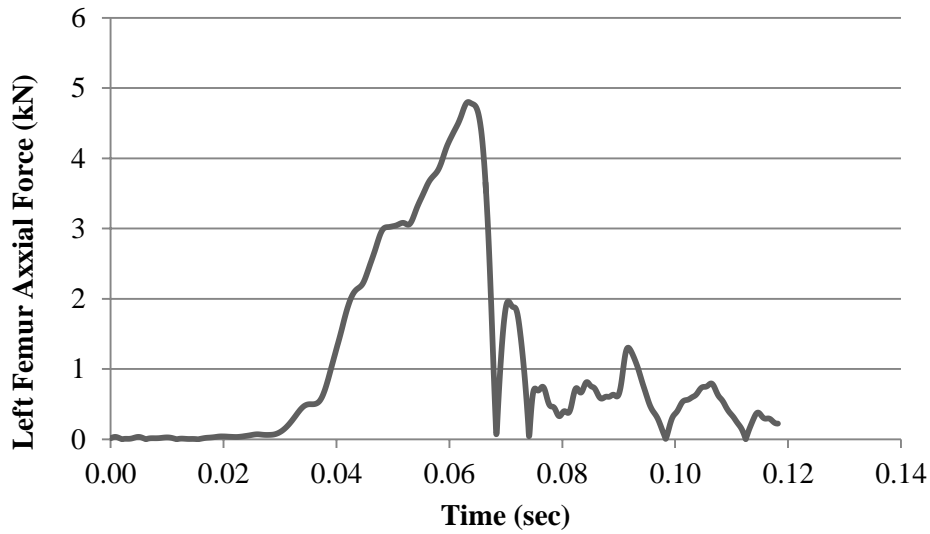


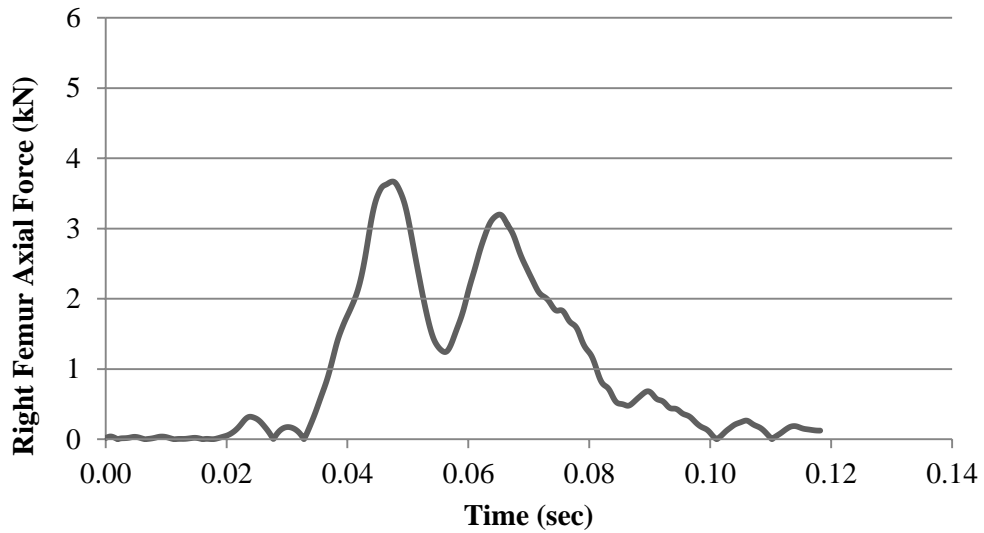
Figure 11-23 Chest deflection time history (35 mph, 4 kN load limiter, no airbag).

1.1.1.19 KTH Injury Criteria

Dummy injury criteria for the KTH are evaluated based on the formulation for probability of injury as a function of femur axial force. Figure 11-24 illustrates details for the KTH injury criteria and the recorded curves from this specific impact condition and passive restraint systems employment.



(a) Left Femur Axial Force Time History

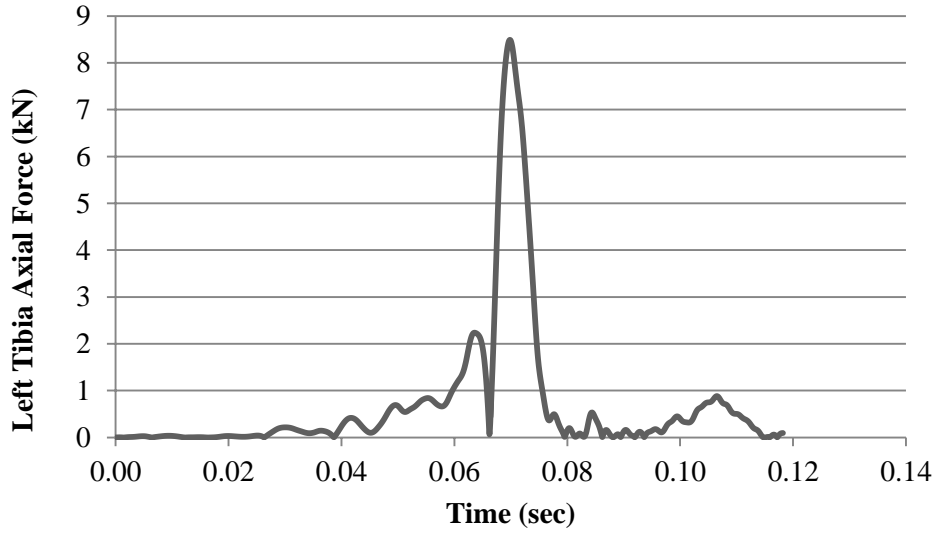


(b) Right Femur Axial Force Time History

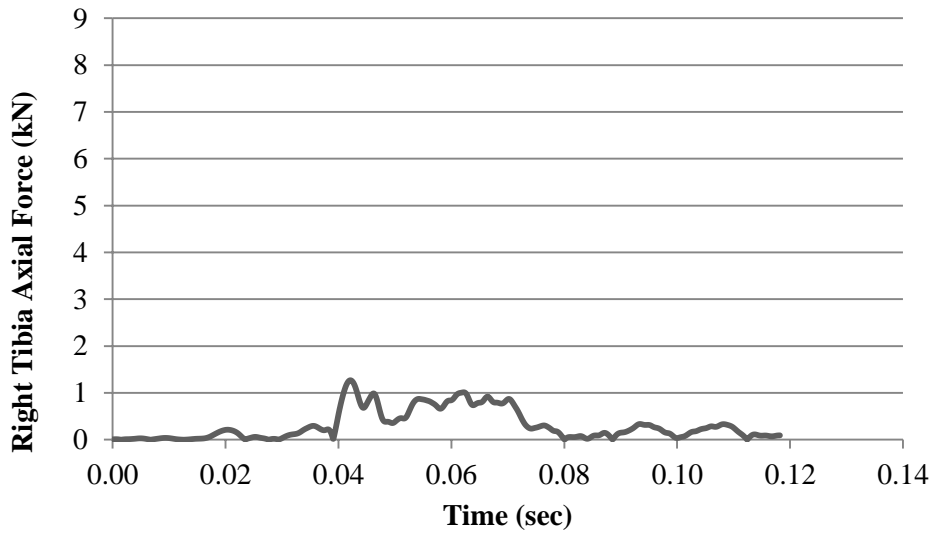
Figure 11-24 KTH injury time history (35 mph, 4 kN load limiter, no airbag).

1.1.1.20 Tibia Plateau Fracture Injury Criteria

Dummy injury criteria for tibia plateau fractures are evaluated based on axial compressive loads. Figure 11-25 illustrates details for the tibia plateau injury criteria and the recorded curves from this specific impact condition and passive restraint systems employment.



(a) Left Tibia Axial Force Time History

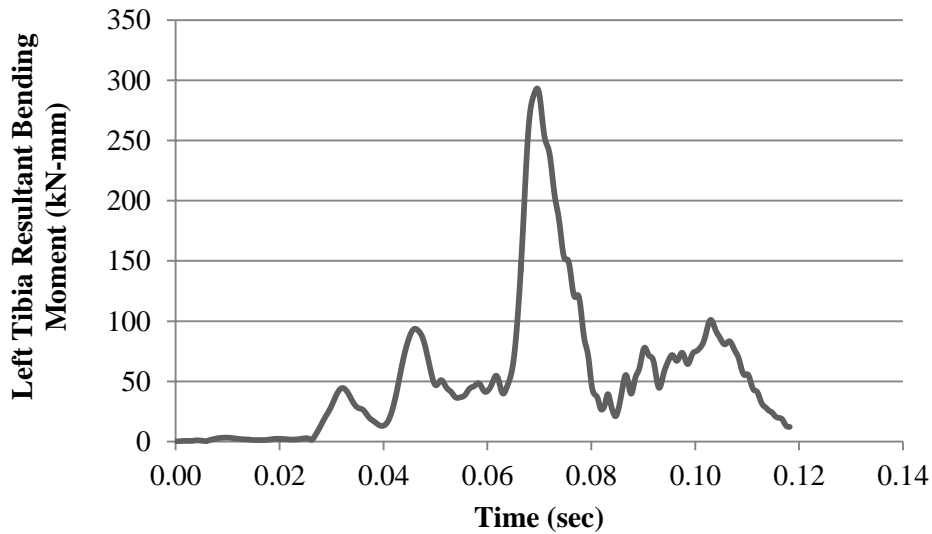


(b) Right Tibia Axial Force Time History

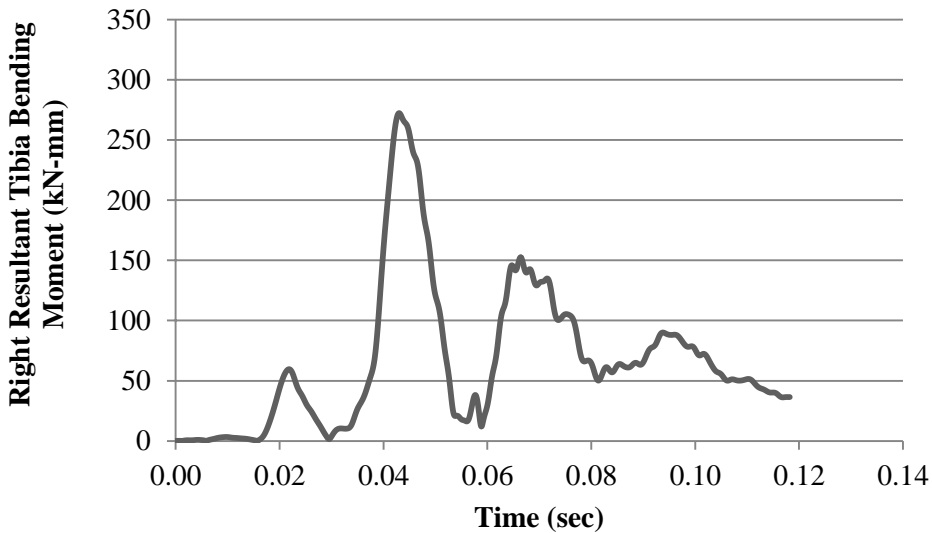
Figure 11-25 Tibia plateau fracture time history (35 mph, 4 kN load limiter, no airbag).

1.1.1.21 Tibia Shaft Fracture Injury Criteria

Dummy injury criteria for tibia shaft fractures are evaluated based on a normalized formulation that combines bending moments and axial compressive loads. Figure 11-26 illustrates details for the tibia shaft injury criteria and the recorded curves from this specific impact condition and passive restraint systems employment.



(a) Left Tibia Resultant Bending Moment Time History



(b) Right Tibia Resultant Bending Moment Time History

Figure 11-26 Tibia shaft fracture time history (35 mph, 4 kN load limiter, no airbag).

1.1.1.22 Conclusions

The injury criteria values for various parts of the body were compared to the IARV requirements. The simulation injury criteria results as a percentage of the IARV values are shown in Figure 11-27.

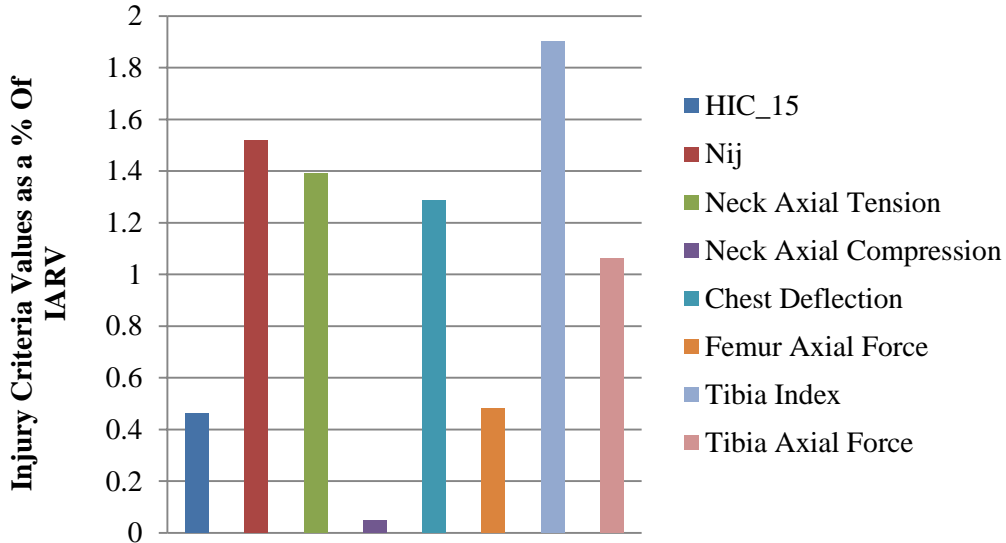


Figure 11-27 Injury probability as a function of IARV (35 mph, 4 kN load limiter, no airbag).

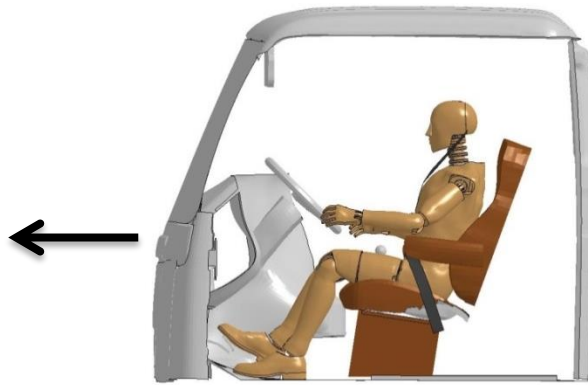
For the frontal 4 kN load limiter simulation without airbag, the probability of injury for the head and KTH regions is unlikely because the injury criteria values stay below the threshold IARV. The injury criteria values for the neck and chest regions exceeded the threshold IARV which is unacceptable according to current standards.

11.1.4 Frontal 8 kN load limiter simulation – 35 mph

11.1.4.1 Simulation frames and summary

The following documents the post processed results of the finite element simulation of a frontal impact event with initial speed of 35 mph, inclusion of a belted HIII 50th percentile male dummy in the driver position, and no application of airbag. Table 11-12 and Table 11-13 summarize the resulting simulation with frames at different times throughout the simulation. The details of the simulation are summarized below and in Figure 11-28:

- Impact Type : Frontal
- Initial Impact Speed : 35 mph
- Seatbelt Condition: Belted (8 kN Load Limiter)
- Airbag : No



(a) Lateral View of the FE Computer Model with Indication of Impact Orientation



(b) Seatbelt Model



(c) No Use of Airbag Model

Figure 11-28 Modeled characteristics of the finite element simulation for the frontal impact (35 mph, 8 kN load limiter, no airbag).

Table 11-12 Frontal impact simulation frames side view (35 mph, 8 kN load limiter, no airbag).









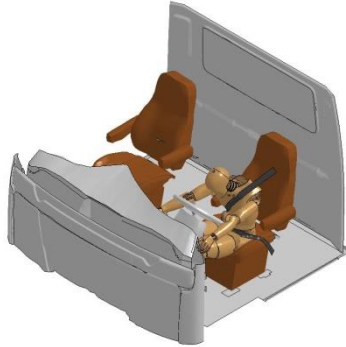





Time (Sec)	Sequential Frames	Time (Sec)	Sequential Frames
0.000		0.074	
0.015		0.089	
0.030		0.99	
0.055			

Table 11-13 Frontal impact simulation frames perspective view (35 mph, 8 kN load limiter, no airbag).

Time (Sec)	Sequential Frames	Time (Sec)	Sequential Frames
0.000		0.074	
0.015		0.089	
0.030		0.99	
0.055			

The seatbelt retractor force for the resulting simulation is plotted in Figure 11-29. The retractor contained an 8 kN load limiter.

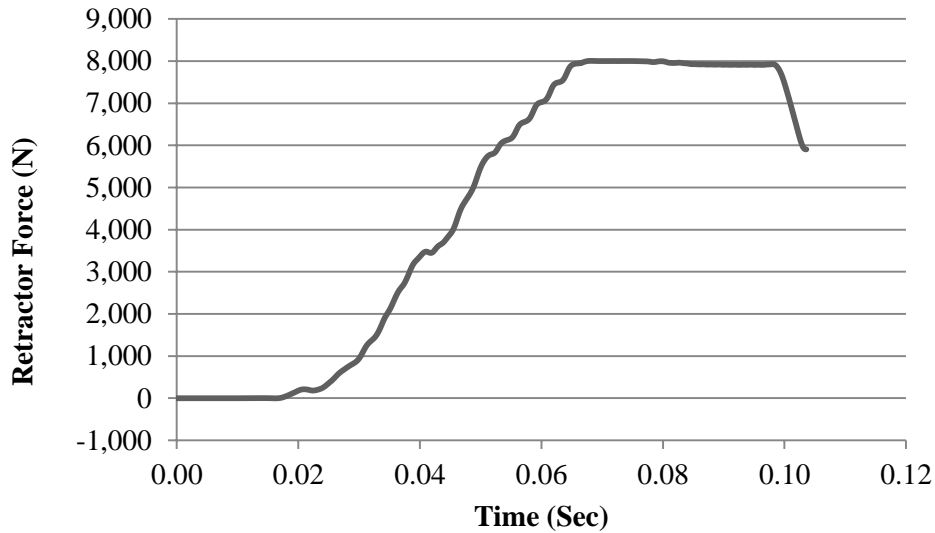


Figure 11-29 Seatbelt retractor force time history (35 mph, 8 kN load limiter, no airbag).

1.1.1.23 Head Injury Criteria

Dummy injury criteria for the head are evaluated with respect to the HIC₁₅ criteria. Head acceleration recorded during the impact event is employed to calculate the HIC₁₅ value. Figure 11-30 illustrates details for the head injury criteria and the recorded curves from this specific impact condition and passive restraint systems employment.

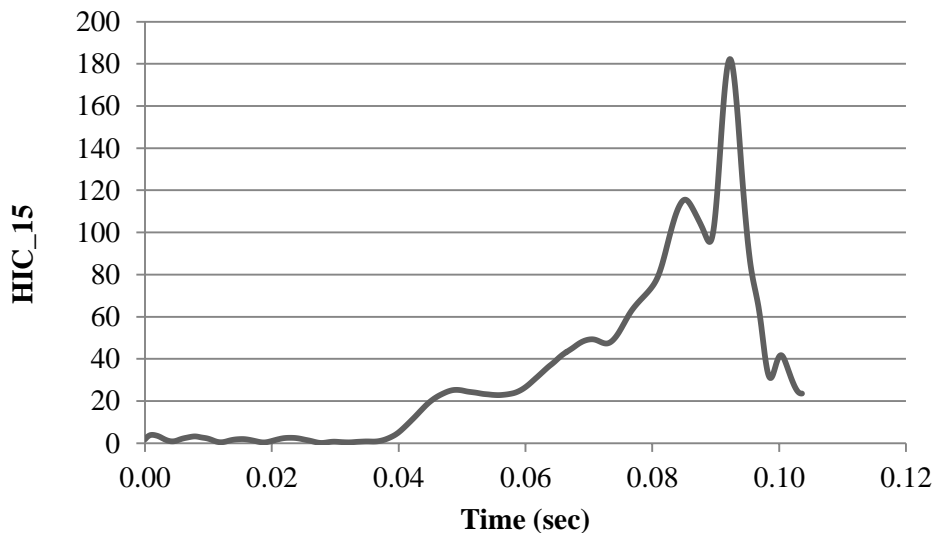
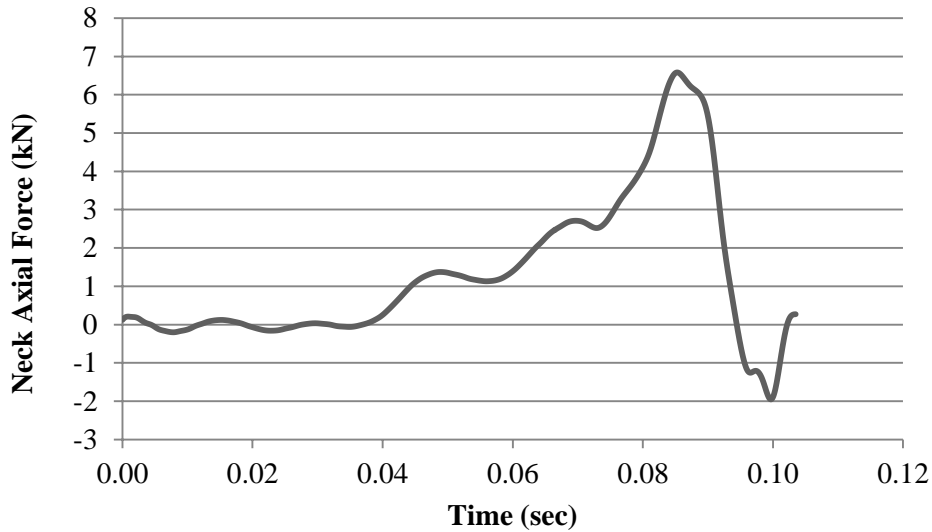


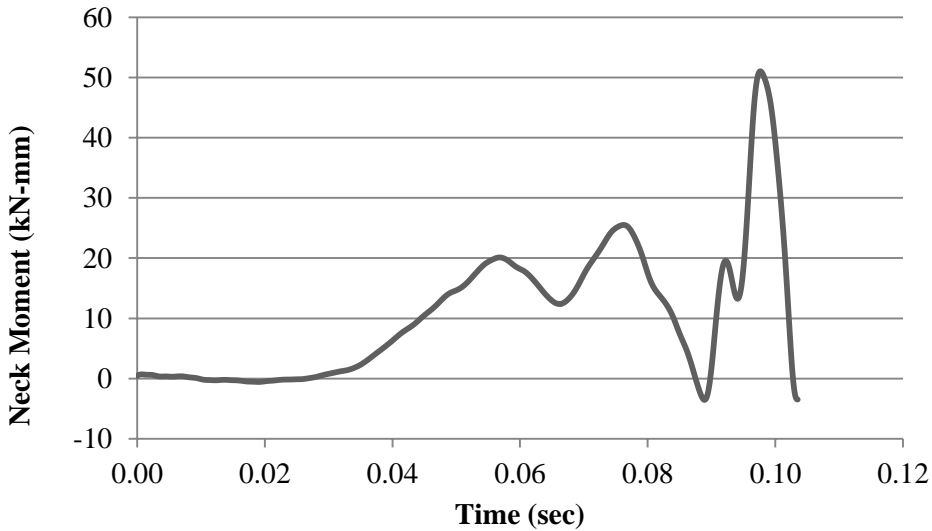
Figure 11-30 HIC time history (35 mph, 8 kN load limiter, no airbag).

1.1.1.24 Neck Injury Criteria

Dummy injury criteria for the neck are evaluated based on the normalized neck injury criteria, N_{ij} , which is defined as the sum of normalized values of loads and moments. Figure 11-31 illustrates details for the neck injury criteria and the recorded curves from this specific impact condition and passive restraint systems employment.



(a) Neck Axial Force Time History



(b) Neck Bending Moment Time History

Figure 11-31 Neck injury time history (35 mph, 8 kN load limiter, no airbag).

1.1.1.25 Chest Injury Criteria

Dummy injury criteria for the chest are evaluated based on the chest deflection values. Figure 11-32 illustrates details for the chest injury criteria and the recorded curves from this specific impact condition and passive restraint systems employment.

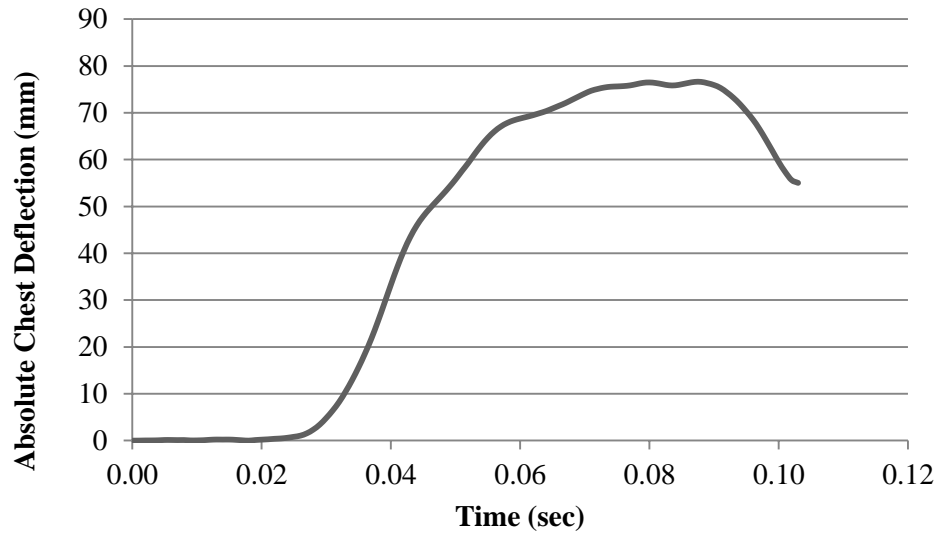
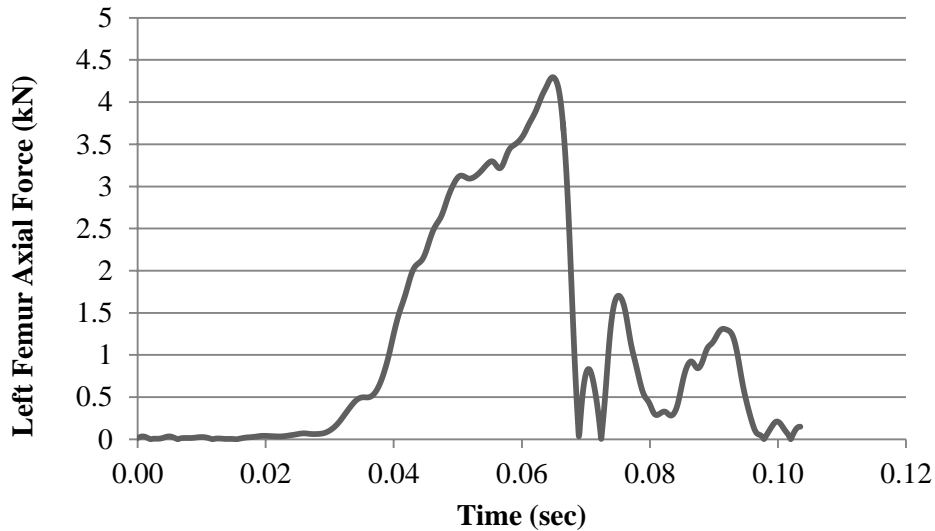


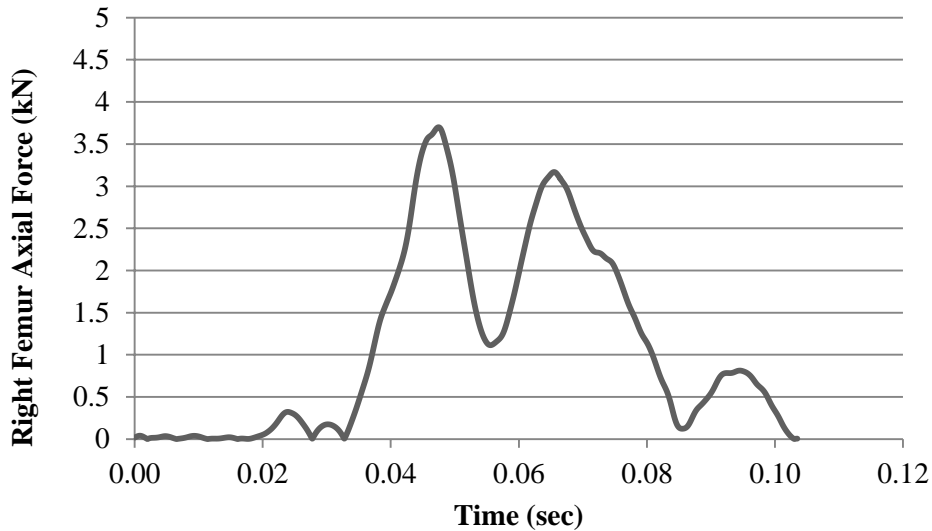
Figure 11-32 Chest deflection time history (35 mph, 8 kN load limiter, no airbag).

1.1.1.26 KTH Injury Criteria

Dummy injury criteria for the KTH are evaluated based on the formulation for probability of injury as a function of femur axial force. Figure 11-33 illustrates details for the KTH injury criteria and the recorded curves from this specific impact condition and passive restraint systems employment.



(a) Left Femur Axial Force Time History

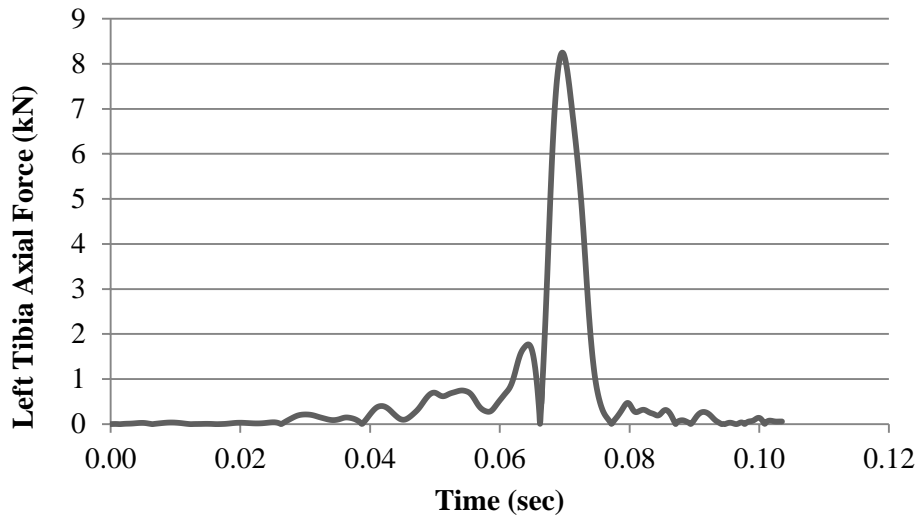


(b) Right Femur Axial Force Time History

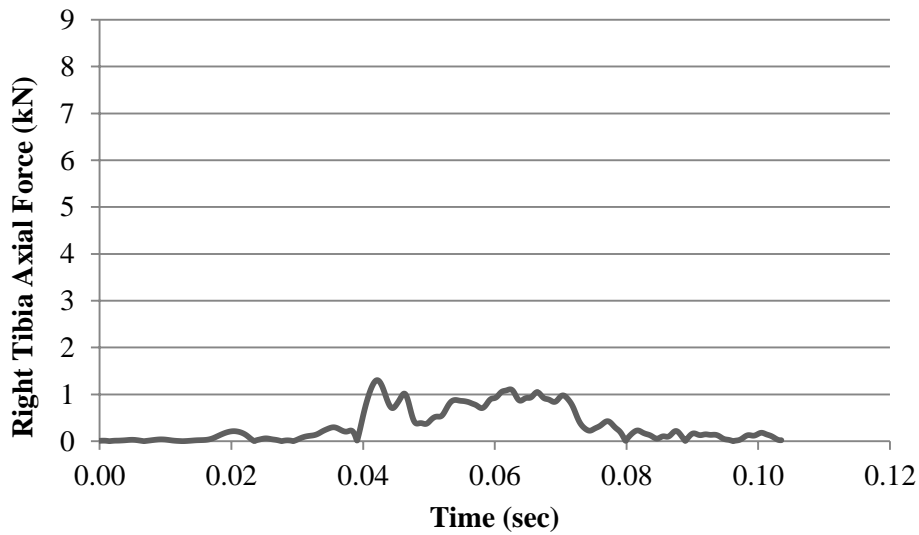
Figure 11-33 KTH injury time history (35 mph, 8 kN load limiter, no airbag).

1.1.1.27 Tibia Plateau Fracture Injury Criteria

Dummy injury criteria for tibia plateau fractures are evaluated based on axial compressive loads. Figure 11-34 illustrates details for the tibia plateau injury criteria and the recorded curves from this specific impact condition and passive restraint systems employment.



(a) Left Tibia Axial Force Time History

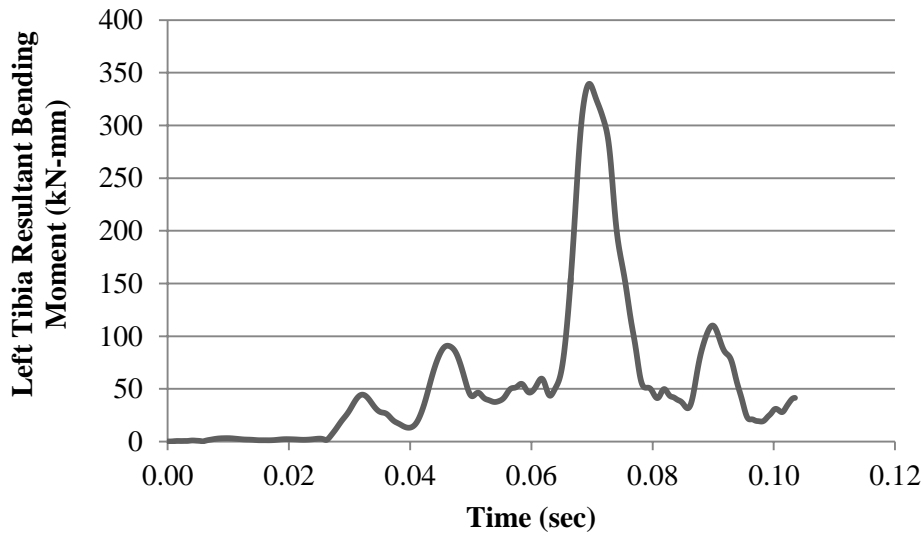


(b) Right Tibia Axial Force Time History

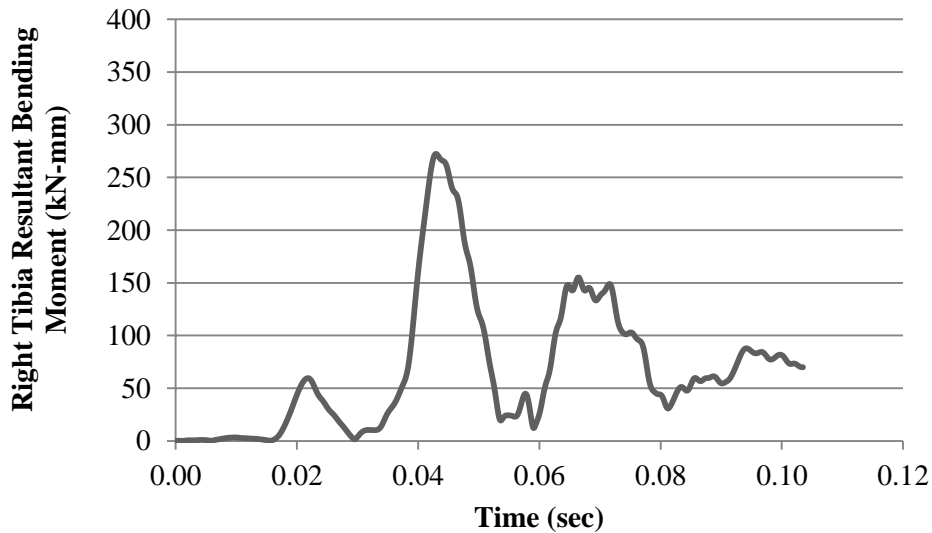
Figure 11-34 Tibia plateau fracture time history (35 mph, 8 kN load limiter, no airbag).

1.1.1.28 Tibia Shaft Fracture Injury Criteria

Dummy injury criteria for tibia shaft fractures are evaluated based on a normalized formulation that combines bending moments and axial compressive loads. Figure 11-35 illustrates details for the tibia shaft injury criteria and the recorded curves from this specific impact condition and passive restraint systems employment.



(a) Left Tibia Resultant Bending Moment Time History



(b) Right Tibia Resultant Bending Moment Time History

Figure 11-35 Tibia shaft fracture time history (35 mph, 8 kN load limiter, no airbag).

1.1.1.29 Conclusions

The injury criteria values for various parts of the body were compared to the IARV requirements. The simulation injury criteria results as a percentage of the IARV values are shown in Figure 11-36.

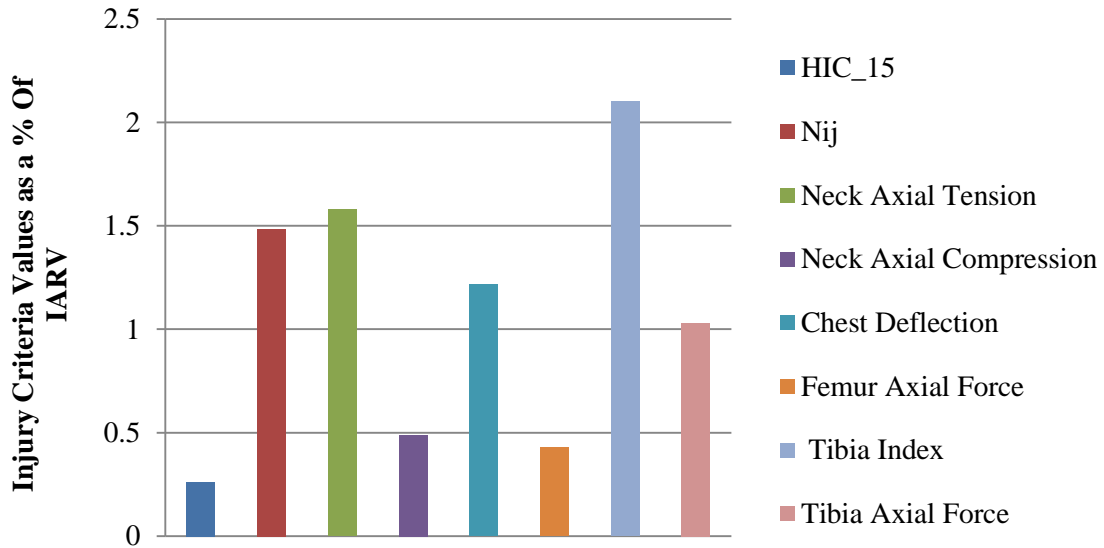


Figure 11-36 Injury probability as a function of IARV (35 mph, 8 kN load limiter, no airbag).

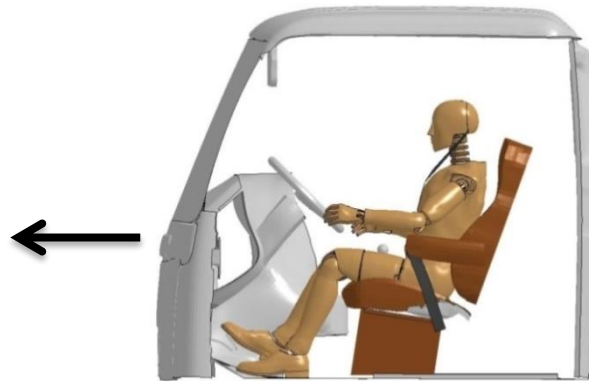
For the frontal 8 kN load limiter simulation without airbag, the probability of injury for the head and KTH regions is unlikely because the injury criteria values stay below the threshold IARV. The injury criteria values for the neck and chest regions exceeded the threshold IARV which is unacceptable according to current standards.

11.1.5 Frontal lowered D-ring simulation – 35 mph

11.1.5.1 Simulation frames and summary

The following documents the post processed results of the finite element simulation of a frontal impact event with initial speed of 35 mph, inclusion of a belted HIII 50th percentile male dummy in the driver position, and no application of airbag. Table 11-14 and Table 11-15 summarize the resulting simulation with frames at different times throughout the simulation. The details of the simulation are summarized below and in Figure 11-37:

- Impact Type : Frontal
- Initial Impact Speed : 35 mph
- Seatbelt Condition: Belted (Lowered D Ring)
- Airbag : No



(a) Lateral View of the FE Computer Model with Indication of Impact Orientation



(b) Seatbelt Model



(c) No Use of Airbag Model

Figure 11-37 Modeled characteristics of the finite element simulation for the frontal impact (35 mph, lowered d-ring, no airbag).

Table 11-14 Frontal impact simulation frames side view (35 mph, lowered d-ring, no airbag).












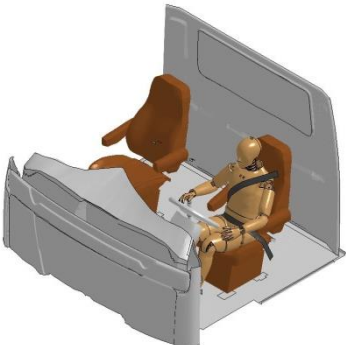


Time (Sec)	Sequential Frames	Time (Sec)	Sequential Frames
0.000		0.074	
0.015		0.089	
0.030		0.120	
0.055			

Table 11-15 Frontal impact simulation frames perspective view (35 mph, lowered d-ring, no airbag).

Time (Sec)	Sequential Frames	Time (Sec)	Sequential Frames
0.000		0.074	
0.015		0.089	
0.030		0.120	
0.055			

The seatbelt retractor force for the resulting simulation is plotted in Figure 11-38. The retractor contained no load limiter for this simulation and reached a peak of about 8.5 kN.

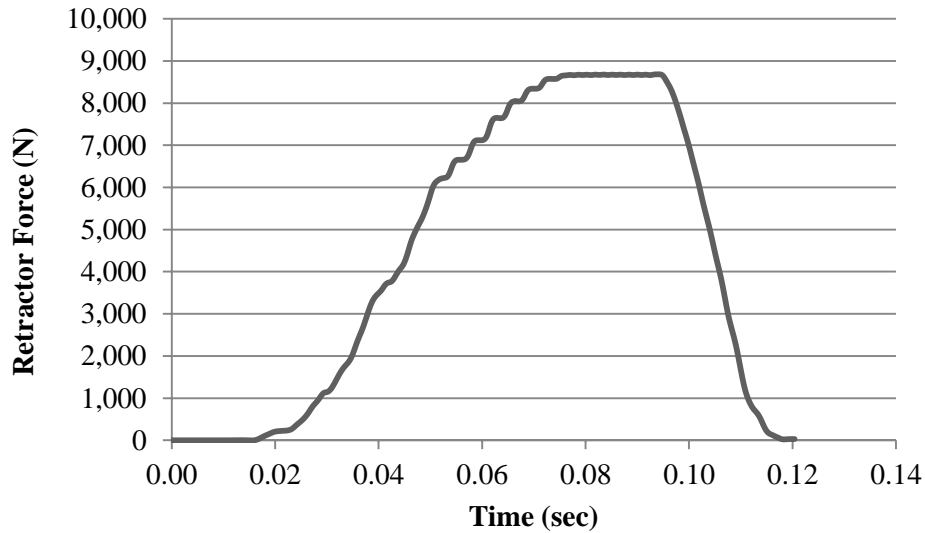


Figure 11-38 Seatbelt retractor force time history (35 mph, lowered d-ring, no airbag).

11.1.5.2 Head injury criteria

Dummy injury criteria for the head are evaluated with respect to the HIC₁₅ criteria. Head acceleration recorded during the impact event is employed to calculate the HIC₁₅ value. Figure 11-39 illustrates details for the head injury criteria and the recorded curves from this specific impact condition and passive restraint systems employment.

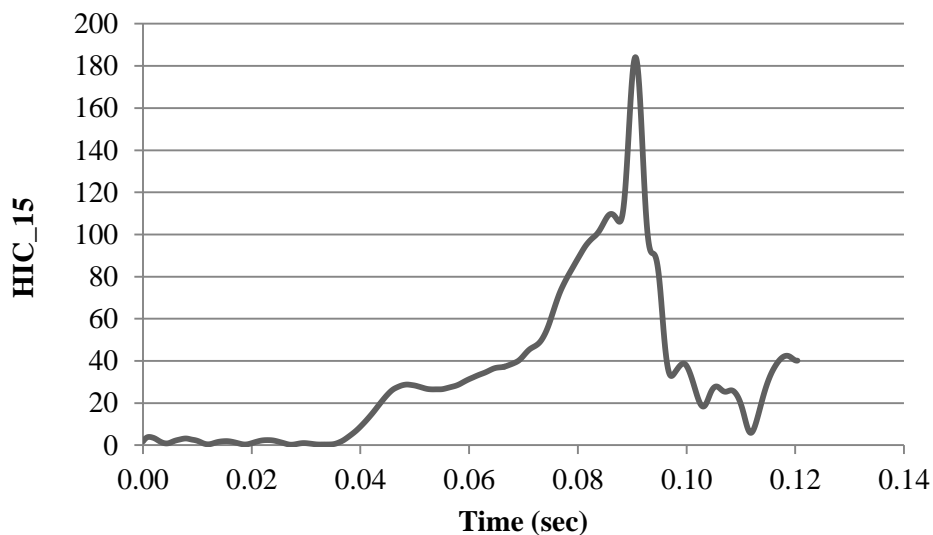
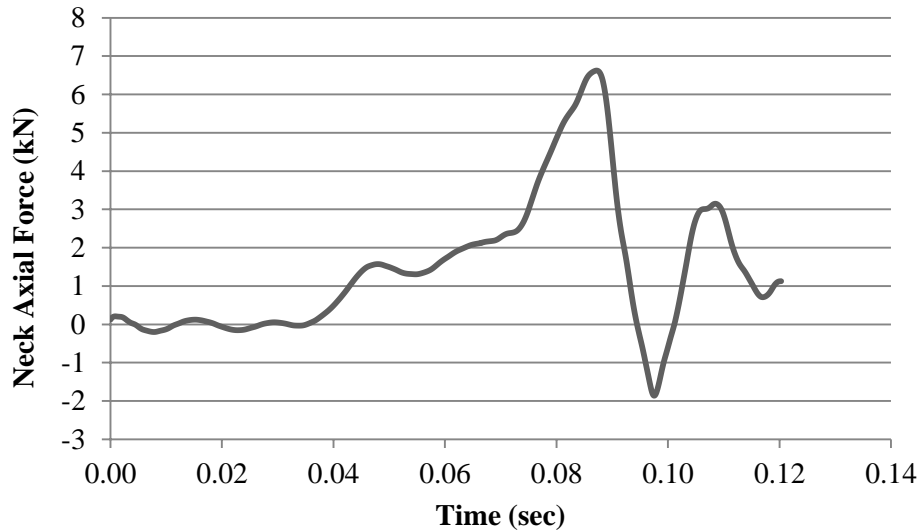


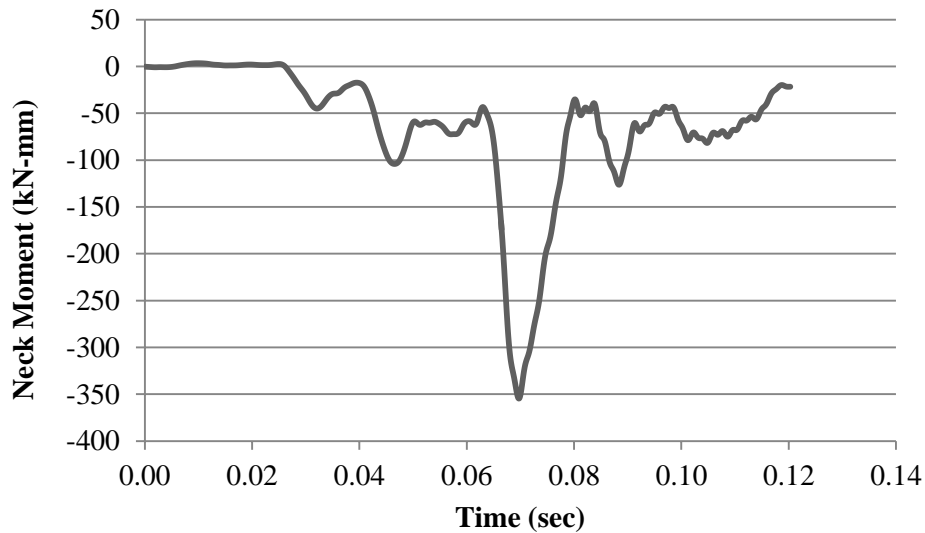
Figure 11-39 HIC time history (35 mph, lowered d-ring, no airbag).

11.1.5.3 Neck injury criteria

Dummy injury criteria for the neck are evaluated based on the normalized neck injury criteria, N_{ij} , which is defined as the sum of normalized values of loads and moments. Figure 11-40 illustrates details for the neck injury criteria and the recorded curves from this specific impact condition and passive restraint systems employment.



(a) Neck Axial Force Time History



(b) Neck Bending Moment Time History

Figure 11-40 Neck injury time history (35 mph, lowered d-ring, no airbag).

11.1.5.4 Chest injury criteria

Dummy injury criteria for the chest are evaluated based on the chest deflection values. Figure 11-41 illustrates details for the chest injury criteria and the recorded curves from this specific impact condition and passive restraint systems employment.

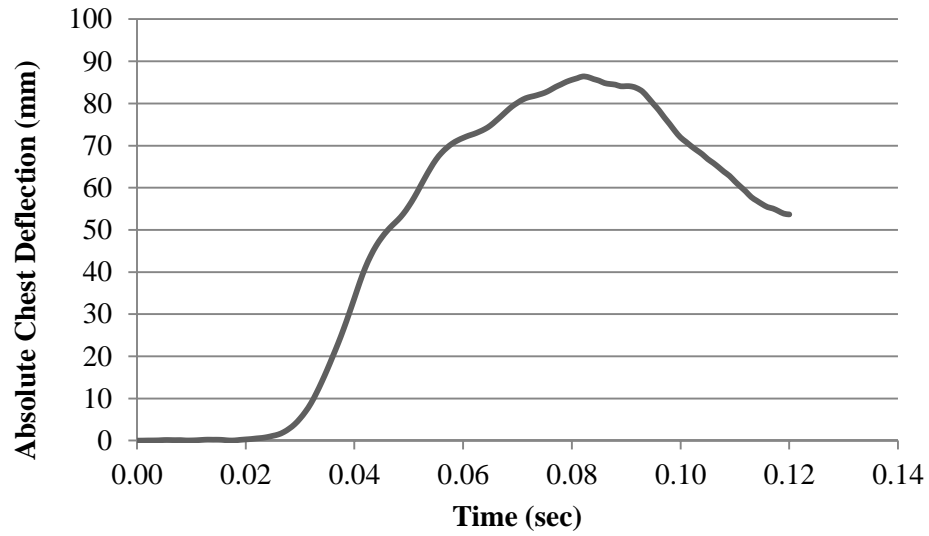
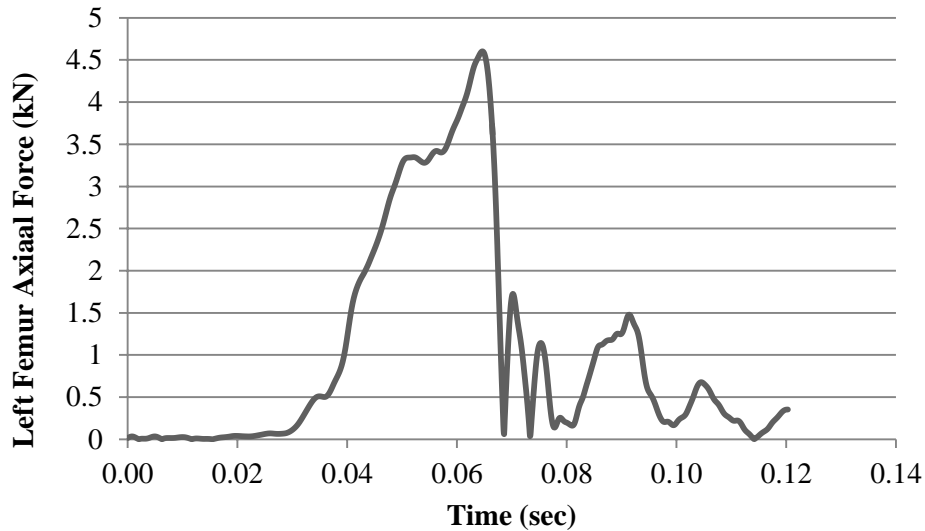


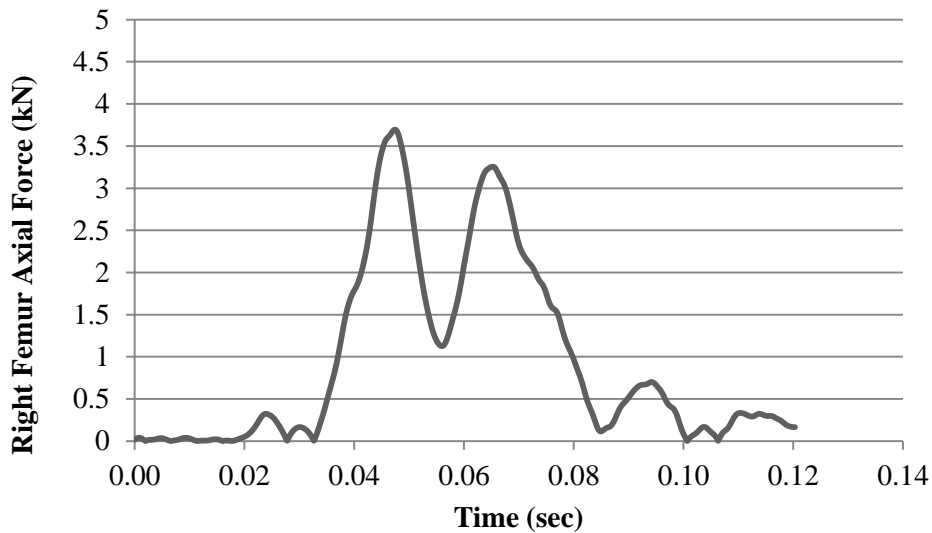
Figure 11-41 Chest deflection time history (35 mph, lowered d-ring, no airbag).

11.1.5.5 KTH injury criteria

Dummy injury criteria for the KTH are evaluated based on the formulation for probability of injury as a function of femur axial force. Figure 11-42 illustrates details for the KTH injury criteria and the recorded curves from this specific impact condition and passive restraint systems employment.



(a) Left Femur Axial Force Time History

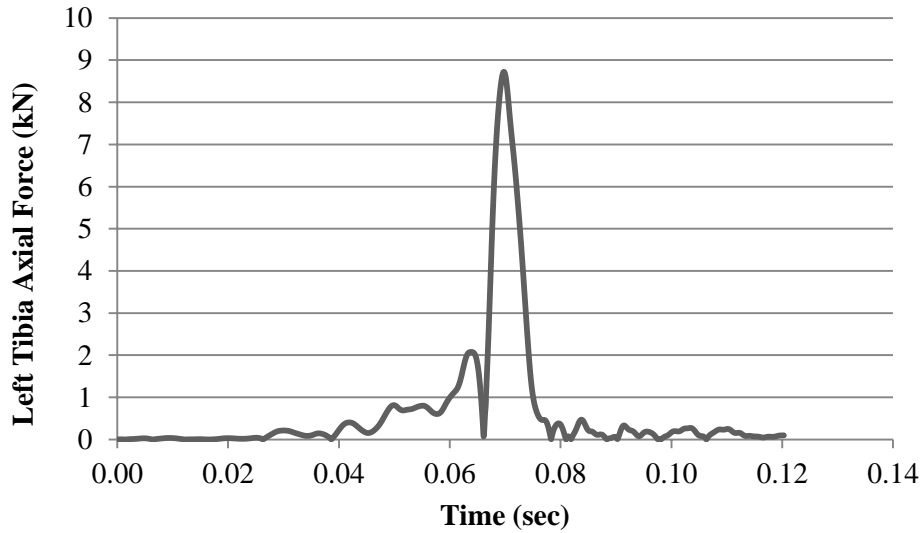


(b) Right Femur Axial Force Time History

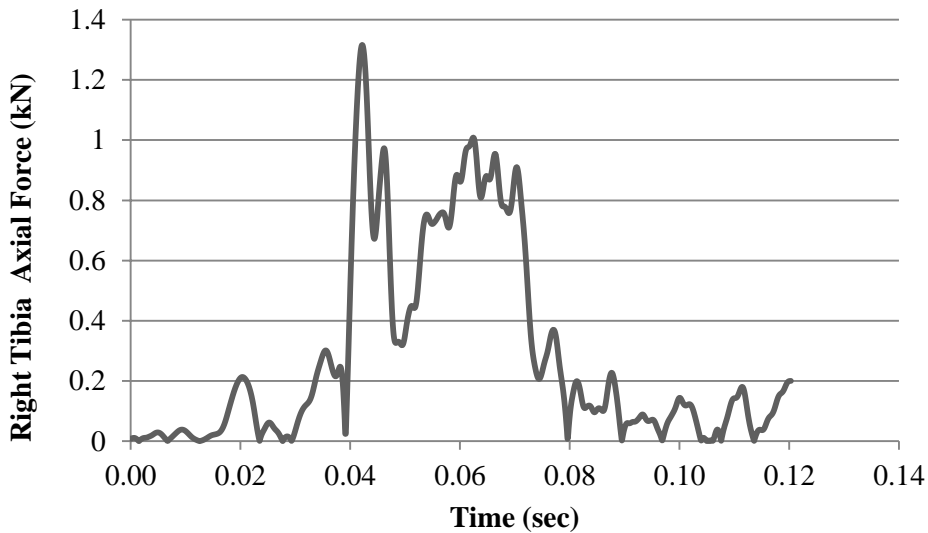
Figure 11-42 KTH injury time history (35 mph, lowered d-ring, no airbag).

1.1.1.30 Tibia Plateau Fracture Injury Criteria

Dummy injury criteria for tibia plateau fractures are evaluated based on axial compressive loads. Figure 11-43 illustrates details for the tibia plateau injury criteria and the recorded curves from this specific impact condition and passive restraint systems employment.



(a) Left Tibia Axial Force Time History

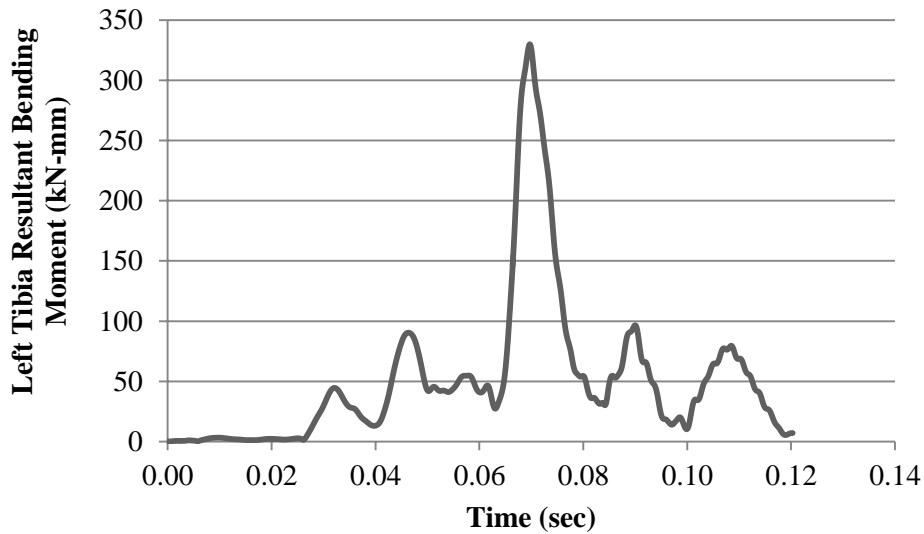


(b) Right Tibia Axial Force Time History

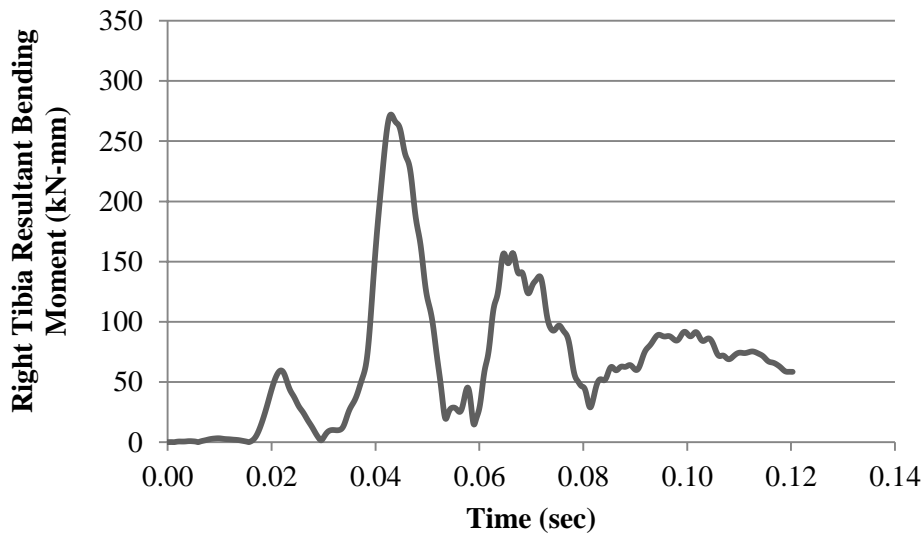
Figure 11-43 Tibia plateau fracture time history (35 mph, lowered d-ring, no airbag).

11.1.5.6 Tibia Shaft Fracture Injury Criteria

Dummy injury criteria for tibia shaft fractures are evaluated based on a normalized formulation that combines bending moments and axial compressive loads. Figure 11-44 illustrates details for the tibia shaft injury criteria and the recorded curves from this specific impact condition and passive restraint systems employment.



(a) Left Tibia Bending Moment Time History



(b) Right Tibia Bending Moment Time History

Figure 11-44 Tibia shaft fracture time history (35 mph, lowered d-ring, no airbag).

11.1.5.7 Conclusions

The injury criteria values for various parts of the body were compared to the IARV requirements. The simulation injury criteria results as a percentage of the IARV values are shown in Figure 11-45.

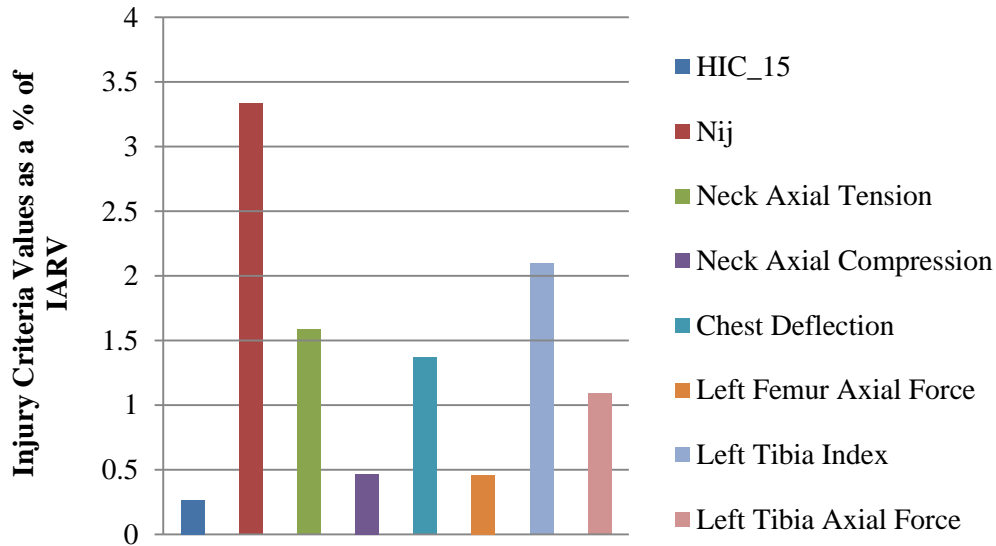


Figure 11-45 Injury probability as a function of IARV (35 mph, lowered d-ring, no airbag).

For the frontal lowered d-ring simulation without airbag, the probability of injury for the head and KTH regions is unlikely because the injury criteria values stay below the threshold IARV. The injury criteria values for the neck and chest regions exceeded the threshold IARV which is unacceptable according to current standards.

11.1.6 Comparison of Frontal Simulations without Airbag – 35 mph

11.1.6.1 Simulation frame comparisons

The five frontal simulations conducted at 35 mph without airbag were compared to see the effects of the different restraint system parameters. Table 11-16 and Table 11-17 summarize the resulting simulations with frames at different times throughout the simulation.

11.1.6.2 Injury criteria comparison for different body regions of ATD

The injury criteria values for various parts of the body were compared to the IARV requirements. The simulation injury criteria results as a percentage of the IARV values are shown in Figure 11-46 through Figure 11-49 for the different regions of the body. The injury criteria results were not included for tibia injury comparison because the IARV for the tibia is not validated. Leg injury is typically analyzed in terms of KTH injury which represents the femur region.

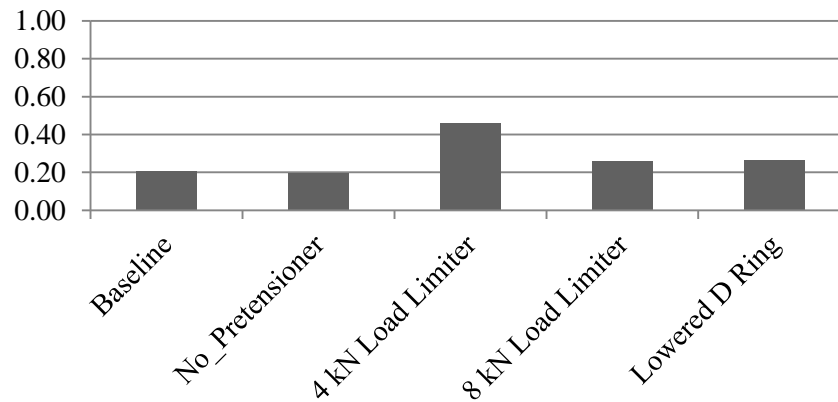


Figure 11-46 Head injury probability comparison as a function of IARV (no airbag).

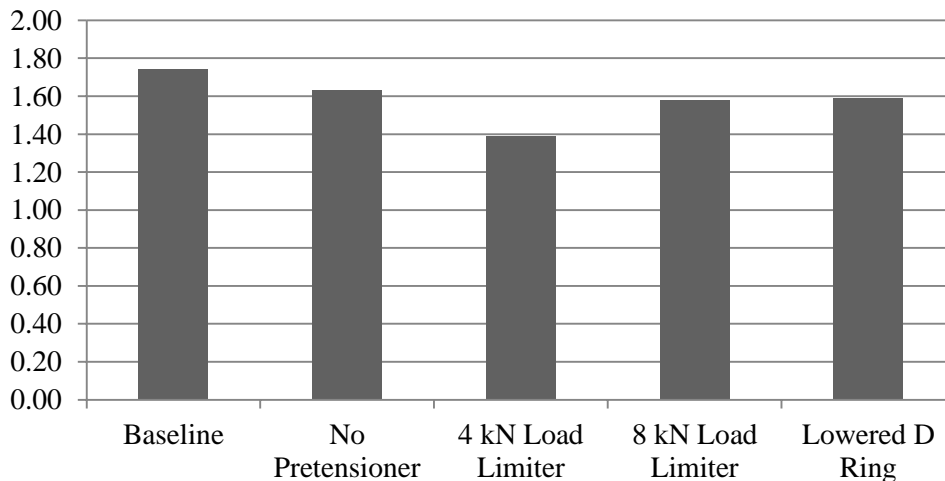





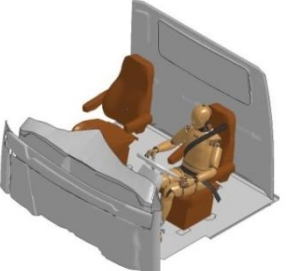
















Figure 11-47 Neck injury probability comparison as a function of IARV (no airbag).

Table 11-16 Sequential frame comparison of frontal simulations at 35 mph without airbag (side view).



Table 11-17 Sequential frame comparison of frontal simulations at 35 mph without airbag (perspective view).

Time (Sec)	Baseline	No Pretensioner	4 kN Load Limiter	8 kN Load Limiter	Lowered D-Ring
0.000					
0.030					
0.074					
End					

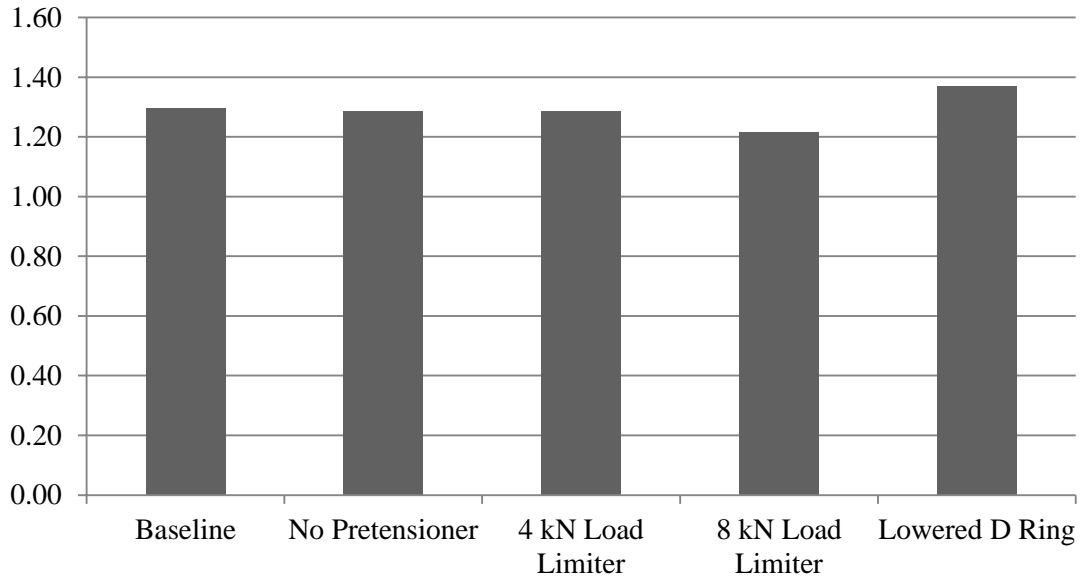


Figure 11-48 Chest injury probability comparison as a function of IARV (no airbag).

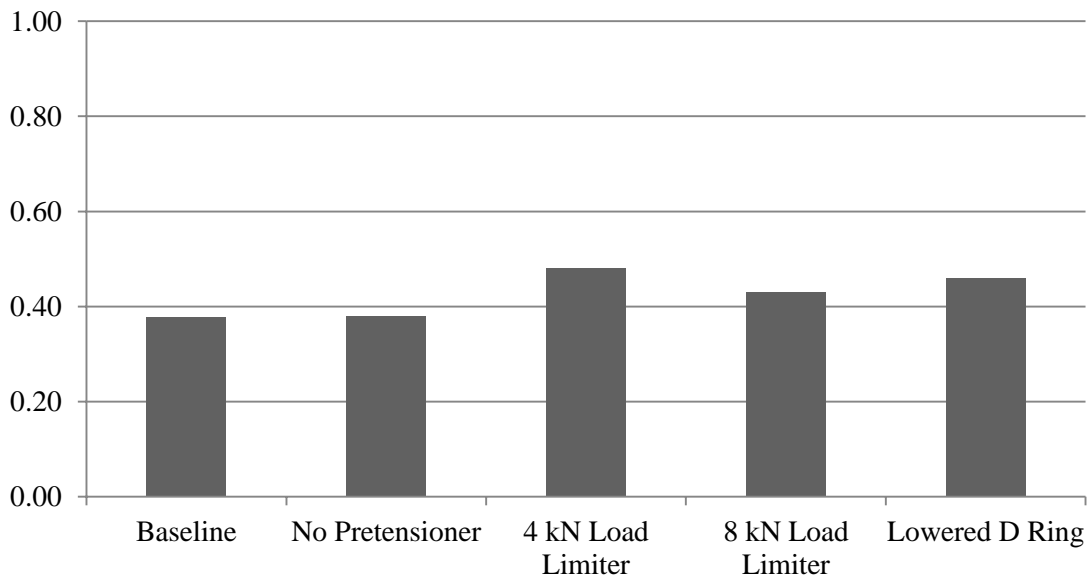


Figure 11-49 KTH injury probability comparison as a function of IARV (no airbag).

Analysis of the injury criteria shows that both the KTH injury and head injury stayed below the threshold IARV, meaning that the probability of leg or head injury is unlikely. Both the neck and chest injury criteria results were higher and contained values above the threshold IARV's which is unacceptable according to current standards. There was not a specific restraint system that clearly produced the lowest injury criteria results in comparison to the others.

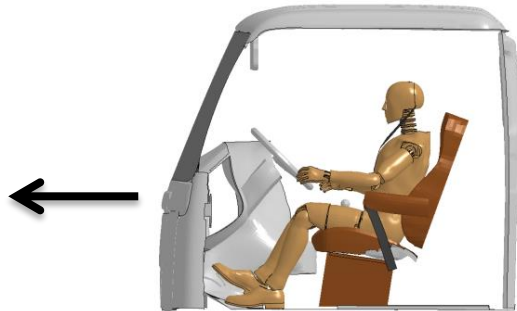
11.2 Frontal simulations with airbag – 35 mph

11.2.1 Frontal baseline simulation – 35 mph

11.2.1.1 Simulation frames and summary

The following documents the post processed results of the finite element simulation of a frontal impact event with initial speed of 35 mph, inclusion of a belted HIII 50th percentile male dummy in the driver position, and application of airbag. Table 11-18 and Table 11-19 summarize the resulting simulation with frames at different times throughout the simulation. The details of the simulation are summarized below and in Figure 11-50:

- Impact Type : Frontal
- Initial Impact Speed : 35 mph
- Seatbelt Condition: Belted
- Airbag : Yes



(a) Lateral View of the FE Computer Model with Indication of Impact Orientation



(b) Seatbelt Model



(c) Use of Airbag Model

Figure 11-50 Modeled characteristics of the finite element simulation for the frontal impact (35 mph, baseline, airbag).

Table 11-18 Frontal impact simulation frames side view (35 mph, baseline, airbag).















Time (Sec)	Sequential Frames	Time (Sec)	Sequential Frames
0.000		0.074	
0.015		0.089	
0.030		0.110	
0.055			

Table 11-19 Frontal impact simulation frames perspective view (35 mph, baseline, airbag).

Time (Sec)	Sequential Frames	Time (Sec)	Sequential Frames
0.000		0.074	
0.015		0.089	
0.030		0.110	
0.055			

The seatbelt retractor force for the resulting simulation is plotted in Figure 11-51. The retractor contained no load limiter for this simulation and reached a peak of about 8.5 kN.

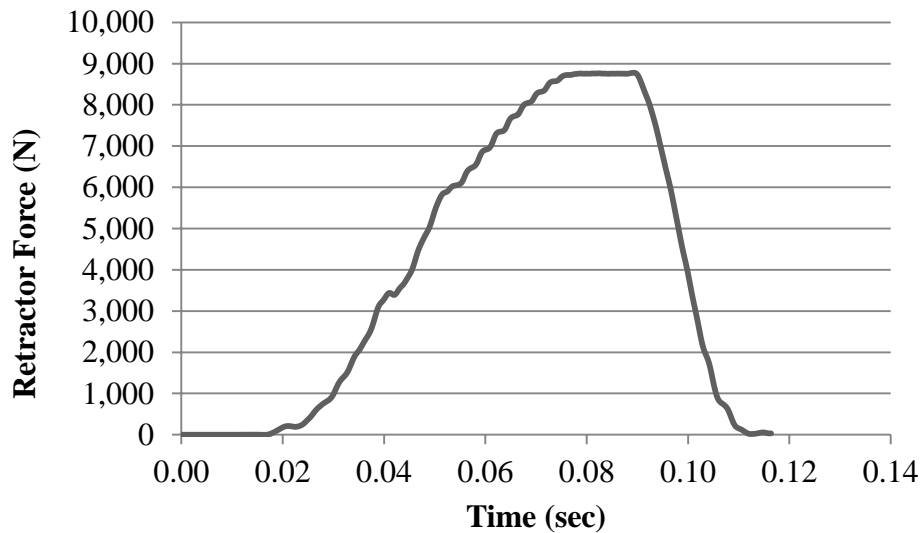


Figure 11-51 Seatbelt retractor force time history (35 mph, baseline, airbag).

11.2.1.2 Head injury criteria

Dummy injury criteria for the head are evaluated with respect to the HIC₁₅ criteria. Head acceleration recorded during the impact event is employed to calculate the HIC₁₅ value. Figure 11-52 illustrates details for the head injury criteria and the recorded curves from this specific impact condition and passive restraint systems employment.

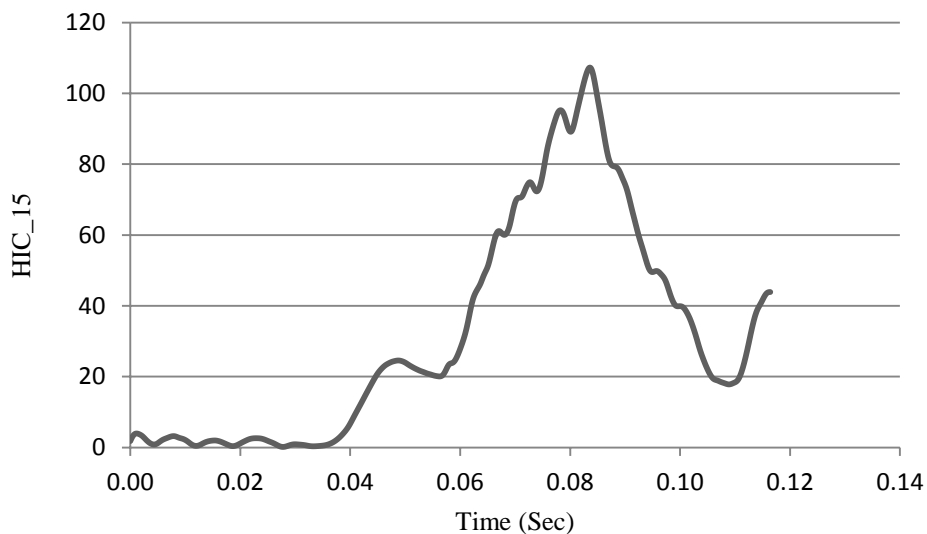
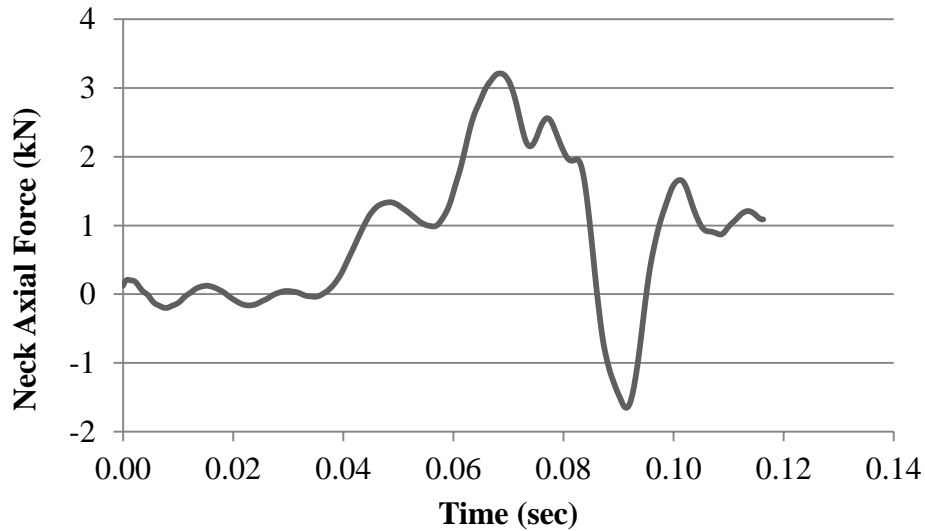


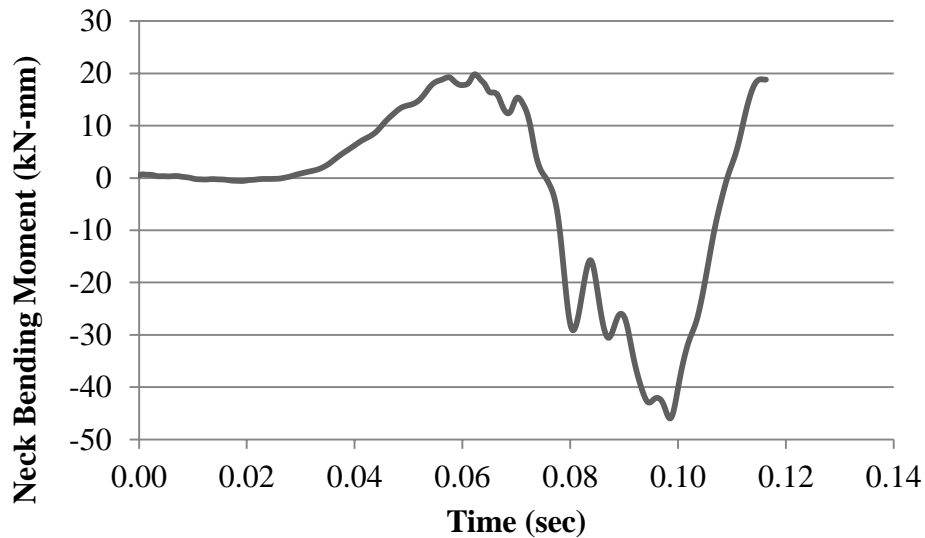
Figure 11-52 HIC time history (35 mph, baseline, airbag).

11.2.1.3 Neck injury criteria

Dummy injury criteria for the neck are evaluated based on the normalized neck injury criteria, N_{ij} , which is defined as the sum of normalized values of loads and moments. Figure 11-53 illustrates details for the neck injury criteria and the recorded curves from this specific impact condition and passive restraint systems employment.



(a) Neck Axial Force Time History



(b) Neck Bending Moment Time History

Figure 11-53 Neck injury time history (35 mph, baseline, airbag).

11.2.1.4 Chest injury criteria

Dummy injury criteria for the chest are evaluated based on the chest deflection values. Figure 11-54 illustrates details for the chest injury criteria and the recorded curves from this specific impact condition and passive restraint systems employment.

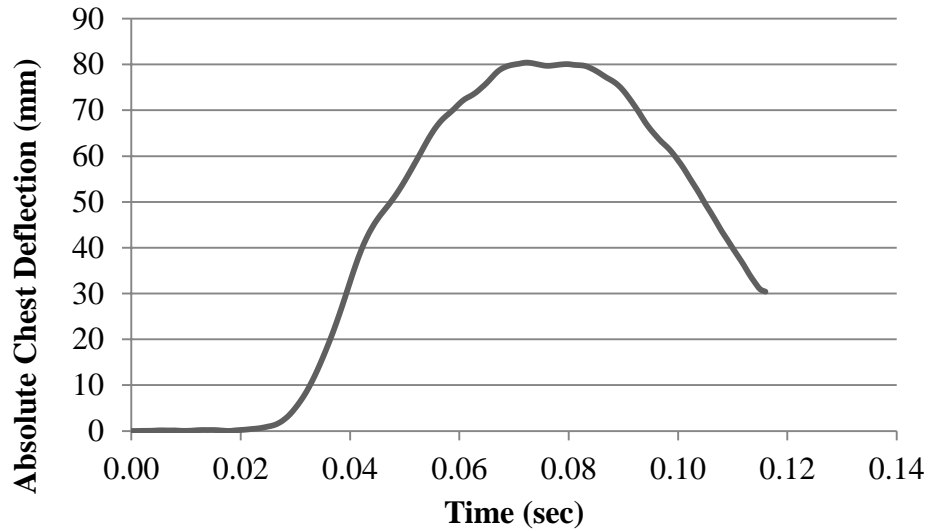
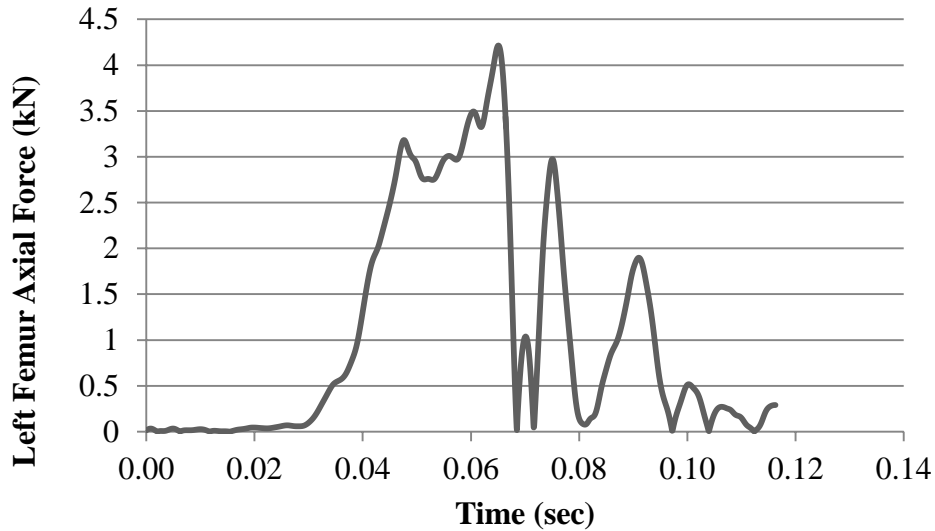


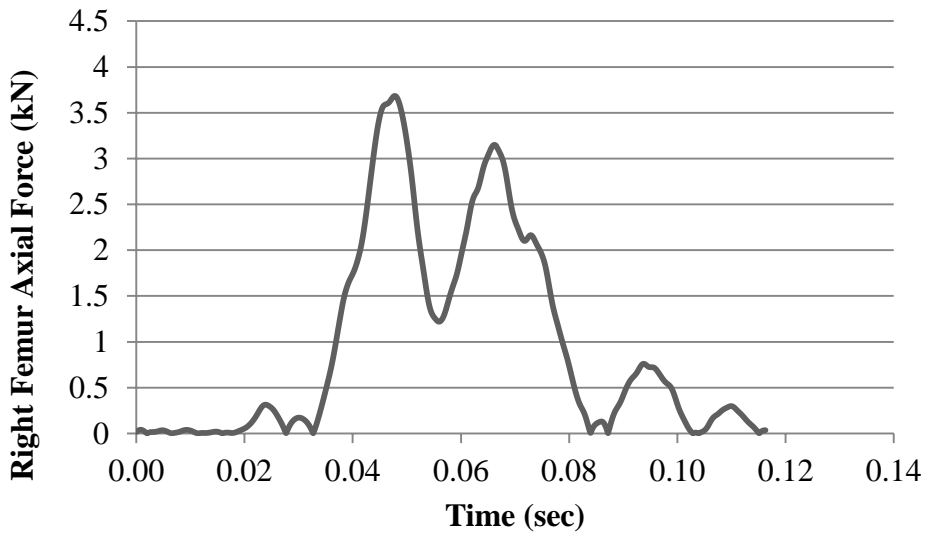
Figure 11-54 Chest deflection time history (35 mph, baseline, airbag).

11.2.1.5 KTH injury criteria

Dummy injury criteria for the KTH are evaluated based on the formulation for probability of injury as a function of femur axial force. Figure 11-55 illustrates details for the KTH injury criteria and the recorded curves from this specific impact condition and passive restraint systems employment.



(a) Left Femur Axial Force Time History

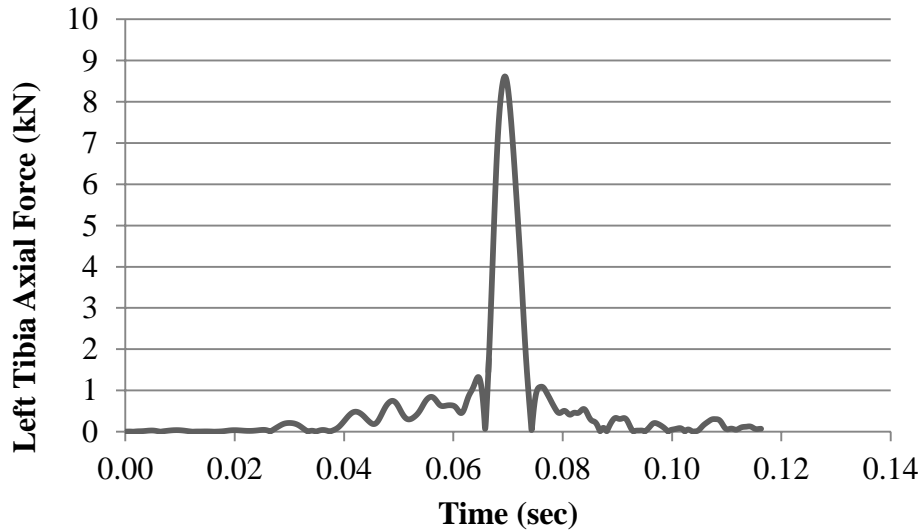


(b) Right Femur Axial Force Time History

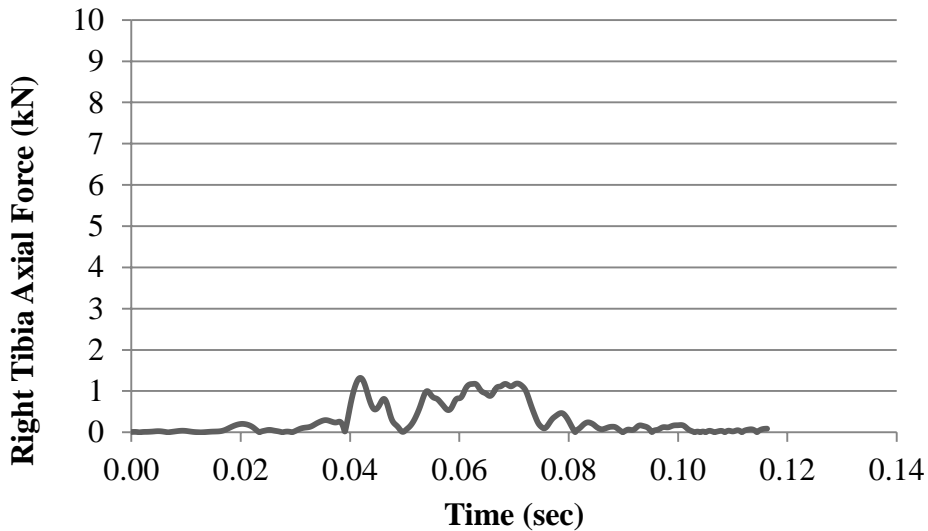
Figure 11-55 KTH injury time histories (frontal, 35 mph, belted, airbag).

11.2.1.6 Tibia plateau fracture injury criteria

Dummy injury criteria for tibia plateau fractures are evaluated based on a normalized formulation that combines bending moments and axial compressive loads. Figure 11-56 illustrates details for the tibia plateau injury criteria and the recorded curves from this specific impact condition and passive restraint systems employment.



(a) Left Tibia Axial Force Time History

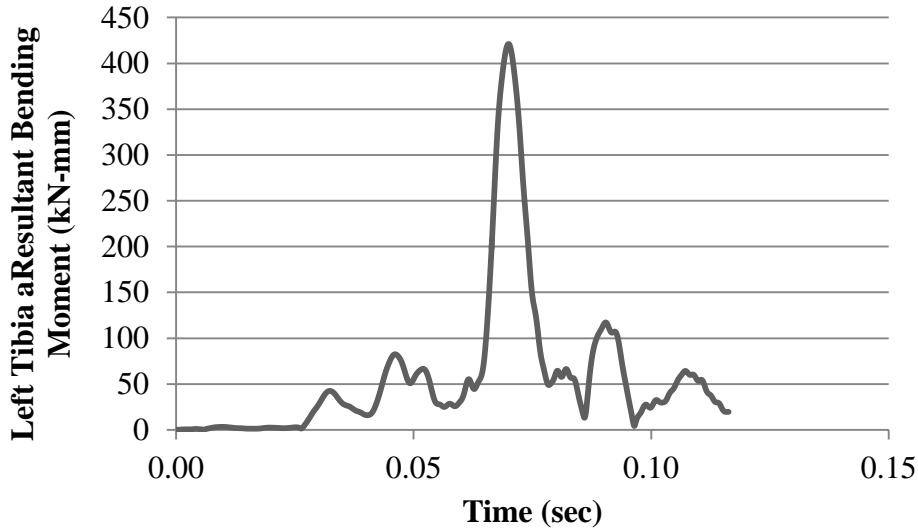


(b) Right Tibia Axial Force Time History

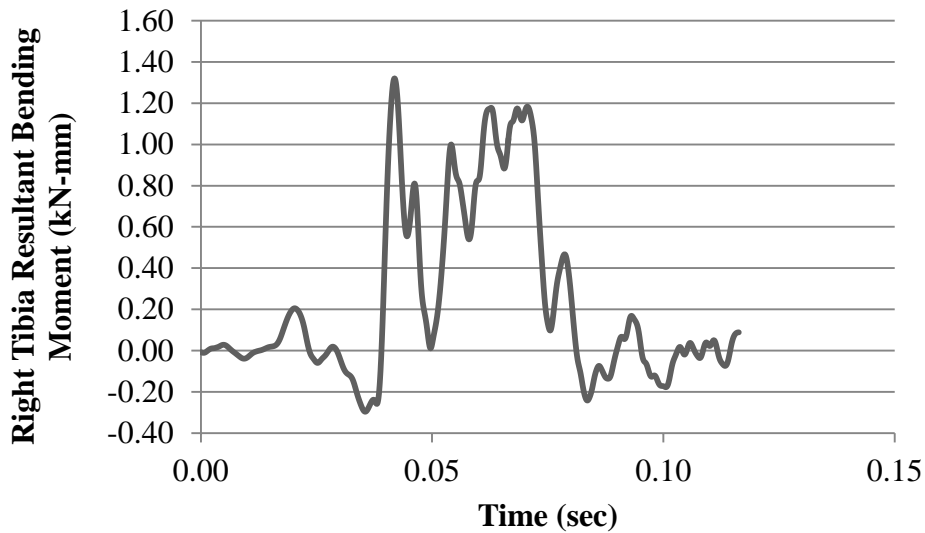
Figure 11-56 Tibia plateau fracture time history (35 mph, baseline, airbag).

11.2.1.7 Tibia shaft fracture injury criteria

Dummy injury criteria for tibia shaft fractures are evaluated based on a normalized formulation that combines bending moments and axial compressive loads along with the Tibia Index. Figure 11-57 illustrates details for the tibia shaft injury criteria and the recorded curves from this specific impact condition and passive restraint systems employment.



(a) Left Tibia Resultant Bending Moment Time History



(b) Right Tibia Resultant Bending Moment Time History

Figure 11-57 Tibia shaft fracture time history (35 mph, baseline, airbag).

11.2.1.8 Conclusions

The injury criteria values for various parts of the body were compared to the IARV requirements. The simulation injury criteria results as a percentage of the IARV values are shown in Figure 11-58.

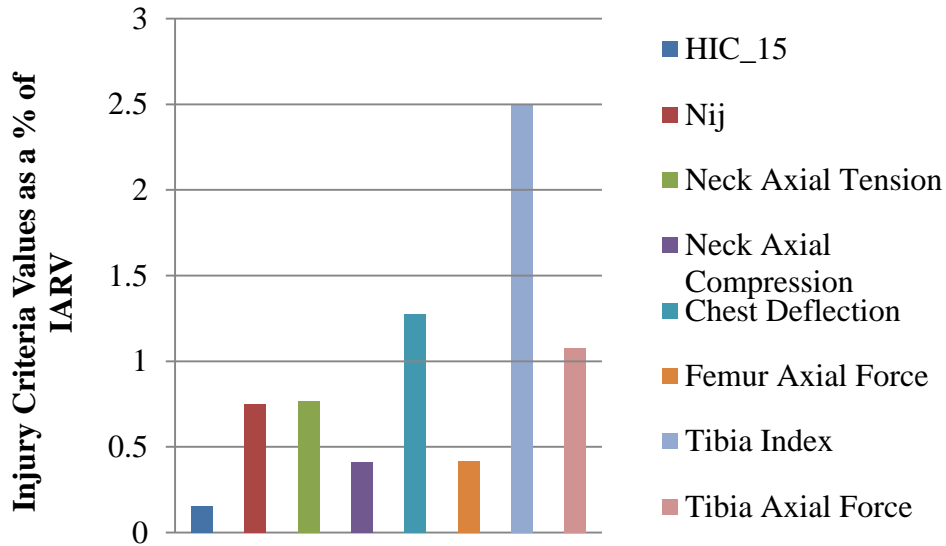


Figure 11-58 Injury probability as a function of IARV (35 mph, baseline, airbag).

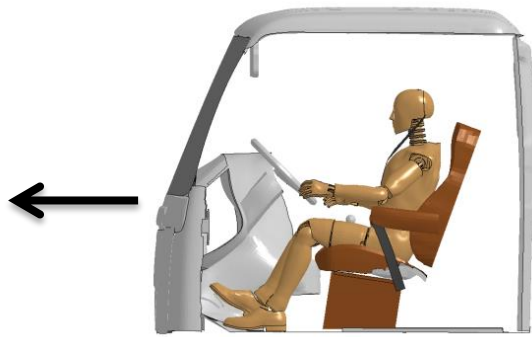
For the frontal baseline simulation with airbag, the probability of injury for the head, KTH and neck regions is unlikely because the injury criteria values stay below the threshold IARV. The injury criteria values for the chest region exceeded the threshold IARV which is unacceptable according to current standards.

11.2.2 Frontal no pretensioner simulation – 35 mph

11.2.2.1 Simulation frames and summary

The following documents the post processed results of the finite element simulation of a frontal impact event with initial speed of 35 mph, inclusion of a belted HIII 50th percentile male dummy in the driver position, and application of airbag. Table 11-20 and Table 11-21 summarize the resulting simulation with frames at different times throughout the simulation. The details of the simulation are summarized below and in Figure 11-59:

- Impact Type : Frontal
- Initial Impact Speed : 35 mph
- Seatbelt Condition: Belted (No Pretensioner)
- Airbag : Yes



(a) Lateral View of the FE Computer Model with Indication of Impact Orientation



(b) Seatbelt Model



(c) Use of Airbag Model

Figure 11-59 Modeled characteristics of the finite element simulation for the frontal impact (35 mph, no pretensioner, airbag).

Table 11-20 Frontal impact simulation frames side view (35 mph, no pretensioner, airbag).








Time (Sec)	Sequential Frames	Time (Sec)	Sequential Frames
0.000		0.074	
0.015		0.089	
0.030		0.110	
0.055			

Table 11-21 Frontal impact simulation frames perspective view (35 mph, no pretensioner, airbag).

**Time
(Sec)**

Sequential Frames

0.000



0.015



0.030



0.055



**Time
(Sec)**

Sequential Frames

0.074



0.089



0.110



The seatbelt retractor force for the resulting simulation is plotted in Figure 11-60. The retractor contained no load limiter for this simulation and reached a peak of about 8.5 kN.

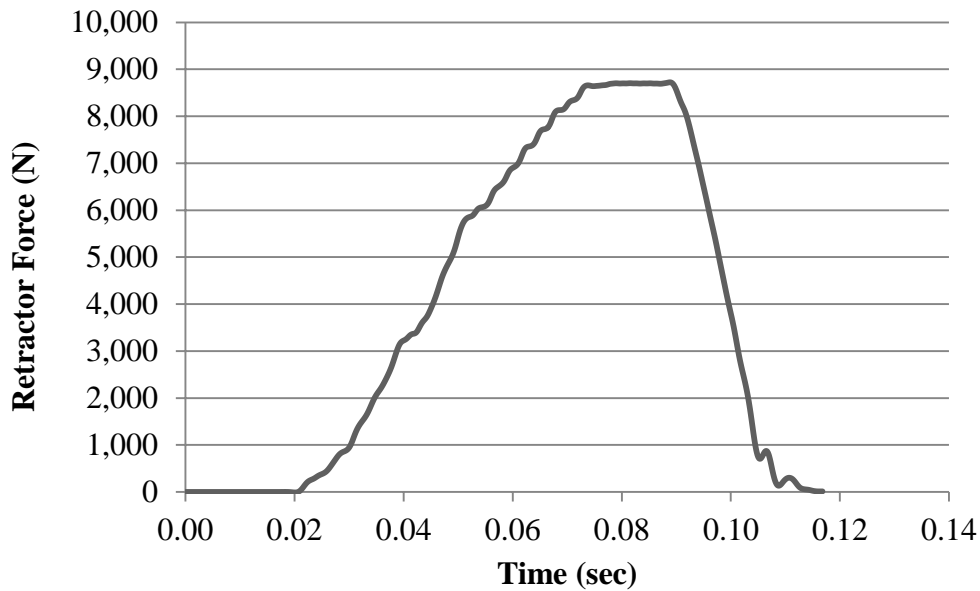


Figure 11-60 Seatbelt retractor force time history (35 mph, no pretensioner, airbag).

11.2.2.2 Head injury criteria

Dummy injury criteria for the head are evaluated with respect to the HIC₁₅ criteria. Head acceleration recorded during the impact event is employed to calculate the HIC₁₅ value. Figure 11-61 illustrates details for the head injury criteria and the recorded curves from this specific impact condition and passive restraint systems employment.

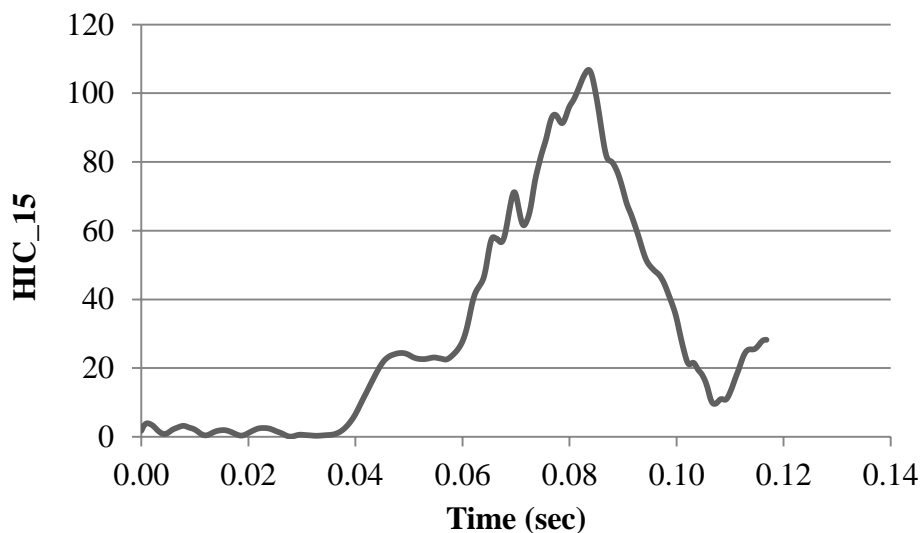
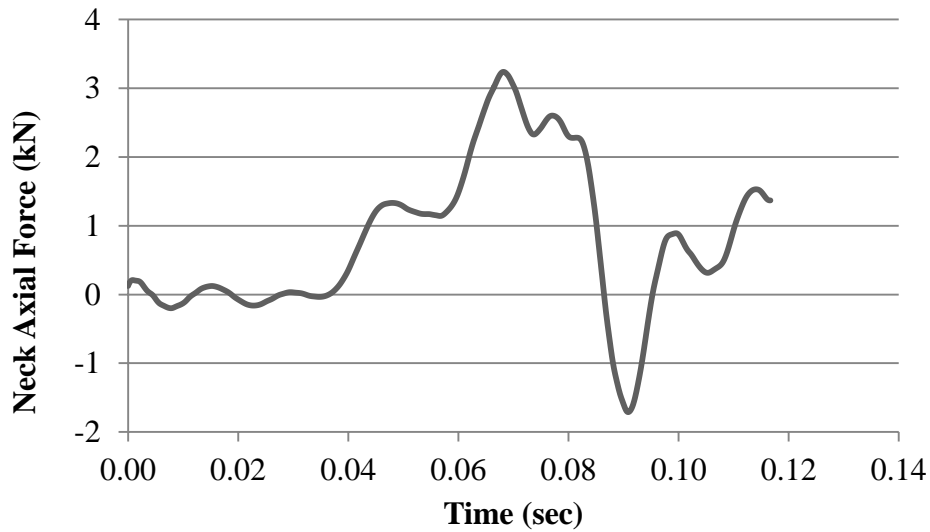


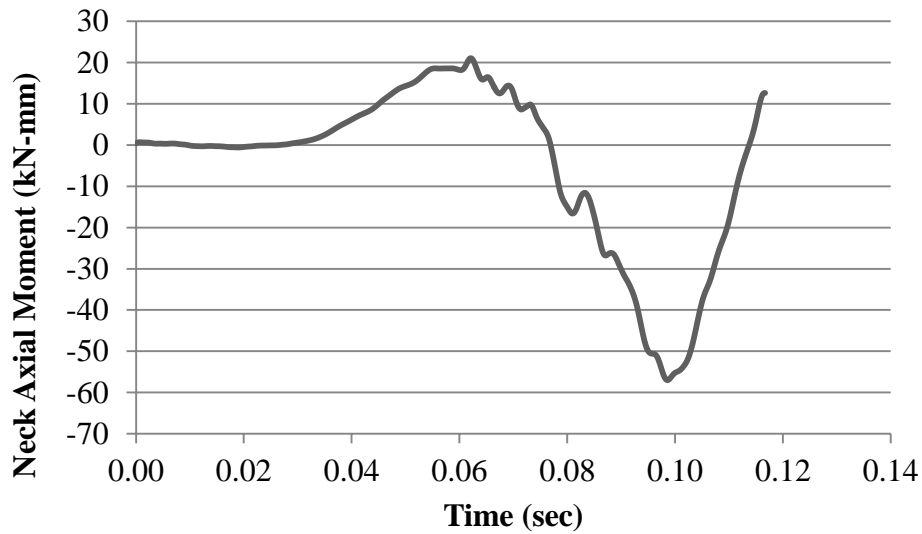
Figure 11-61 HIC time history (35 mph, no pretensioner, airbag).

11.2.2.3 Neck injury criteria

Dummy injury criteria for the neck are evaluated based on the normalized neck injury criteria, N_{ij} , which is defined as the sum of normalized values of loads and moments. Figure 11-62 illustrates details for the neck injury criteria and the recorded curves from this specific impact condition and passive restraint systems employment.



(a) Neck Axial Force Time History



(b) Neck Bending Moment Time History

Figure 11-62 Neck injury time history (35 mph, no pretensioner, airbag).

11.2.2.4 Chest injury criteria

Dummy injury criteria for the chest are evaluated based on the chest deflection values. Figure 11-63 illustrates details for the chest injury criteria and the recorded curves from this specific impact condition and passive restraint systems employment.

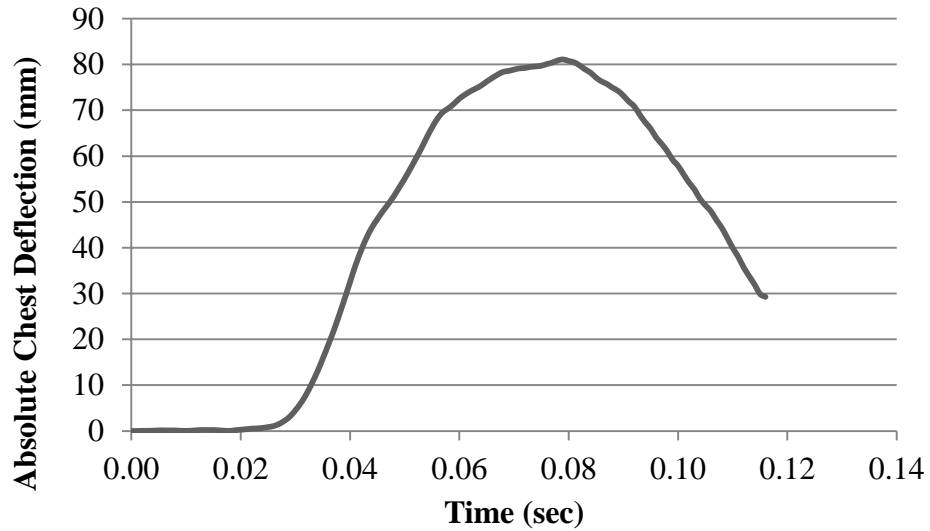
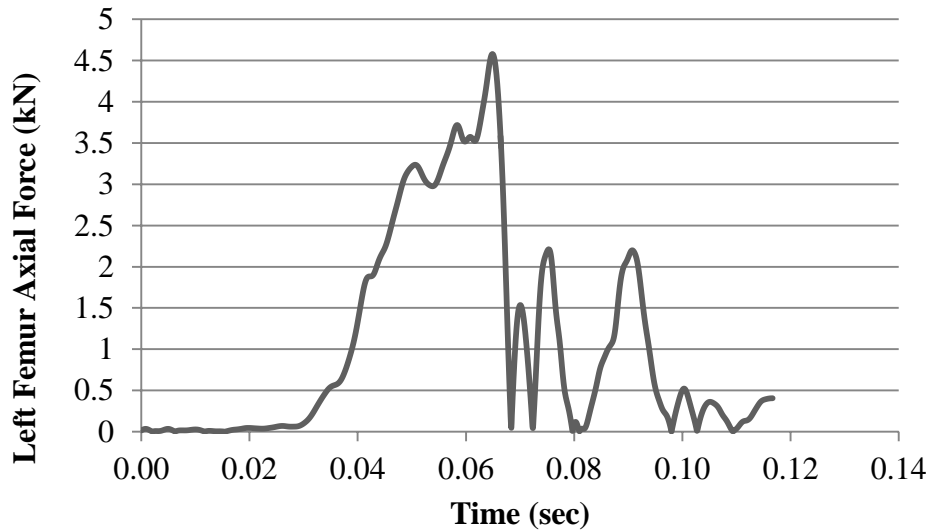


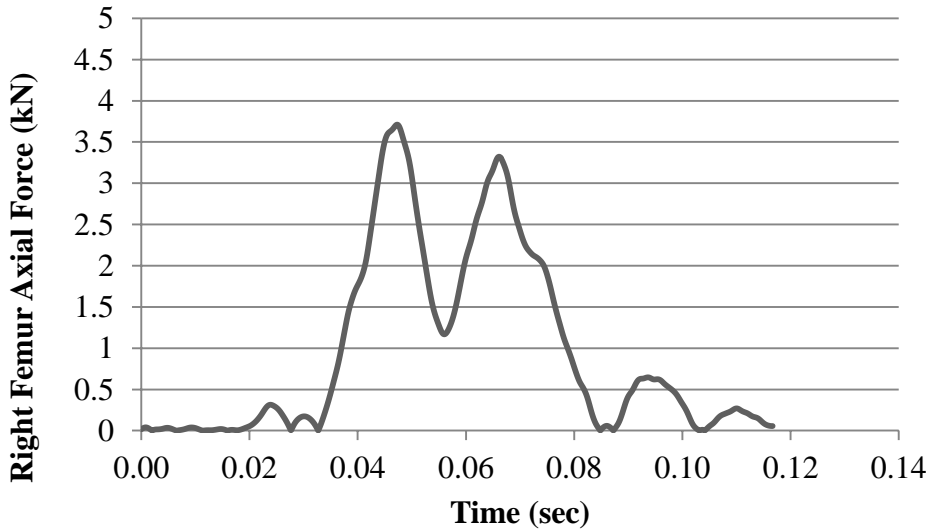
Figure 11-63 Chest deflection time history (35 mph, no pretensioner, airbag).

11.2.2.5 KTH injury criteria

Dummy injury criteria for the KTH are evaluated based on the formulation for probability of injury as a function of femur axial force. Figure 11-64 illustrates details for the KTH injury criteria and the recorded curves from this specific impact condition and passive restraint systems employment.



(a) Left Femur Axial Force Time History

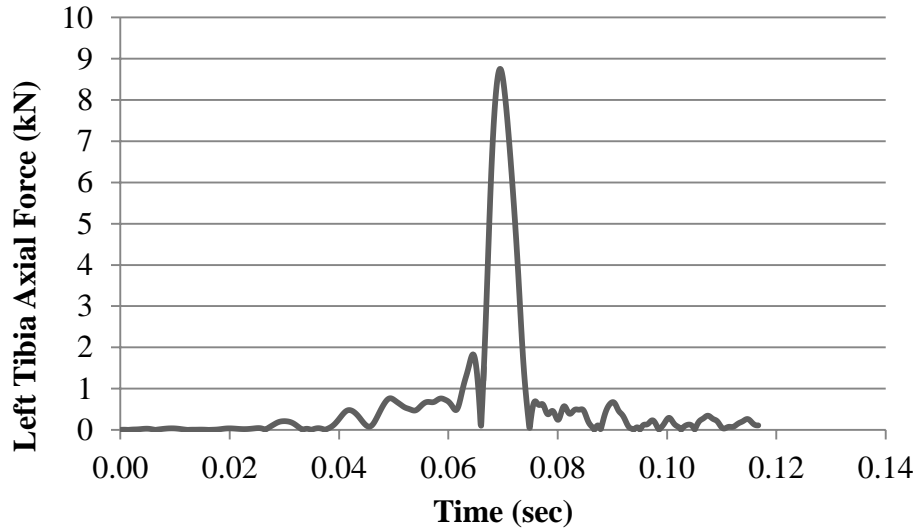


(b) Right Femur Axial Force Time History

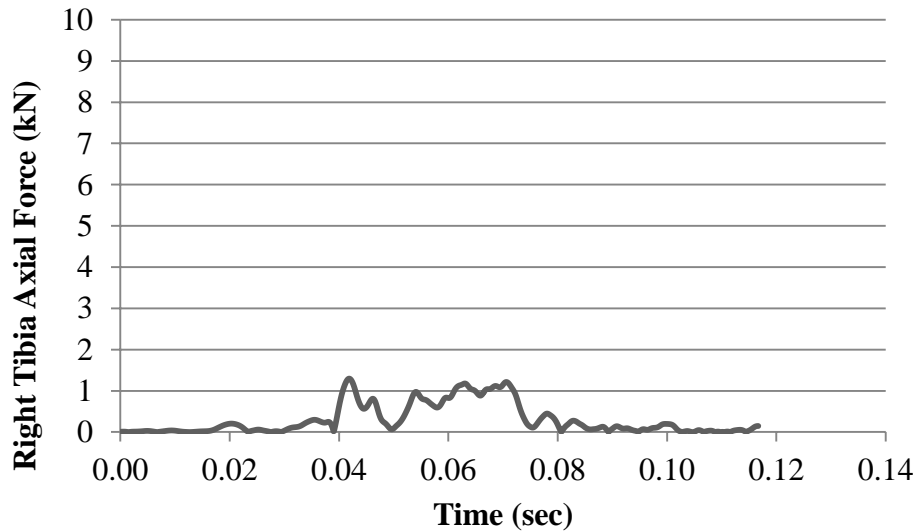
Figure 11-64 KTH injury time history (35 mph, no pretensioner, airbag).

11.2.2.6 Tibia plateau fracture injury criteria

Dummy injury criteria for tibia plateau fractures are evaluated based on axial compressive loads. Figure 11-65 illustrates details for the tibia plateau injury criteria and the recorded curves from this specific impact condition and passive restraint systems employment.



(a) Left Tibia Axial Force Time History

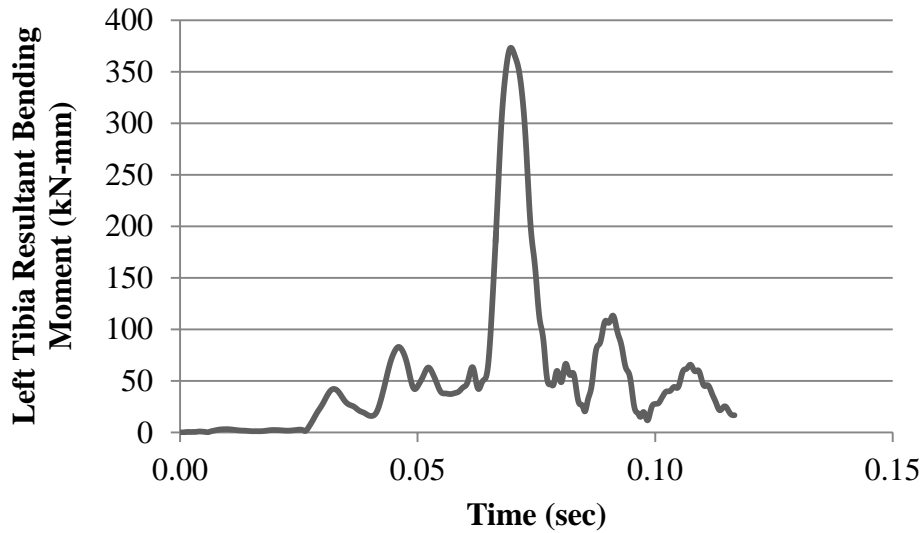


(b) Right Tibia Axial Force Time History

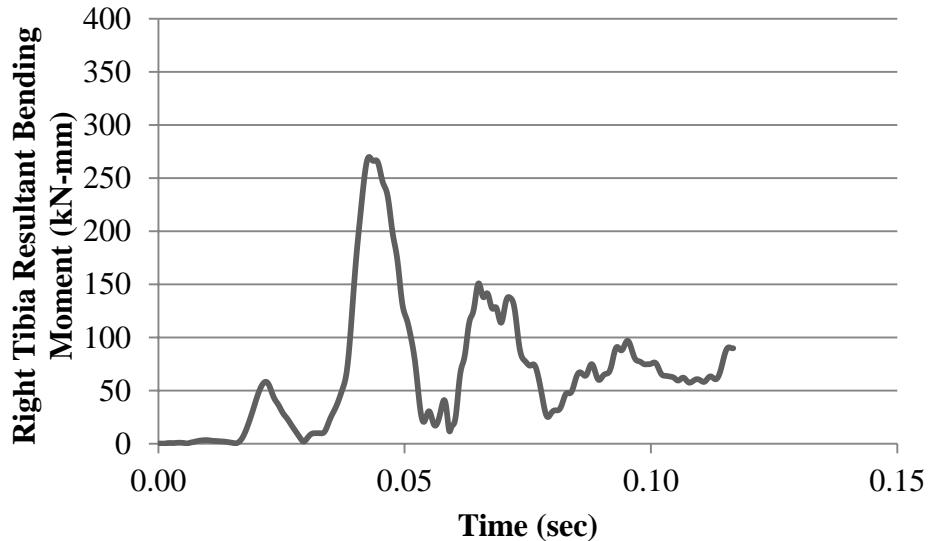
Figure 11-65 Tibia plateau fracture time history (35 mph, no pretensioner, airbag).

11.2.2.7 Tibia shaft fracture criteria

Dummy injury criteria for tibia shaft fractures are evaluated based on a normalized formulation that combines bending moments and axial compressive loads. Figure 11-66 illustrates details for the tibia shaft injury criteria and the recorded curves from this specific impact condition and passive restraint systems employment.



(a) Left Tibia Resultant Bending Moment Time History



(b) Right Tibia Resultant Bending Moment Time History

Figure 11-66 Tibia shaft fracture time history (35 mph, no pretensioner, airbag).

11.2.2.8 Conclusions

The injury criteria values for various parts of the body were compared to the IARV requirements. The simulation injury criteria results as a percentage of the IARV values are shown in Figure 11-67.

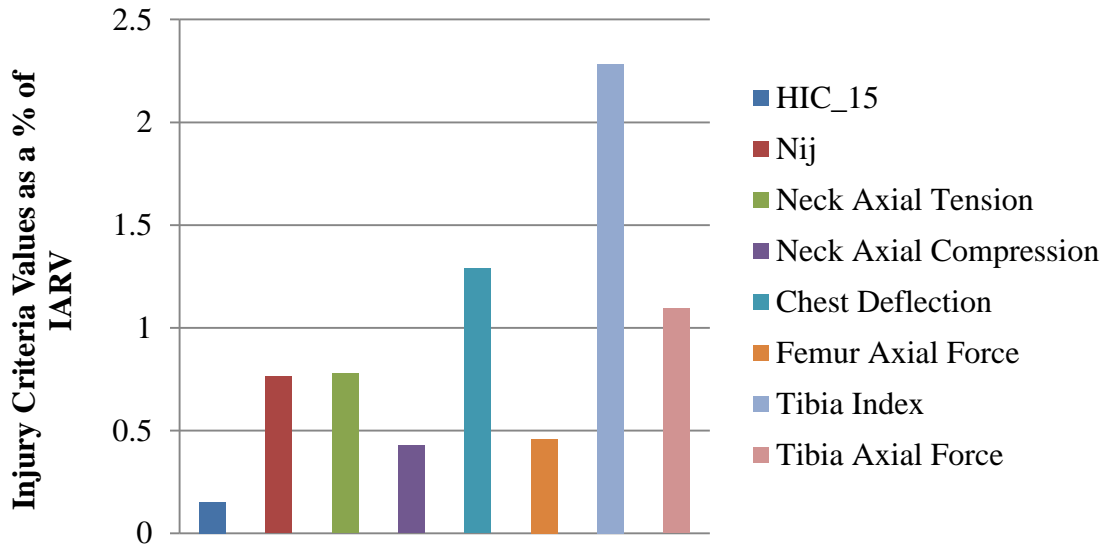


Figure 11-67 Injury probability as a function of IARV (35 mph, no pretensioner, airbag).

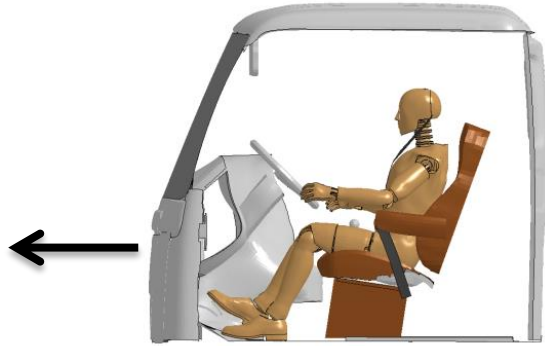
For the frontal no pretensioner simulation with airbag, the probability of injury for the head, KTH and neck regions is unlikely because the injury criteria values stay below the threshold IARV. The injury criteria values for the chest region exceeded the threshold IARV which is unacceptable according to current standards.

11.2.3 Frontal 4 kN load limiter simulation – 35 mph

11.2.3.1 Simulation frames and summary

The following documents the post processed results of the finite element simulation of a frontal impact event with initial speed of 35 mph, inclusion of a belted H3 50th percentile male dummy in the driver position, and no application of airbag. Table 11-22 and Table 11-23 summarize the resulting simulation with frames at different times throughout the simulation. The details of the simulation are summarized below and in Figure 11-68:

- Impact Type : Frontal
- Initial Impact Speed : 35 mph
- Seatbelt Condition: Belted (4 kN Load Limiter)
- Airbag : Yes



(a) Lateral View of the FE Computer Model with Indication of Impact Orientation



(b) Seatbelt Model



(c) Use of Airbag Model

Figure 11-68 Modeled characteristics of the finite element simulation for the frontal impact (35 mph, 4 kN load limiter, airbag).

Table 11-22 Frontal impact simulation frames side view (35 mph, 4 kN load limiter, airbag).









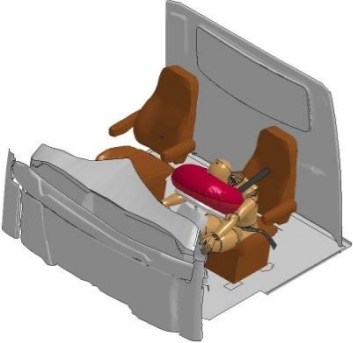




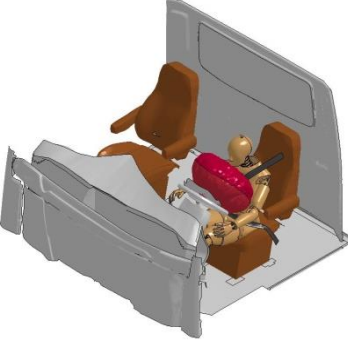
Time (Sec)	Sequential Frames	Time (Sec)	Sequential Frames
0.000		0.074	
0.015		0.089	
0.030		0.110	
0.055			

Table 11-23 Frontal impact simulation frames perspective view (35 mph, 4 kN load limiter, airbag).

Time (Sec)	Sequential Frames	Time (Sec)	Sequential Frames
0.000		0.074	
0.015		0.089	
0.030		0.110	
0.055			

The seatbelt retractor force for the resulting simulation is plotted in Figure 11-69. The retractor contained a 4 kN load limiter.

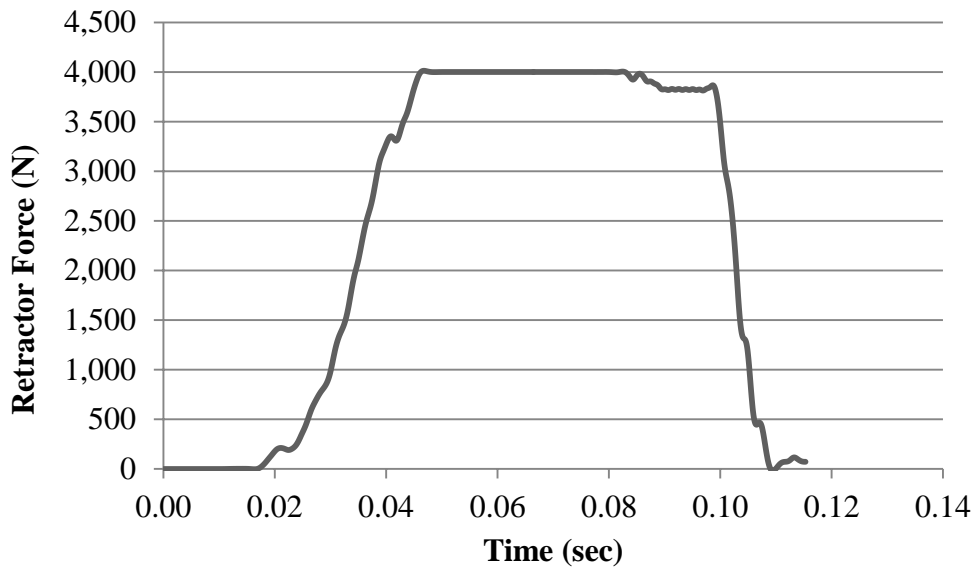


Figure 11-69 Seatbelt retractor force time history (frontal, 35 mph, belted, airbag).

11.2.3.2 Head injury criteria

Dummy injury criteria for the head are evaluated with respect to the HIC₁₅ criteria. Head acceleration recorded during the impact event is employed to calculate the HIC₁₅ value. Figure 11-70 illustrates details for the head injury criteria and the recorded curves from this specific impact condition and passive restraint systems employment.

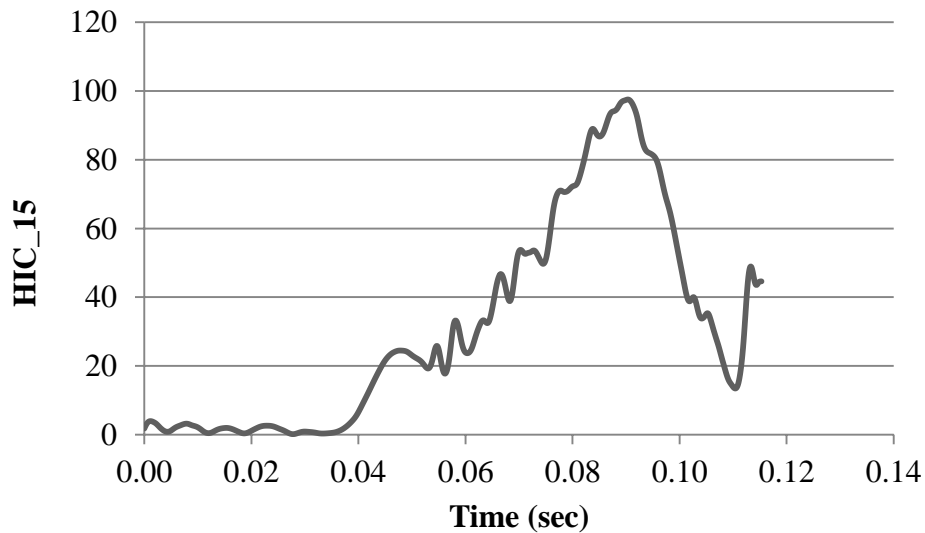
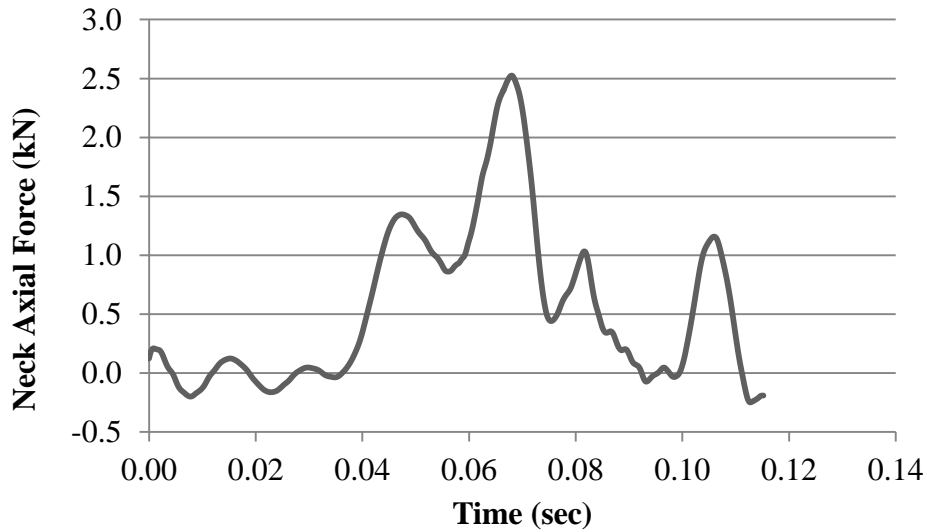


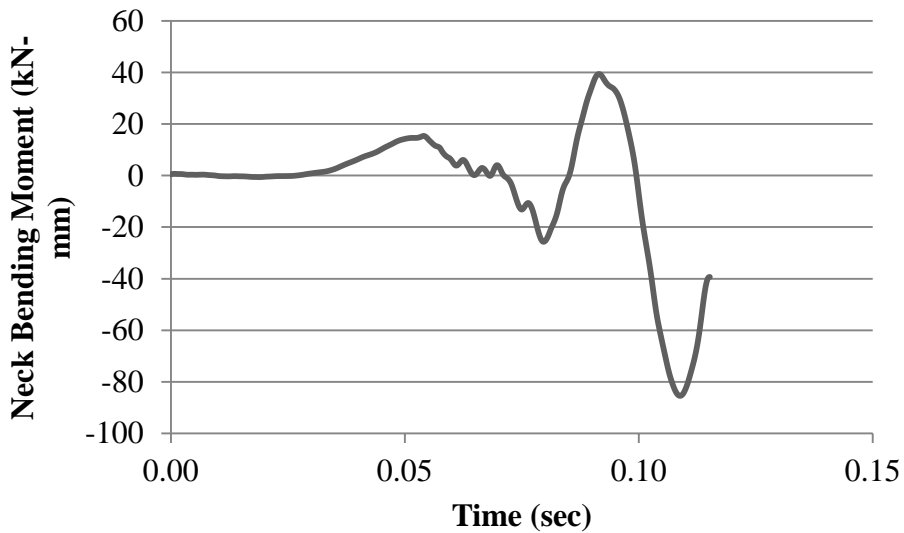
Figure 11-70 HIC time history (35 mph, 4 kN load limiter, airbag).

11.2.3.3 Neck injury criteria

Dummy injury criteria for the neck are evaluated based on the normalized neck injury criteria, N_{ij} , which is defined as the sum of normalized values of loads and moments. Figure 11-71 illustrates details for the neck injury criteria and the recorded curves from this specific impact condition and passive restraint systems employment.



(a) Neck Axial Force Time History



(b) Neck Bending Moment Time History

Figure 11-71 Neck injury time history (35 mph, 4 kN load limiter, airbag).

11.2.3.4 Chest injury criteria

Dummy injury criteria for the chest are evaluated based on the chest deflection values. Figure 11-72 illustrates details for the chest injury criteria and the recorded curves from this specific impact condition and passive restraint systems employment.

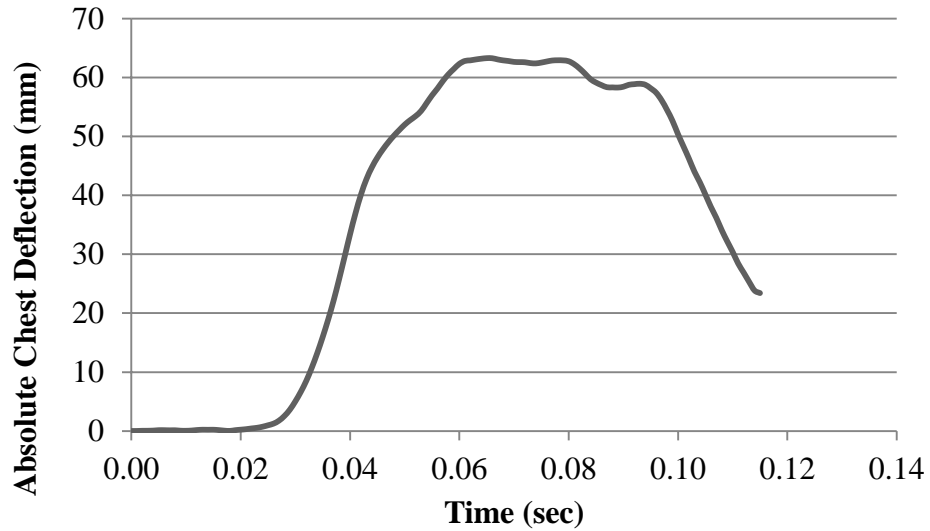
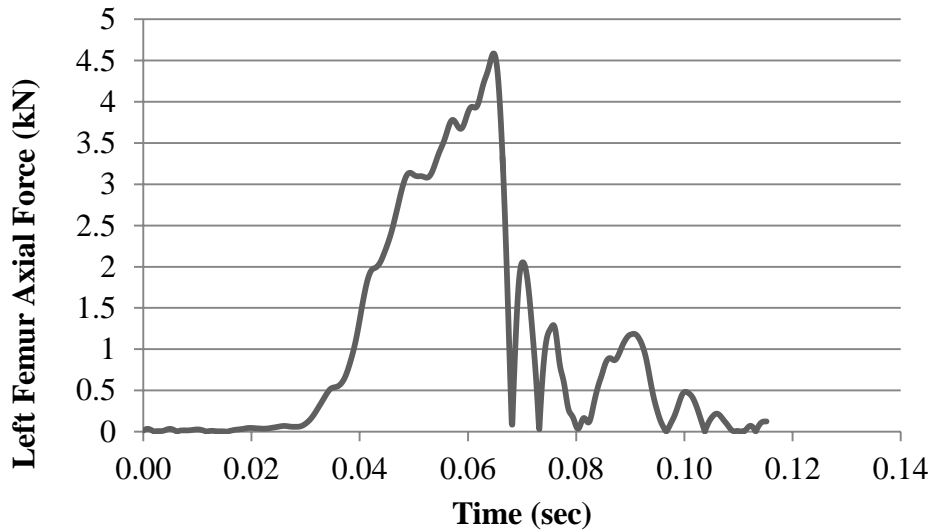


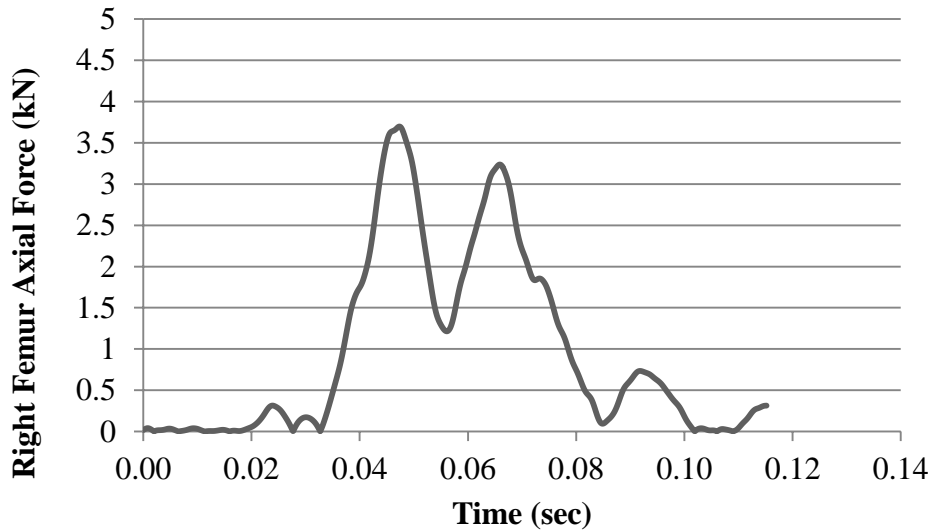
Figure 11-72 Chest deflection time history (35 mph, 4 kN load limiter, airbag).

11.2.3.5 KTH injury criteria

Dummy injury criteria for the KTH are evaluated based on the formulation for probability of injury as a function of femur axial force. Figure 11-73 illustrates details for the KTH injury criteria and the recorded curves from this specific impact condition and passive restraint systems employment.



(a) Left Femur Axial Force Time History

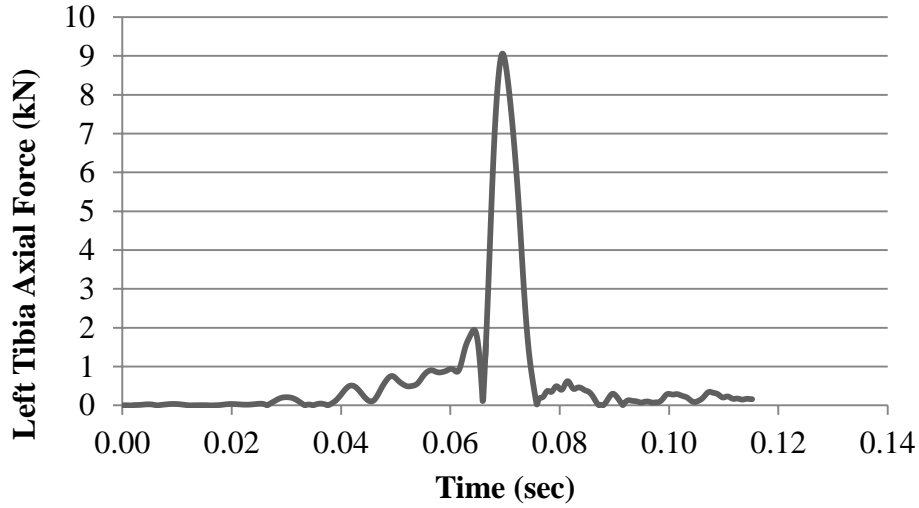


(b) Right Femur Axial Force Time History

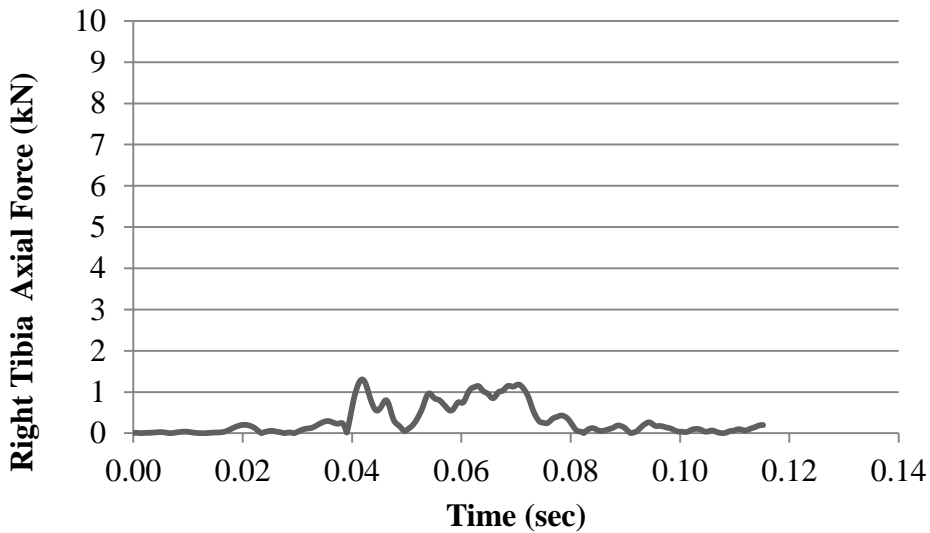
Figure 11-73 KTH injury time history (35 mph, 4 kN load limiter, airbag).

11.2.3.6 Tibia plateau fracture injury criteria

Dummy injury criteria for tibia plateau fractures are evaluated based on axial compressive loads. Figure 11-74 illustrates details for the tibia plateau injury criteria and the recorded curves from this specific impact condition and passive restraint systems employment.



(a) Left Tibia Axial Force Time History

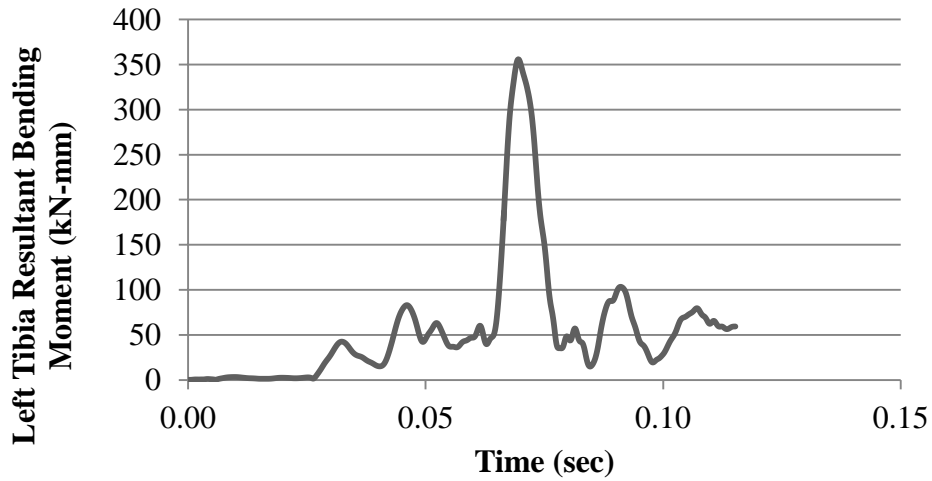


(b) Right Tibia Axial Force Time History

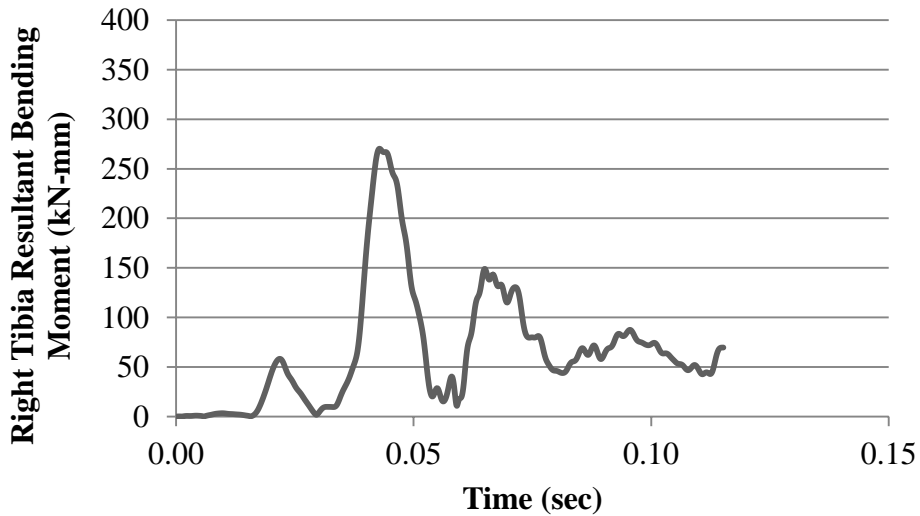
Figure 11-74 Tibia plateau fracture time history (35 mph, 4 kN load limiter, airbag).

11.2.3.7 Tibia shaft fracture injury criteria

Dummy injury criteria for tibia shaft fractures are evaluated based on a normalized formulation that combines bending moments and axial compressive loads. Figure 11-75 illustrates details for the tibia shaft injury criteria and the recorded curves from this specific impact condition and passive restraint systems employment.



(a) Left Tibia Resultant Bending Moment Time History



(b) Right Tibia Resultant Bending Moment Time History

Figure 11-75 Tibia shaft fracture time history (35 mph, 4 kN load limiter, airbag).

11.2.3.8 Conclusions

The injury criteria values for various parts of the body were compared to the IARV requirements. The simulation injury criteria results as a percentage of the IARV values are shown in Figure 11-76.

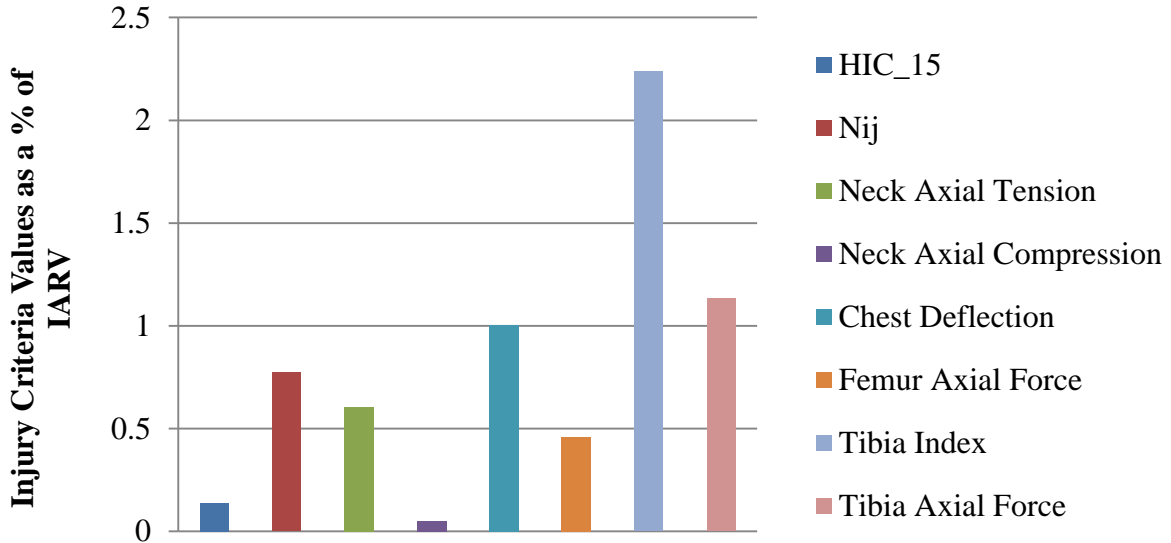


Figure 11-76 Injury probability as a function of IARV (35 mph, 4 kN load limiter, airbag).

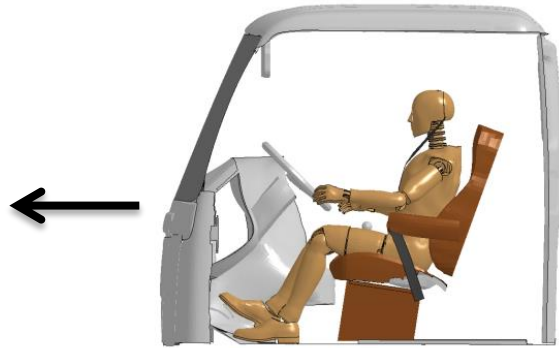
For the frontal 4 kN load limiter simulation with airbag, the probability of injury for the head, KTH, neck regions is unlikely because the injury criteria values stay below the threshold IARV. The injury criteria values for the chest region exceeded the threshold IARV which is unacceptable according to current standards.

11.2.4 Frontal 8 kN load limiter simulation – 35 mph

11.2.4.1 Simulation frames and summary

The following documents the post processed results of the finite element simulation of a frontal impact event with initial speed of 35 mph, inclusion of a belted HIII 50th percentile male dummy in the driver position, and no application of airbag. Table 11-24 and Table 11-25 summarize the resulting simulation with frames at different times throughout the simulation. The details of the simulation are summarized below and in Figure 11-77:

- Impact Type : Frontal
- Initial Impact Speed : 35 mph
- Seatbelt Condition: Belted (8 kN Load Limiter)
- Airbag : Yes



(a) Lateral View of the FE Computer Model with Indication of Impact Orientation



(b) Seatbelt Model



(c) Use of Airbag Model

Figure 11-77 Modeled characteristics of the finite element simulation for the frontal impact (35 mph, 8 kN load limiter, airbag).

Table 11-24 Frontal impact simulation frames side view (35 mph, 8 kN load limiter, airbag).









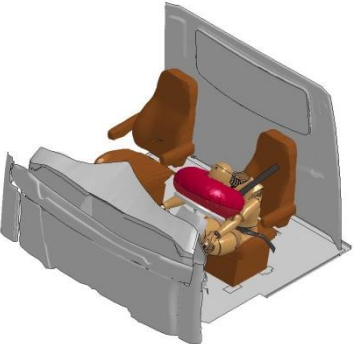

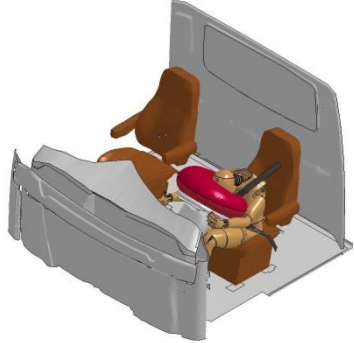


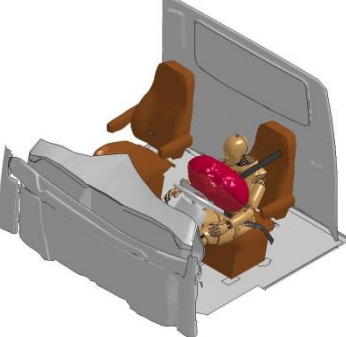
Time (Sec)	Sequential Frames	Time (Sec)	Sequential Frames
0.000		0.074	
0.015		0.089	
0.030		0.110	
0.055			

Table 11-25 Frontal impact simulation frames perspective view (35 mph, 8 kN load limiter, airbag).

Time (Sec)	Sequential Frames	Time (Sec)	Sequential Frames
0.000		0.074	
0.015		0.089	
0.030		0.110	
0.055			

The seatbelt retractor force for the resulting simulation is plotted in Figure 11-78. The retractor contained an 8 kN load limiter.

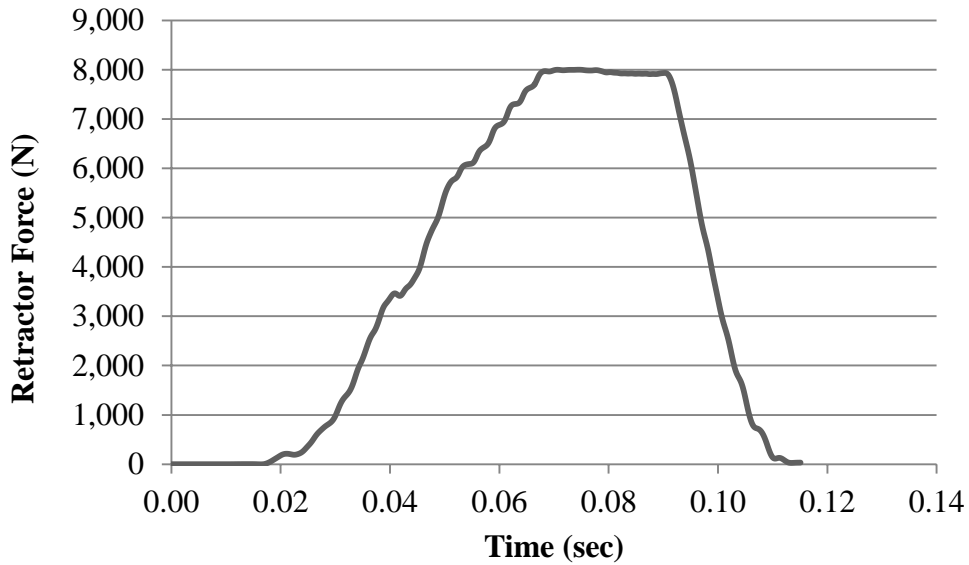


Figure 11-78 Seatbelt retractor force time history (35 mph, 8 kN load limiter, airbag).

11.2.4.2 Head injury criteria

Dummy injury criteria for the head are evaluated with respect to the HIC-15 criteria. Head acceleration recorded during the impact event is employed to calculate the HIC₁₅ value. Figure 11-79 illustrates details for the head injury criteria and the recorded curves from this specific impact condition and passive restraint systems employment.

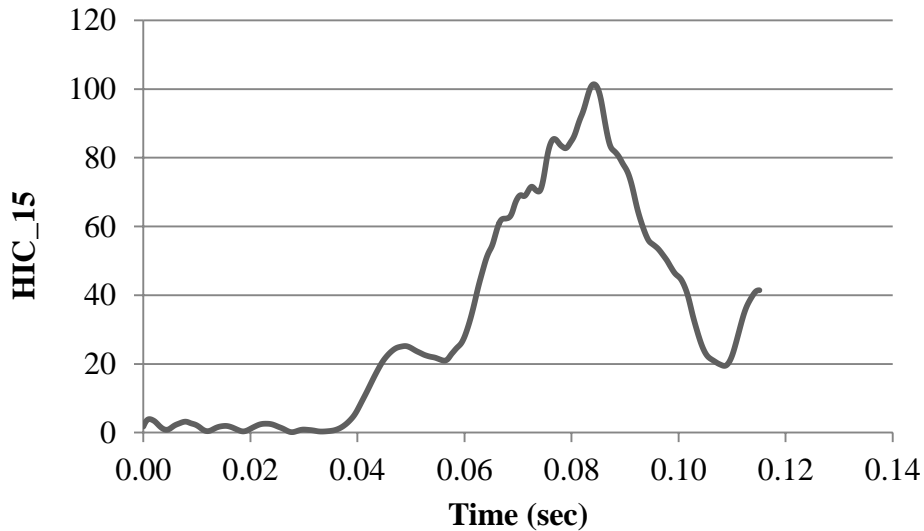
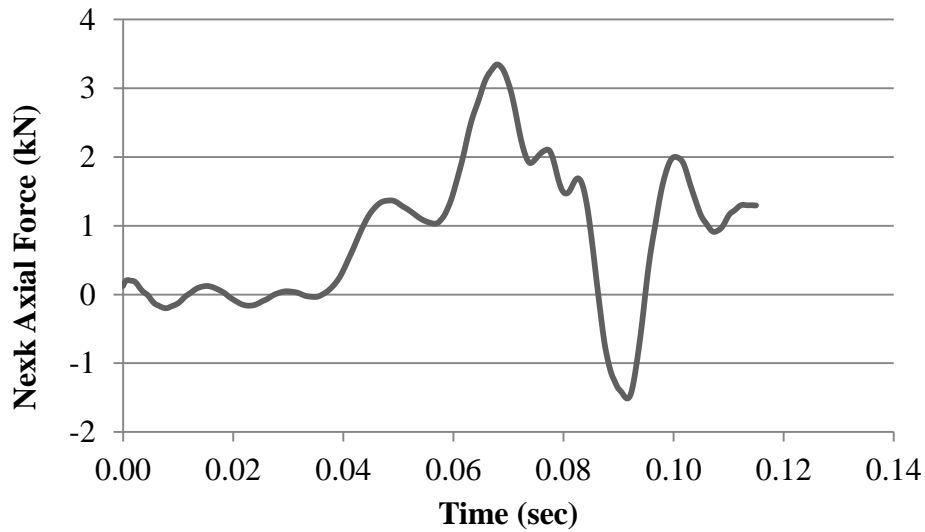


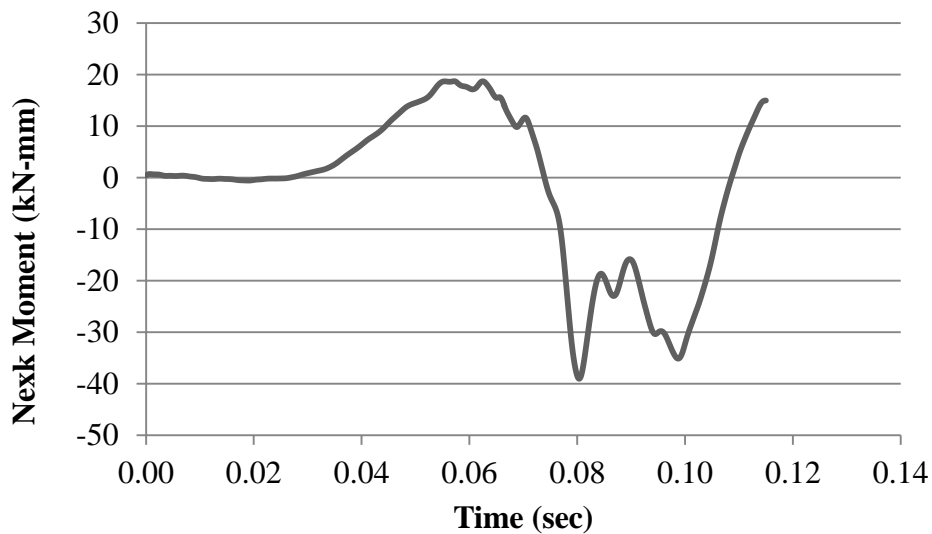
Figure 11-79 HIC time history (35 mph, 8 kN load limiter, airbag).

11.2.4.3 Neck injury criteria

Dummy injury criteria for the neck are evaluated based on the normalized neck injury criteria, N_{ij} , which is defined as the sum of normalized values of loads and moments. Figure 11-80 illustrates details for the neck injury criteria and the recorded curves from this specific impact condition and passive restraint systems employment.



(a) Neck Axial Force Time History



(b) Neck Bending Moment Time History

Figure 11-80 Neck injury time history (35 mph, 8 kN load limiter, airbag).

11.2.4.4 Chest injury criteria

Dummy injury criteria for the chest are evaluated based on the chest deflection values. Figure 11-81 illustrates details for the chest injury criteria and the recorded curves from this specific impact condition and passive restraint systems employment.

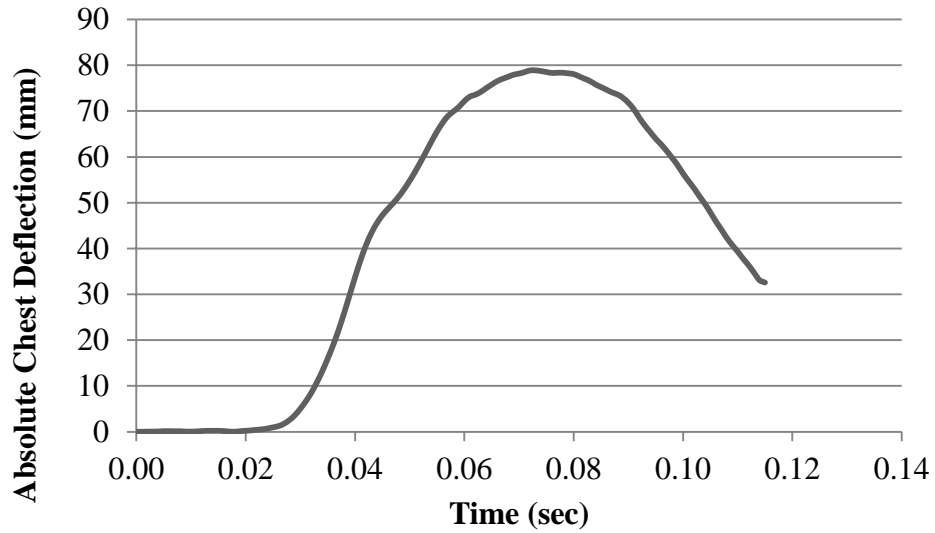
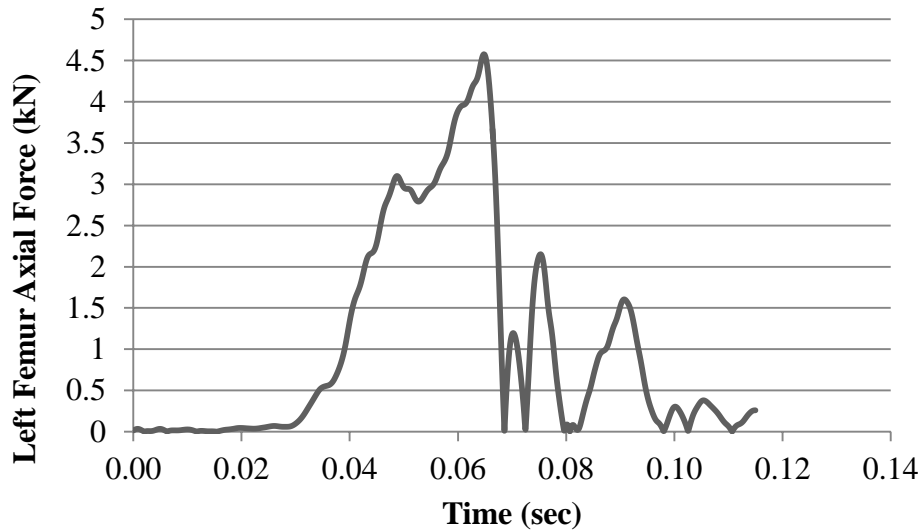


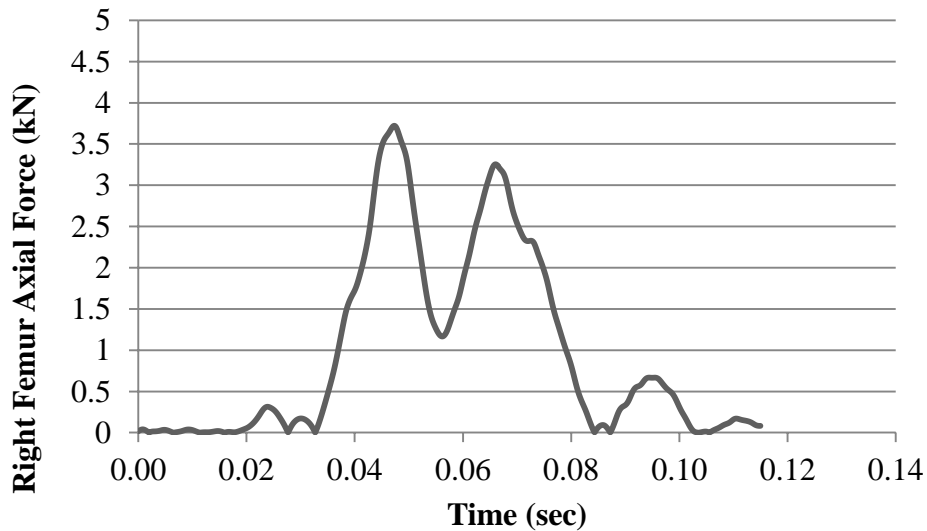
Figure 11-81 Chest deflection time history (35 mph, 8 kN load limiter, airbag).

11.2.4.5 KTH injury criteria

Dummy injury criteria for the KTH are evaluated based on the formulation for probability of injury as a function of femur axial force. Figure 11-82 illustrates details for the KTH injury criteria and the recorded curves from this specific impact condition and passive restraint systems employment.



(a) Left Femur Axial Force Time History

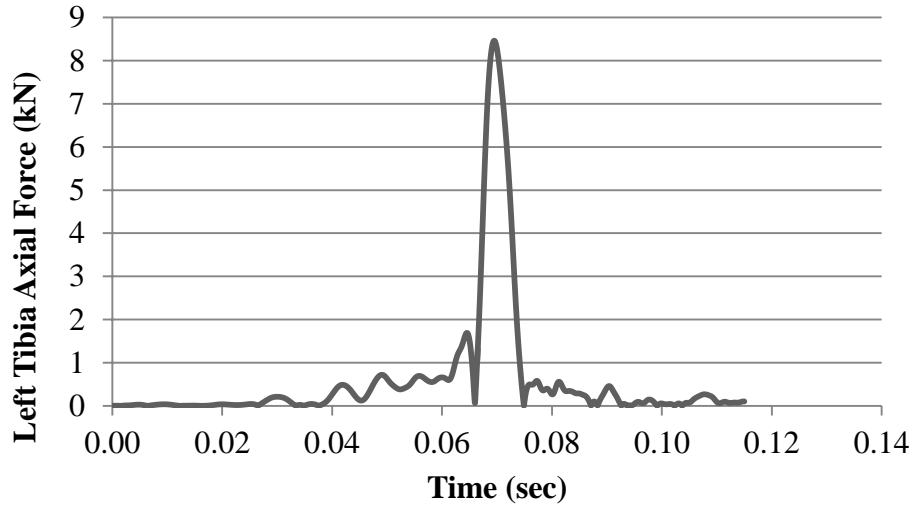


(b) Right Femur Axial Force Time History

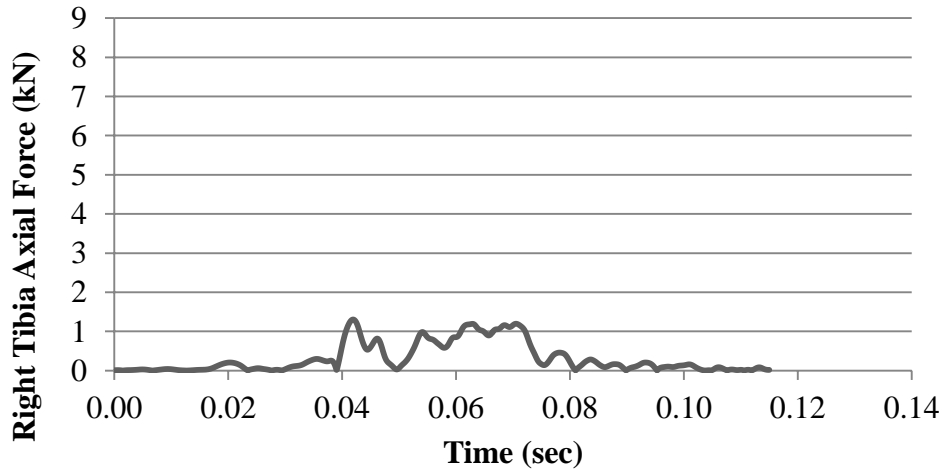
Figure 11-82 KTH injury time history (35 mph, 8 kN load limiter, airbag).

11.2.4.6 Tibia plateau fracture injury criteria

Dummy injury criteria for tibia plateau fractures are evaluated based on axial compressive loads. Figure 11-83 illustrates details for the tibia plateau injury criteria and the recorded curves from this specific impact condition and passive restraint systems employment.



(a) Left Tibia Axial Force Time History

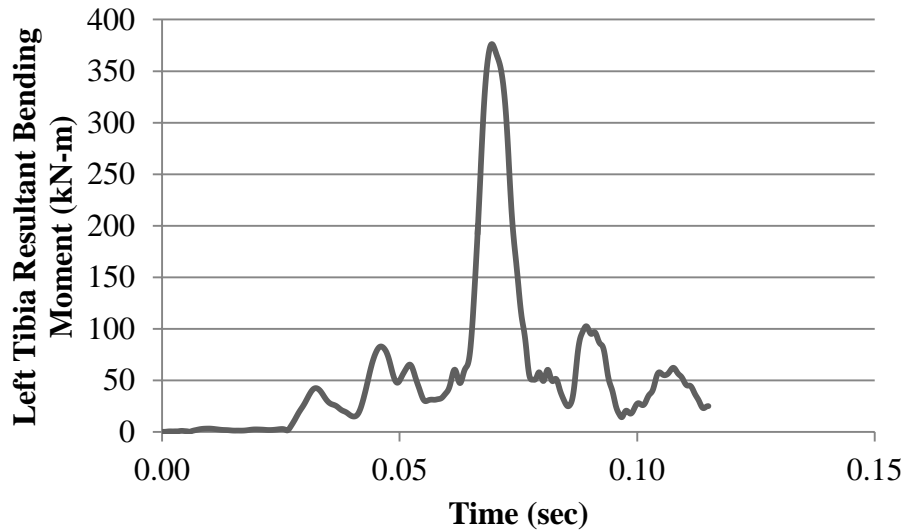


(b) Right Tibia Axial Force Time History

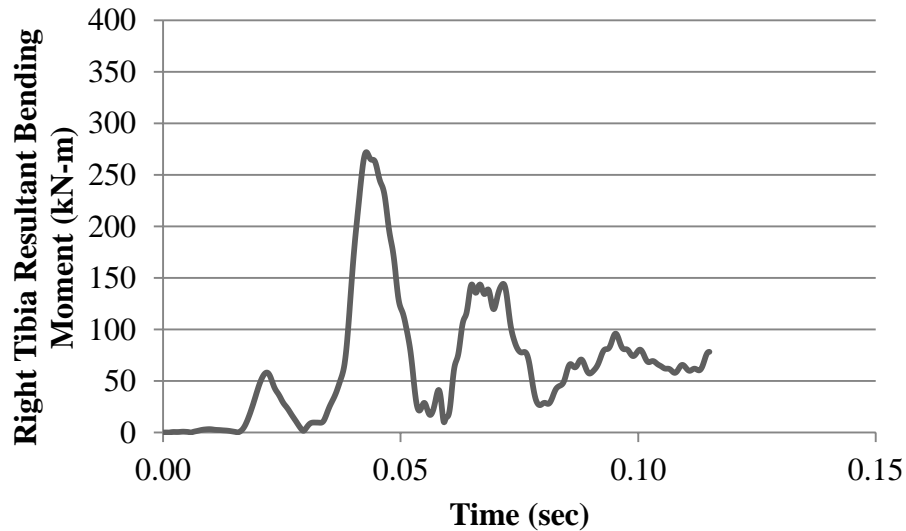
Figure 11-83 Tibia plateau fracture time history (35 mph, 8 kN load limiter, airbag).

11.2.4.7 Tibia shaft fracture injury criteria

Dummy injury criteria for tibia shaft fractures are evaluated based on a normalized formulation that combines bending moments and axial compressive loads. Figure 11-84 illustrates details for the tibia shaft injury criteria and the recorded curves from this specific impact condition and passive restraint systems employment.



(a) Left Tibia Resultant Bending Moment Time History



(b) Right Tibia Resultant Bending Moment Time History

Figure 11-84 Tibia shaft fracture time history (35 mph, 8 kN load limiter, airbag).

11.2.4.8 Conclusions

The injury criteria values for various parts of the body were compared to the IARV requirements. The simulation injury criteria results as a percentage of the IARV values are shown in Figure 11-85.

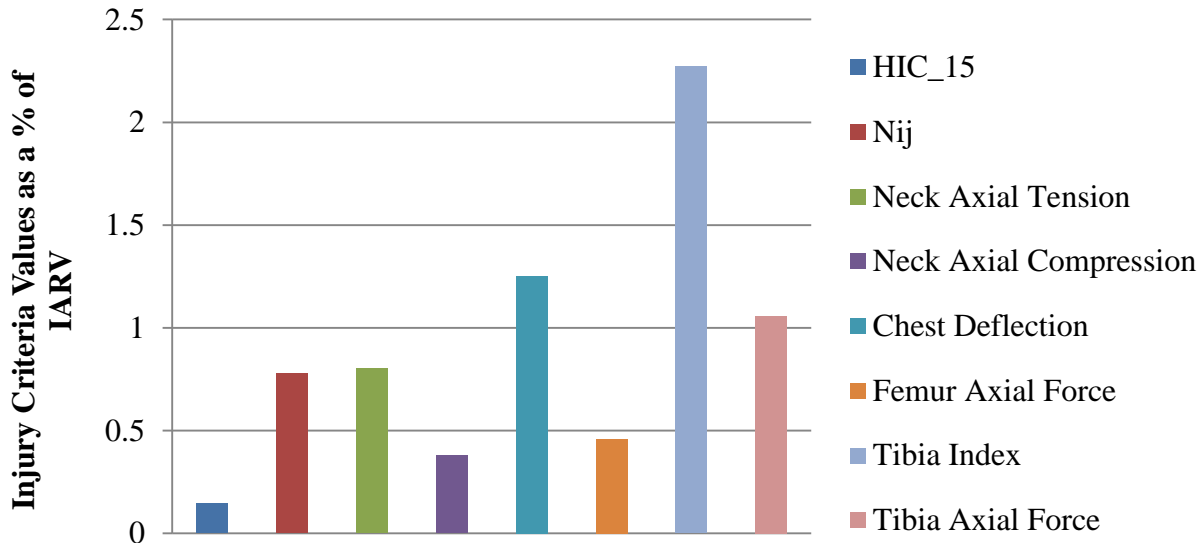


Figure 11-85 Injury probability as a function of IARV (35 mph, 8 kN load limiter, airbag).

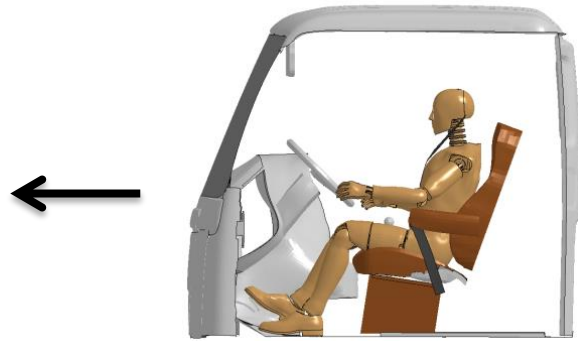
For the frontal 8 kN load limiter simulation with airbag, the probability of injury for the head, KTH, neck regions is unlikely because the injury criteria values stay below the threshold IARV. The injury criteria values for the chest region exceeded the threshold IARV which is unacceptable according to current standards.

11.2.5 Frontal lowered D-ring simulation – 35 mph

11.2.5.1 Simulation frames and summary

The following documents the post processed results of the finite element simulation of a frontal impact event with initial speed of 35 mph, inclusion of a belted HIII 50th percentile male dummy in the driver position, and no application of airbag. Table 11-26 and Table 11-27 summarize the resulting simulation with frames at different times throughout the simulation. The details of the simulation are summarized below and in Figure 11-86:

- Impact Type : Frontal
- Initial Impact Speed : 35 mph
- Seatbelt Condition: Belted (Lowered D-Ring)
- Airbag : Yes



(a) Lateral View of the FE Computer Model with Indication of Impact Orientation



(b) Seatbelt Model



(c) Use of Airbag Model

Figure 11-86 Modeled characteristics of the finite element simulation for the frontal impact (35 mph, lowered d-ring, airbag).

Table 11-26 Frontal impact simulation frames side view (35 mph, lowered d-ring, airbag).







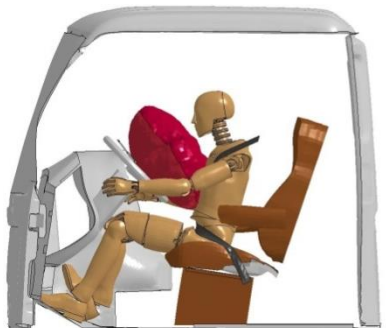







Time (Sec)	Sequential Frames	Time (Sec)	Sequential Frames
0.000		0.074	
0.015		0.089	
0.030		0.115	
0.055			

Table 11-27 Frontal impact simulation frames perspective view (35 mph, lowered d-ring, airbag).

Time (Sec)	Sequential Frames	Time (Sec)	Sequential Frames
0.000		0.074	
0.015		0.089	
0.030		0.115	
0.055			

The seatbelt retractor force for the resulting simulation is plotted in Figure 11-87. The retractor contained no load limiter for this simulation and reached a peak of about 11.0 kN.

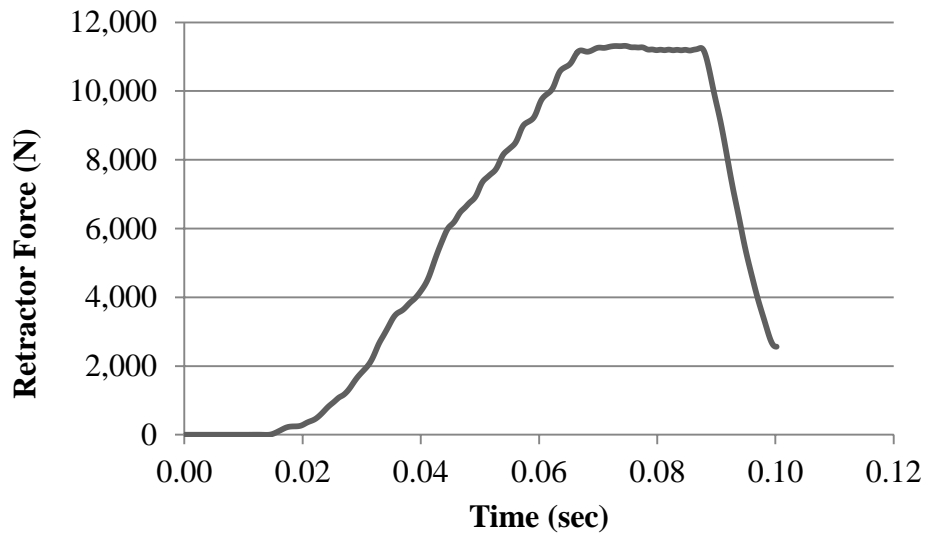


Figure 11-87 Seatbelt retractor force time history (35 mph, lowered d-ring, airbag).

11.2.5.2 Head injury criteria

Dummy injury criteria for the head are evaluated with respect to the HIC₁₅ criteria. Head acceleration recorded during the impact event is employed to calculate the HIC₁₅ value. Figure 11-88 illustrates details for the head injury criteria and the recorded curves from this specific impact condition and passive restraint systems employment.

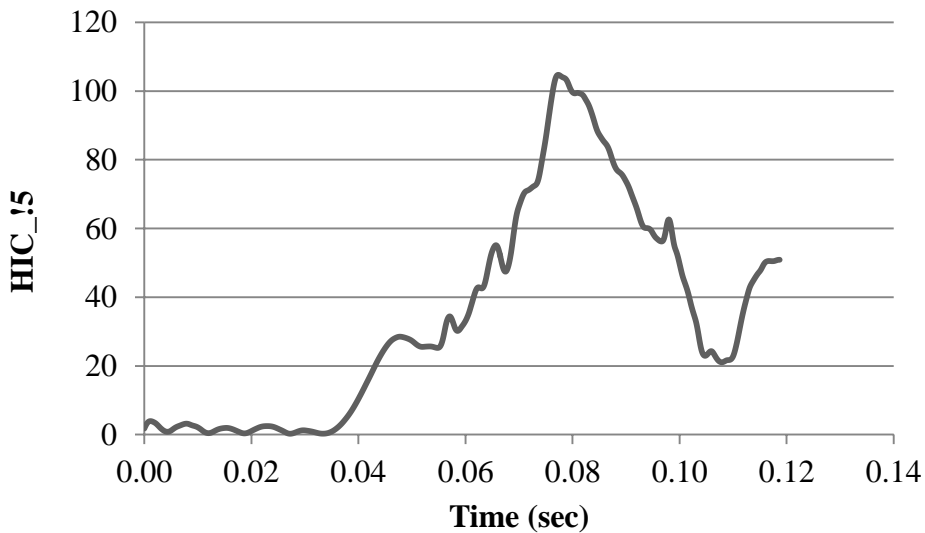
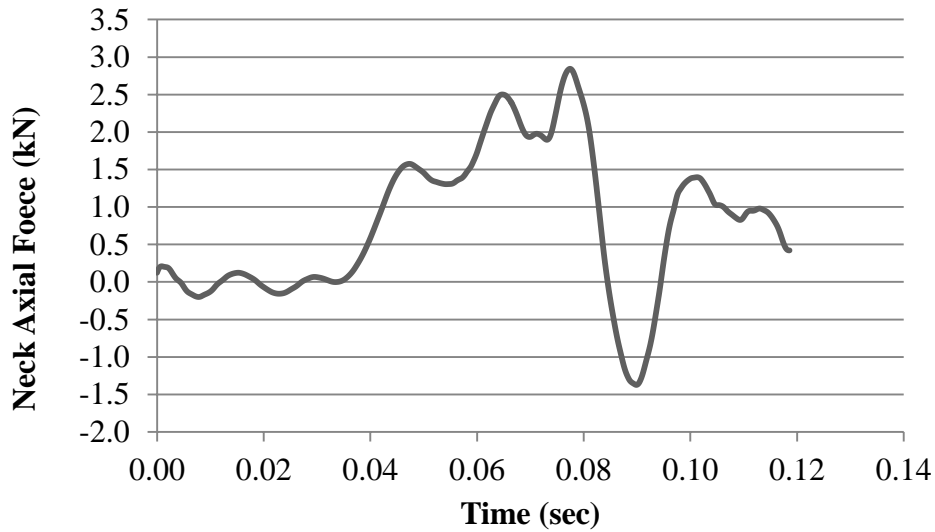


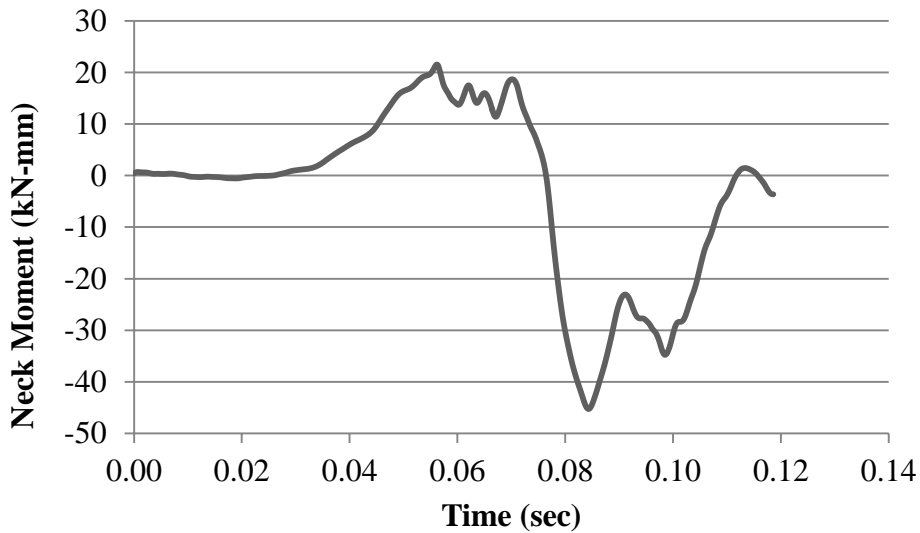
Figure 11-88 HIC time history (35 mph, lowered d-ring, airbag).

11.2.5.3 Neck injury criteria

Dummy injury criteria for the neck are evaluated based on the normalized neck injury criteria, N_{ij} , which is defined as the sum of normalized values of loads and moments. Figure 11-89 illustrates details for the neck injury criteria and the recorded curves from this specific impact condition and passive restraint systems employment.



(a) Neck Axial Force Time History



(b) Neck Bending Moment Time History

Figure 11-89 Neck injury time history (35 mph, lowered d-ring, airbag).

11.2.5.4 Chest injury criteria

Dummy injury criteria for the chest are evaluated based on the chest deflection values. Figure 11-90 illustrates details for the chest injury criteria and the recorded curves from this specific impact condition and passive restraint systems employment.

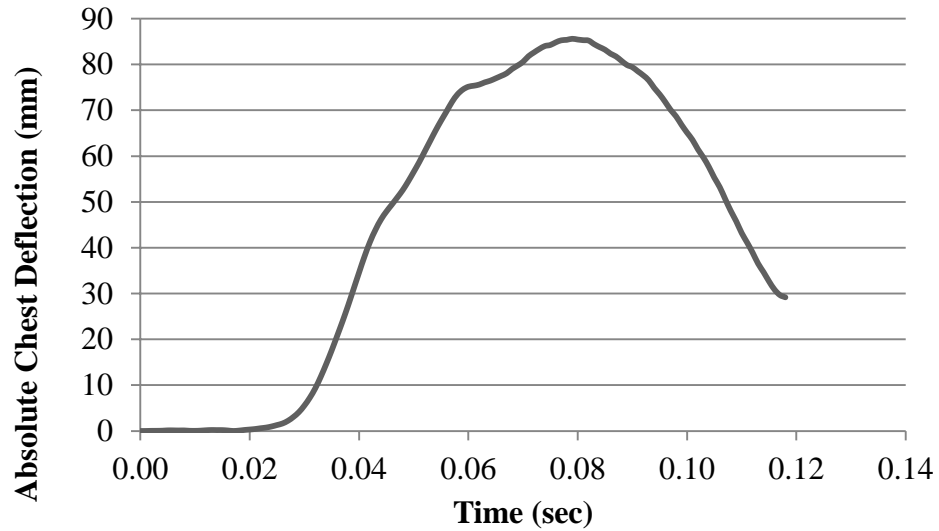
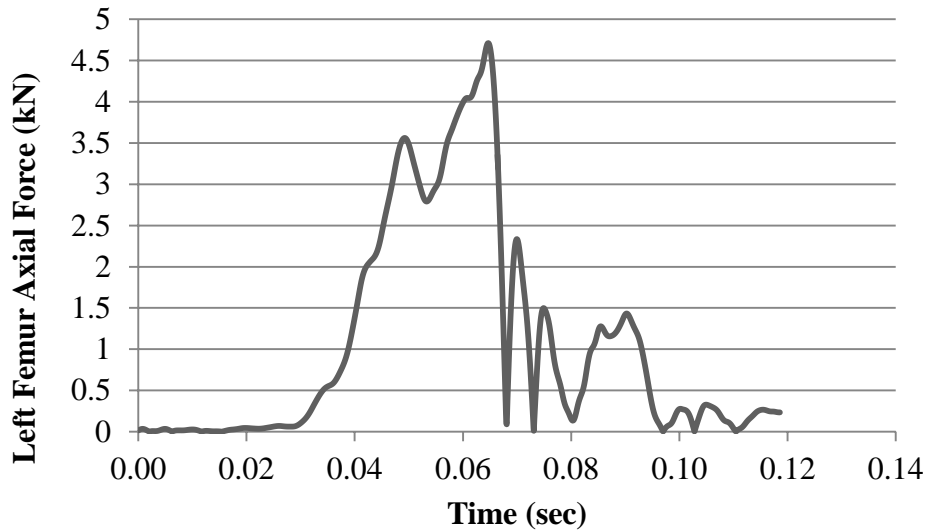


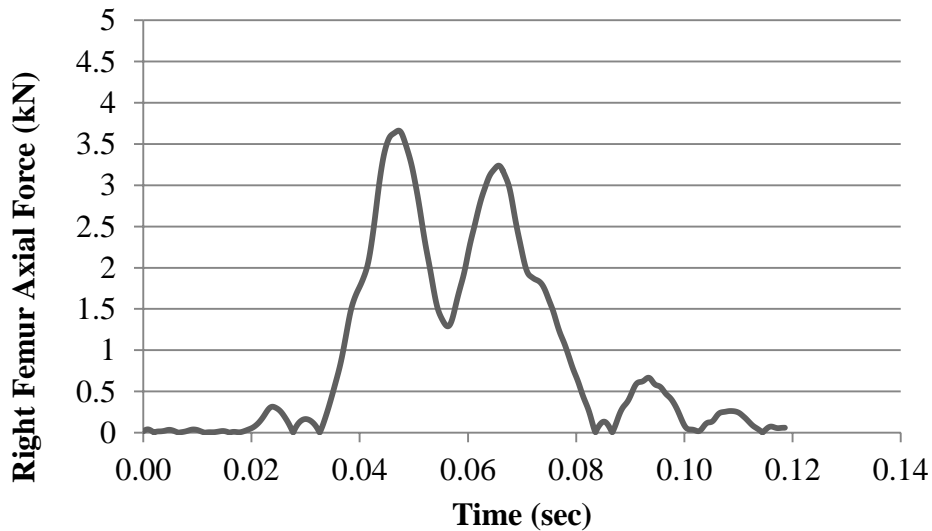
Figure 11-90 Chest deflection time history (35 mph, lowered d-ring, airbag).

11.2.5.5 KTH injury criteria

Dummy injury criteria for the KTH are evaluated based on the formulation for probability of injury as a function of femur axial force. Figure 11-91 illustrates details for the KTH injury criteria and the recorded curves from this specific impact condition and passive restraint systems employment.



(a) Left Femur Axial Force Time History

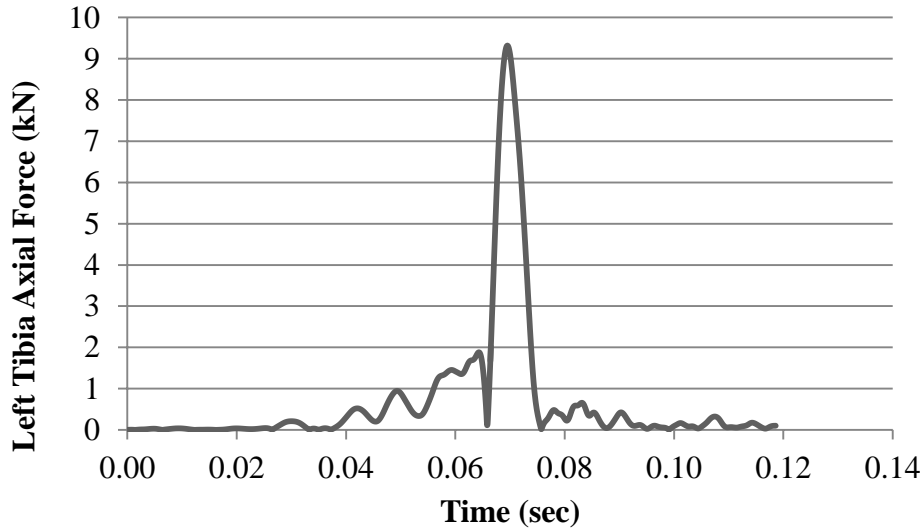


(b) Right Femur Axial Force Time History

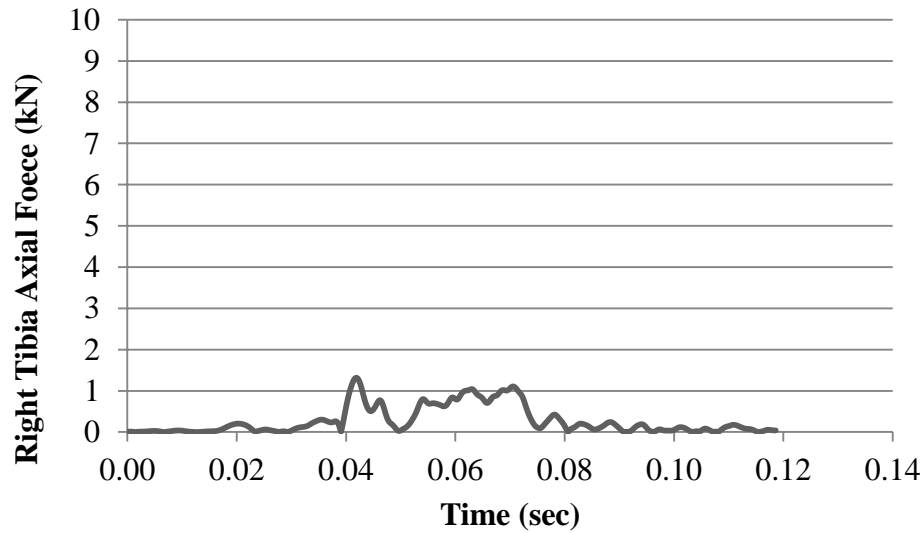
Figure 11-91 KTH injury time history (35 mph, lowered d-ring, airbag).

11.2.5.6 Tibia plateau fracture injury criteria

Dummy injury criteria for tibia plateau fractures are evaluated based on axial compressive loads. Figure 11-92 illustrates details for the tibia plateau injury criteria and the recorded curves from this specific impact condition and passive restraint systems employment.



(a) Left Tibia Axial Force Time History

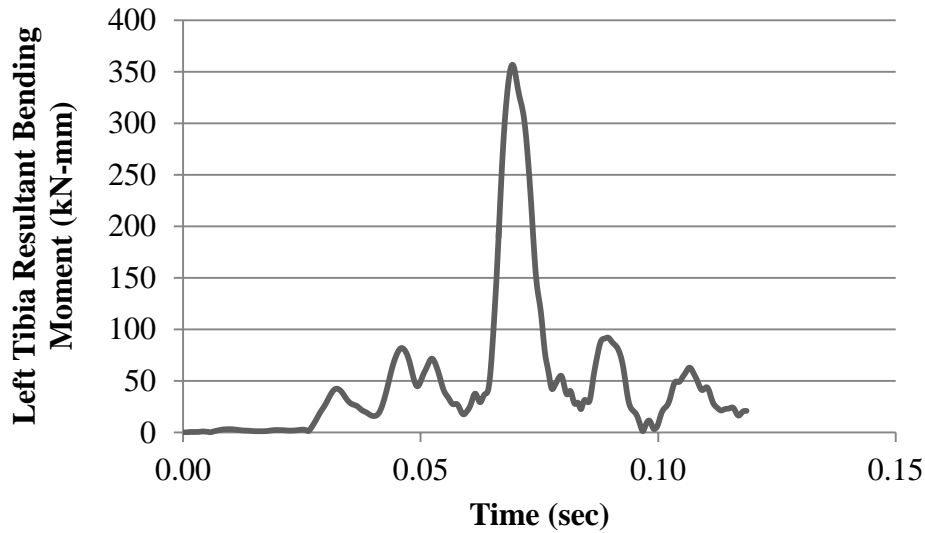


(b) Right Tibia Axial Force Time History

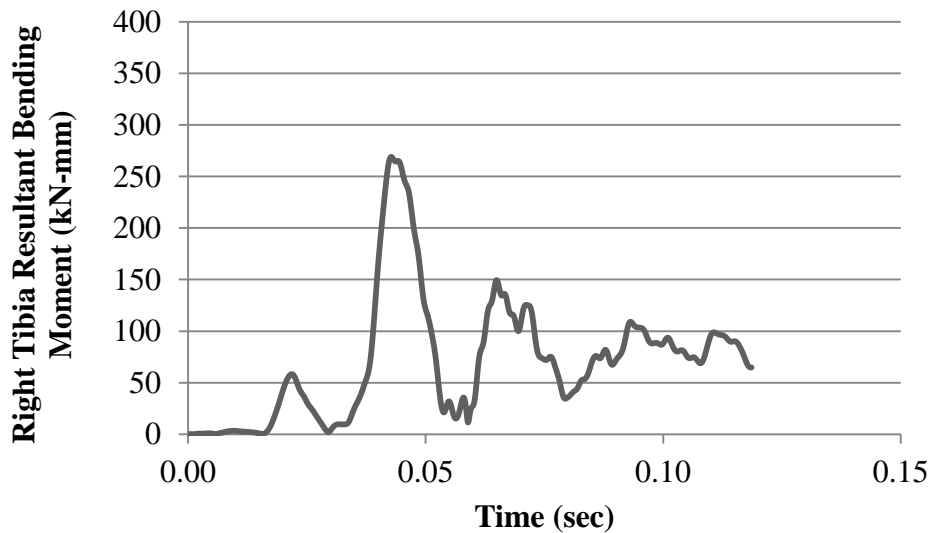
Figure 11-92 Tibia plateau fracture time history (35 mph, lowered d-ring, airbag).

11.2.5.7 Tibia shaft fracture injury criteria

Dummy injury criteria for tibia shaft fractures are evaluated based on a normalized formulation that combines bending moments and axial compressive loads. Figure 11-93 illustrates details for the neck injury criteria and the recorded curves from this specific impact condition and passive restraint systems employment.



(a) Left Tibia Bending Moment Time History



(b) Right Tibia Bending Moment Time History

Figure 11-93 Tibia shaft fracture time history (35 mph, lowered d-ring, airbag).

11.2.5.8 Conclusions

The injury criteria values for various parts of the body were compared to the IARV requirements. The simulation injury criteria results as a percentage of the IARV values are shown in Figure 11-94.

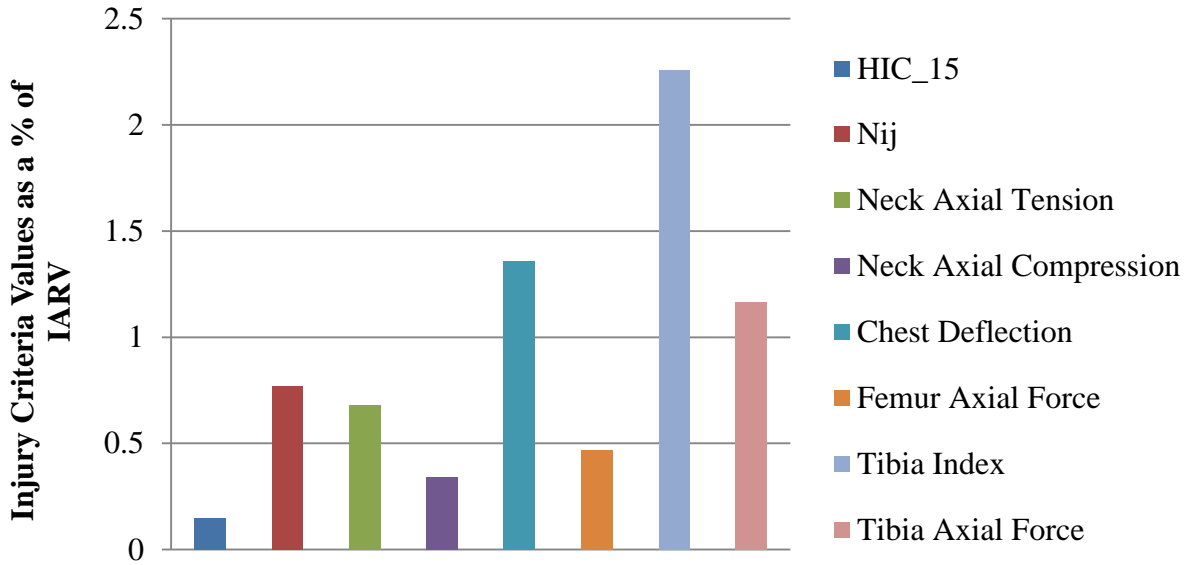


Figure 11-94 Injury probability as a function of IARV (35 mph, lowered d-ring, airbag).

For the frontal lowered d-ring simulation with airbag, the probability of injury for the head, KTH, neck regions is unlikely because the injury criteria values stay below the threshold IARV. The injury criteria values for the chest region exceeded the threshold IARV which is unacceptable according to current standards.

11.2.6 Comparison of frontal simulations with airbag – 35 mph

11.2.6.1 Simulation frame comparisons

The five frontal simulations conducted at 35 mph with airbag were compared to see the effects of the different restraint system parameters. Table 11-28 and Table 11-29 summarize the resulting simulations with frames at different times throughout the simulation.

11.2.6.2 Injury criteria comparison for different body regions of ATD

The injury criteria values for various parts of the body were compared to the IARV requirements. The simulation injury criteria results as a percentage of the IARV values are shown in Figure 11-95 through Figure 11-98 for the different regions of the body. The injury criteria results were not included for tibia injury comparison because tibia injury criteria results are not predictable. Leg injury is typically analyzed in terms of KTH injury which represents the femur region.

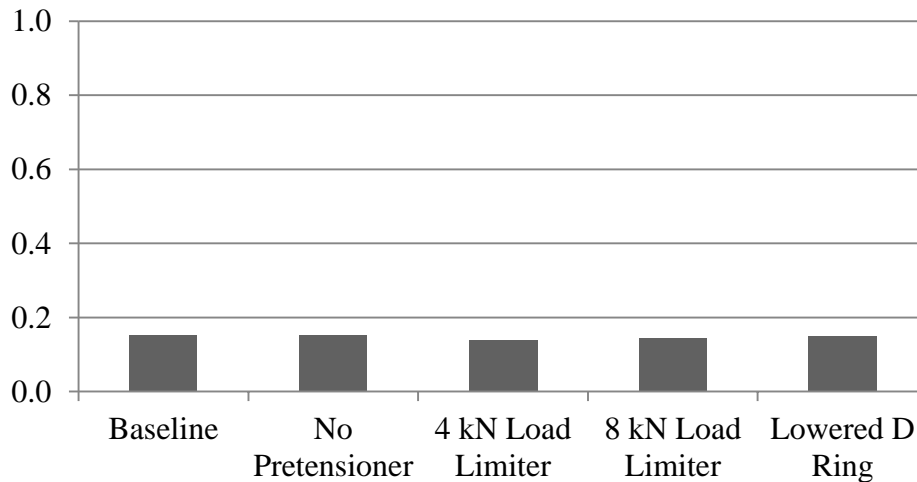


Figure 11-95 Head injury probability comparison as a function of IARV (airbag).

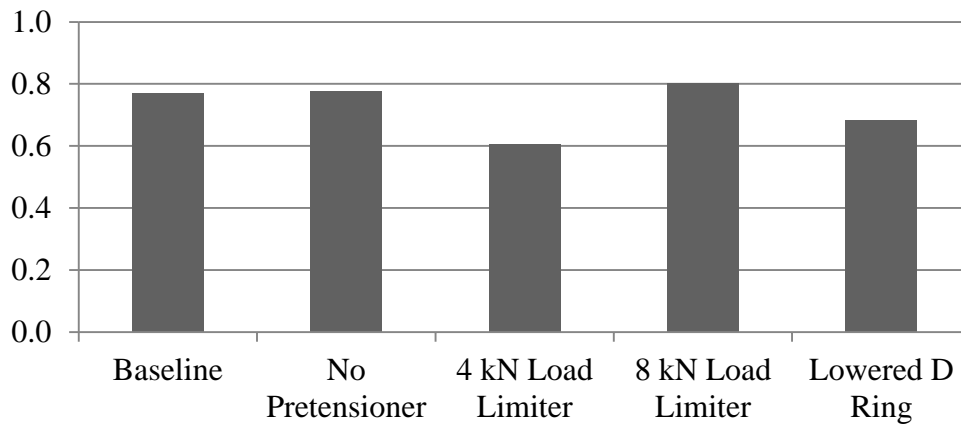











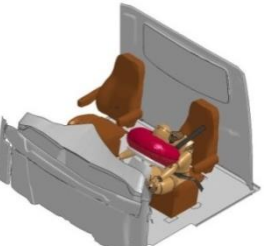


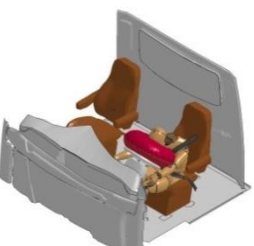







Figure 11-96 Neck injury probability comparison as a function of IARV (airbag).

Table 11-28 Sequential frame comparison of frontal simulations at 35 mph with airbag (side view).



Table 11-29 Sequential frame comparison of frontal simulations at 35 mph with airbag (perspective view).

Time (Sec)	Baseline	No Pretensioner	4 kN Load Limiter	8 kN Load Limiter	Lowered D-Ring
0.000					
0.030					
0.074					
End					

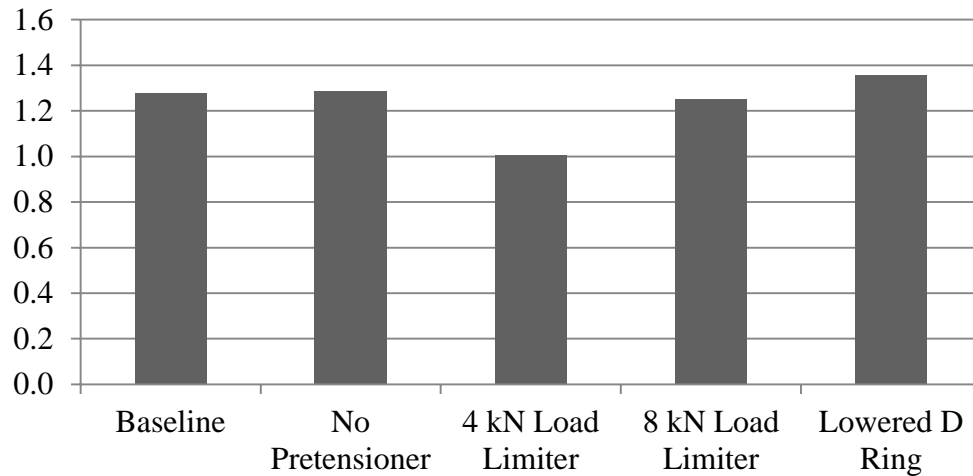


Figure 11-97 Chest injury probability comparison as a function of IARV (airbag).

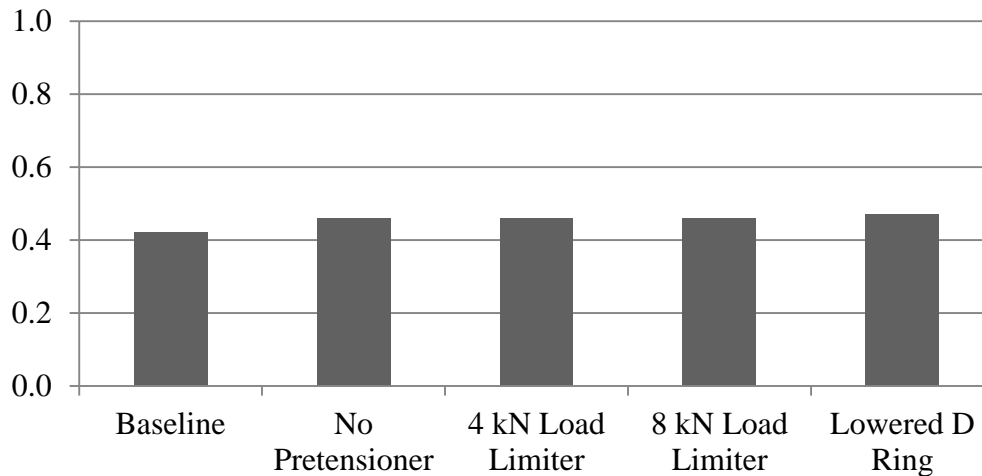


Figure 11-98 KTH injury probability comparison as a function of IARV (airbag).

Analysis of the injury criteria shows that the KTH, head and neck injury stayed below the threshold IARV, meaning that the probability of leg, head and neck injury is unlikely. The chest injury criteria results did have values slightly above the threshold which is unacceptable according to current standards. The restraint system that contained the lowest injury criteria results was the 4 kN load limiter seatbelt design. The inclusion of the airbag significantly reduced neck injury criteria values for all five simulations when compared to the simulations with no airbag. The other body regions did have not much effect with the inclusion of the airbag.

12. FE rollover computer simulation results

The methodology approach for the rollover simulation was implemented to analyze occupant kinematics and injury criteria for three different simulation types. Restraint systems have a critical role in occupant kinematics and injury criteria during a rollover crash. As a result, simulations were conducted to analyze the effects of different types of seatbelt restraint systems. The different cases include: unbelted, lap belt, and shoulder and lap belt.

It was also necessary to compare the fast hybrid dummy model to the detailed hybrid dummy model to ensure accuracy of the fast dummy model.

12.1 Comparison of fast dummy model to detailed dummy model

In order to conduct a comparison of the two dummies one of the frontal simulation scenario was re-run with the fast dummy model. The simulation setup remained the same, except for the employment of the different dummy model. The simulation was a 35 mph frontal speed with an 8 kN load limiter and no airbag. Table 12-1 summarizes the resulting IARV's for the fast dummy model and detailed dummy model. As can be seen in the table the resulting injury criteria for the fast dummy are significantly different from the injury criteria for the detailed dummy. The only similar resulting injury criteria values are chest deflection and right tibia axial force.

Due to the resulting significant difference in injury criteria researchers did not focus on injury criteria results for the rollover simulations. The accuracy of the results for the fast dummy model was questionable and it was not possible to conduct further research to improve the accuracy of the fast dummy model. Therefore, for the three different rollover simulations researchers focused on occupant behavior throughout the simulation and did not analyze the injury criteria.

Table 12-1 Comparison of injury criteria for fast dummy and detailed dummy.

	Fast Dummy			Detailed Dummy		
	IARV	Injury Criteria	% of IARV	IARV	Injury Criteria	% of IARV
HIC-15	700	70.4	0.10	700	182.2	0.26
Neck Axial Tension (kN)	4.17	0.99	0.24	4.17	6.6	1.58
Neck Axial Compression (kN)	4	0.02	0.01	4	2.0	0.49
Chest Deflection (mm)	63	73.4	1.17	63	76.6	1.22
Left Femur Axial Force (kN)	-10	-1.7	0.17	-10	-4.3	0.43
Right Axial Femur Force (kN)	-10	-7.6	0.76	-10	-3.7	0.37
Left Tibia Axial Force (kN)	-8	-1.9	0.23	-8	-8.3	1.03
Right Tibia Axial Force (kN)	-8	-1.2	0.15	-8	-1.3	0.16

12.2 Unbelted rollover simulation

The first rollover simulation was conducted with an unbelted occupant. Table 12-2 and Table 12-3 summarize the simulation with frames at different times throughout the simulation. The truck cabin was made transparent in order to see the behavior of the dummy.

Table 12-2 Rollover unbelted simulation frames (front view).

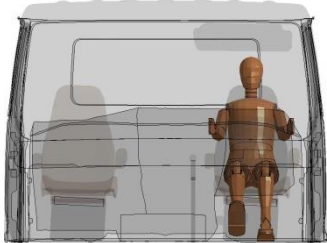
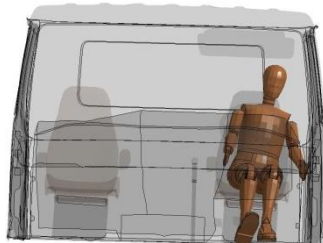
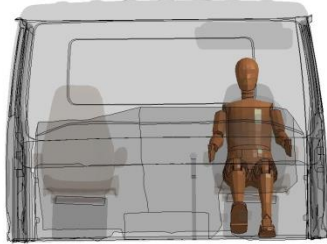
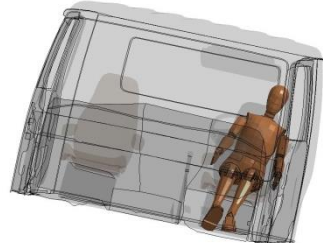
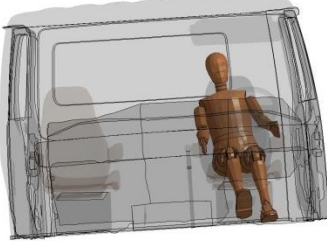
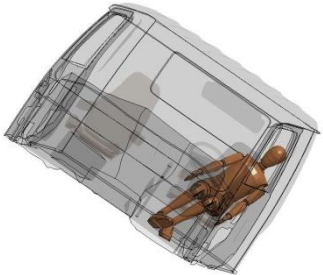
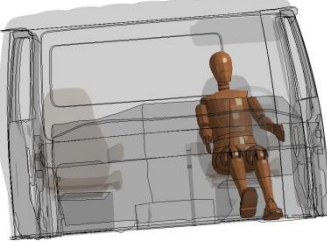
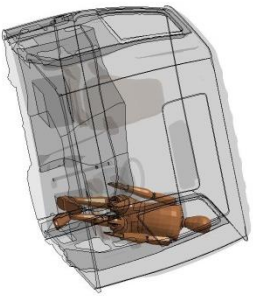
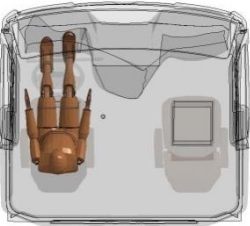
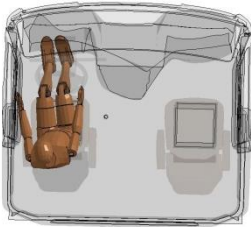
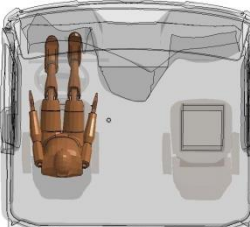
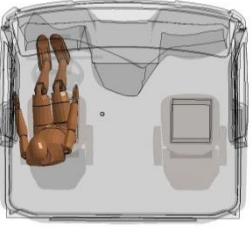
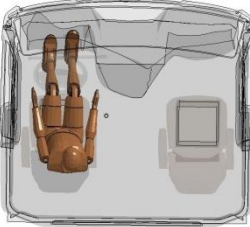
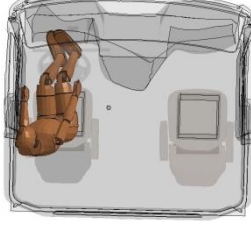
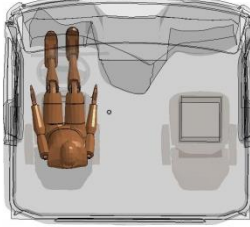
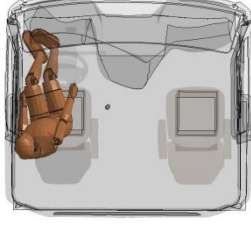
Time (Sec)	Sequential Frames	Time (Sec)	Sequential Frames
0.0		2.0	
0.5		2.5	
1.0		3.0	
1.5		3.4	

Table 12-3 Rollover unbelted simulation frames (top view).

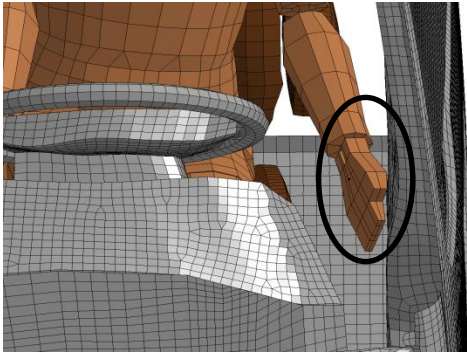
Time (Sec)	Sequential Frames	Time (Sec)	Sequential Frames
0.0		2.0	
0.5		2.5	
1.0		3.0	
1.5		3.4	

During the simulation it was noted that the following parts came into contact with the truck cabin:

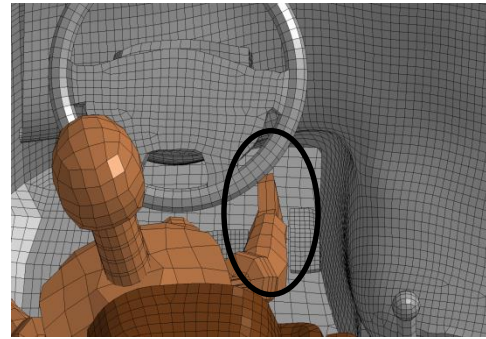
- Dummy head to left door.
- Dummy left hand to left door.
- Dummy right hand to steering wheel.
- Dummy right knee to steering wheel.

Table 12-4 shows the four different major contacts that occur during the rollover simulation. Researchers proceeded to output the lateral or y-displacement of the dummy head. In LS-PrePost a node was selected on the top of the head and the y-displacement history was plotted as seen in Figure 12-1.

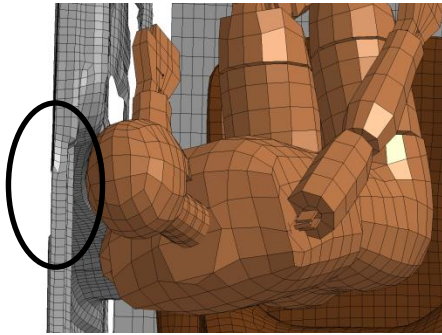
Table 12-4 Description of different contact points during rollover unbelted simulation.



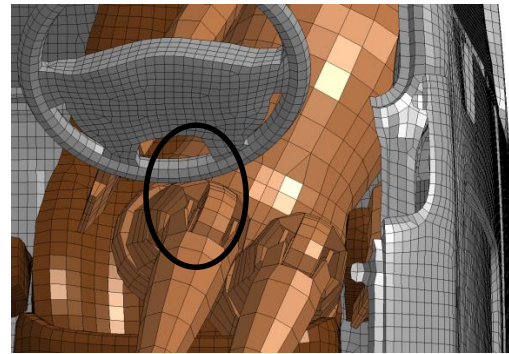
(a) Contact between dummy left hand and left door at 1.76 seconds.



(b) Contact between dummy right hand and steering wheel at 1.81 seconds.



(c) Contact between dummy head and left door at 2.9 seconds.



(d) Contact between dummy right knee and steering wheel at 3.22 seconds.

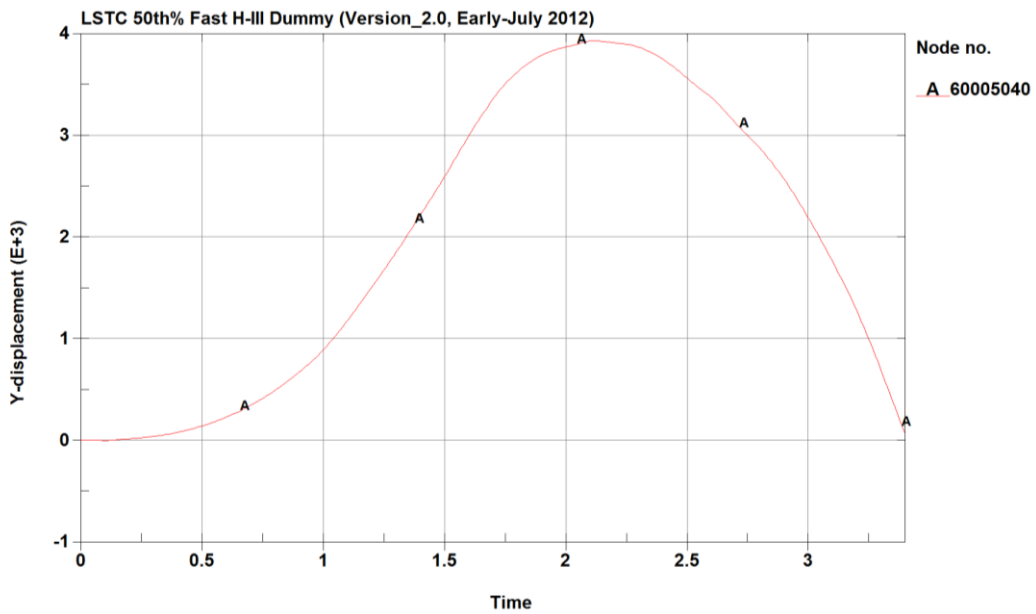


Figure 12-1 Lateral displacement of dummy head during rollover unbelted simulation.

12.3 Lap belt rollover simulation

The second rollover simulation was conducted with a lap belt restraint system. Table 12-5 and Table 12-6 summarize the simulation with frames at different times throughout the simulation. The truck cabin was made transparent in order to see the behavior of the dummy.

During the simulation it was noted that the following parts came into contact with the truck cabin:

- Dummy head to left door.
- Dummy left hand to left door.
- Dummy right hand to steering wheel.

Table 12-7 shows the three different major contacts that occur during the rollover simulation.

Researchers proceeded to output the lateral or y-displacement of the dummy head. In LS-PrePost a node was selected on the top of the head and the y-displacement history was plotted as seen in Figure 12-2.

Table 12-5 Rollover lap belt simulation frames (front view).

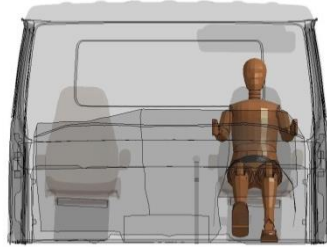
**Time
(Sec)**

Sequential Frames

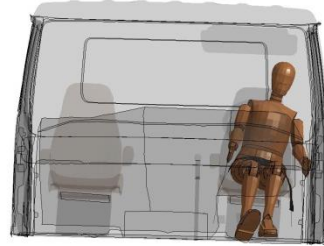
**Time
(Sec)**

Sequential Frames

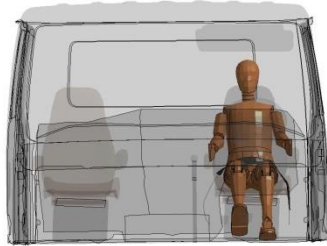
0.0



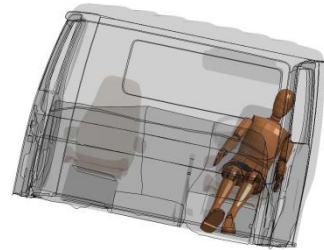
2.0



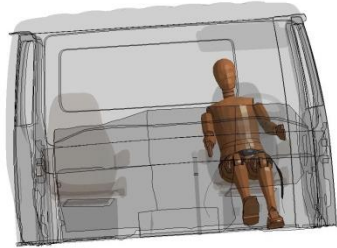
0.5



2.5



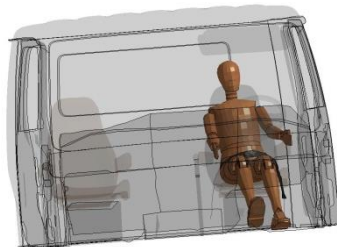
1.0



3.0



1.5



3.4

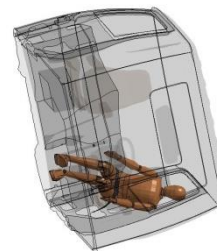


Table 12-6 Rollover lap belt simulation frames (top view).

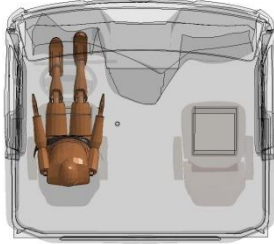
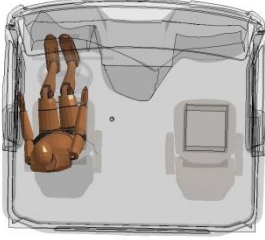
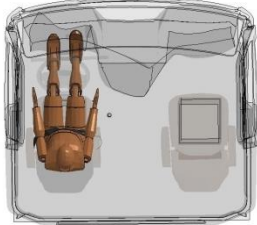
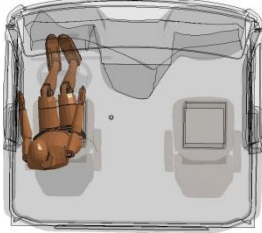
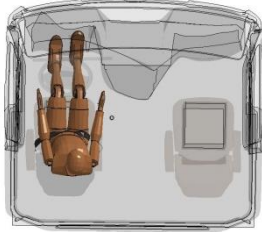
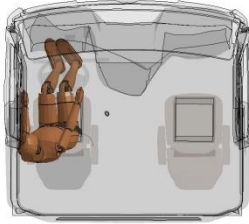
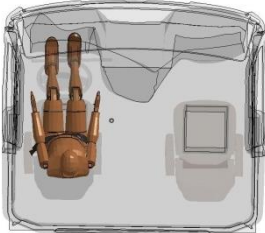
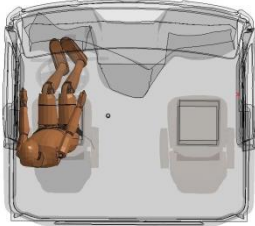
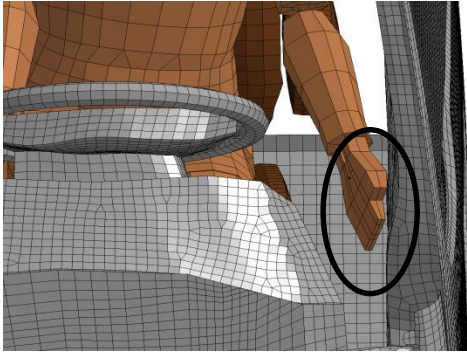
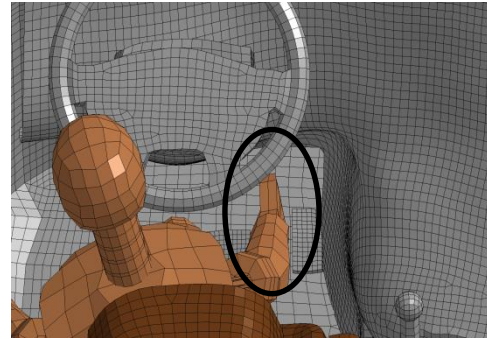
Time (Sec)	Sequential Frames	Time (Sec)	Sequential Frames
0.0		2.0	
0.5		2.5	
1.0		3.0	
1.5		3.4	

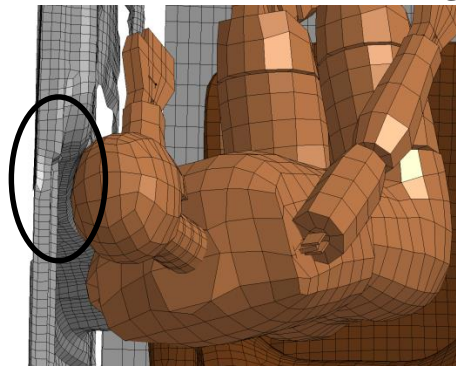
Table 12-7 Description of different contact points during rollover lap belt simulation.



(a) Contact between dummy left hand and left door at 1.75 seconds.



(b) Contact between dummy right hand and steering wheel at 1.80 seconds.



(c) Contact between dummy head and left door at 2.85 seconds.

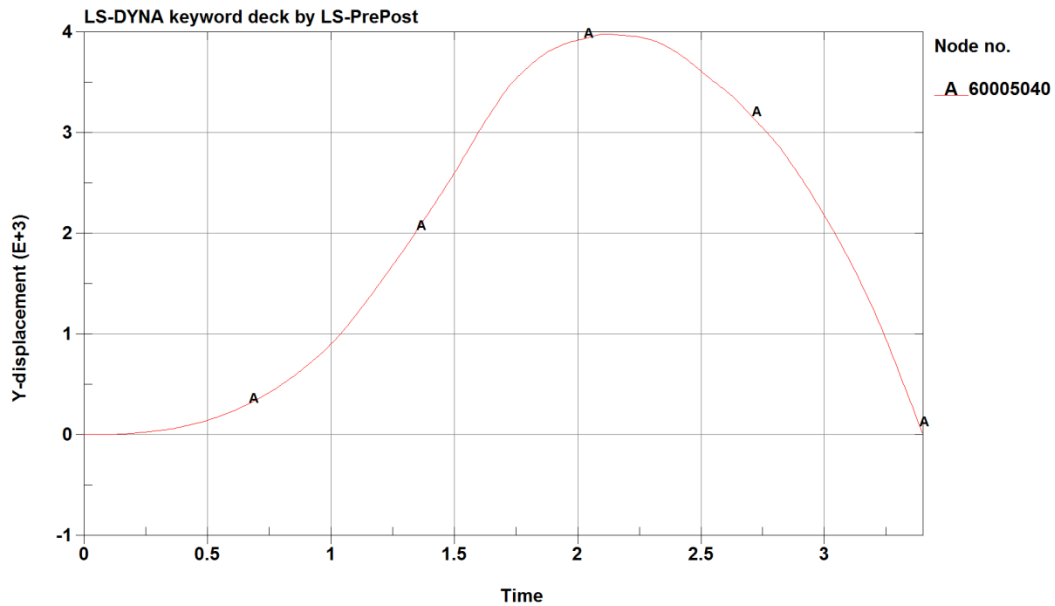


Figure 12-2 Lateral displacement of dummy head during rollover lap belt simulation.

12.4 Shoulder and lap belt rollover simulation

The third rollover simulation was conducted with a shoulder and lap belt restraint system. Table 12-8 and Table 12-9 summarize the simulation with frames at different times throughout the simulation. The truck cabin was made transparent in order to see the behavior of the dummy.

During the simulation it was noted that the following parts came into contact with the truck cabin:

- Dummy left hand to left door.
- Dummy right hand to steering wheel.

Table 12-10 shows the four different major contacts that occur during the rollover simulation.

Researchers proceeded to output the lateral or y-displacement of the dummy head. In LS-PrePost a node was selected on the top of the head and the y-displacement history was plotted as seen in Figure 12-3.

Table 12-8 Rollover shoulder and lap belt simulation frames (front view).

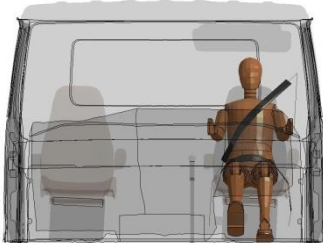
**Time
(Sec)**

Sequential Frames

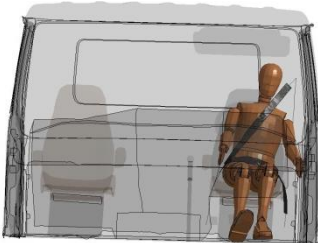
**Time
(Sec)**

Sequential Frames

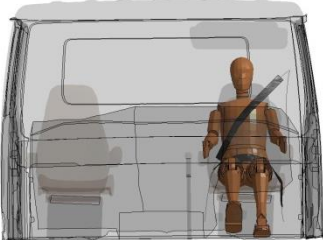
0.0



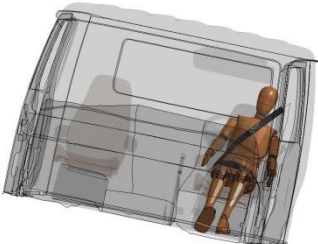
2.0



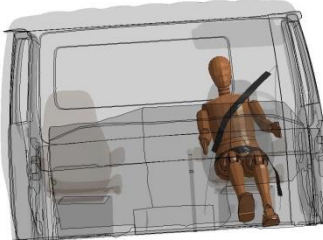
0.5



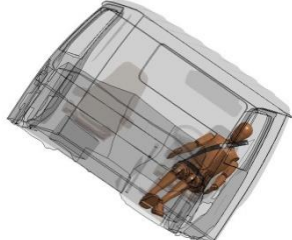
2.5



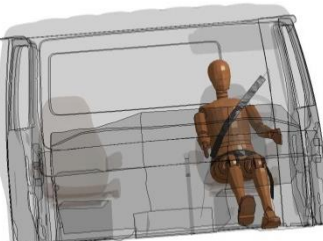
1.0



3.0



1.5



3.4

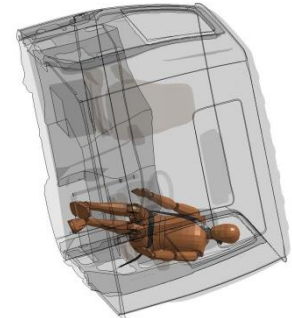


Table 12-9 Rollover shoulder and lap belt simulation frames (top view).

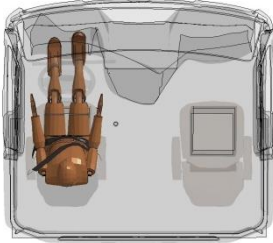
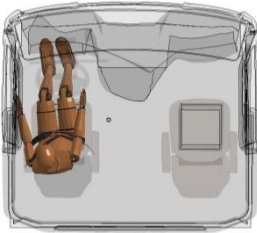
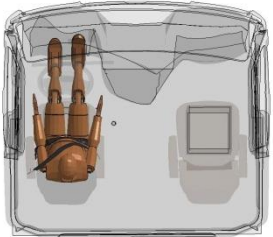
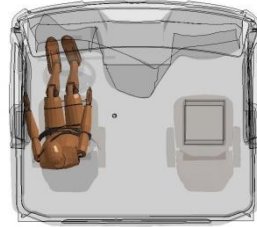
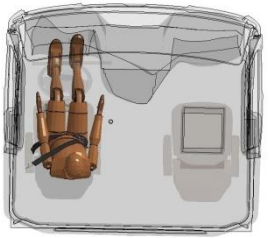
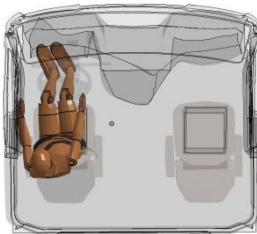
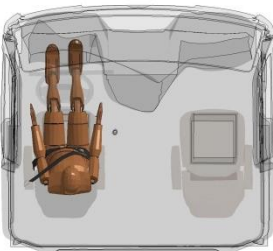
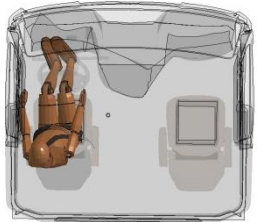
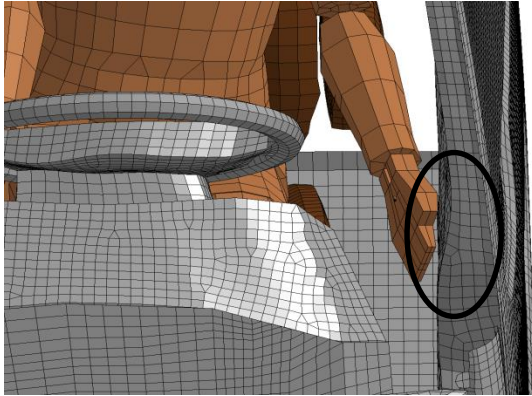
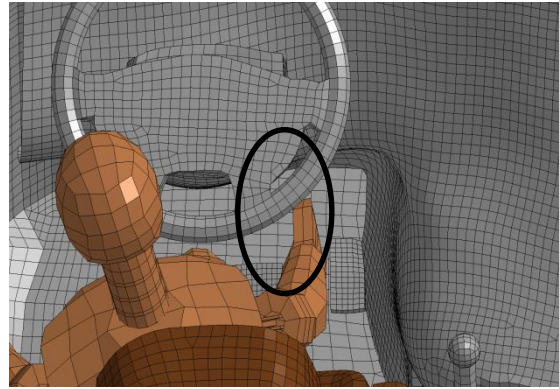
Time (Sec)	Sequential Frames	Time (Sec)	Sequential Frames
0.0		2.0	
0.5		2.5	
1.0		3.0	
1.5		3.4	

Table 12-10 Description of different contact points during rollover shoulder and lap belt simulation.



(a) Contact between dummy left hand and left door at 1.9 seconds.



(b) Contact between dummy right hand and steering wheel at 1.75 seconds.

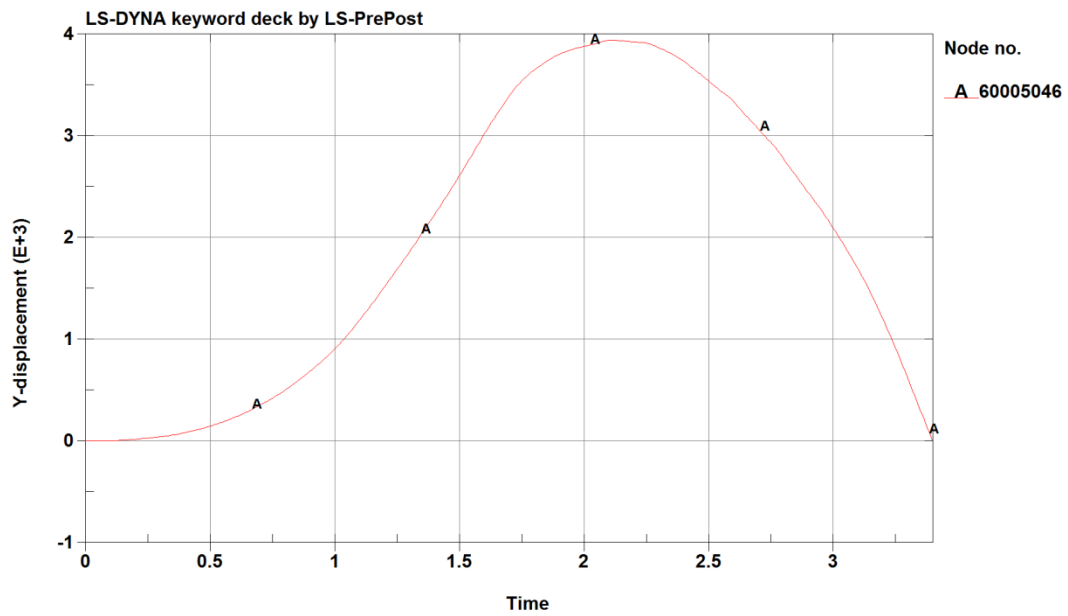


Figure 12-3 Lateral displacement of dummy head during rollover shoulder and lap belt simulation.

12.5 Comparison of rollover simulations

The three different rollover simulations were compared to see the effects of the different restraint systems on occupant behavior. Table 12-11 and Table 12-12 compare sequential frames of the rollover simulations. The truck cabin was made transparent in order to see the behavior of the dummy.

Table 12-11 Comparison of rollover sequential frames for different restraint systems (front view).

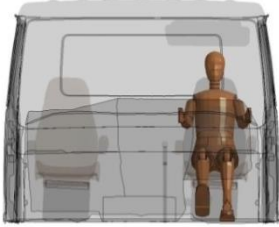
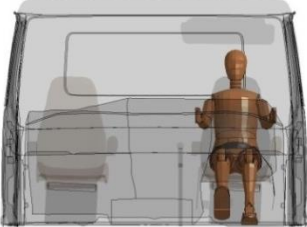
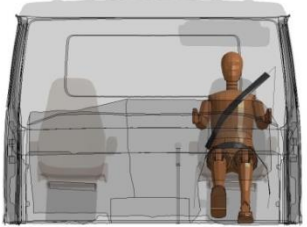
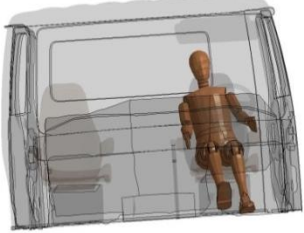
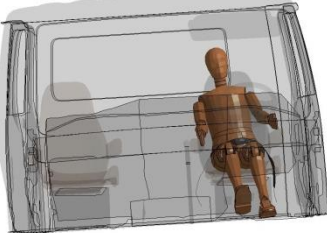
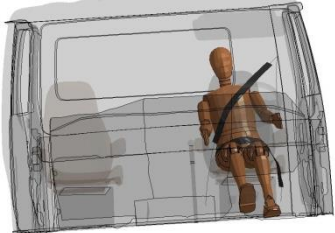
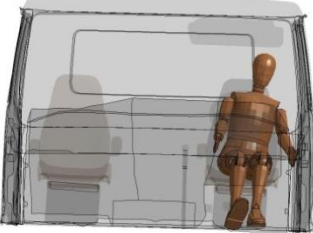
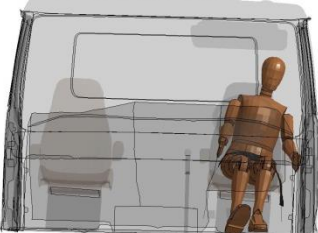
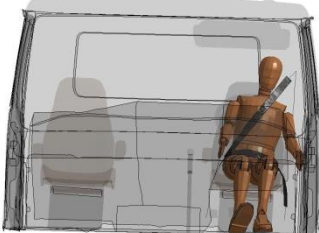
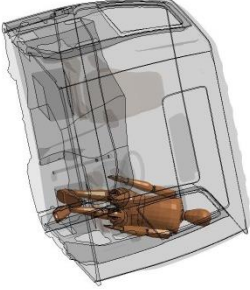
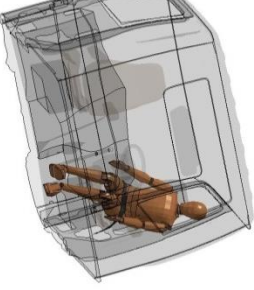
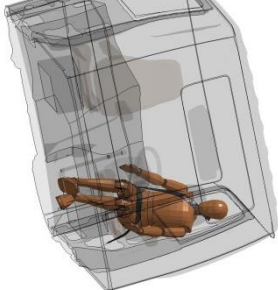
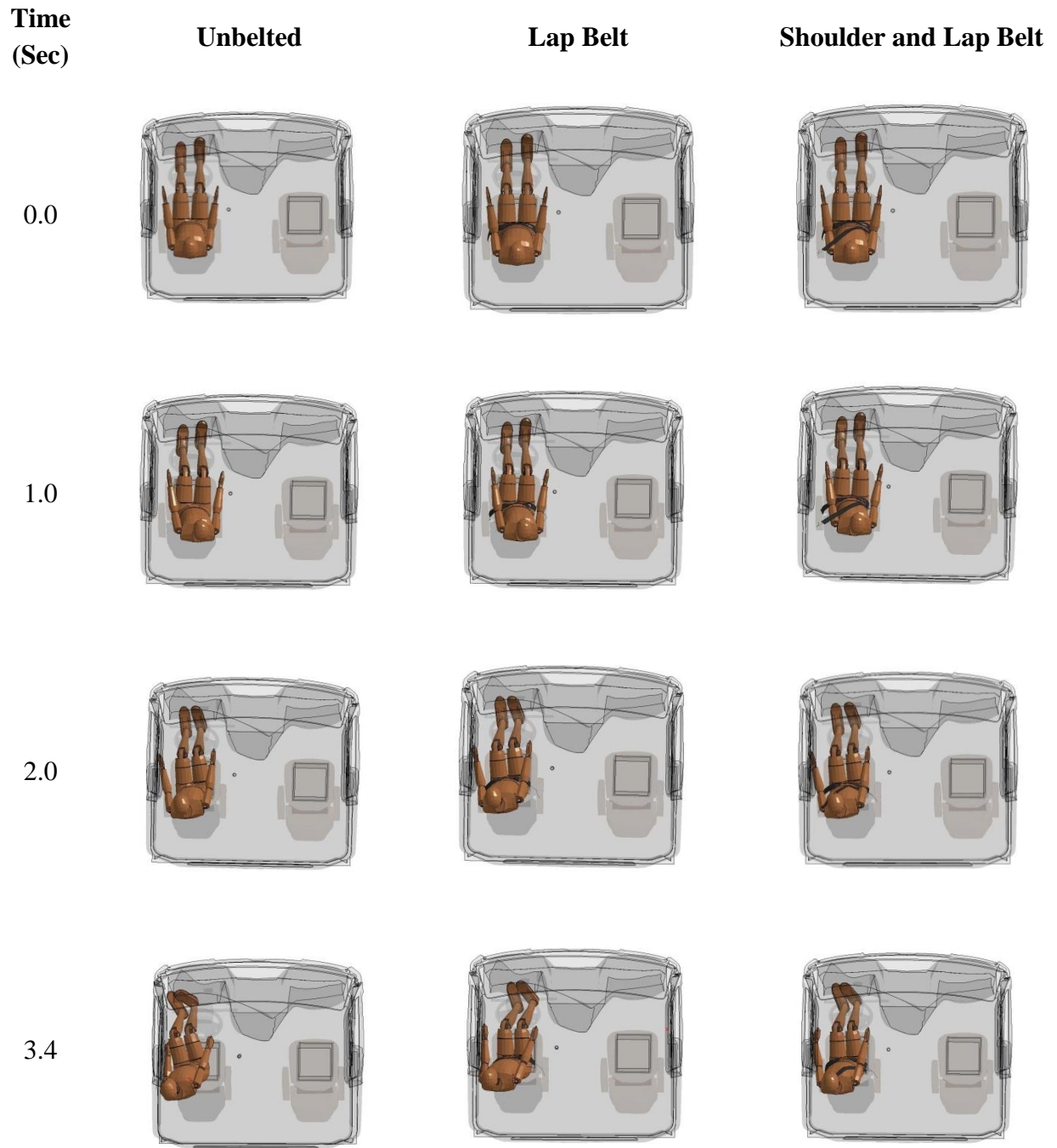
Time (Sec)	Unbelted	Lap Belt	Shoulder and Lap Belt
0.0			
1.0			
2.0			
3.4			

Table 12-12 Comparison of rollover sequential frames for different restraint systems (top view).



For the unbelted and lap belt rollover simulations it can be seen in the previous tables that the dummy head came into contact with the left door. Although researchers were unable to computer injury criteria as a result of this contact it is still not ideal behavior for the dummy. The lap and shoulder belt rollover simulation did not have contact between the dummy head and left door. The reason being is that the dummy neck came into contact with the shoulder belt which prevented the dummy head from falling farther towards the door. Despite the avoided contact with the door, the contact occurrence between the dummy neck and seatbelt was not ideal behavior.

To compare head movement during the different rollover simulations, the maximum lateral displacement is recorded in Table 12-13 for the three rollover simulations. The resulting lateral displacement was very similar among the three simulations and did not show much change.

Table 12-13 Comparison of maximum lateral displacement for rollover simulations.

	Unbelted	Lap Belt	Shoulder and Lap Belt
Max Y-Lateral Displacement (mm)	3934.76	3978.1	3936.91

Researchers were able to develop three successful rollover simulations that captured occupant behavior. Two different seatbelt restraint systems were developed to analyze the different effects on occupant dynamics during the simulation. These seatbelt restraint systems did not result in ideal occupant behavior and contact with truck cabin interior components. Researchers suggest future work be conducted to analyze additional seatbelt restraint systems along with airbag systems to improve occupant behavior during a rollover crash.

13. Summary and conclusions

Little research has been conducted in the field of heavy truck occupant protection, especially with the use of computer simulations to analyze occupant kinematics. This research represented here is the product of a joint project to identify opportunities to reduce truck driver fatalities and injuries in traffic crashes in the context of the projected full deployment of ACATs.

This project was intended to represent a pilot study for the investigation of overall heavy trucks crashworthiness and areas of improvement for occupant safety. Researchers focused on identifying specific areas for future research aiming at improving occupant protection for truck drivers. Additionally, researchers developed a methodology that can be employed and /or adapted to conduct future research within heavy truck occupant safety with use of computational analysis.

Crash scenarios were identified that capture the highest risk to truck drivers and account for the most fatalities and injuries. The two primary crash types identified were rollover and frontal collisions with other trucks or with hard roadside objects, such as bridge abutments or embankments. The effect of the primary current crash avoidance technologies on the crash population was overlaid on the crash population to determine the residual population of crashes that would remain after full deployment. This allowed researchers to focus on impact conditions that are overrepresented in the real world crash data, but that would not be addressed by crash avoidance technologies, and to define opportunities for improved truck crashworthiness to reduce truck driver fatalities and injuries.

The crash-reduction potential of ESC, RSC, LDW, and FCW with CMB were applied to the crash population. It was estimated that the joint effect of these technologies would be to reduce overall tractor-semitrailer crashes by about 10%. However, the evaluation showed that the effect would be significantly higher for the crashes that were most harmful to truck drivers. It is expected that full deployment would reduce truck driver fatalities by about one-third and A-injuries by about 30%. Rollovers as a crash type would be reduced by almost 40%, and frontal collisions by about 20%.

Despite the significant decrease in the number of rollovers and frontal collisions, the crash analysis suggested that those two crash types would remain as the primary injury mechanism for tractor-semitrailer drivers. Rollover would still account for about half of truck driver fatalities, and frontal impact would still account for almost 60% of the collision-related fatalities.

Thus, two crash scenarios were identified as the most critical for heavy truck occupant safety: frontal crash and rollover crash caused by a specific maneuver. FE computer simulations were used to replicate these crash scenarios and to investigate occupant safety during the crash.

Researchers employed a currently available FE anthropomorphic test device (dummy) model in their computer simulations to analyze occupant kinematics during simulated crash scenarios. This allowed collecting acceleration data experienced by the dummy as consequence of impacts with interior components of the truck occupant compartment. Occupant body injury levels were then calculated for each simulated crash scenario. Crash scenarios were identified using preliminary results obtained by crash data analysis. Researchers focused on overrepresented impact conditions from real world crash data, for which it is believed to be room for improvement in terms of occupant safety. In addition, researchers evaluated the effectiveness of passive safety restraints by comparing occupant injury results obtained from FE computer simulations performed with and without use of these restraints.

An essential area of the FE simulations was the development of the truck cabin model. The limited time and budget of this pilot study did not allow use of an FE full tractor-trailer model for computer simulations. Instead, researchers developed a simplified truck cabin model that was used in the simulated crash scenarios. Crash pulses representing different crash scenarios were then applied to this simplified truck cabin model to replicate the accelerations that the occupant would experience during the simulated events.

An integral part in developing the truck cabin model was the development of occupant compartment components. Currently no publicly available FE tractor-trailer models exist which include occupant compartment components. In order to model these components, cloud point scans of a Peterbilt 387 truck model were used to define the geometry of several key interior components which were later meshed and included in the full FE truck cabin model.

Furthermore, researchers developed FE models of seatbelt and airbag restraint systems which were included in the truck cabin model with the scope of investigating their effects on occupant dynamics and injury.

The injury criteria values calculated through use of the FE model of the Hybrid III 50th percentile male were compared to IARV's to determine risk of injury to the occupant.

The frontal simulations were conducted at a speed of 35 mph replicating a tractor-trailer impacting a rigid barrier. A parametric evaluation of the seatbelt and airbag restraint system was conducted to determine effectiveness of occupant restraint systems. In frontal simulations without an airbag both the neck and chest injury criteria were higher than IARV's which is unacceptable according to current standards. The simulation with an 8 kN load limiting seatbelt produced the best injury criteria results in comparison to the other simulations but was still unacceptable when compared to the IARV's. In frontal simulations with an airbag only the chest injury criteria values were above the IARV's which is unacceptable. The inclusion of an airbag system significantly reduced injury criteria values for the neck and produced acceptable values that were below the IARV's. The simulation with a 4 kN load limiter seatbelt produced

the best injury criteria results in comparison to the other simulations but still contained chest injury criteria values above the IARV's. Despite trying different types of seatbelt designs and inclusion of an airbag system the dummy still produced injury criteria values above the threshold IARV's.

The rollover simulations were conducted at a speed of 60 mph replicating a complex rollover maneuver. The maneuver entailed the vehicle performing an evasive maneuver to the left followed by an overcorrecting maneuver to the right. Several limitations were encountered during the development of the rollover simulations. As a result, researchers focused on occupant kinematic behavior and did not analyze injury criteria values. Simulations were conducted analyzing occupant behavior with no seatbelt, a lap belt, and a lap and shoulder belt. For the unbelted and lap belt rollover simulations it was noted that the dummy head came into contact with the left door. The dummy head did not impact the left door with the shoulder and lap belt but contact between the dummy neck and shoulder belt was observed. The behavior of the dummy was not ideal for the different simulations and could result in severe injury for the dummy head.

13.1 Limitations

The effectiveness of the ACATs may be different in actual deployment. The real effects may be greater or less. The evaluations of individual ACATs focused on relatively narrow and simple crash types. In addition, they make many simplifying assumptions. The focus on narrow crash types is reasonable, since it simplifies the problem of detecting any significant differences in crashes. But some of the technologies may affect other crashes than the ones they were tested against. We saw some evidence of that in the effect of LDW on untripped rollovers. Some real-world untripped rollovers were preceded by running off the road. Rollover occurred when the driver over-corrected back onto the road, but the overcorrection resulted in sufficient lateral acceleration to overturn the vehicle. There may be other unanticipated synergies. In addition, drivers may change their driving behavior, resulting in safer operations. For example, some FOTs of LDW noted that drivers tended to improve their lane following and use turn signals more often.

However, the positive effects of deployment may also turn out to be less than the clinical studies estimate. In full deployment, the population of drivers and carriers using the technologies will be more varied. Drivers may choose to disable some of the devices. For example, drivers frustrated with LDW or FCW alerts may simply choose to turn the devices off. Carriers may not maintain the technologies appropriately. It is also possible that some drivers may come to rely on the warnings from FCW or LDW and reduce their vigilance, thus resulting in more, rather than fewer crashes.

This project was conducted as a pilot study and there were important limitations encountered during the development of the computer simulations. Deformation of the truck cabin exterior was not considered during the frontal and rollover crashes. Although this is not a realistic assumption, still it was considered to simplify modeling techniques and produce shorter simulations. Researchers suggest inclusion of cabin interior into tractor-trailer model to consider deformation of tractor-trailer vehicle.

Interior component material properties were not validated for the truck cabin model. Validated material properties for heavy truck interiors are not publicly available and due to budget constraints researchers were unable to conduct material coupon testing for the different interior parts.

The rollover simulation did not consider subsequent collision with the ground during the rollover event. Impact with the ground can cause significant injury to the occupant during the rollover crash.

Despite the limitations of this project a successful methodology was produced and followed to replicate a frontal and rollover crash. Researchers suggest future work be conducted to address the limitations of the project. This includes conducting interior material testing, consideration of deformation, and consideration of subsequent contact with the ground during a rollover crash.

13.2 Implications for future research

Crash analysis showed that the primary crash types in which tractor-semitrailer drivers were injured were in rollovers and in frontal collisions with other trucks or which hard fixed objects. Thus, protecting drivers in rollover and frontal impact is the priority of occupant protection, whether from improved restraints, air bags, more protective interior surfaces within the cab, or stronger cab structures.

In terms of crash avoidance, it appears that, beyond increasing the effectiveness of existing technologies, addressing residual crash types will be more challenging. For example, a higher proportion of residual rollovers is likely to be tripped, i.e., following a collision with another vehicle, object, or tripped by curbs or other environmental feature. The remaining collisions will likely to be more complex geometrically and involving more other vehicles. Future advances in crash avoidance along current lines may be more difficult. Other avenues, such as vehicle-to-vehicle (V2V) and vehicle-to-infrastructure (V2I) may be more promising.

In addition, more real-world evaluation of the technologies in actual deployment is needed. Existing studies generally incorporated the experience of the technologies as deployed at some level. Some studies were based on FOTs, in which the technologies were deployed in actual operations. But few if any crashes occurred, so effectiveness estimates could not be based on observed crash reduction. Instead, estimates of crash reduction were inferred based on reduction

in the traffic conflicts observed, on the assumption that the mechanisms that produce conflicts are the same as those that result in crashes. Other studies incorporated some analysis of the crashes of fleets that had deployed the technologies. Some of these studies did indeed have enough data to draw statistically valid conclusions from crash occurrence. But in these studies there are questions of how representative the carriers studied are of the whole population of truck operators.

Researchers suggest future work be conducted to analyze the effects of different types of seatbelt designs such as a four-point seatbelt and a five-point seat integrated belt to improve occupant safety during frontal and rollover crashes. Furthermore, researchers suggest analysis of side curtain air bag system to prevent occupant head contact with the left door during a rollover crash.

14. References

- Belzowski, B. M., D. Blower, et al. (2009). Tracking the Use of Onboard Safety Technologies Across the Truck Fleet. Ann Arbor, Michigan, UMTRI.
- Blower, D. (2014). Assessment of the Effectiveness of Advanced Collision Avoidance Technologies. Ann Arbor, MI, University of Michigan Transportation Research Institute: 43.
- Bureau of Labor Statistics (2015). Current Population Survey, Census of Fatal Occupational Injuries, U.S. Bureau of Labor Statistics, U.S. Department of Labor.
- Cheng, L. Y., T. P. Khatua, et al. (1994). Heavy Truck Crashworthiness. Phase I, Task C. Occupant Dynamics Simulation.
- Chinni, J., M. Miller, et al. (2007). Tractor-Trailer Rollover Crash Test.
- Eppinger, R.; E. Sun, et al. (1999). Development of Improved Injury Criteria for the Assessment of Advanced Automotive Restraint Systems - II. Report from the National Highway Traffic Safety Administration concerning Federal Motor Vehicle Safety Standard 208, Occupant Crash Protection. Docket Document No. 1999-6407-5. Washington, DC: U.S. Department of Transportation.
- FMCSA. (2007). Safety Belt Usage by Commercial Motor Vehicle Drivers (SBU CMVD) 2007 Survey. <http://www.fmcsa.dot.gov/safety-security/safety-belt/exec-summary-2007.htm>.
- FMCSA (2014). Commercial Motor Vehicle Safety Belt Facts. Washington, DC.
- Guha, S., D. Bhalsod, et al. (2008). LSTC Hybrid III Dummies, Positioning and Post-Processing Documentation. Livermore Software Technology Corporation, Livermore, California, USA.
- Guha, S. (2008). Learning Aid: Vehicle and Hybrid III 50th Percentile Belted Driver. Livermore Software Technology Corporation, Livermore, California, USA.
- Hallquist, J.O. (2015). LS-DYNA Keyword User's Manual, Volume 1. Livermore Software Technology Corporation, Livermore, California.
- Hershman, L. (2001). The U.S. New Car Assessment Program (NCAP): Past, Present, and Future. 17th International Technical Conference on the Enhanced Safety of Vehicles (ESV). Amsterdam, The Netherlands.
- Hickman, J., F. Guo, et al. (2013). Onboard Safety Systems Effectiveness Evaluation Final Report. Washington, DC, Federal Motor Carrier Safety Administration: 267.
- Houser, A., D. Murray, et al. (2007). Onboard Safety Technology Survey Synthesis Final Report. Washington, DC: 93.
- Houser, A., D. Murray, et al. (2009). Analysis of Benefits and Costs of Lane Departure Warning Systems for the Trucking Industry. Washington, DC: 75.
- Houser, A., J. Pierowicz, et al. (2005a). Concept of Operations and Voluntary Operational Requirements for Lane Departure Warning System (LDWS) On-board Commercial Motor Vehicles. Washington, DC, Federal Motor Carrier Safety Administration, : 22.
- Houser, A., J. Pierowicz, et al. (2005b). Concept of Operations and Voluntary Operational Requirements for Vehicular Stability Systems (VSS) On-board Commercial Motor Vehicles. Washington, DC, Federal Motor Carrier Safety Administration, : 23.

- Kuppa, S., J. Wang , et al. (2001). Lower Extremity Injuries and Associated Injury Criteria. Proceedings of the 17th International Technical Conference on the Enhanced Safety of Vehicles, National Highway Traffic Safety Administration, Washington, DC, Paper Number: 457.
- McMillan, N., R. Carnell, et al. (2007). Evaluation of the Volvo Intelligent Vehicle Initiative Field Operation Test, Version 1.3. Washington, DC.
- Mertz, H. (2002). Injury Risk Assessments Based on Dummy Responses.
- Murray, D., S. Shackelford, et al. (2009a). Analysis of Benefits and Costs of Forward Crash Warning Systems for the Trucking Industry. Washington, DC: 67.
- Murray, D., S. Shackelford, et al. (2009b). Analysis of Benefits and Costs of Roll Stability Control Systems for the Trucking Industry. Washington, DC: 69.
- National Crash Analysis Center. Finite element model archive, Driver side Airbag, <http://www.ncac.gwu.edu/vml/models.html> (March 2007) .
- NHTSA (2011a). National Automotive Sampling System (NASS) General Estimates System (GES) 2010 Coding and Editing Manual. Washington, DC.
- NHTSA (2011b). National Automotive Sampling System (NASS) General Estimates System (GES) Analytical Users Manual 1988-2010. Washington, DC.
- NHTSA (2014). Fatality Analysis Reporting System (FARS) Analytical Users Manual, 1975-2013. Washington, DC, USDOT NHTSA.
- Office of Regulatory Analysis and Evaluation (2012). FMVSS No. 136 Electronic Stability Control Systems on Heavy Vehicles Preliminary Regulatory Impact Analysis. N. C. f. S. a. Analysis. Washington DC, US DOT.
- Orban, J., J. Hadden, et al. (2006). Evaluation of the Mack Intelligent Vehicle Initiative Field Operational Test. Washington, DC, Federal Motor Carrier Safety Administration: 246.
- Truck & Engine Manufacturers Association (2012). Comment on Notice of Proposed Rulemaking: Electronic Stability Control Systems for Heavy Vehicles. Docket NHTSA-2012-0065.
- Woodrooffe, J. and D. Blower (2013). Heavy Truck Crashworthiness: Injury Mechanisms and Countermeasures to Improve Occupant Safety. Ann Arbor, MI, University of Michigan Transportation Research Institute: 112.
- Woodrooffe, J., D. Blower, et al. (2012). Performance Characterization and Safety Effectiveness of Collision Mitigation Braking and Forward Collision Warning Systems for Commercial Vehicles. Ann Arbor, Michigan, University of Michigan Transportation Research Institute: 138.
- Woodrooffe, J., D. Blower, et al. (2009). Safety Benefits of Stability Control Systems for Tractor-Semitrailers. Washington, DC.
- Yu, M. (2010). Finite Element Analysis of Passenger Multiple Belt Restraint Configurations.

Appendix A. FE frontal computer simulation results – 50 mph

In addition to the 35 mph frontal simulations, researchers conducted extra simulations at an impact speed of 50 mph. The same methodology used to develop simulations for the 35 mph was used for the 50 mph frontal simulations. The 50 mph impact speed is based on crash data analysis that resulted in 50 mph as the average impact condition. TTI researchers performed an array of crash tests to determine the crashworthiness of the heavy truck. The variations in crash tests were based on initial impact speed and seatbelt condition. As previously stated the impact speed was set to be 50 mph. The other category for differentiation among crash tests was the seat belt condition. The baseline simulation incorporated the basic seatbelt model with a pretensioner and no load limiter. The second type did not include the pretensioner. The following two types included a 4 and 8 kN load limiters, respectively. Lastly, in the final simulation, the location of the D-Ring was lowered compared to the baseline simulation. Table A-1 summarizes the different simulation types. Researchers were unable to investigate airbag effects in conjunction with the seatbelt restraint system due to numerical instability in the simulations with included airbag. Due to limited time and budget, the problem was not fixed and the simulations were focused on the seatbelt restraint system without the effect of an airbag system.

Table A-1 Summary of simulation types, impact information, and seatbelt.

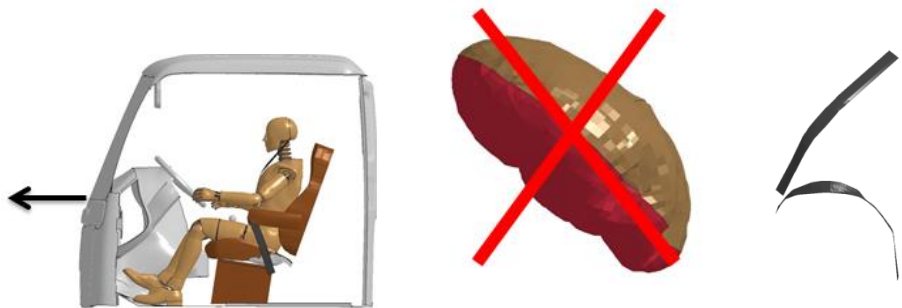
Impact Type : Frontal

Initial Impact Speed : 50 mph

Seatbelt Conditions:

- Baseline
- No Pretensioner
- 4 kN Load Limiter
- 8 kN Load Limiter
- Lowered D-Ring

Airbag : No

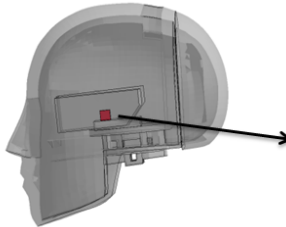


To assess the potential threat to occupants, the injury criteria of the HIII 50th percentile male dummy was analyzed and a parametric evaluation was performed. The injury criterion used for the evaluation included head and neck injury criteria, chest injury criteria, and leg injury criteria. Table A-2 through Table A-4 summarize the injury criteria parameters for the different body regions.

Table A-2 Injury criteria parameters for head and neck region.

c) Head Injury Criteria (HIC₁₅)

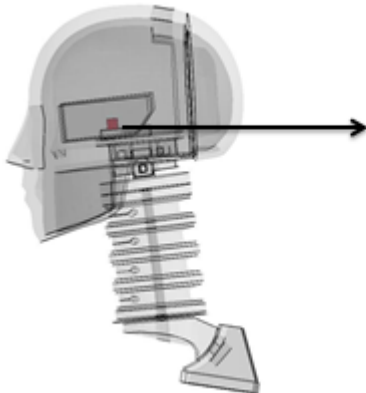
Head acceleration recorded during the impact event is employed to calculate the HIC₁₅ value, which represents the probability of skull fracture



$$HIC = \max \left[\frac{\int_{t_1}^{t_2} a(t) dt}{t_2 - t_1} \right]^{2.5} (t_2 - t_1)$$

d) Neck Injury Criteria

Dummy injury criteria for the neck are evaluated based on the Normalized Neck Injury Criteria- Nij which is defined as the sum of normalized values of loads and moments.



$$N_{ij} = \frac{F_z}{F_{intz}} + \frac{M_y}{M_{inty}}$$

Table A-3 Injury criteria parameters for chest region

c) Chest Injury Criteria

Chest deflection recorded during the impact event is employed to calculate the chest injury criteria value and probability of injury.

$$p(AIS3+) = \frac{1}{1 + e^{10.5456 - 1.568 * D^{0.4612}}}$$

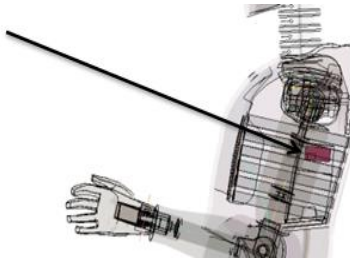
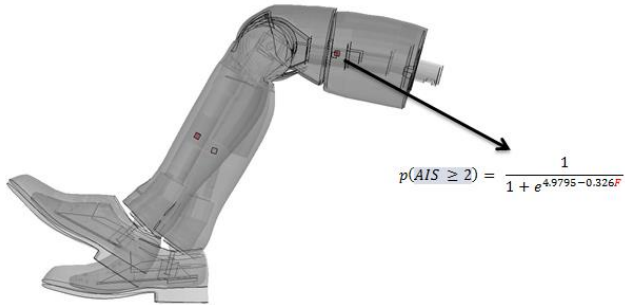


Table A-4 Injury criteria parameters for leg region.

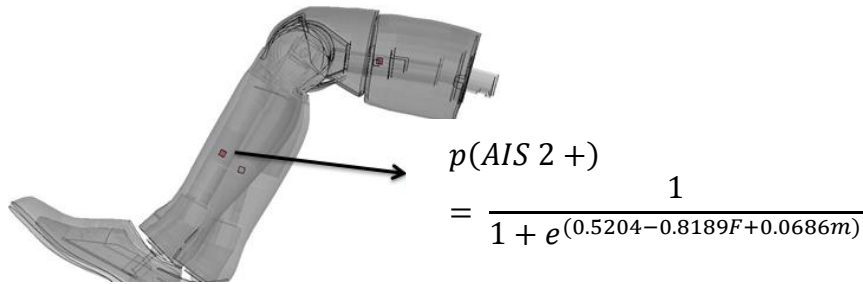
b) KTH Injury Criteria

Dummy injury criteria for the KTH are evaluated based on the formulation for probability of injury as a function of femur axial force.



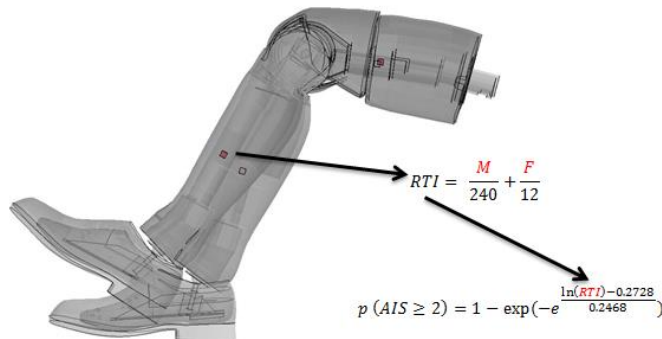
d) Tibia Plateau Fractures

Dummy injury criteria for tibia plateau fractures are evaluated based on upper tibia axial forces and dummy mass.



e) Leg Shaft Fracture

Dummy injury criteria for tibia plateau fractures are evaluated based on a normalized formulation that combines bending moments and axial compressive loads.



In 1978, Mertz developed the Injury assessment reference values (IARVs) to assess the efficacy of General Motors (GM) restraint system designs under a series of simulated frontal crash events using the Hybrid III midsize adult male dummy as the occupant. It was a comparative analysis which evaluated whether or not the values from the simulation exceeded the IARVs. The injury event was termed “unlikely” if the associated injury value did not exceed the IARVs. They were published as a part of the GM petition of the National Highway Safety Administration (NHTSA) to authorize the use of the Hybrid III midsize adult male dummy in Federal Motor Vehicle Safety Standard (FMVSS) 208 testing. Table A-5 contains IARVs for the different injury criteria parameters analyzed in the simulations. Typically, injury criteria values are represented as a percentage of IARV, and this approach was used for each simulation.

Table A-5 Summary of IARVs for injury criteria parameters.

Head and Neck	Parameter	IARV
	HIC-15	700
	Nij	1
	Neck axial tension(kN)	4.17
	Neck axial compression(kN)	4
Chest		
	Deflection (mm)	63
Leg and Foot		
	Left Femur axial force(kN)	-10
	Right Femur axial force(kN)	-10
	Left Tibia Index	1
	Right Tibia Index	1
	Left Tibia axial force(kN)	-8
	Right Tibia axial force (kN)	-8

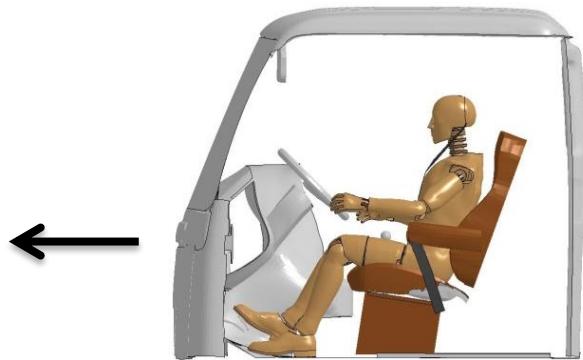
A1 Frontal simulations without airbag – 50 mph

A1.1 Frontal baseline simulation – 50 mph

A1.1.1 Simulation frames and summary

The following documents the post processed results of the finite element simulation of a frontal impact event with initial speed of 50 mph, inclusion of a belted HIII 50th percentile male dummy in the driver position, and no application of airbag. Table A-6 and Table A-7 summarize the resulting simulation with frames at different times throughout the simulation. The details of the simulation are summarized below and in Figure A-1:

- Impact Type : Frontal
- Initial Impact Speed : 50 mph
- Seatbelt Condition: Belted (Baseline)
- Airbag : No



(a) Lateral View of the FE Computer Model with Indication of Impact Orientation



(b) Seatbelt Model



(c) No Use of Airbag Model

Figure A-1 Modeled characteristics of the finite element simulation for the frontal impact (50 mph, baseline, no airbag).

Table A-6 Frontal impact simulation frames side view (50 mph, baseline, no airbag).







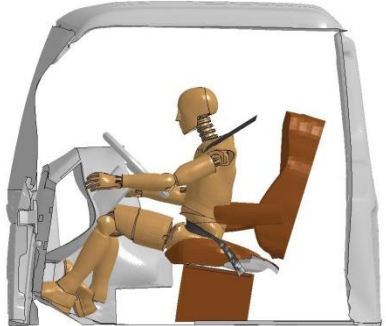

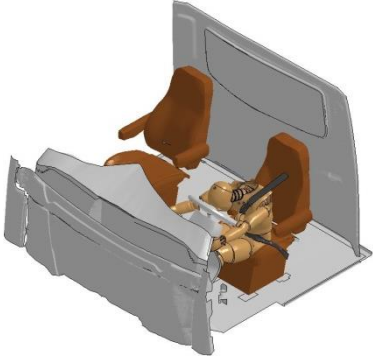
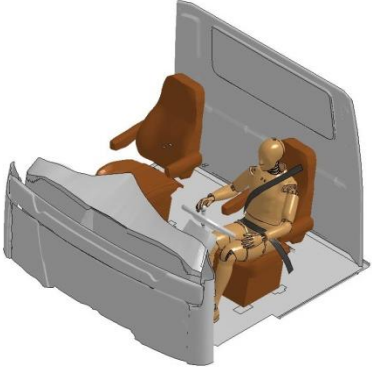

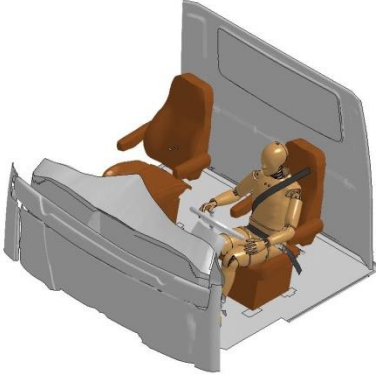
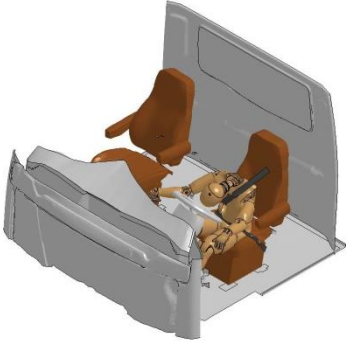
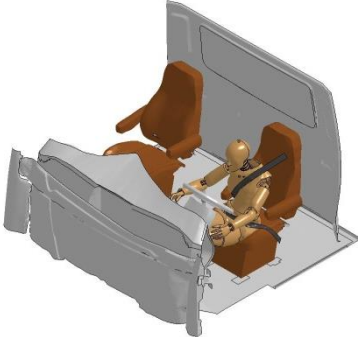
Time (Sec)	Sequential Frames	Time (Sec)	Sequential Frames
0.000		0.074	
0.015		0.089	
0.030		0.105	
0.055			

Table A-7 Frontal impact simulation frames perspective view (50 mph, baseline, no airbag).

Time (Sec)	Sequential Frames	Time (Sec)	Sequential Frames
0.000		0.074	
0.015		0.089	
0.030		0.105	
0.055			

The seatbelt retractor force for the resulting simulation is plotted in Figure A-2. The retractor contained no load limiter for this simulation and reached a peak of about 11.5 kN.

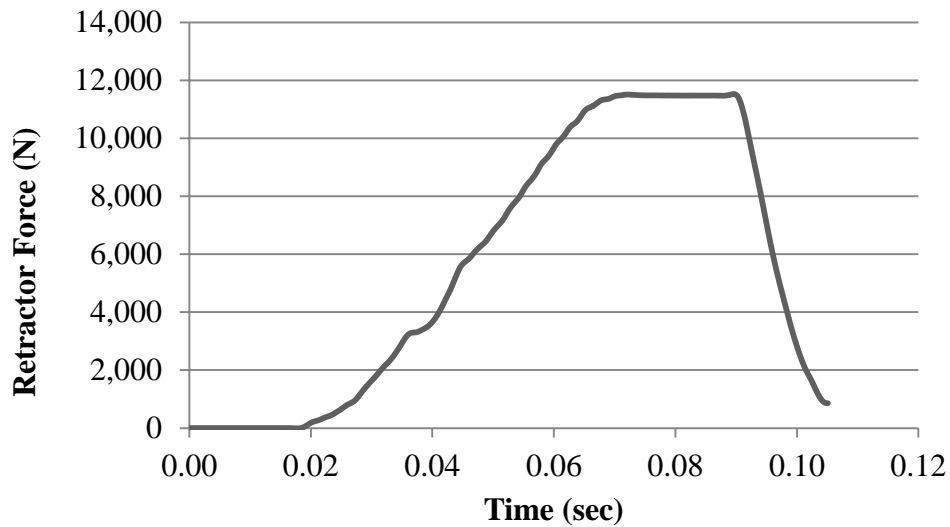


Figure A-2 Seatbelt retractor force time history (50 mph, baseline, no airbag).

A1.1.2 Head Injury Criteria

Dummy injury criteria for the head are evaluated with respect to the HIC₁₅ criteria. Head acceleration recorded during the impact event is employed to calculate the HIC₁₅ value. Figure A-3 illustrates details for the head injury criteria and the recorded curves from this specific impact condition and passive restraint systems employment.

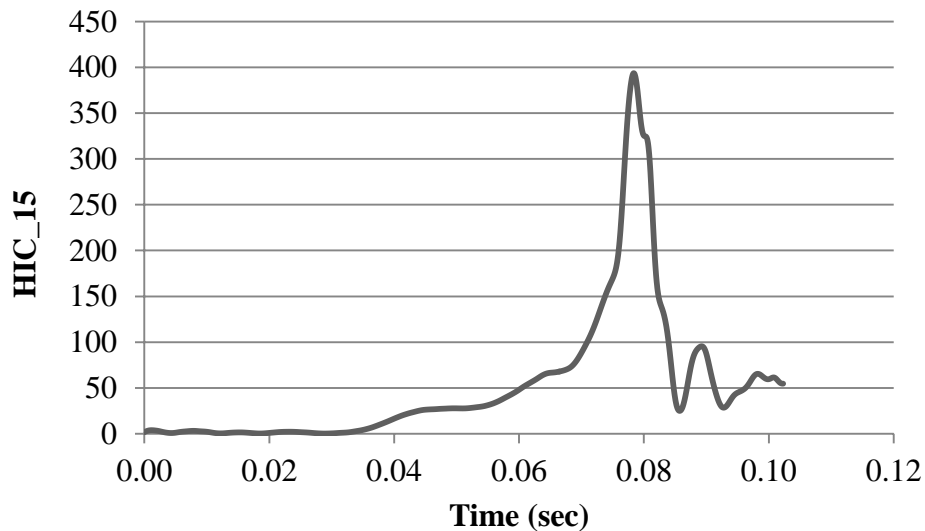
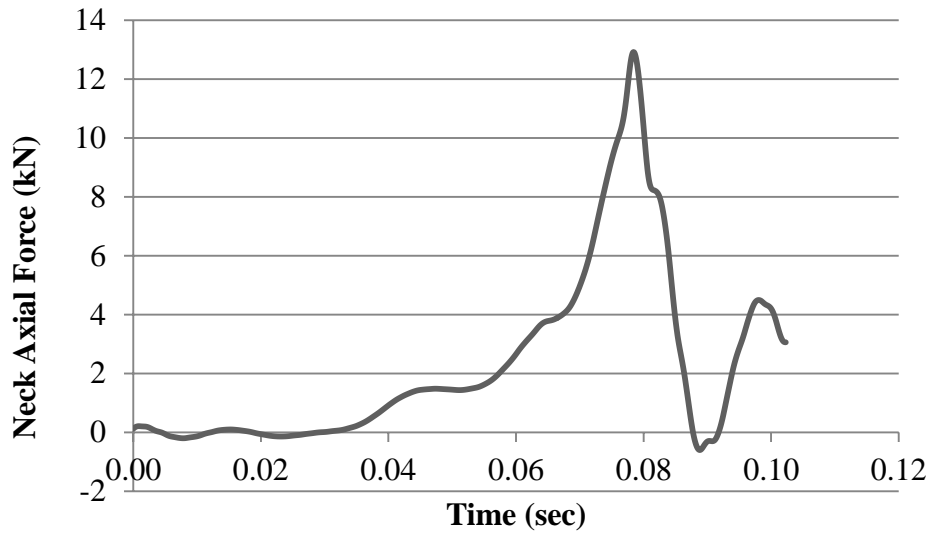


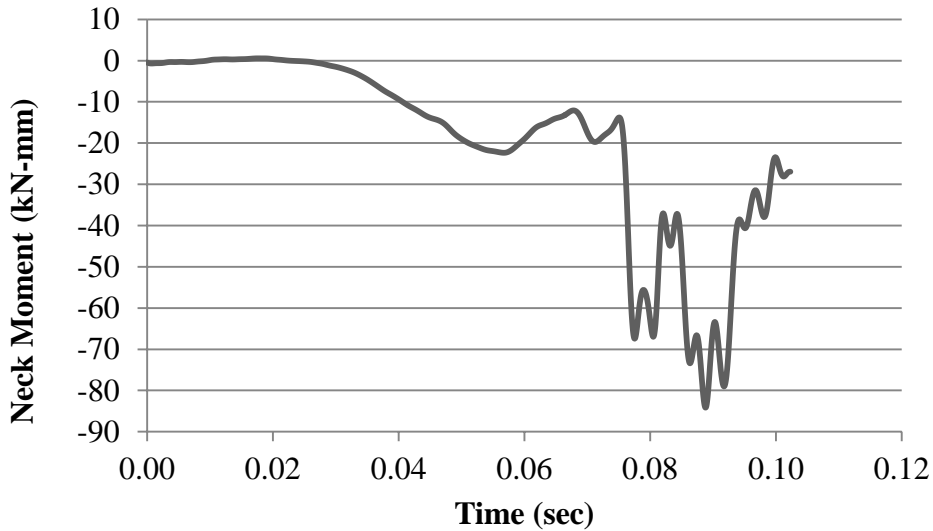
Figure A-3 HIC time history (50 mph, baseline, no airbag).

A1.1.3 Neck injury criteria

Dummy injury criteria for the neck are evaluated based on the normalized neck injury criteria, N_{ij} , which is defined as the sum of normalized values of loads and moments. Figure A-4 illustrates details for the neck injury criteria and the recorded curves from this specific impact condition and passive restraint systems employment.



(a) Neck Axial Force Time History



(b) Neck Bending Moment Time History

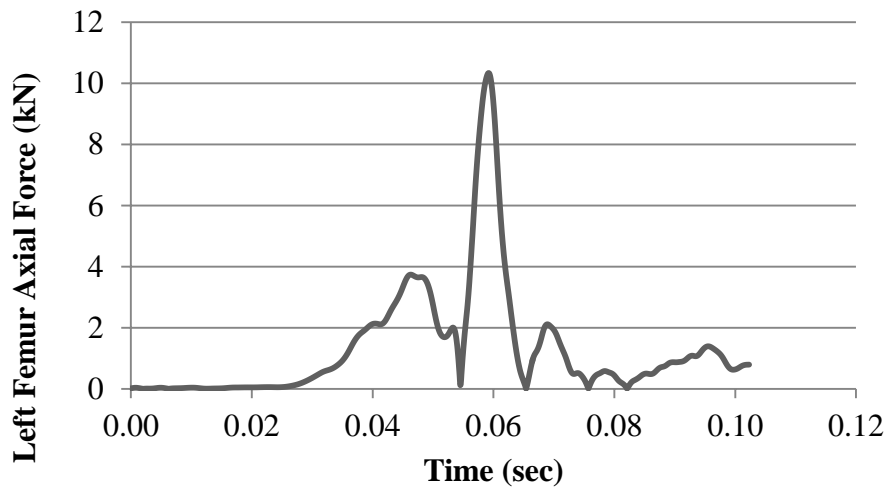
Figure A-4 Neck injury time history (50 mph, baseline, no airbag).

A1.1.4 Chest injury criteria

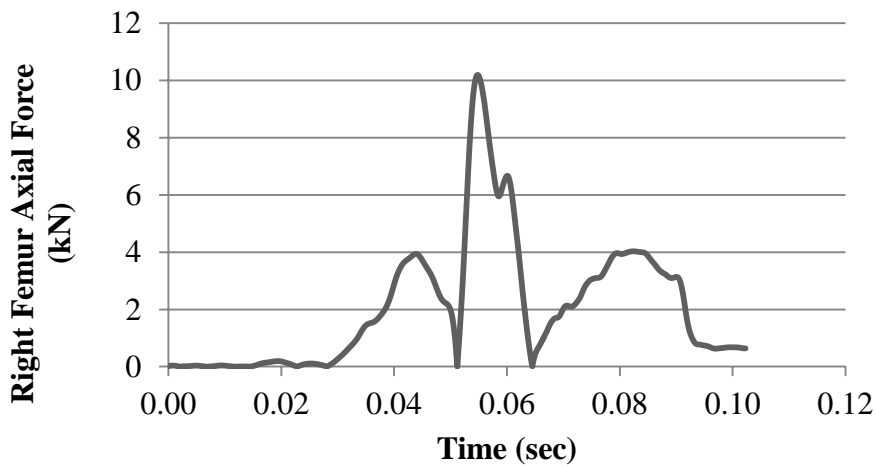
Dummy injury criteria for the chest are evaluated based on the chest deflection values. Researchers were unable to post-process chest deflection values and therefore did not evaluate chest injury criteria for this simulation case.

A1.1.5 KTH injury criteria

Dummy injury criteria for the KTH are evaluated based on the formulation for probability of injury as a function of femur axial force. Figure A-5 illustrates details for the KTH injury criteria and the recorded curves from this specific impact condition and passive restraint systems employment.



(a) Left Femur Axial Force Time History

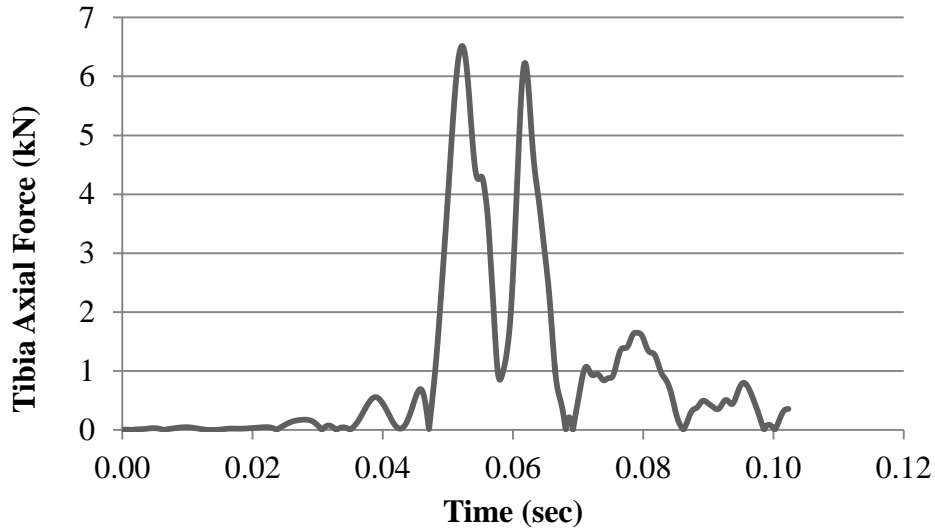


(b) Right Femur Axial Force Time History

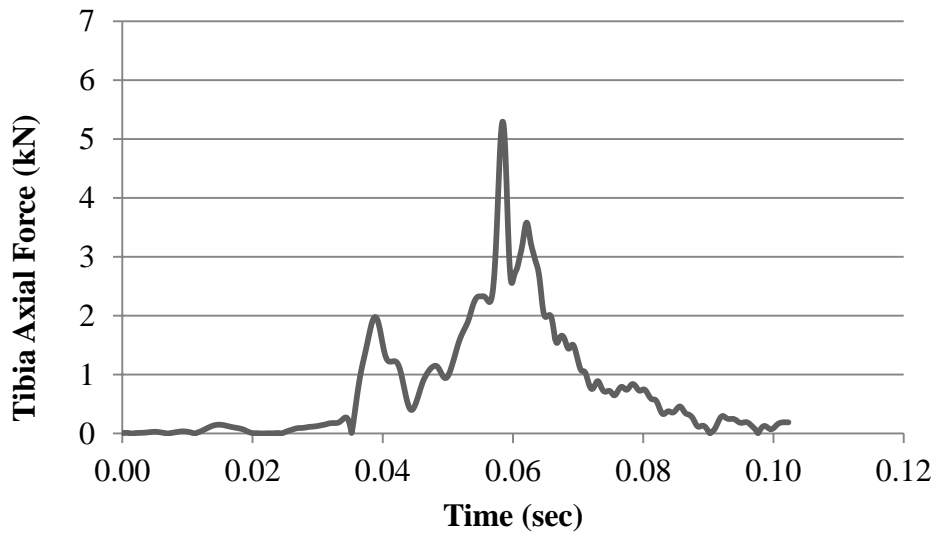
Figure A-5 KTH injury time history (50 mph, baseline, no airbag).

A1.1.6 Tibia plateau fracture injury criteria

Dummy injury criteria for tibia plateau fractures are evaluated based on axial compressive loads. Figure A-6 illustrates details for the tibia plateau injury criteria and the recorded curves from this specific impact condition and passive restraint systems employment.



(a) Left Tibia Axial Force Time History

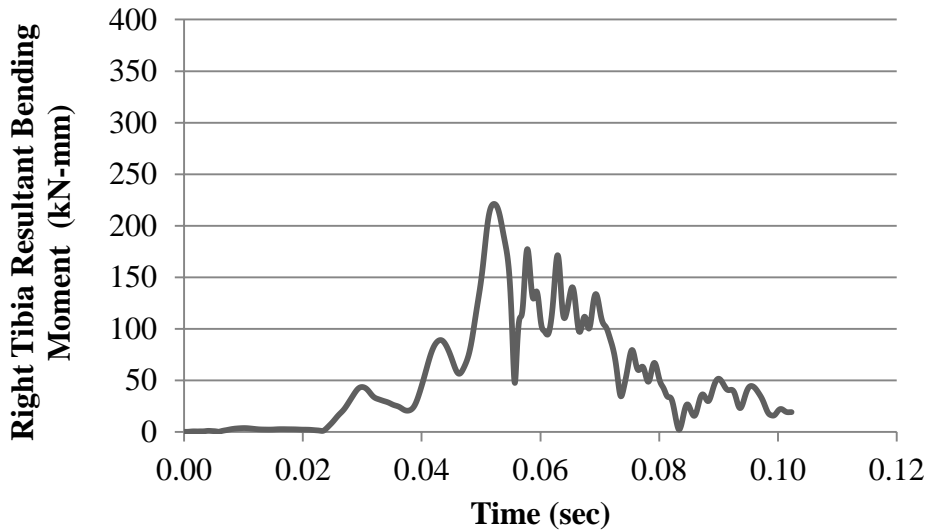


(b) Right Tibia Axial Force Time History

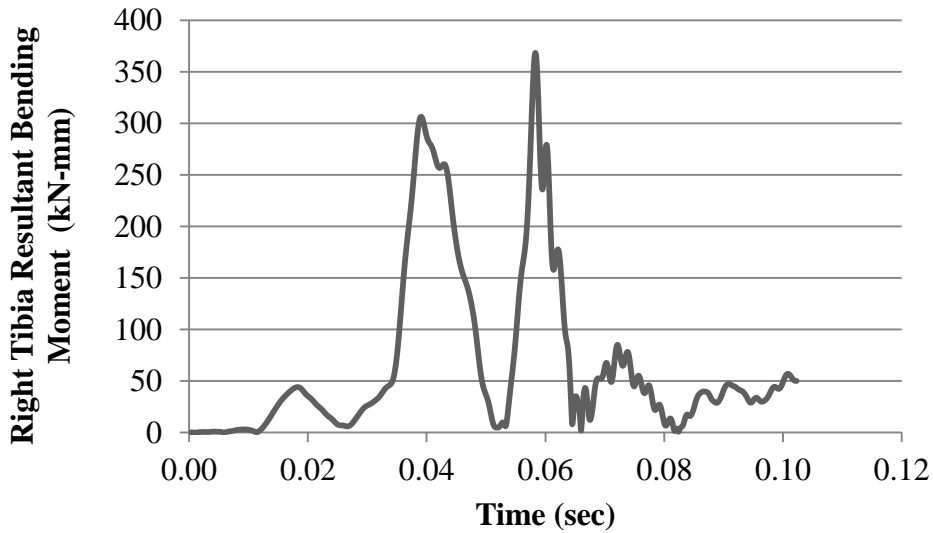
Figure A-6 Tibia plateau fracture time history (50 mph, baseline, no airbag).

A1.1.7 Tibia shaft fracture injury criteria

Dummy injury criteria for tibia shaft fractures are evaluated based on a normalized formulation that combines bending moments and axial compressive loads. Figure A-7 illustrates details for the tibia shaft injury criteria and the recorded curves from this specific impact condition and passive restraint systems employment.



(a) Left Tibia Resultant Bending Moment Time History



(b) Right Tibia Resultant Bending Moment Time History

Figure A-7 Tibia shaft fracture time history (50 mph, baseline, no airbag).

A1.1.8 Conclusions

The injury criteria values for various parts of the body were compared to the IARV requirements. The simulation injury criteria results as a percentage of the IARV values are shown in Figure A-8.

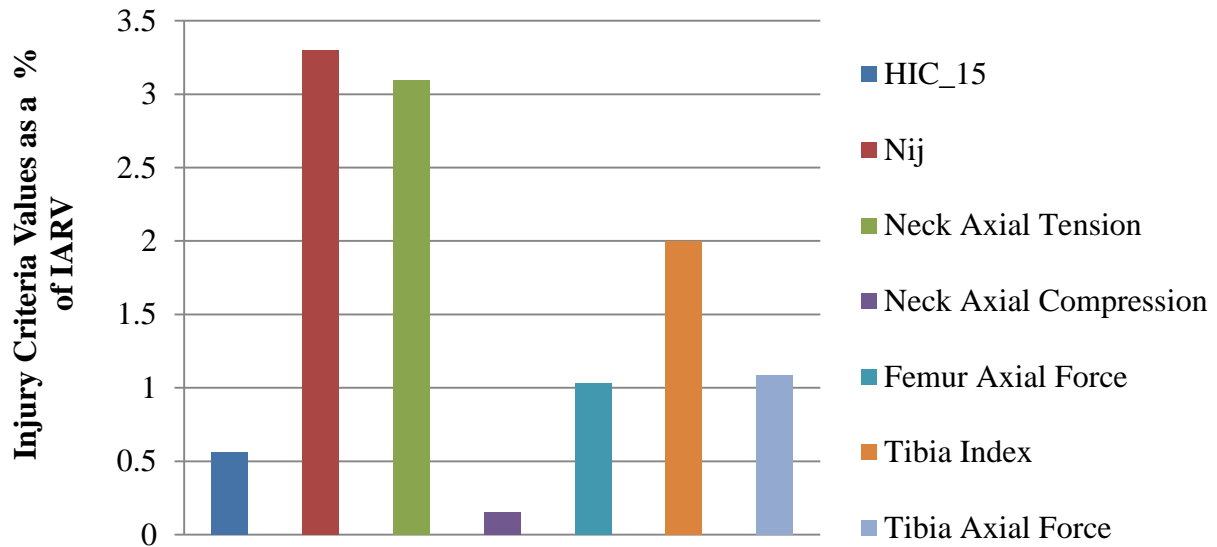


Figure A-8 Injury probability as a function of IARV (50 mph, baseline, no airbag).

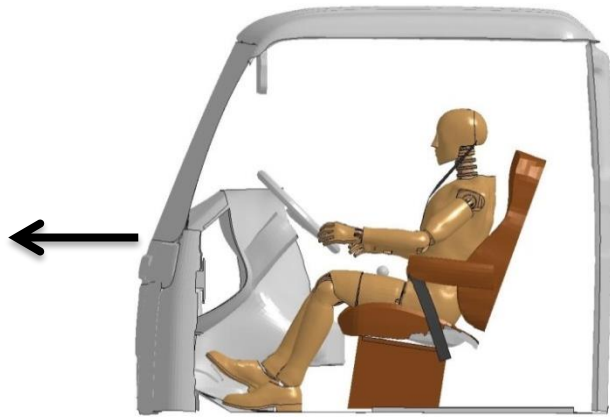
For the frontal baseline simulation without airbag, the probability of injury for the head region is unlikely because the injury criteria values stay below the threshold IARV. The injury criteria values for the neck, and KTH regions exceeded the threshold IARV which is unacceptable according to current standards.

A1.2 Frontal no pretensioner simulation – 50 mph

A1.2.1 Simulation frames and summary

The following documents the post processed results of the finite element simulation of a frontal impact event with initial speed of 50 mph, inclusion of a belted HIII 50th percentile male dummy in the driver position, and no application of airbag. Table A-8 and Table A-9 summarize the resulting simulation with frames at different times throughout the simulation. The details of the simulation are summarized below and in Figure A-9:

- Impact Type : Frontal
- Initial Impact Speed : 50 mph
- Seatbelt Condition: Belted (No Pretensioner)
- Airbag : No



(a) Lateral View of the FE Computer Model with Indication of Impact Orientation



(b) Seatbelt Model



(c) No Use of Airbag Model

Figure A-9 Modeled characteristics of the finite element simulation for the frontal impact (50 mph, no pretensioner, no airbag).

Table A-8 Frontal impact simulation frames side view (50 mph, no pretensioner, no airbag).







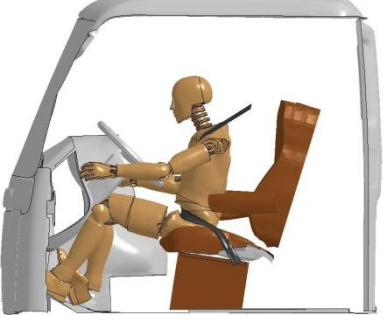






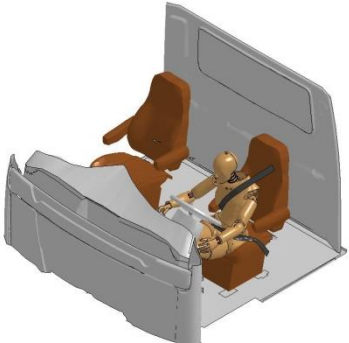
Time (Sec)	Sequential Frames	Time (Sec)	Sequential Frames
0.000		0.074	
0.015		0.089	
0.030		0.105	
0.055			

Table A-9 Frontal impact simulation frames perspective view (50 mph, no pretensioner, no airbag).

Time (Sec)	Sequential Frames	Time (Sec)	Sequential Frames
0.000		0.074	
0.015		0.089	
0.030		0.105	
0.055			

The seatbelt retractor force for the resulting simulation is plotted in Figure A-10. The retractor contained no load limiter for this simulation and reached a peak of about 11.5 kN.

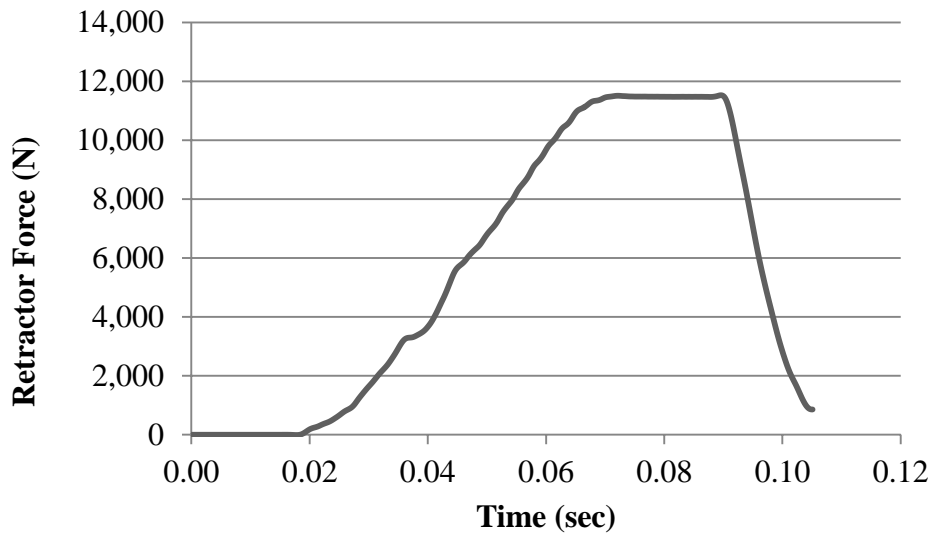


Figure A-10 Seatbelt retractor force time history (50 mph, no pretensioner, no airbag).

A1.2.2 Head injury criteria

Dummy injury criteria for the head are evaluated with respect to the HIC₁₅ criteria. Head acceleration recorded during the impact event is employed to calculate the HIC₁₅ value. Figure A-11 illustrates details for the head injury criteria and the recorded curves from this specific impact condition and passive restraint systems employment.

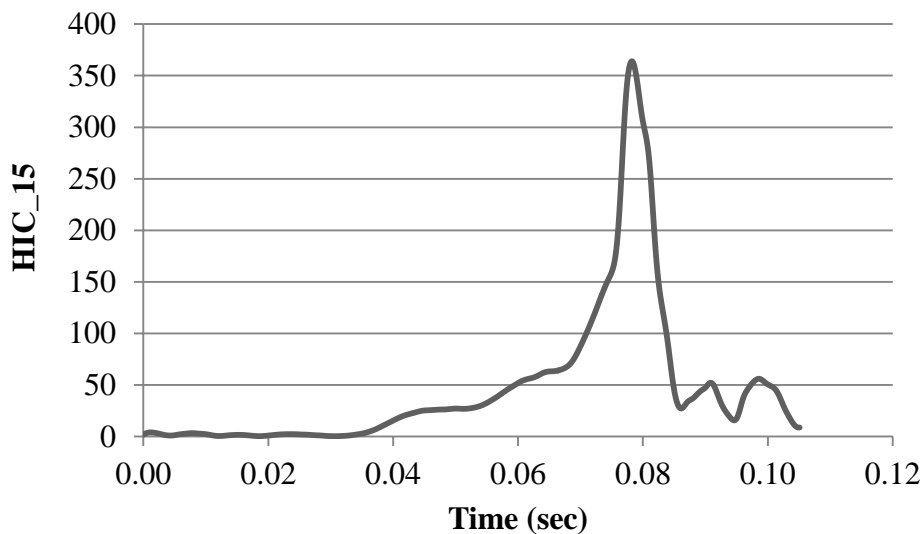
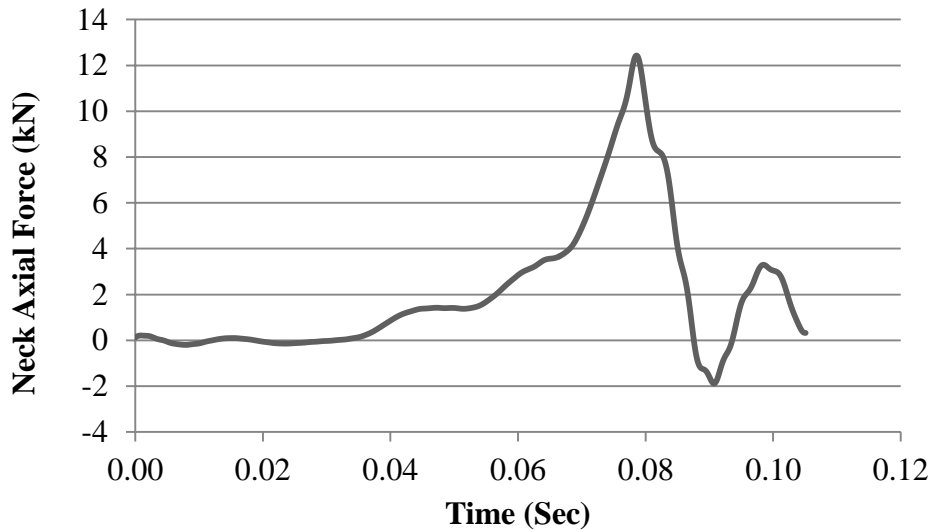


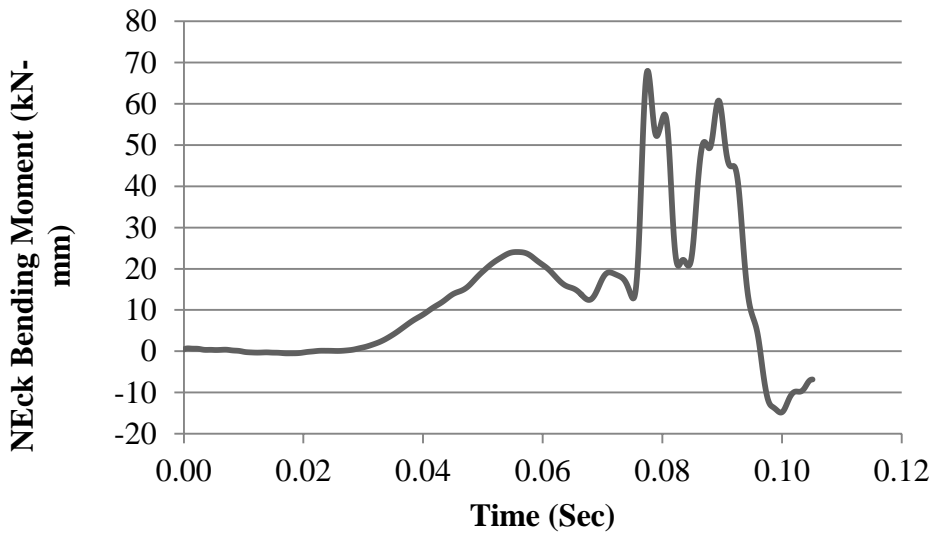
Figure A-11 HIC time history (50 mph, no pretensioner, no airbag).

A1.2.3 Neck injury criteria

Dummy injury criteria for the neck are evaluated based on the normalized neck injury criteria, N_{ij} , which is defined as the sum of normalized values of loads and moments. Figure A-12 illustrates details for the neck injury criteria and the recorded curves from this specific impact condition and passive restraint systems employment.



(a) Neck Axial Force Time History



(b) Neck Bending Moment Time History

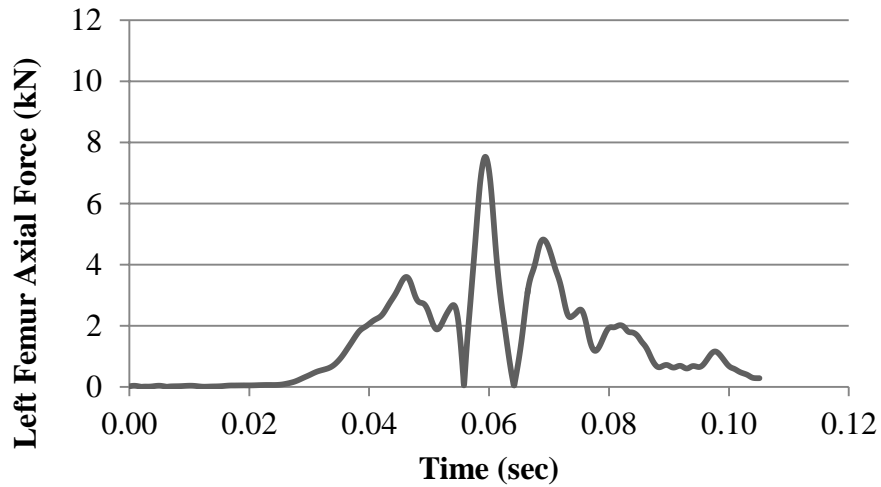
Figure A-12 Neck injury time history (50 mph, no pretensioner, no airbag).

A1.2.4 Chest injury criteria

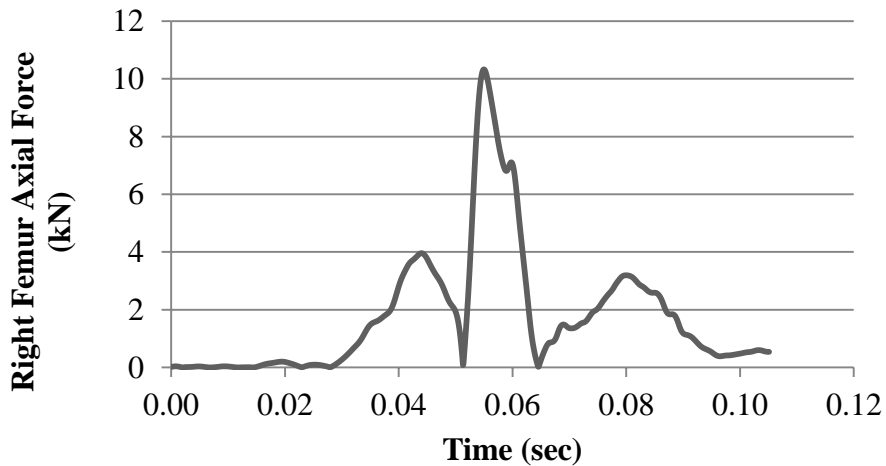
Dummy injury criteria for the chest are evaluated based on the chest deflection values. Researchers were unable to post-process chest deflection values and therefore did not evaluate chest injury criteria for this simulation case.

A1.2.5 KTH injury criteria

Dummy injury criteria for the KTH are evaluated based on the formulation for probability of injury as a function of femur axial force. Figure A-13 illustrates details for the KTH injury criteria and the recorded curves from this specific impact condition and passive restraint systems employment.



(a) Left Femur Axial Force Time History

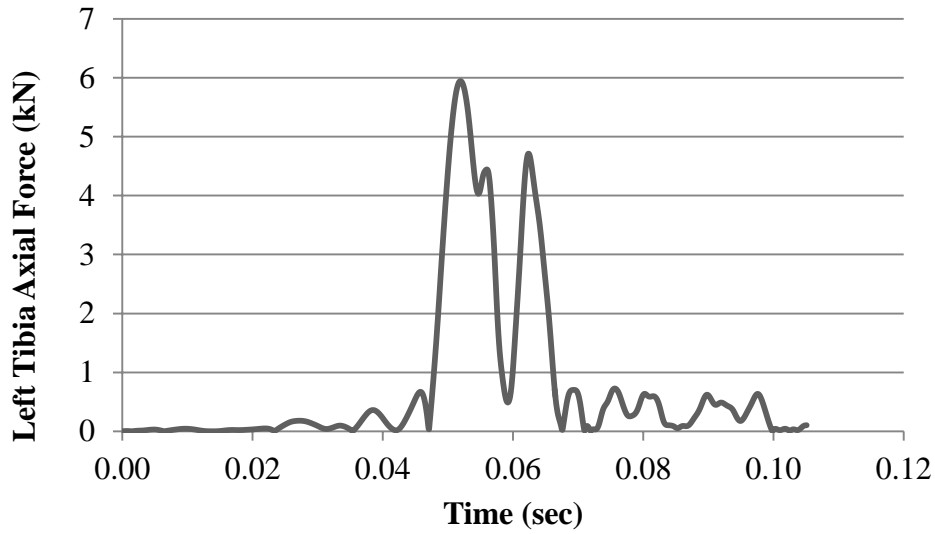


(b) Right Femur Axial Force Time History

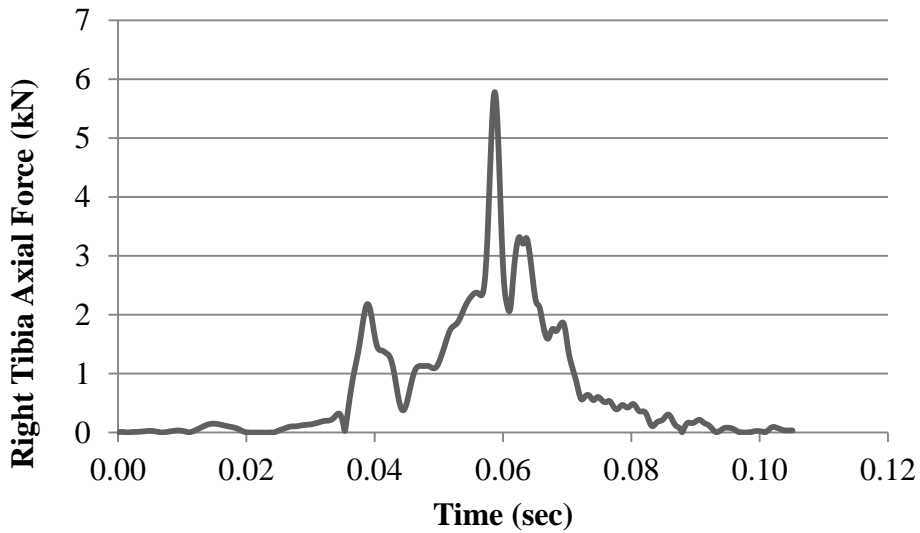
Figure A-13 KTH injury time history (50 mph, no pretensioner, no airbag).

A1.2.6 Tibia plateau fracture injury criteria

Dummy injury criteria for tibia plateau fractures are evaluated based on axial compressive loads. Figure A-14 illustrates details for the tibia plateau injury criteria and the recorded curves from this specific impact condition and passive restraint systems employment.



(a) Left Tibia Axial Force Time History

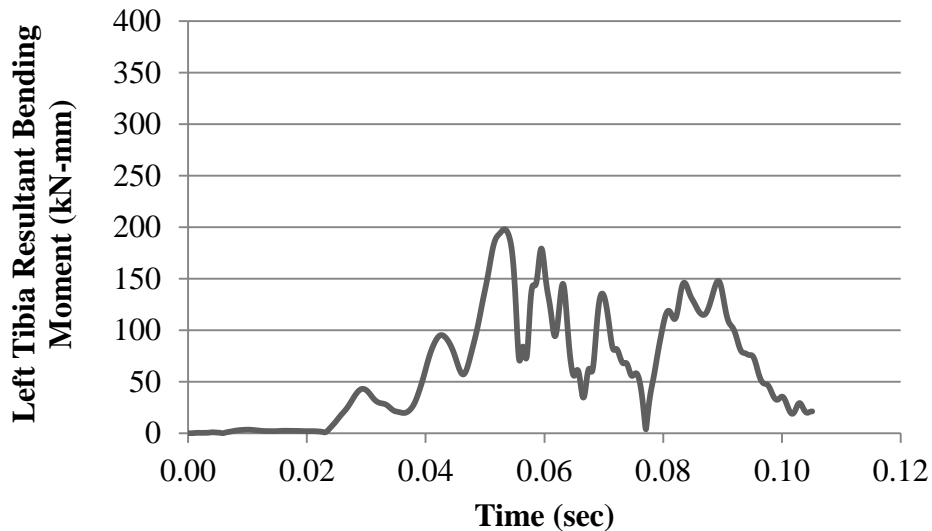


(b) Right Tibia Axial Force Time History

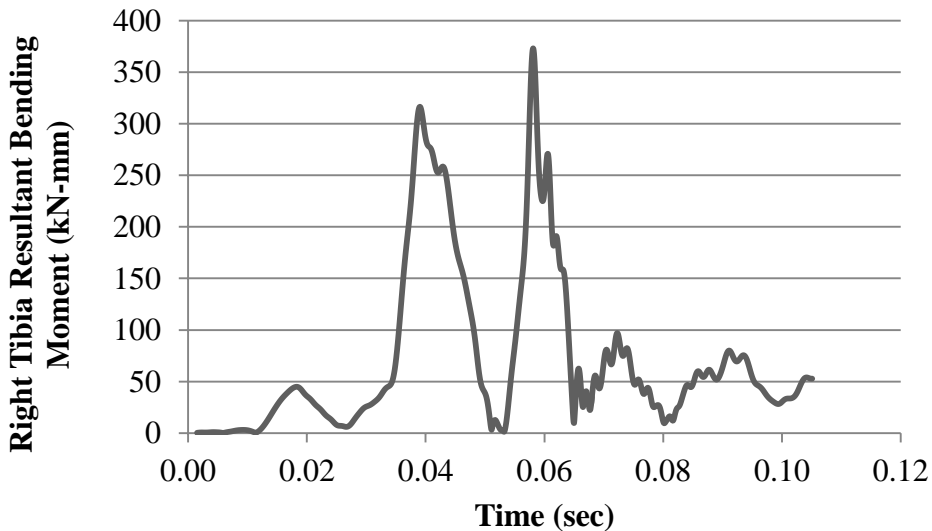
Figure A-14 Tibia plateau fracture time history (50 mph, no pretensioner, no airbag).

A1.2.7 *Tibia shaft fracture injury criteria*

Dummy injury criteria for tibia shaft fractures are evaluated based on a normalized formulation that combines bending moments and axial compressive. Figure A-15 illustrates details for the tibia shaft injury criteria and the recorded curves from this specific impact condition and passive restraint systems employment.



(a) **Left Tibia Resultant Bending Moment Time History**



(b) **Right Tibia Resultant Bending Moment Time History**

Figure A-15 Tibia shaft fracture time history (50 mph, no pretensioner, no airbag).

A1.2.8 Conclusions

The injury criteria values for various parts of the body were compared to the IARV requirements. The simulation injury criteria results as a percentage of the IARV values are shown in Figure A-16.

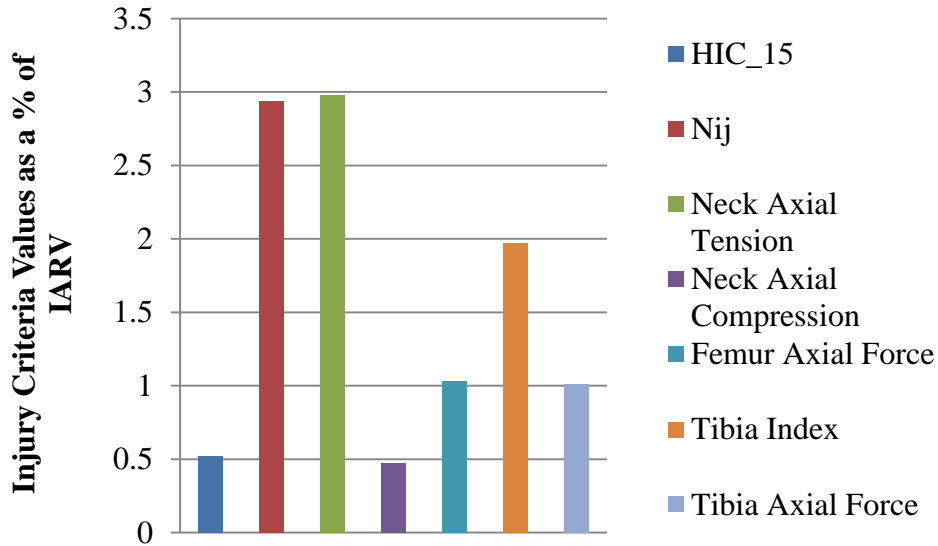


Figure A-16 Injury probability as a function of IARV (50 mph, no pretensioner, no airbag).

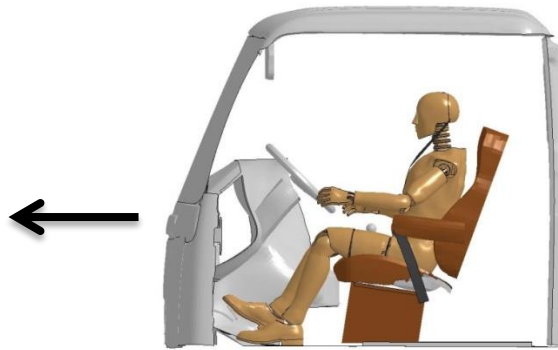
For the frontal no pretensioner baseline simulation without airbag, the probability of injury for the head region is unlikely because the injury criteria values stay below the threshold IARV. The injury criteria values for the neck, and KTH regions exceeded the threshold IARV which is unacceptable according to current standards.

A1.3 Frontal 4 kN load limiter simulation – 50 mph

A1.3.1 Simulation frames and summary

The following documents the post processed results of the finite element simulation of a frontal impact event with initial speed of 50 mph, inclusion of a belted HIII 50th percentile male dummy in the driver position, and no application of airbag. Table A-10 and Table A-11 summarize the resulting simulation with frames at different times throughout the simulation. The details of the simulation are summarized below and in Figure A-17:

- Impact Type : Frontal
- Initial Impact Speed : 50 mph
- Seatbelt Condition: Belted (4 kN Load Limiter)
- Airbag : No



(a) Lateral View of the FE Computer Model with Indication of Impact Orientation



(b) Seatbelt Model



(c) No Use of Airbag Model

Figure A-17 Modeled characteristics of the finite element simulation for the frontal impact (50 mph, 4 kN load limiter, no airbag).

Table A-10 Frontal impact simulation frames side view (50 mph, 4 kN load limiter, no airbag).




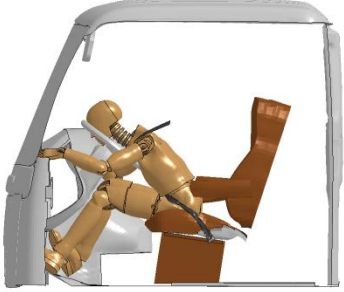
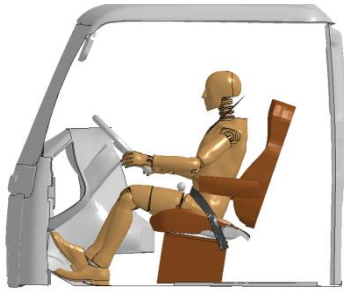
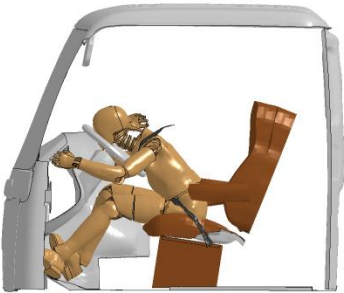


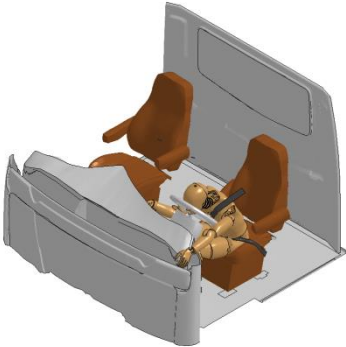
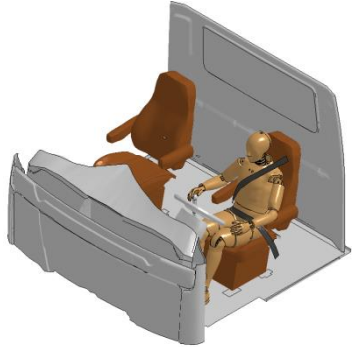
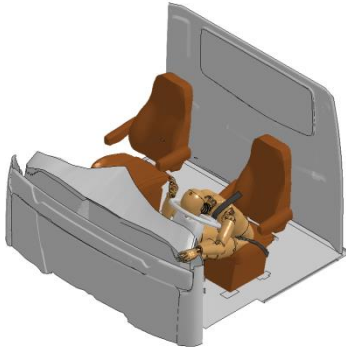

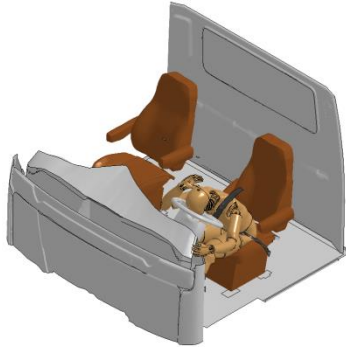
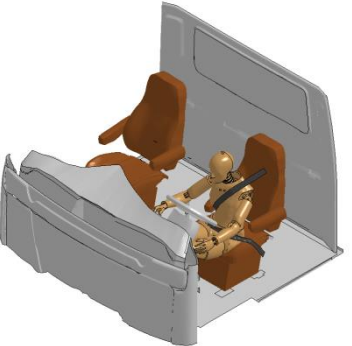
Time (Sec)	Sequential Frames	Time (Sec)	Sequential Frames
0.000		0.074	
0.015		0.089	
0.030		0.105	
0.055			

Table A-11 Frontal impact simulation frames perspective view (50 mph, 4 kN load limiter, no airbag).

Time (Sec)	Sequential Frames	Time (Sec)	Sequential Frames
0.000		0.074	
0.015		0.089	
0.030		0.105	
0.055			

The seatbelt retractor force for the resulting simulation is plotted in Figure A-18. The retractor contained a 4 kN load limiter.

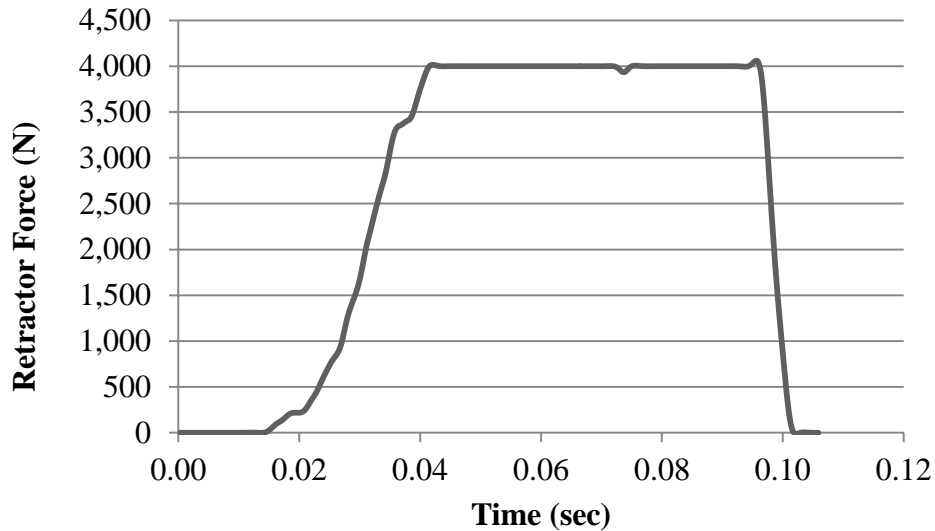


Figure A-18 Seatbelt retractor force time history (50 mph, 4 kN load limiter, no airbag).

A1.3.2 Head Injury Criteria

Dummy injury criteria for the head are evaluated with respect to the HIC₁₅ criteria. Head acceleration recorded during the impact event is employed to calculate the HIC₁₅ value. Figure A-19 illustrates details for the head injury criteria and the recorded curves from this specific impact condition and passive restraint systems employment.

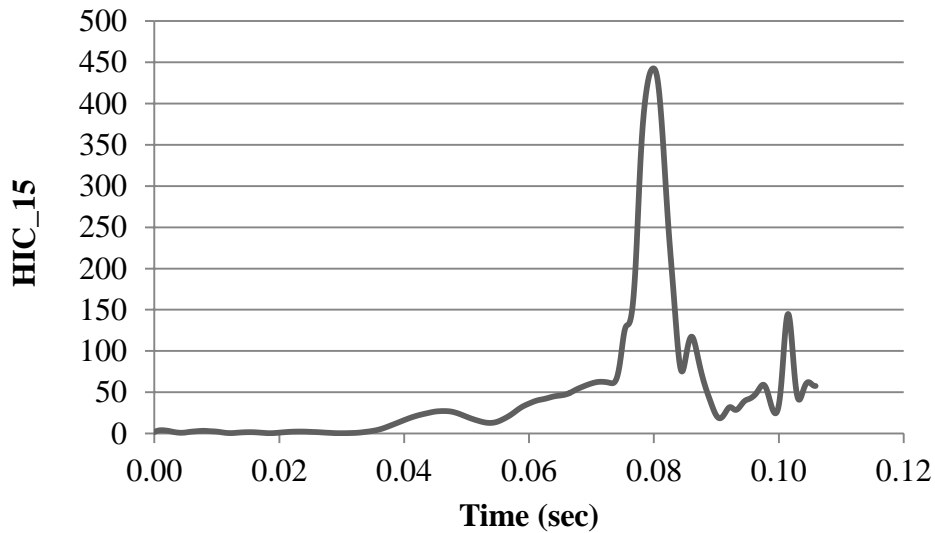
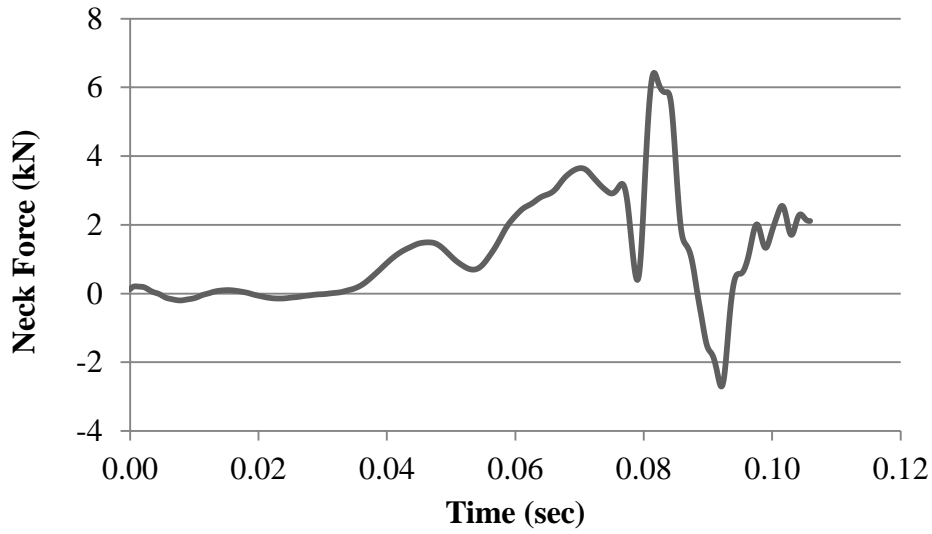


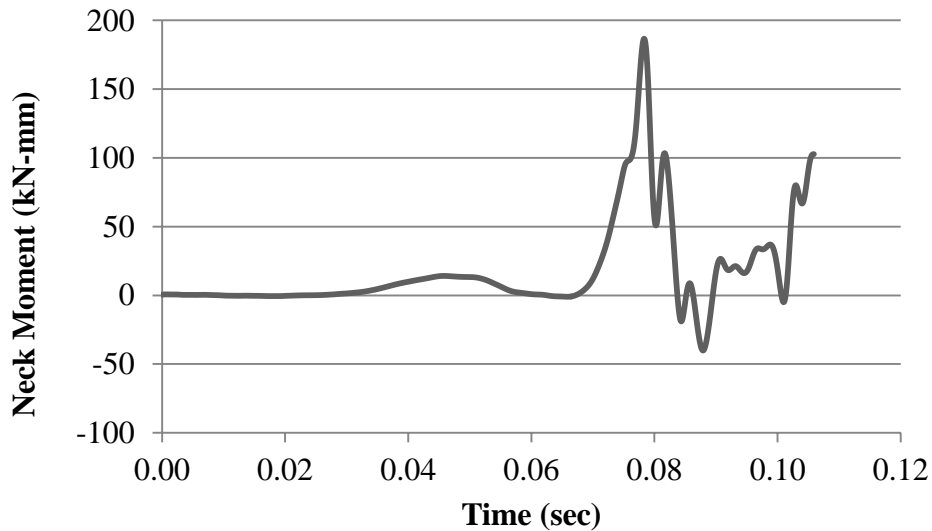
Figure A-19 HIC time history (50 mph, 4 kN load limiter, no airbag).

A1.3.3 Neck injury criteria

Dummy injury criteria for the neck are evaluated based on the normalized neck injury criteria, Nij, which is defined as the sum of normalized values of loads and moments. Figure A-20 illustrates details for the neck injury criteria and the recorded curves from this specific impact condition and passive restraint systems employment.



(a) Neck Axial Force Time History



(b) Neck Bending Moment Time History

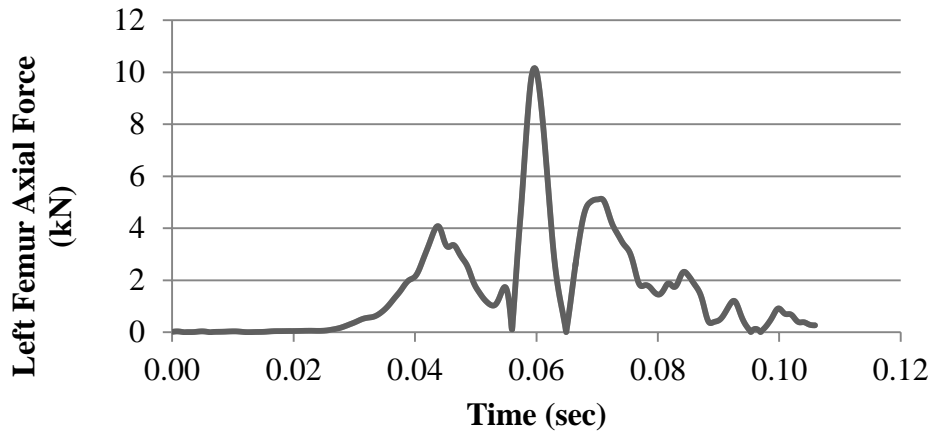
Figure A-20 Neck injury time history (50 mph, 4 kN load limiter, no airbag).

A1.3.4 Chest injury criteria

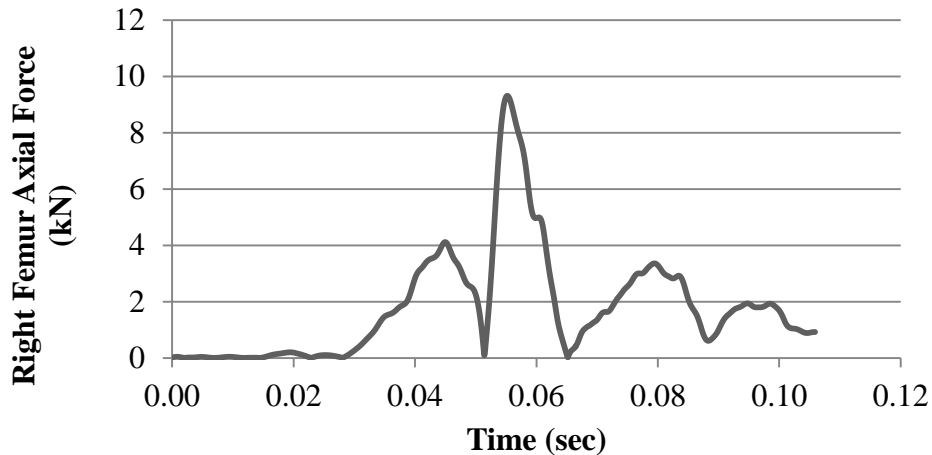
Dummy injury criteria for the chest are evaluated based on the chest deflection values. Researchers were unable to post-process chest deflection values and therefore did not evaluate chest injury criteria for this simulation case.

A1.3.5 KTH injury criteria

Dummy injury criteria for the KTH are evaluated based on the formulation for probability of injury as a function of femur axial force. Figure A-21 illustrates details for the KTH injury criteria and the recorded curves from this specific impact condition and passive restraint systems employment.



(a) Left Femur Axial Force Time History

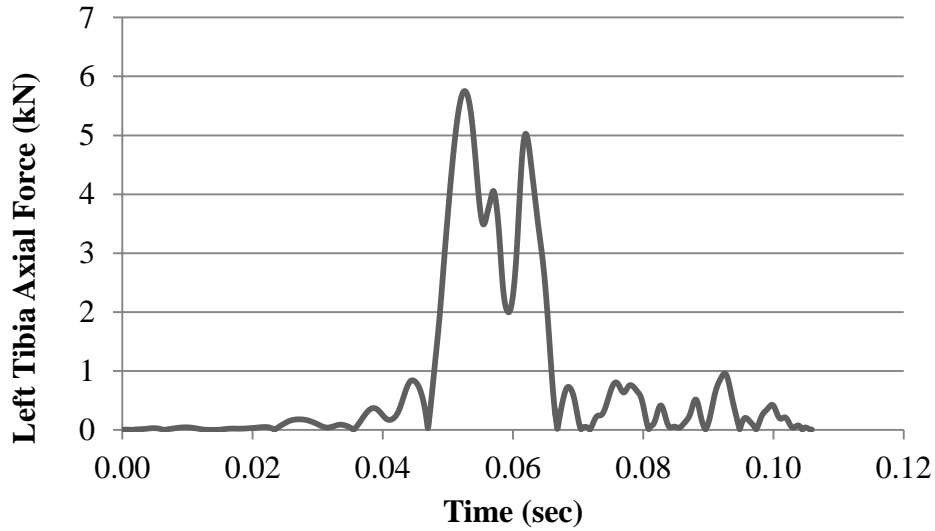


(b) Right Femur Axial Force Time History

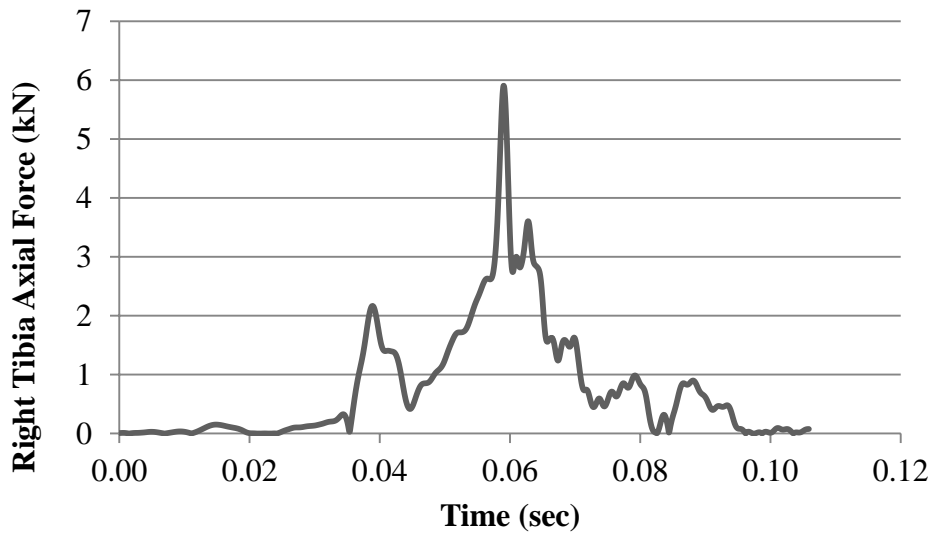
Figure A-21 KTH injury time history (50 mph, 4 kN load limiter, no airbag).

A1.3.6 *Tibia plateau fracture injury criteria*

Dummy injury criteria for tibia plateau fractures are evaluated based on axial compressive loads. Figure A-22 illustrates details for the tibia plateau injury criteria and the recorded curves from this specific impact condition and passive restraint systems employment.



(a) Left Tibia Axial Force Time History

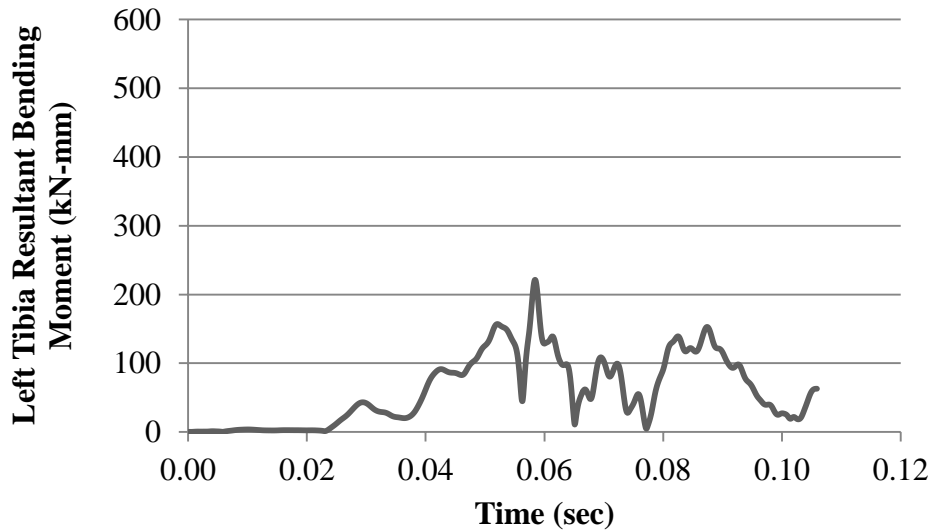


(b) Right Tibia Axial Force Time History

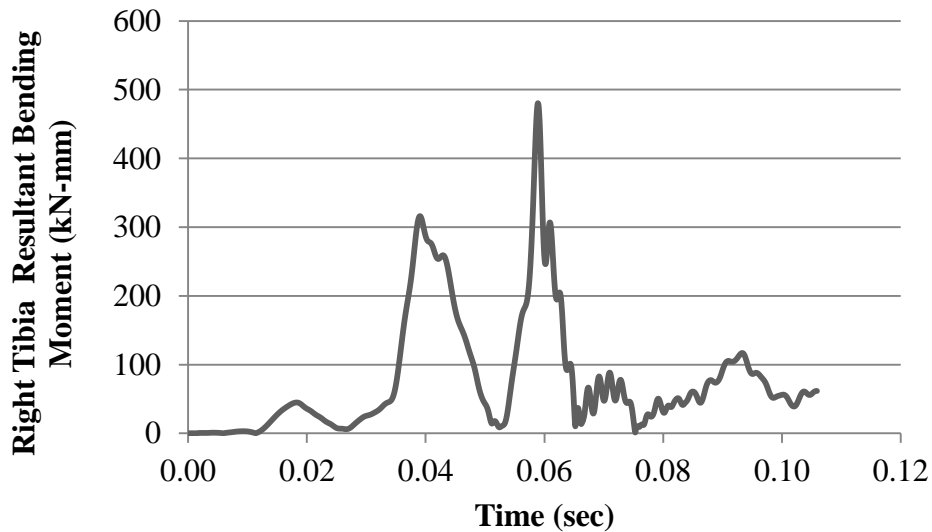
Figure A-22 Tibia plateau fracture time history (50 mph, 4 kN load limiter, no airbag).

A1.3.7 Tibia shaft fracture injury criteria

Dummy injury criteria for tibia shaft fractures are evaluated based on a normalized formulation that combines bending moments and axial compressive loads. Figure A-23 illustrates details for the tibia shaft injury criteria and the recorded curves from this specific impact condition and passive restraint systems employment.



(a) Left Tibia Resultant Bending Moment Time History



(b) Right Tibia Resultant Bending Moment Time History

Figure A-23 Tibia shaft fracture time history (50 mph, 4 kN load limiter, no airbag).

A1.3.8 Conclusions

The injury criteria values for various parts of the body were compared to the IARV requirements. The simulation injury criteria results as a percentage of the IARV values are shown in Figure A-24.

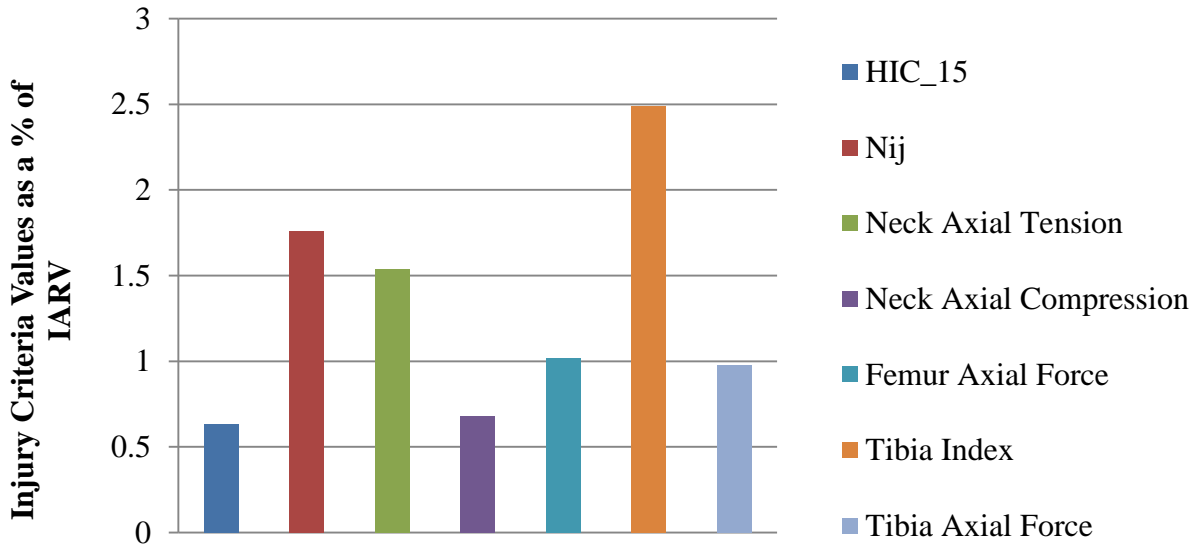


Figure A-24 Injury probability as a function of IARV (50 mph, 4 kN load limiter, no airbag).

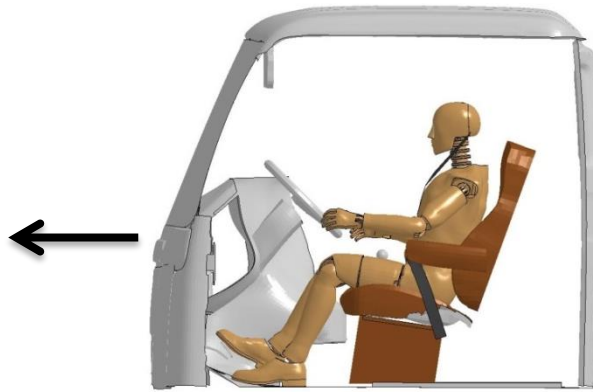
For the frontal 4 kN load limiter simulation without airbag, the probability of injury for the head region is unlikely because the injury criteria values stay below the threshold IARV. The injury criteria values for the neck, and KTH regions exceeded the threshold IARV which is unacceptable according to current standards.

A1.4 Frontal 8 kN load limiter simulation – 50 mph

A1.4.1 Simulation frames and summary

The following documents the post processed results of the finite element simulation of a frontal impact event with initial speed of 50 mph, inclusion of a belted HIII 50th percentile male dummy in the driver position, and no application of airbag. Table A-12 and Table A-13 summarize the resulting simulation with frames at different times throughout the simulation. The details of the simulation are summarized below and in Figure A-25:

- Impact Type : Frontal
- Initial Impact Speed : 50 mph
- Seatbelt Condition: Belted (8 kN Load Limiter)
- Airbag : No



(a) Lateral View of the FE Computer Model with Indication of Impact Orientation



(b) Seatbelt Model



(c) No Use of Airbag Model

Figure A-25 Modeled characteristics of the finite element simulation for the frontal impact (50 mph, 8 kN load limiter, no airbag).

Table A-12 Frontal impact simulation frames side view (50 mph, 8 kN load limiter, no airbag).




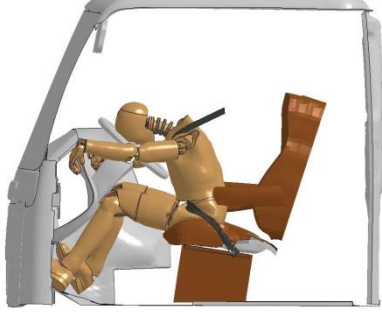




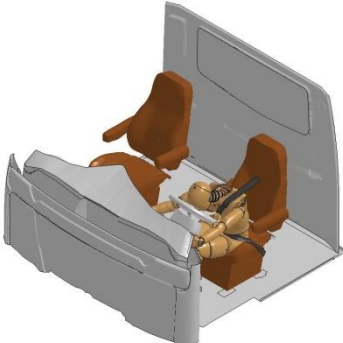


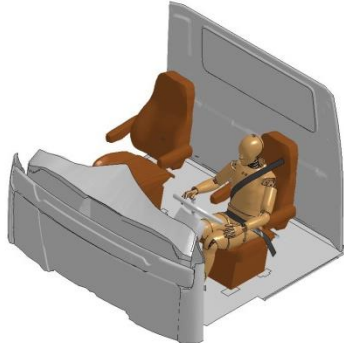
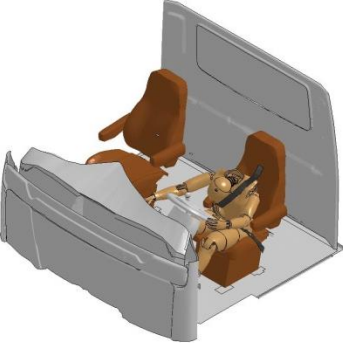
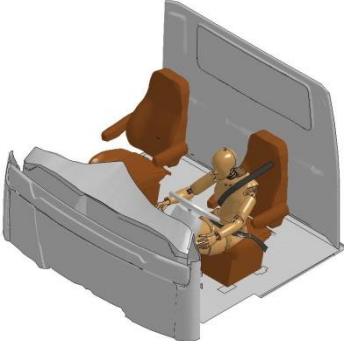
Time (Sec)	Sequential Frames	Time (Sec)	Sequential Frames
0.000		0.074	
0.015		0.089	
0.030		0.130	
0.055			

Table A-13 Frontal impact simulation frames perspective view (50 mph, 8 kN load limiter, no airbag).

Time (Sec)	Sequential Frames	Time (Sec)	Sequential Frames
0.000		0.074	
0.015		0.089	
0.030		0.130	
0.055			

The seatbelt retractor force for the resulting simulation is plotted in Figure A-26. The retractor contained an 8 kN load limiter.

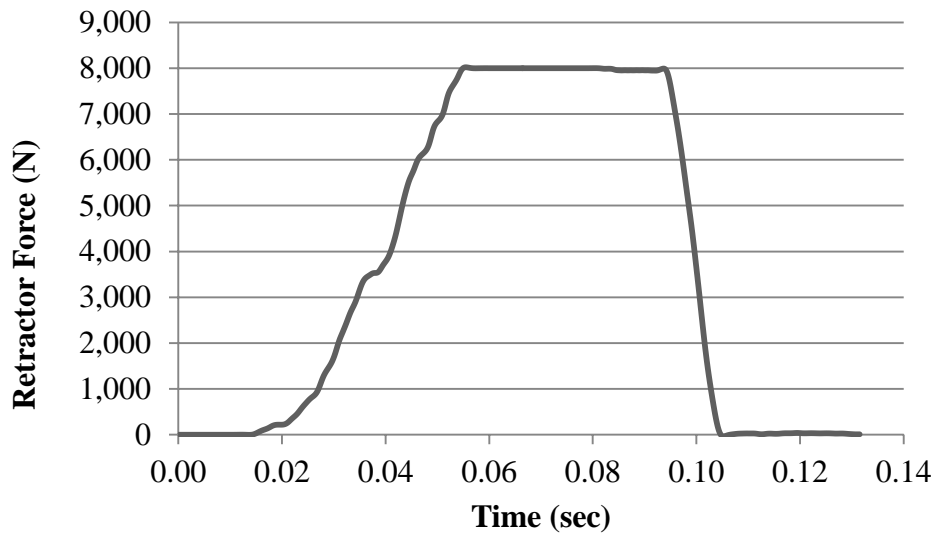


Figure A-26 Seatbelt retractor force time history (50 mph, 8 kN load limiter, no airbag).

A1.4.2 Head injury criteria

Dummy injury criteria for the head are evaluated with respect to the HIC₁₅ criteria. Head acceleration recorded during the impact event is employed to calculate the HIC₁₅ value. Figure A-27 illustrates details for the head injury criteria and the recorded curves from this specific impact condition and passive restraint systems employment.

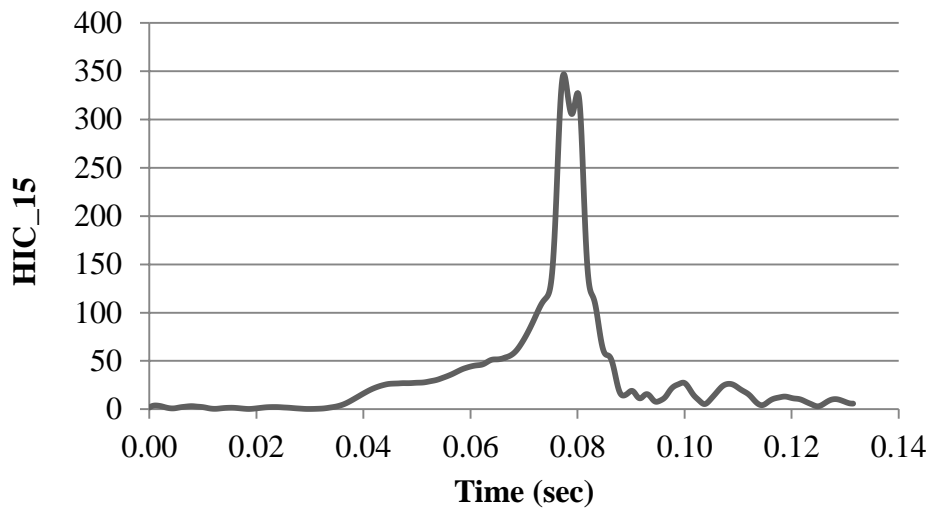
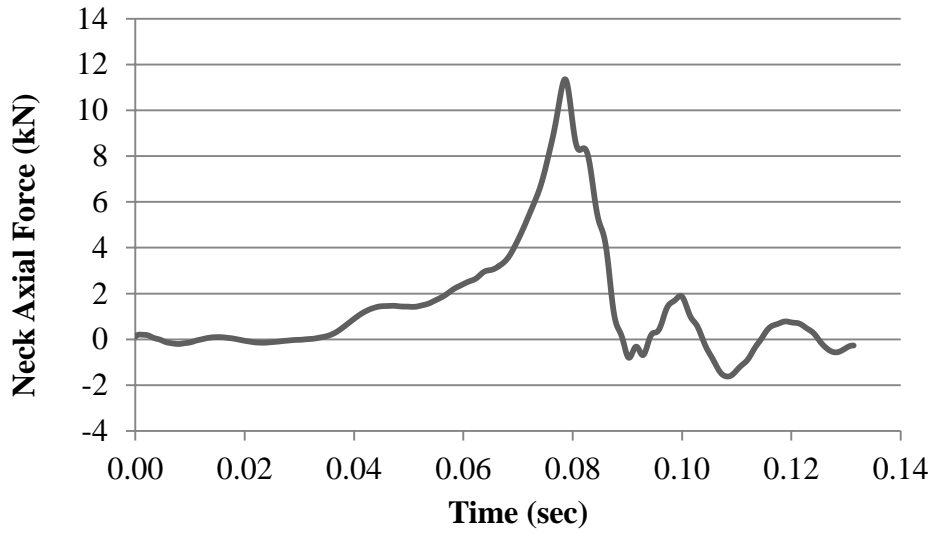


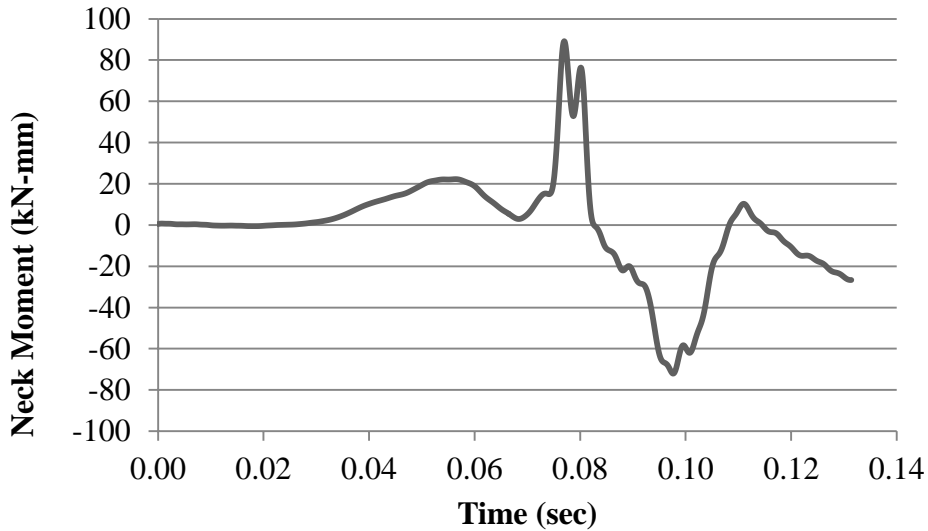
Figure A-27 HIC time history (50 mph, 8 kN load limiter, no airbag).

A1.4.3 Neck injury criteria

Dummy injury criteria for the neck are evaluated based on the normalized neck injury criteria, N_{ij} , which is defined as the sum of normalized values of loads and moments. Figure A-28 illustrates details for the neck injury criteria and the recorded curves from this specific impact condition and passive restraint systems employment.



(a) Neck Axial Force Time History



(b) Neck Bending Moment Time History

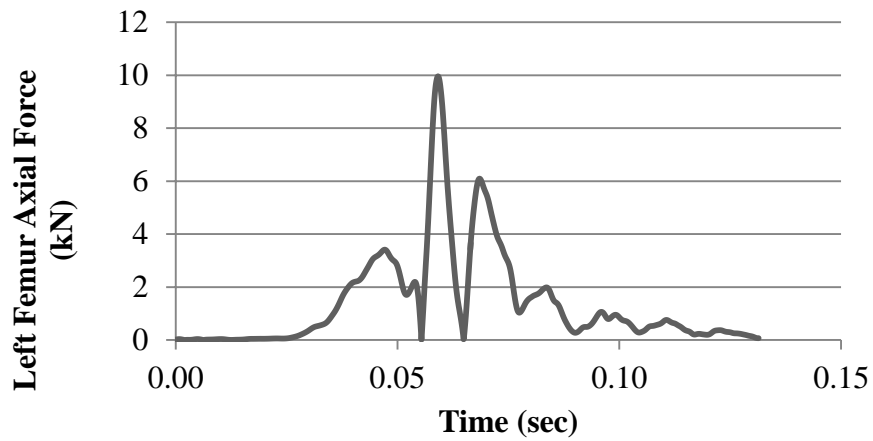
Figure A-28 Neck injury time history (50 mph, 8 kN load limiter, no airbag).

A1.4.4 Chest injury criteria

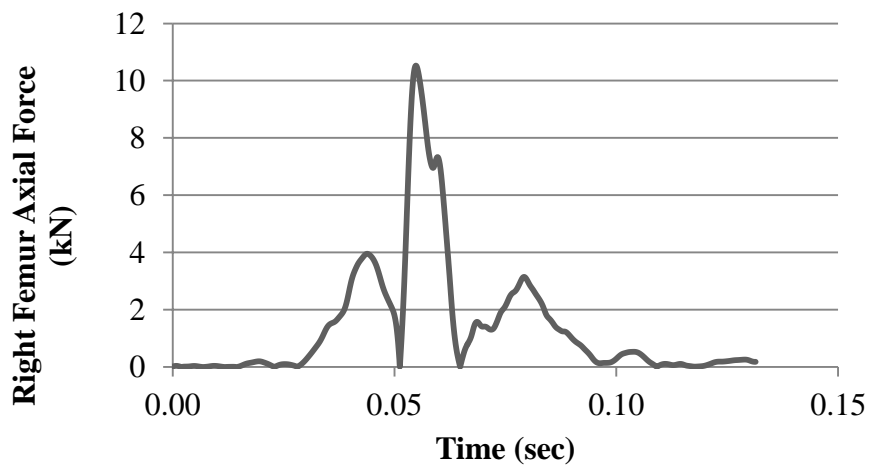
Dummy injury criteria for the chest are evaluated based on the chest deflection values. Researchers were unable to post-process chest deflection values and therefore did not evaluate chest injury criteria for this simulation case.

A1.4.5 KTH injury criteria

Dummy injury criteria for the KTH are evaluated based on the formulation for probability of injury as a function of femur axial force. Figure A-29 illustrates details for the KTH injury criteria and the recorded curves from this specific impact condition and passive restraint systems employment.



(a) Left Femur Axial Force Time History

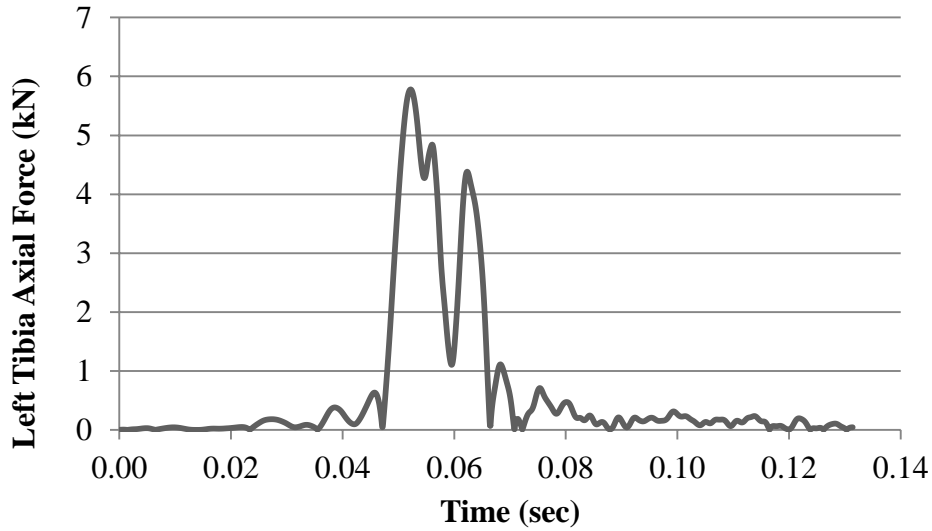


(b) Right Femur Axial Force Time History

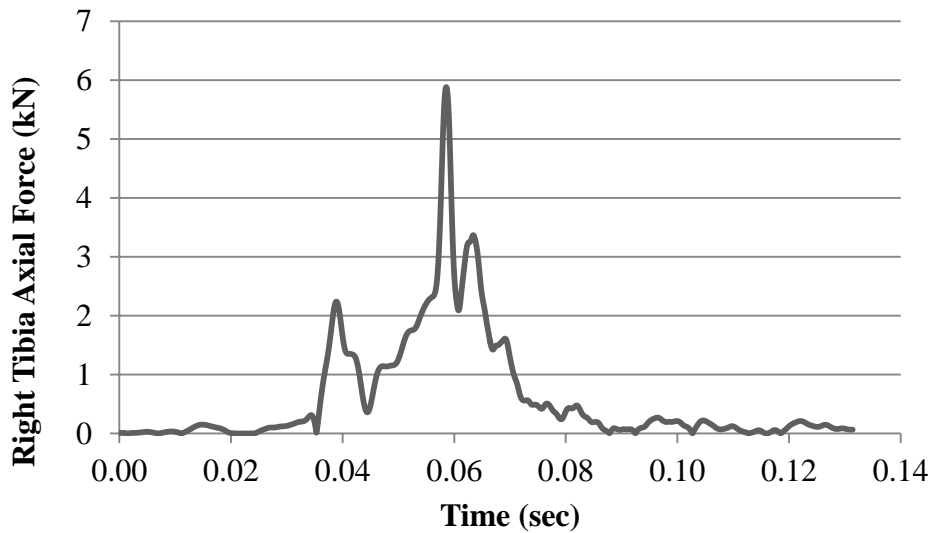
Figure A-29 KTH injury time history (50 mph, 8 kN load limiter, no airbag).

A1.4.6 Tibia plateau fracture injury criteria

Dummy injury criteria for tibia plateau fractures are evaluated based on axial compressive loads. Figure A-30 illustrates details for the neck injury criteria and the recorded curves from this specific impact condition and passive restraint systems employment.



(a) Left Tibia Axial Force Time History

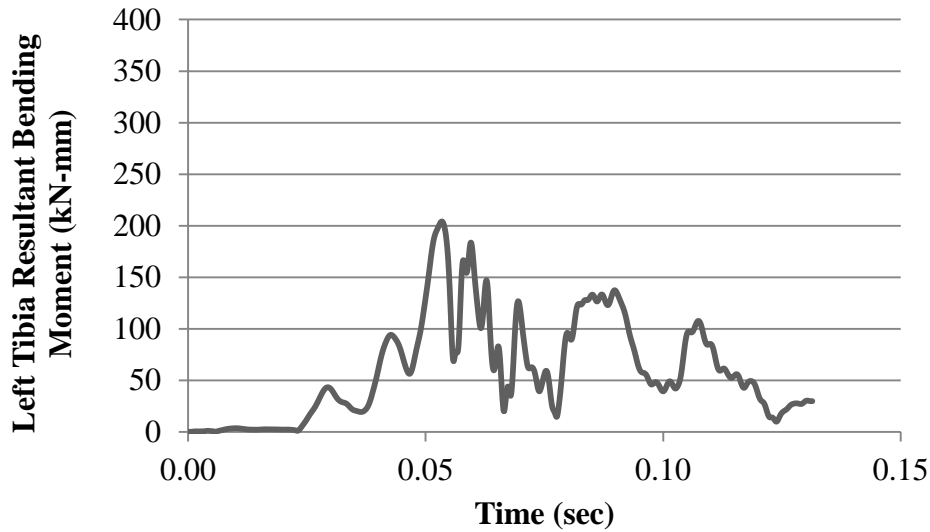


(b) Right Tibia Axial Force Time History

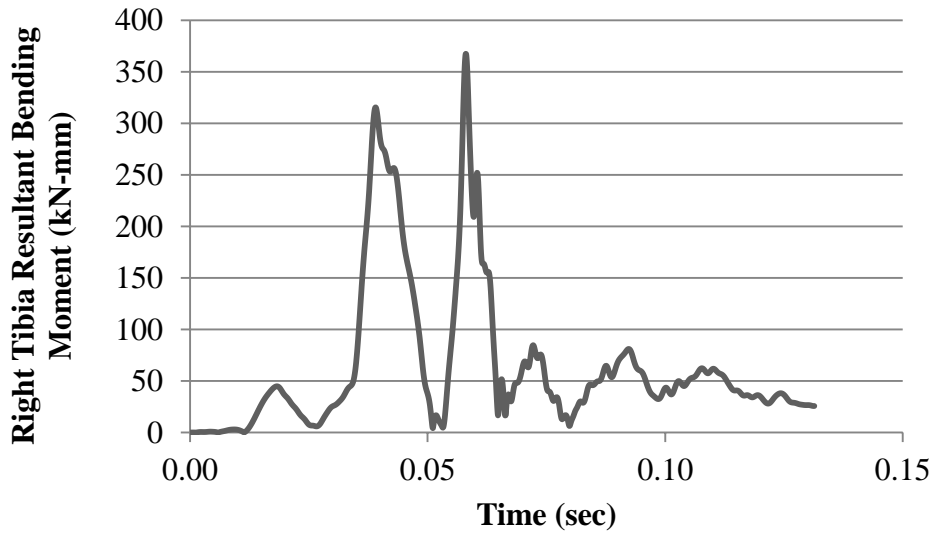
Figure A-30 Tibia plateau fracture time history (50 mph, 8 kN load limiter, no airbag).

A1.4.7 Tibia shaft fracture injury criteria

Dummy injury criteria for tibia shaft fractures are evaluated based on a normalized formulation that combines bending moments and axial compressive loads. Figure A-31 illustrates details for the tibia shaft injury criteria and the recorded curves from this specific impact condition and passive restraint systems employment.



(a) Left Tibia Resultant Bending Moment Time History



(b) Right Tibia Resultant Bending Moment Time History

Figure A-31 Tibia shaft fracture time history (50 mph, 8 kN load limiter, no airbag).

A1.4.8 Conclusions

The injury criteria values for various parts of the body were compared to the IARV requirements. The simulation injury criteria results as a percentage of the IARV values are shown in Figure A-32.

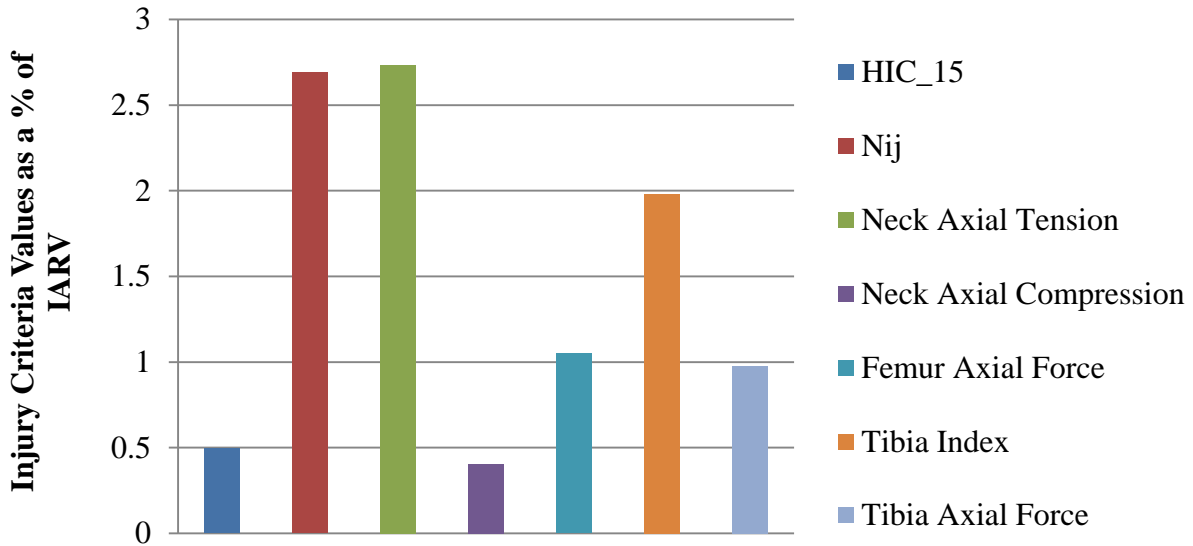


Figure A-32 Injury probability as a function of IARV (50 mph, 8 kN load limiter, no airbag).

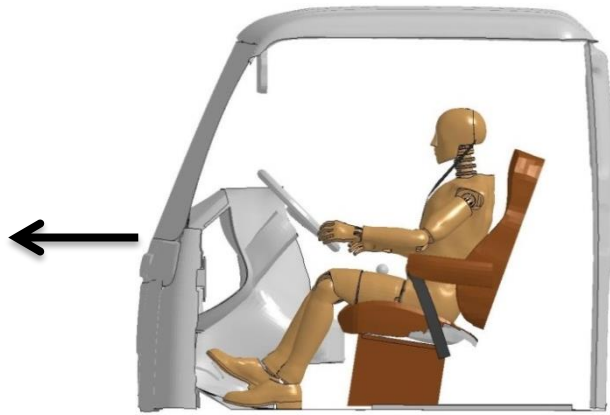
For the frontal 8 kN load limiter simulation without airbag, the probability of injury for the head region is unlikely because the injury criteria values stay below the threshold IARV. The injury criteria values for the neck, and KTH regions exceeded the threshold IARV which is unacceptable according to current standards.

A1.5 Frontal lowered D-ring simulation – 50 mph

A1.5.1 Simulation frames and summary

The following documents the post processed results of the finite element simulation of a frontal impact event with initial speed of 50 mph, inclusion of a belted HIII 50th percentile male dummy in the driver position, and no application of airbag. Table A-14 and Table A-15 summarize the resulting simulation with frames at different times throughout the simulation. The details of the simulation are summarized below and in Figure A-33:

- Impact Type : Frontal
- Initial Impact Speed : 50 mph
- Seatbelt Condition: Belted (Lowered D Ring)
- Airbag : No



(a) Lateral View of the FE Computer Model with Indication of Impact Orientation



(b) Seatbelt Model



(c) No Use of Airbag Model

Figure A-33 Modeled characteristics of the finite element simulation for the frontal impact (50 mph, lowered d-ring, no airbag).

Table A-14 Frontal impact simulation frames side view (50 mph, lowered d-ring, no airbag).














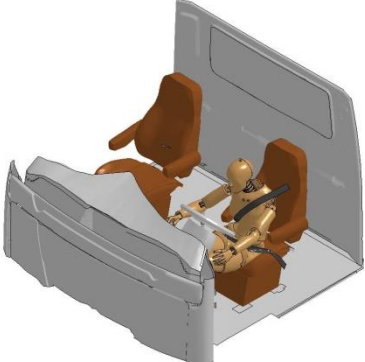
Time (Sec)	Sequential Frames	Time (Sec)	Sequential Frames
0.000		0.074	
0.015		0.089	
0.030		0.99	
0.055			

Table A-15 Frontal impact simulation frames perspective view (50 mph, lowered d-ring, no airbag).

Time (Sec)	Sequential Frames	Time (Sec)	Sequential Frames
0.000		0.074	
0.015		0.089	
0.030		0.99	
0.055			

The seatbelt retractor force for the resulting simulation is plotted in Figure A-34. The retractor contained no load limiter for this simulation and reached a peak of about 11.5 kN.

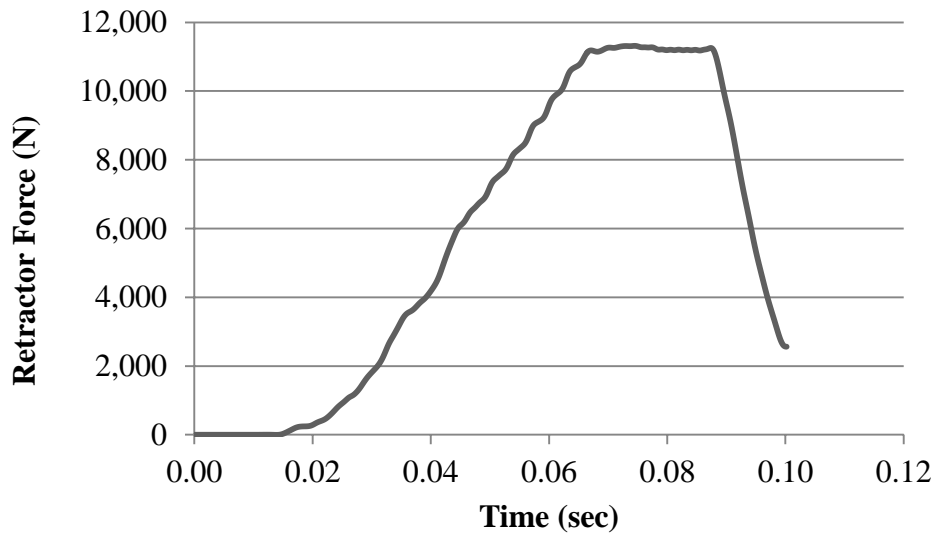


Figure A-34 Seatbelt retractor force time history (50 mph, lowered d-ring, no airbag).

A1.5.2 Head injury criteria

Dummy injury criteria for the head are evaluated with respect to the HIC₁₅ criteria. Head acceleration recorded during the impact event is employed to calculate the HIC₁₅ value. Figure A-35 illustrates details for the head injury criteria and the recorded curves from this specific impact condition and passive restraint systems employment.

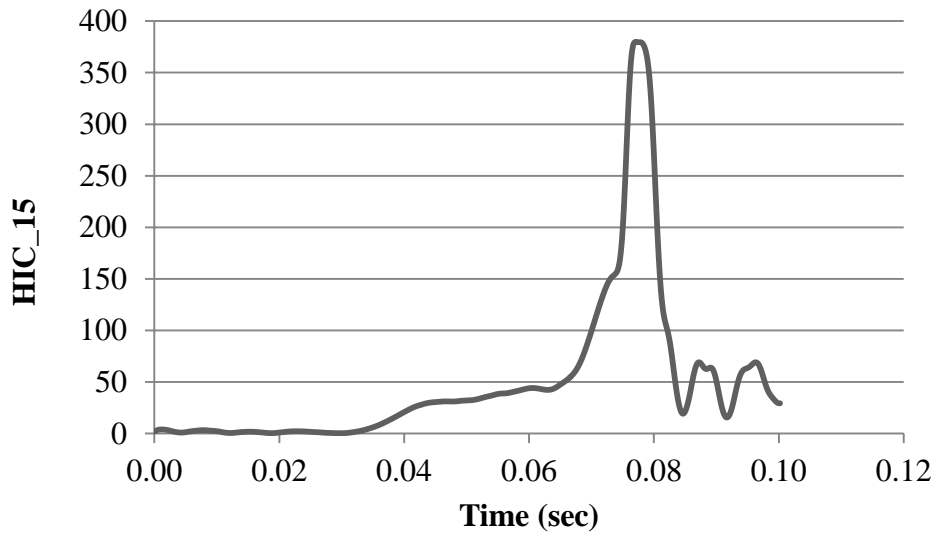
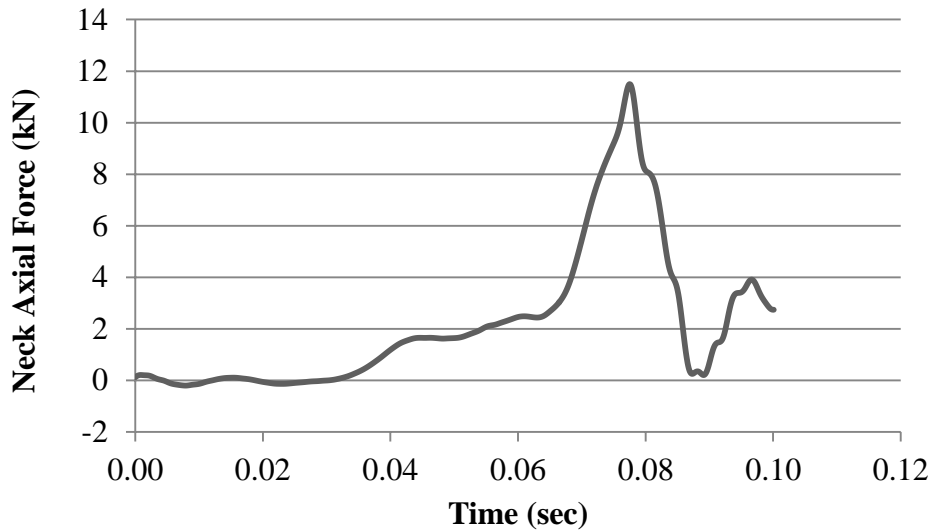


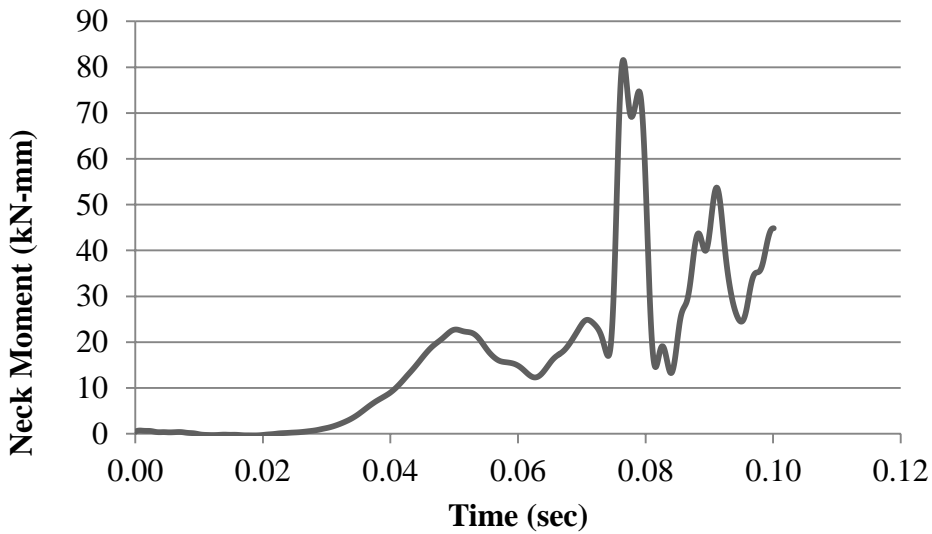
Figure A-35 HIC time history (50 mph, lowered d-ring, no airbag).

A1.5.3 Neck injury criteria

Dummy injury criteria for the neck are evaluated based on the normalized neck injury criteria, N_{ij} , which is defined as the sum of normalized values of loads and moments. Figure A-36 illustrates details for the neck injury criteria and the recorded curves from this specific impact condition and passive restraint systems employment.



(a) Neck Axial Force Time History



(b) Neck Bending Moment Time History

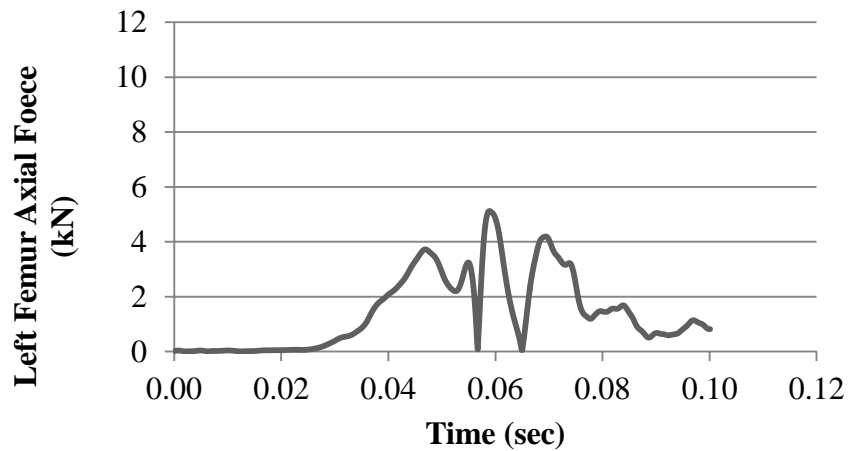
Figure A-36 Neck injury time history (50 mph, lowered d-ring, no airbag).

A1.5.4 Chest injury criteria

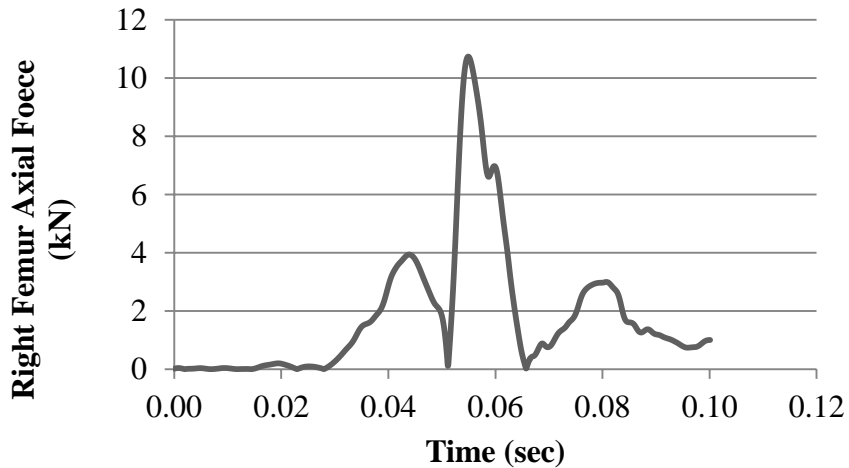
Dummy injury criteria for the chest are evaluated based on the chest deflection values. Researchers were unable to post-process chest deflection values and therefore did not evaluate chest injury criteria for this simulation case.

A1.5.5 KTH injury criteria

Dummy injury criteria for the KTH are evaluated based on the formulation for probability of injury as a function of femur axial force. Figure A-37 illustrates details for the KTH injury criteria and the recorded curves from this specific impact condition and passive restraint systems employment.



(a) Left Femur Axial Force Time History

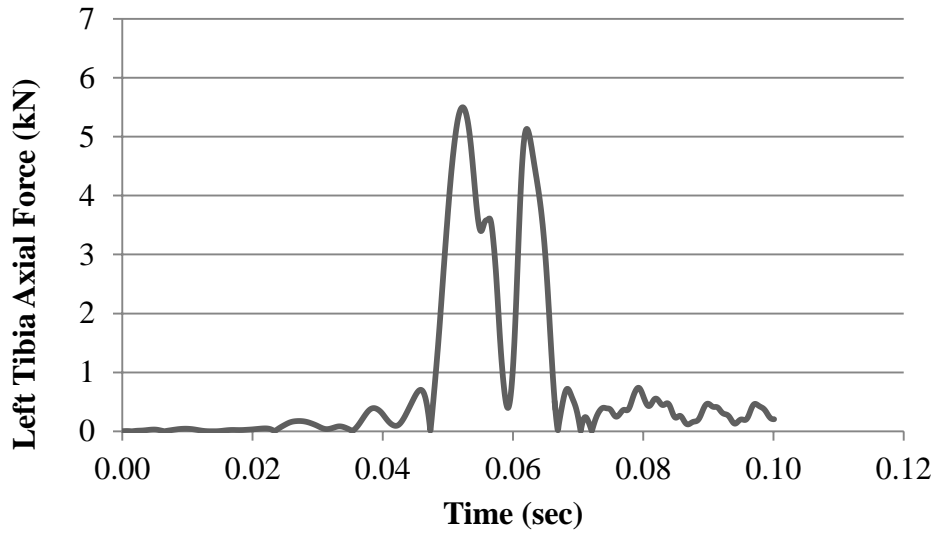


(b) Right Femur Axial Force Time History

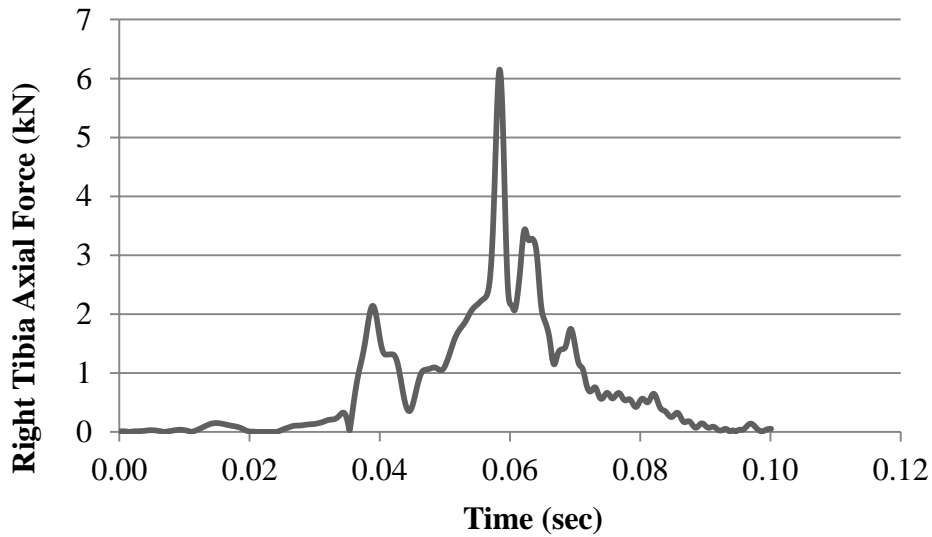
Figure A-37 KTH injury time history (50 mph, lowered d-ring, no airbag).

A1.5.6 *Tibia plateau fracture injury criteria*

Dummy injury criteria for tibia plateau fractures are evaluated based on axial compressive loads. Figure A-38 illustrates details for the neck injury criteria and the recorded curves from this specific impact condition and passive restraint systems employment.



(a) Left Tibia Axial Force Time History

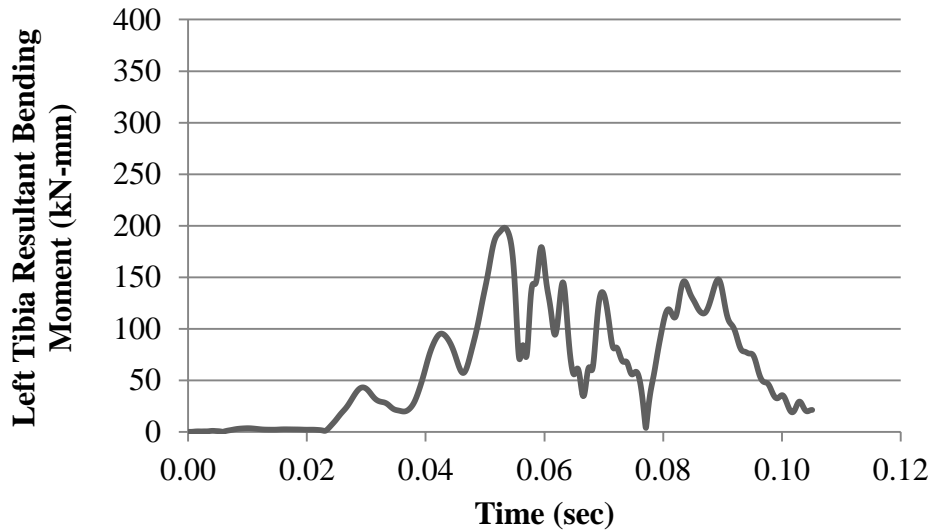


(b) Right Tibia Axial Force Time History

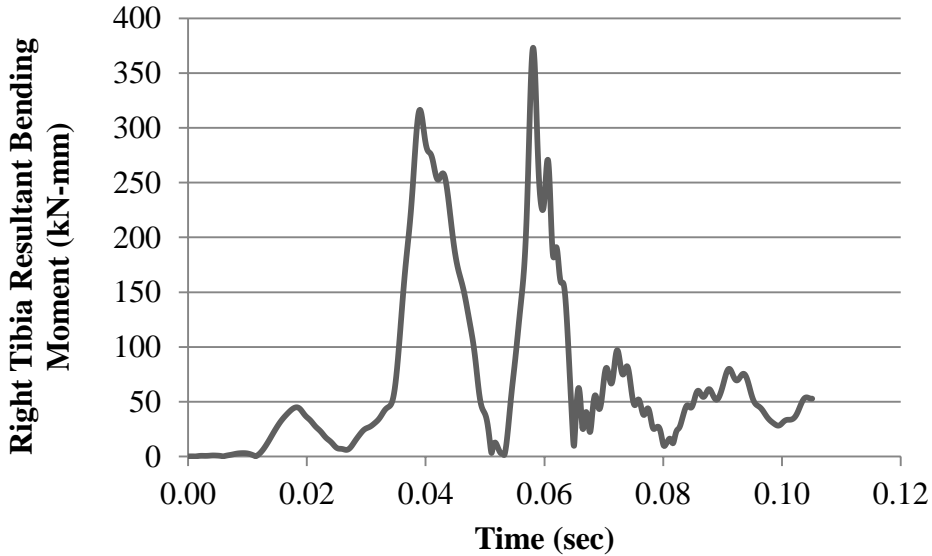
Figure A-38 Tibia plateau fracture time history (50 mph, lowered d-ring, no airbag).

A1.5.7 Tibia shaft fracture injury criteria

Dummy injury criteria for tibia shaft fractures are evaluated based on a normalized formulation that combines bending moments and axial compressive loads. Figure A-39 illustrates details for the tibia shaft injury criteria and the recorded curves from this specific impact condition and passive restraint systems employment.



(a) Left Tibia Resultant Bending Moment Time History



(b) Right Tibia Resultant Bending Moment Time History

Figure A-39 Tibia shaft fracture time history (50 mph, lowered d-ring, no airbag).

A1.5.8 Conclusions

The injury criteria values for various parts of the body were compared to the IARV requirements. The simulation injury criteria results as a percentage of the IARV values are shown in Figure A-40.

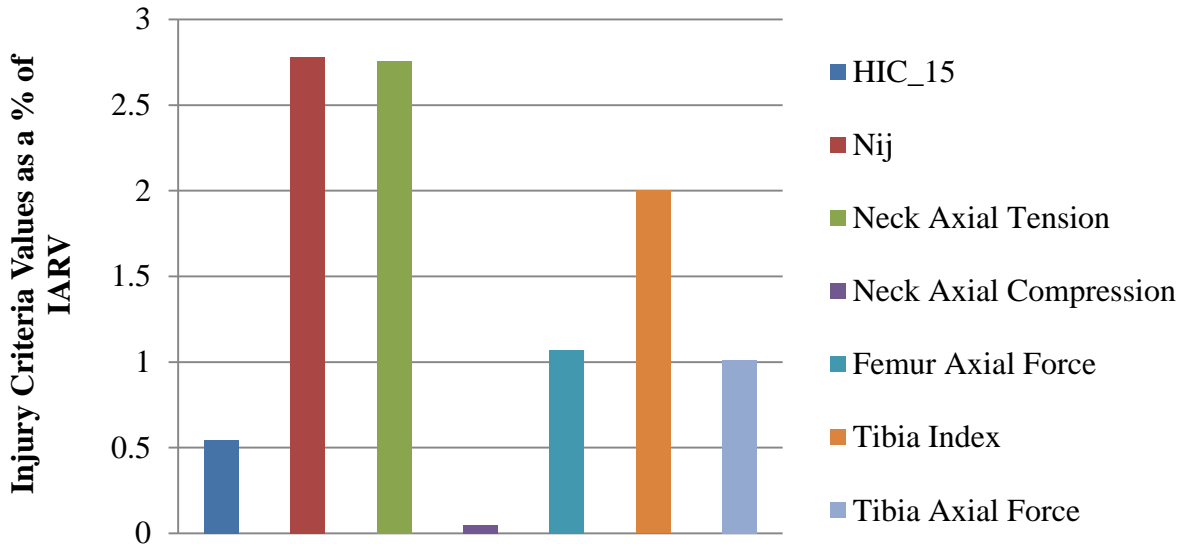


Figure A-40 Injury probability as a function of IARV (50 mph, lowered d-ring, no airbag).

For the frontal lowered d-ring simulation without airbag, the probability of injury for the head region is unlikely because the injury criteria values stay below the threshold IARV. The injury criteria values for the neck, and KTH regions exceeded the threshold IARV which is unacceptable according to current standards.

A1.6 Comparison of frontal simulations without airbag – 50 mph

A1.6.1 Simulation frame comparisons

The five frontal simulations conducted at 50 mph without airbag were compared to see the effects of the different restraint system parameters. Table A-16 and Table A-17 summarize the resulting simulations with frames at different times throughout the simulation.

A1.6.1 Injury criteria comparison for different regions of dummy

The injury criteria values for various parts of the body were compared to the IARV requirements. The simulation injury criteria results as a percentage of the IARV values are shown in Figure A-41 through Figure A-43 for the different regions of the body. The injury criteria results were not included for tibia injury comparison because the IARV for the tibia is not validated. Leg injury is typically analyzed in terms of KTH injury which represents the femur region.

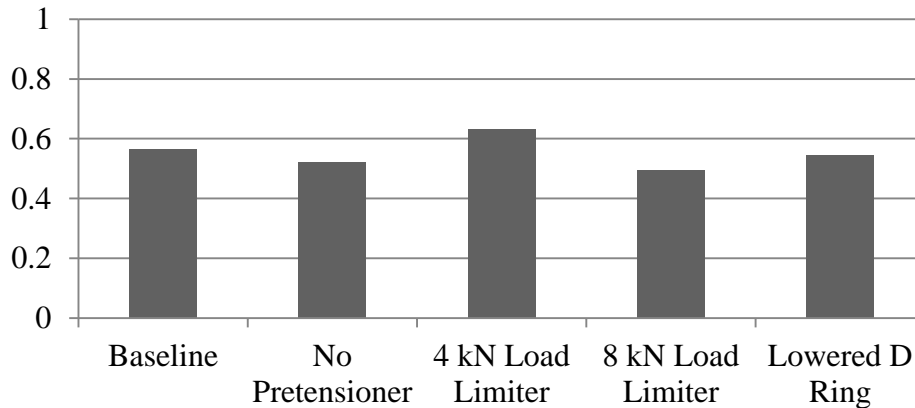


Figure A-41 Head injury probability comparison as a function of IARV (no airbag).

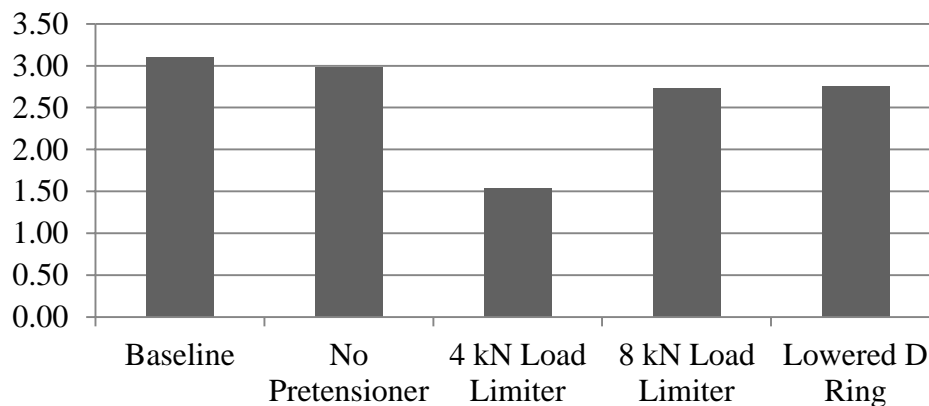


Figure A-42 Neck injury probability comparison as a function of IARV (no airbag).

Table A-16 Sequential frame comparison of frontal simulations at 50 mph without airbag (side view).

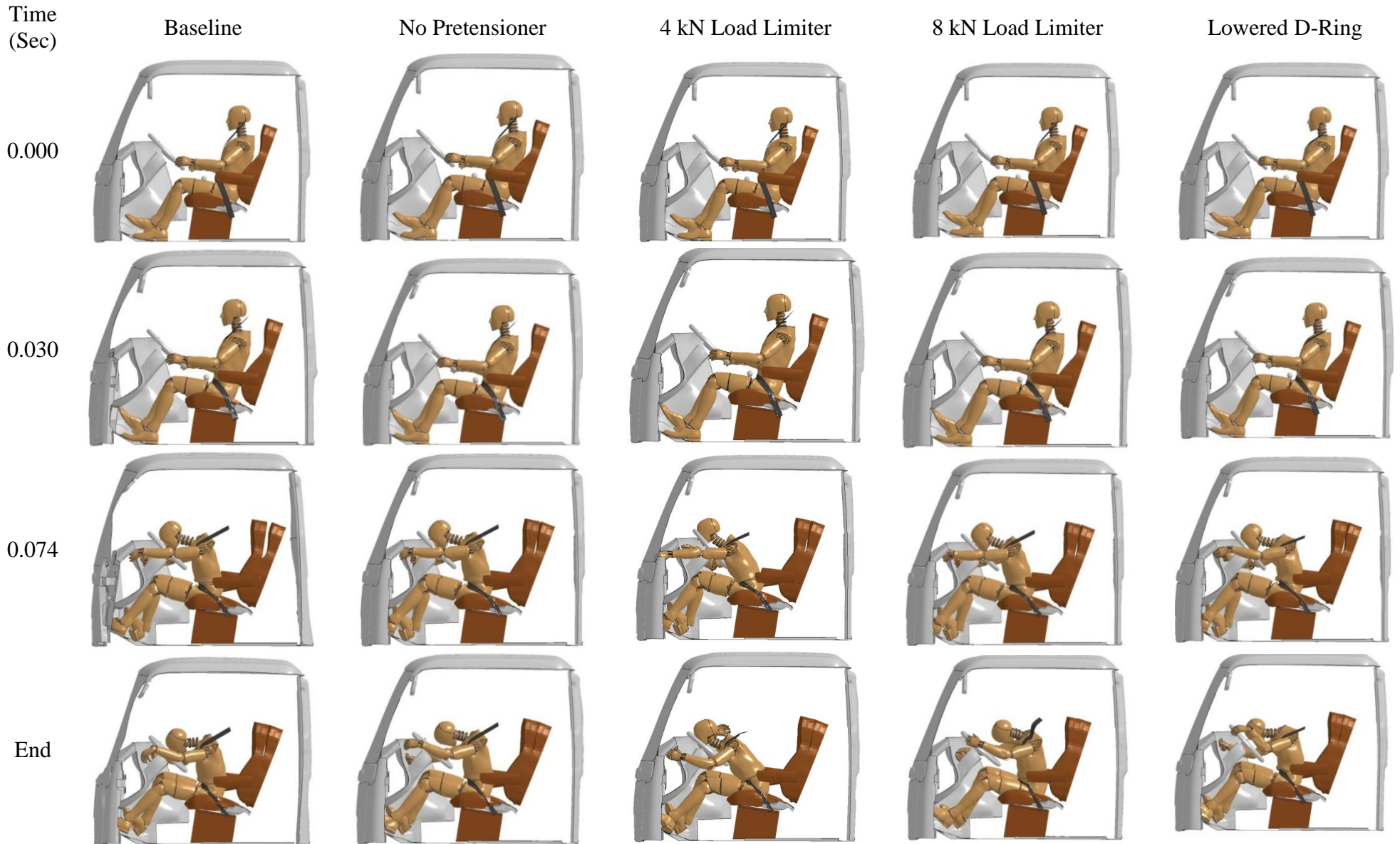










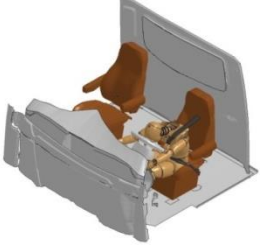






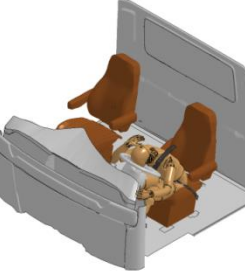




Table A-17 Sequential frame comparison of frontal simulations at 50 mph without airbag (perspective view).

Time (Sec)	Baseline	No Pretensioner	4 kN Load Limiter	8 kN Load Limiter	Lowered D-Ring
0.000					
0.030					
0.074					
End					

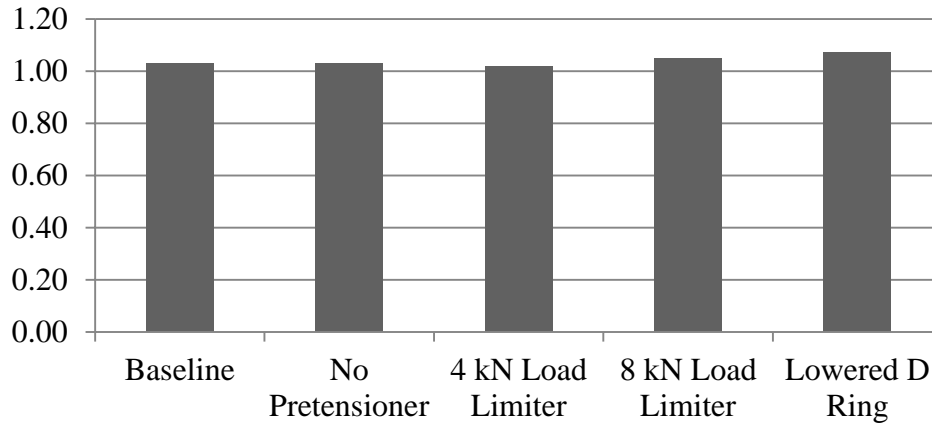


Figure A-43 KTH injury probability comparison as a function of IARV (no airbag).

Analysis of the injury criteria shows that both the head injury stayed below the threshold IARV, meaning that the probability of head injury is unlikely. Both the neck and KTH injury criteria results were higher and contained values above the threshold IARV's which is unacceptable according to current standards.